Salmonella:
Characterization of the Type III Effector SrfH and Proteomic Identification of the Secretome

by
George Stephan Niemann

A DISSERTATION

Presented to the Department of Molecular Microbiology and Immunology
and the Oregon Health and Science University
School of Medicine
in partial fulfillment of
the requirements for the degree of
Doctor of Philosophy
January 2010

School of Medicine

Oregeon Health and Science University

CERTIFICATE OF APPROVAL

This is to certify that the Ph.D. dissertation of

George Stephan Niemann

has been approved

Fred Heffron, Ph.D., Thesis Advisor

Jorge Crosa, Ph.D., Member

David Parker, Ph.D., Member

Erik Barkliss, Ph.D., Member

Peter Rotwein, Ph.D., Member

Ujwal Shinde, Ph.D., Member

Acknowledgments

I would like thank my mentor, Fred Heffron, for his advice and flexibility, but most importantly for his desire to help people even when I thought they didn't deserve it. I would also like to acknowledge the members of my committee for their guidance and support: Jorge Crosa, David Parker, Erik Barkliss, Peter Rotwein, and Ujwal Shinde. Numerous people at OHSU aided in my development as a scientist, but in particular I would like to mention Micah Worley, Kaoru Geddes, Lidia Crosa, Hyunjin Yoon, Afke Stufkens, and Afshan Kidwai. They taught me that collaboration is the key to efficiency. I give special thanks to my friends, especially Andy Simpson, Jayme and Tony Gallegos, Richard Locke, Devin Synder, Josh Anderson, and Matt Miller. None of my accomplishments were possible without the love of my family: Hildegard, Franz, Peter, Paul, Willfried, and Joe Niemann, their loved ones, Dave and Lee Shoemaker, and especially my wife, Jennifer, and son, Max.

I dedicate this work to my father, Peter Niemann, a welder and artist who always had a silly joke that didn't make much sense.

Table of Contents

List of Tables

Chapter 3

Chapter 4

Chapter 5

Appendices

List of Figures

Chapter 1

Chapter 2

Chapter 3

Chapter 4

Chapter 5

Appendices

ABSTRACT

Salmonella:
Characterization of the Type III Effector SrfH and
Proteomic Identification of the Secretome
George Stephan Niemann, B.S.

Doctor of Philosophy
Department of Molecular Microbiology and Immunology
and the Oregon Health and Science University
School of Medicine

January 2010
Thesis Advisor: Fred Heffron

Salmonella afflicts millions of people across the globe, is the leading cause of death among HIV infected individuals in sub-Saharan Africa, and is estimated to cost billions of dollars in lost productivity and wages every year. The relevance of this pathogen cannot be disputed and in light of emerging antibiotic resistant strains, it is of upmost importance that we understand the molecular mechanisms by which it mediates virulence. *Salmonella* is an intracellular pathogen and its virulence is in large part mediated by the secretion of effector proteins into host cells. Type III secretion systems (TSSS) are the best understood secretion mechanism, and they function as molecular syringes that directly inject effectors from bacteria to the eukaryotic cytosol. *Salmonella enteriditis* serovar Typhimurium has two TTSS which are encoded on *Salmonella* pathogenicity island 1 (SPI-1) and *Salmonella* pathogenicity island 2 (SPI-2). SPI-1 is required for the invasion of non-phagocytic cells and the intestinal phase of infection, while SPI-2 mediates intracellular survival and is required for systemic disease.

Following oral infection, a small population of $CD18^{+}$ cells rapidly carry *Salmonella* from the lumen of the intestine to the blood – this is the rapid septiciemia phenotype. My work demonstrates that the SPI-2 effector SrfH is responsible for rapid

septicemia. Then I attempted to gain an understanding of the host mechanisms involved. I present evidence showing that rapid septicemia is mediated by SrfH interaction with host TRIP6, and that this phenotype may occur via a c-Src signaling cascade.

To date 37 type III effectors have been reported in the literature, but when I initiated my thesis only a few had been described. However, such numbers underestimate the effector repertoire. Thus the second half of this thesis focuses upon the identification of novel secreted proteins. Two approaches were used to address this objective. First, I describe a transposon based strategy that was designed to generate effector fusions with an enzyme linked reporter. Although it was a sensitive way to evaluate secretion of individual effectors, only three novel effector proteins were identified. An alternative, mass-spectrometry based approach is presented next. We used LC-MS/MS to identify over 200 proteins secreted into SPI-2 inducing, defined media. By employing various genetic mutants, we selectively identified the majority of type III substrates and have developed the most efficient screen for *Salmonella* effector proteins to date. Moreover, this study identified several effector proteins that were secreted into host cells independent of TTS, suggesting that *Salmonella* employs alternative secretion systems during infection. It will take many years to define the function of these proteins.

Chapter 1

Salmonella Pathogenesis is Effector Driven

Background and significance

Introduction

Non-typhoidal *Salmonella* (NTS) serovars such as Typhimurium do not generally cause sepsis but are a leading cause of gastroenteritis in the US and a major cause of childhood mortality in developing countries. In sub-Saharan Africa NTS is the leading cause of death in HIV-positive patients. Typhoid fever is still common outside developed nations. This statistic may be surprising given the availability of effective vaccines [1] but their more widespread use is limited by cost. *Salmonella* virulence is largely mediated by the secretion of effector proteins, and there are numerous ways in which to discuss them. Excellent reviews have focused on themes such as inflammation, vesicular trafficking, ubiquitination, and the activities of the virulence factors themselves [2-6]. This short review is based on *S*. Typhimurium infection of mice because it is a model of typhoid-like disease in humans. I have organized effectors in terms of events that happen during the infection cycle and how secreted effectors may be involved.

Salmonella pathogenesis in human and mouse models of infection

After oral ingestion the initial contact between *Salmonella* and the intestinal wall results in an inflammatory response. Pro-inflammatory cytokines are released to attract $CD18^+$ phagocytes such as neutrophils, macrophages, and dendritic cells [7]. *Salmonella* lives within multiple cell types. Epithelial cells, B cells, T cells, macrophages, neutrophils, and dendritic cells are all known to harbor *Salmonella*. Bacterial replication occurs in the intestinal lumen and in various epithelial cell types. Bacteria are shed into stool for dissemination to new hosts [7,8]. Additionally, $CD18^+$ phagocytes carry bacteria from the intestine to systemic sites such as the spleen and liver. While the lymph is the major route by which *S*. Typhimurium becomes systemic, a small population of monocytes rapidly carries intracellular bacteria from the lumen of the intestine to the blood stream [9-11]. During the systemic phase of infection $CD18^+$ phagocytes are thought to be the dominant reservoirs of bacterial replication [7]. An adaptive immune response is required for clearance. However, the response is usually delayed or weak indicating that *Salmonella* actively subverts host immunity [12]. *Salmonella* employs multiple strategies to accomplish this subversion, and the topic is described in more detail

in subsequent sections. Alternatively, infected mice succumb to bacteremia or, in a small percentage of cases, become long term carriers. Long term carriers continually shed *Salmonella* into stool, a phenomenon that is not well understood.

Unlike *S.* Typhimurium infection in humans, mice do not show a very strong inflammatory response in the intestine following oral infection. One possible explanation for the different inflammatory responses is that mice express lower levels of Toll-like receptors (TLR) on the luminal side of intestinal enterocytes [13]. However, the inflammatory response to *Salmonella* is exacerbated if mice are first treated with streptomycin, thus providing a mouse model for gastroenteritis and inflammatory bowel disease [14,15]. The antibiotic removes a part of the intestinal flora that normally dampens inflammation although the precise change in microbiome is not yet known (pers. comm. B. Finlay).

C56/BL6 and BALB/c are the most common strains of mice used to study *Salmonella* infection, but they both carry a mutation in macrophage associated resistance protein (Nramp1/ Slc11a1). This gene encodes a metal ion transporter that is expressed in cells of myeloid origin and inhibits growth of some intracellular pathogens by reducing iron and manganese concentrations within the phagosome [16,17]. As a result, C56/BL6 and BALB/c mice are more susceptible to infection when compared to $Nramp^{+}$ 129/SvJ mice. The LD_{50} values for BALB/c, C56/BL6, and 129/SvJ mice after oral infection are ~1×10^4, 2×10^5, and >10^9 CFU, respectively [8,18]. Furthermore, 129/SvJ mice will not resolve a *Salmonella* infection for weeks, a characterisitic that more closely resembles typhoid-like disease in humans and which makes them a valuable persistence model [8,18].

Type III secretion systems (TTSS)

The interaction between bacterial pathogens and the host depends on cell surface proteins and secreted virulence factors. Many secreted effectors are injected into the eukaryotic cell via the type III secretion system. Two type III secretion systems (TTSS) are encoded by *Salmonella* – one at 63 minutes on the chromosome (SPI-1) and the other at 31 minutes (SPI-2). Both are about forty kilobases in length and encode the major structural components of the apparatus.

SPI-1 effectors are required for invasion of epithelial cells, intestinal inflammation, and gastroenteritis in the case of humans. The SPI-I secretion apparatus is also required to kill M cells that sample antigens and occlude the access to the lymphatic system [19]. Cell invasion is inherently inflammatory because of exposure to bacterial associated molecular patterns (PAMPs) that bind TLR, intracellular nod-like receptors (NLR), and potentially other receptors as well. The inflammatory response is also required for spread of infection through feces and the transmission of the bacteria across the intestinal barrier.

SPI-1 is not necessary for internalization by macrophages nor for survival within macrophages *in vitro*. Interestingly, SPI-1 is required for virulence with an *in vivo* persistence model. Persistence in 129/SvJ mice required the SPI-1 secretion apparatus and regulators HilA, HilD, InvF, and HilC [20]. SPI-1 effectors presumably improve the conditions for *Salmonella* replication and dissemination from the lower bowel, but it is unknown how SPI-1 affects persistence at systemic sites such as the spleen and liver where *Salmonella* resides within phagocytic cells that do not require SPI-1 for internalization. The mechanism for persistence may be a consequence of growth in cell types other than professional phagocytes, but this remains to be demonstrated. SPI-2, on the other hand, promotes *Salmonella* survival and replication within phagocytic cells. Since these cells constitute the main reservoirs of bacterial replication at the systemic sites, a SPI-2 mutant fails to persist after infection [21]. See Fig. 1-1 for an overview of these processes.

TTS and the intestinal phase of infection

SPI-1 effectors SopE, SopE2, SopB, and the SPI-1/2 effector SptP

Four secreted effectors are required for the invasion of non-phagocytic cells as has been shown elegantly by the Galan laboratory: SopE, SopE2, SopB, and SptP. SopE and SopE2 function as guanine exchange factors (GEF) for Rac1 and CDC42. Rac1 and CDC42 are small Rho GTPases that coordinate cellular activities such as actin polymerization, cell motility, and cell adhesion. Activation by SopE and SopE2 leads to actin rearrangements, localized membrane ruffling, and macropinocytosis of bacteria.

Intestinal phase

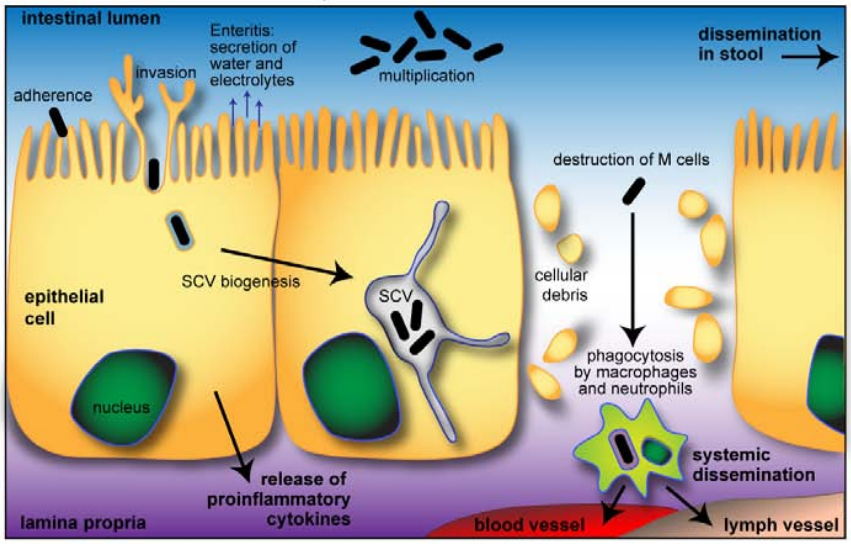

-Invasion of non-phagocytic cells
  ▪SipA, SipC, SopE, SopE2, SopB, SopD, SptP

-SCV biogenesis
  ▪SopB, SptP

Transit to the systemic sites and intracellular replication

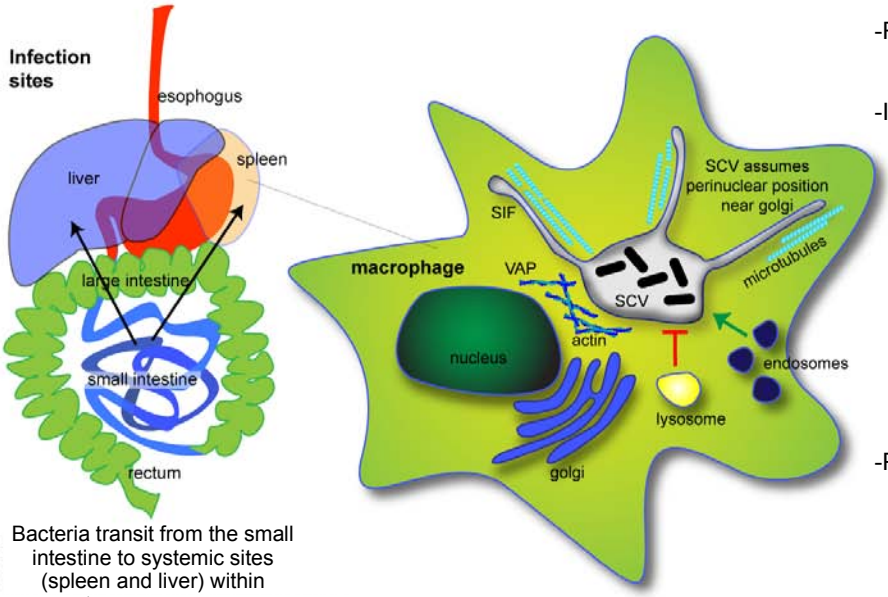

Bacteria transit from the small intestine to systemic sites (spleen and liver) within $CD18^{+}$ phagocytes via the lymph and blood

-Rapid Septicemia
  ▪SrfH

-Intracellular replication
  ▪SIF
    ◦SifA, SseJ, SopD2
  ▪SIF extension
    ◦PipB2
  ▪SCV positioning
    ◦SseF, SseG
  ▪VAP phenotype
    ◦SpvB, SteC

-Persistence
  ▪SrfH, SopD2, SseJ, PipD, SseK2, SopD, SteA, SipA, SipD, SopE2

Fig. 1-1

Characteristics of the intestinal and systemic phases of *Salmonella* infection. (Instetinal phase) *Salmonella* adheres to and invades epithelial cells of the intestinal lumen. This is a SPI-1 dependent process that involves the activities of multiple type type III effectors, particularly SopE, SopE2, SopB, SipA, SipC, SopD, and SptP. Recognition of bacterial PAMPs by the innate immune system as well as effector activities stimulate the secretion of pro-inflammatory cytokines that recruit $CD18^{+}$ phagocytes such as neutrophils and macrophages. M cells of the Peyer's patch are destroyed as a consequence of infection and are thought to be one route by which *Salmonella* is taken up by macrophages and neutrophils. (Systemic phase) These cells carry *Salmonella* from the intestinal lumen to the systemic sites of infection via the lymph and blood. *Salmonella* survives and replicates within $CD18^{+}$ cells in the spleen and liver. Salmonella replication occurs in a modified phagosome called the *Salmonella* containing vacuole (SCV). Although the SPI-1 effector SopB and SPI-1/2 effector SptP participate in SCV biogenesis, intracellular replication is dependent upon the SPI-2 effectors SifA, SseJ, SseF, SseG, PipB2, SopD2, SpvB, and SteC. These effectors mediate many of the phenotypes associated with the SCV such as *Salmonella* induced filaments (SIF), SCV associated actin polymerization (VAP), perinuclear localization of the SCV near the golgi, and modulation of the endocytic pathway.

SopE2 activates CDC42 more strongly than SopE, but SopE activation of Rac1 alone is sufficient for internalization (rev. in [22,23]). Surprisingly, neither SopE nor SopE2 has primary sequence homology with a mammalian GEF, but they are structural homologs [24,25]. SopE and SopE2 also pro-inflammatory and act redundantly to stimulate IL-8 secretion via mitogen-activated protein kinases (MAPK) JNK, p38 and ERK [26,27]. IL-8 is a CXC chemokine and potent chemoattractant for neutrophils and macrophages [26].

SptP is a GTPase activating protein (GAP) that deactivates Rac1 and CDC42 and functions as an antagonist of SopE and SopE2 activities [28]. SptP is thought to return the cellular cytoskeleton to a resting state following bacterial uptake. SptP can be secreted by both SPI-1 and SPI-2 TTSS, but approximately five fold less efficiently through the SPI-2 apparatus [29]. SptP has a longer, cellular half life than SopE, ensuring the reversal of bacterial mediated actin rearrangements associated with CDC42 and Rac1 activation [30]. In addition, SptP activity dampens pro-inflammatory signaling by inhibiting Raf-1 activation of the MAPK ERK[31]. However, half-life is not the only mechanism by which effectors coordinate their activities.

Amazing pictures of *Salmonella* injecting type III effectors have shown that both SopE2 and SptP were expressed prior to secretion, and that SopE2 was injected more efficiently than SptP. As described above SptP is an antagonist of SopE2 GEF activity, and when taken together this data suggests that effector tranlocation is coordinated [32]. In a similar set of experiments, Schlumberger et al. demonstrated that both SipA and SopE were expressed prior to secretion and translocated to the eukaryotic cell within 90 minutes of contact, but in this case translocation occurred at similar rates. This finding was not surprising considering the roles both SipA and SopE perform in bacterial uptake [33]. These examples demonstrate exquisite regulation, a property that likely applies to many secreted effector proteins.

SopB is a phosphoinositide phosphatase of PI(4,5)P2 [34], the products of which activate SH3-containing guanine nucleotide exchange factor (SGEF). SopB activation of SGEF in turn activates the small GTP binding protein RhoG which remodels actin via Arp2/3 [35]. Hydrolysis of PI(4,5)P2 also coincides with recruitment of host SNARE protein VAMP8 which promotes membrane fission and macropinosome formation to engulf bacteria [36]. The phosphoinositide activity of the SPI-1 effector SopB is also

known to activate Akt1 [27,37], a serine-threonine kinase that promotes bacterial invasion, inhibits apoptosis, and aids in the maturation of the *Salmonella* containing vacuole (SCV). The first phenotype is attributable to PAK4, and adaptor protein that links Cdc42 and Rac1 to the actin cytoskeleton [38]. Since Cdc42 and Rac1 are also targeted by SopE and SopE2, *Salmonella* appears to manipulate Rho GTPases from multiple directions to promote internalization. Akt1 may inhibit apoptosis by phosphorylation and inactivation of FoxO and GSK-3β. FoxO is a transcription factor that likely functions as a trigger for apoptosis by upregulating genes necessary for cell death such as Bim and PUMA or by down-regulating of anti-apoptotic proteins like FLIP. A role for GSK-3β in apoptosis has not been reported [27]. The effects on SCV maturation occur through Akt1 activation of AS160, the Rab14-GAP, which blocks Rab14 mediated phagosome-lysosome fusion. In human macrophages Akt1 inhibitors blocked *Salmonella* replication but did not affect bacterial viability, demonstrating that Akt1 activation was required for intracellular replication. Moreover, chemical and siRNA inhibitors of Akt1 blocked the intracellular replication of many intracellular pathogens, suggesting that this signaling network plays a central role in regulating replication and, therefore, may be a good therapeutic target [38].

SPI-1 secreted effectors SipA, SipC, and SopD

SipA and SipC increase the efficiency of cell invasion by targeting actin [39]. SipA prevents actin depolymerization by displacing and preventing F-actin interactions with cellular actin depolymerizing proteins ADF and cofilin [40]. SipA also potentiates SipC actin polymerization [41]. SipC is an example of the complexity of type III effectors as it also forms part of the translocon pore in the eukaryotic membrane [42]. SipC interaction with actin occurs via two separate domains. The N-terminus bundles actin whereas the C-terminus nucleates actin assembly leading to filament growth from barbed ends [43]. Both SipC and SipA effectors limit the membrane ruffling to the point of bacterial contact [40,44]. SipA also possesses a pro-inflammatory phenotype because it activates protein kinase C alpha (PKCα) signaling pathways that lead to the secretion of IL-8 via Jun and p38 [45]. In addition to SopE and SopE2, SipA is the third effector known to stimulate the secretion of this cytokine. The function of SopD is less clear. SopD was first identified in *Salmonella* Dublin as a SPI-1 secreted effector that, along

with SopB, induced inflammation in ileal mucosa [46]. SopD increases invasion efficiency and is recruited to the site of cell invasion through a process that requires the inositol phosphatase activity of SopB [47].

TTS and the systemic phase of infection

Salmonella containing vacuole (SCV)

Intracellular *Salmonella* resides and replicates within a vesicle known as the SCV, and it modifies the cellular architecture to permit replication by altering vesicular trafficking ([48]; reviewed in [49]). Vesicular transport initiates at the Golgi where an amino acid sequence determines a protein's glycosylation pattern, which in turn directs its transport within the cell. At least one effector, SteA, is targeted to the Golgi and required for virulence, but its precise role is unknown [29]. Vesicular compartments bud from the trans-Golgi and are transported along microtubules. Vesicles are distinguished by both v- and t-SNAREs and specific Rabs. The former are proteins that fuse membranes whereas the later are small GTP binding proteins related to the cytoplasmic portion of G-coupled receptors. Rabs attach to vesicles via lipidation (prenylation) of a C-terminal cysteine. Vesicle fusion requires the appropriate t-SNARE, Rab, and Rab binding proteins. There are about 60 conserved Rabs encoded within the mammalian genome and at least that number of v- and t-SNARE proteins. Rabs associate with specific vesicles and are required for membrane fusion, but the precise steps are still being investigated.

Salmonella has evolved strategies to avoid anti-microbial components by blocking fusion with vesicles that contain NADPH oxidase and inducible nitric oxide synthase while allowing fusion with other vesicles that presumably contain nutrients (reviewed in [50]). Rab manipulation likely facilitates these phenotypes. See Fig. 1-2 reprinted from Smith et al. [51] illustrating the complexity of Rab recruitment to a vesicle containing live *Salmonella* or one containing *Salmonella* unable to synthesize effectors.

The SCV is remarkably different from cellular vesicles. Following phagocytosis the SCV contains early endosomal markers EEA1, transferin receptor, Rab4, Rab5, and Rab11. Further maturation results in the recruitment of vATPase, Rab7, Rab11a, Rab11b, and lysosomal glycoproteins such as LAMP1. vATPase acidifies the SCV, and Rab7

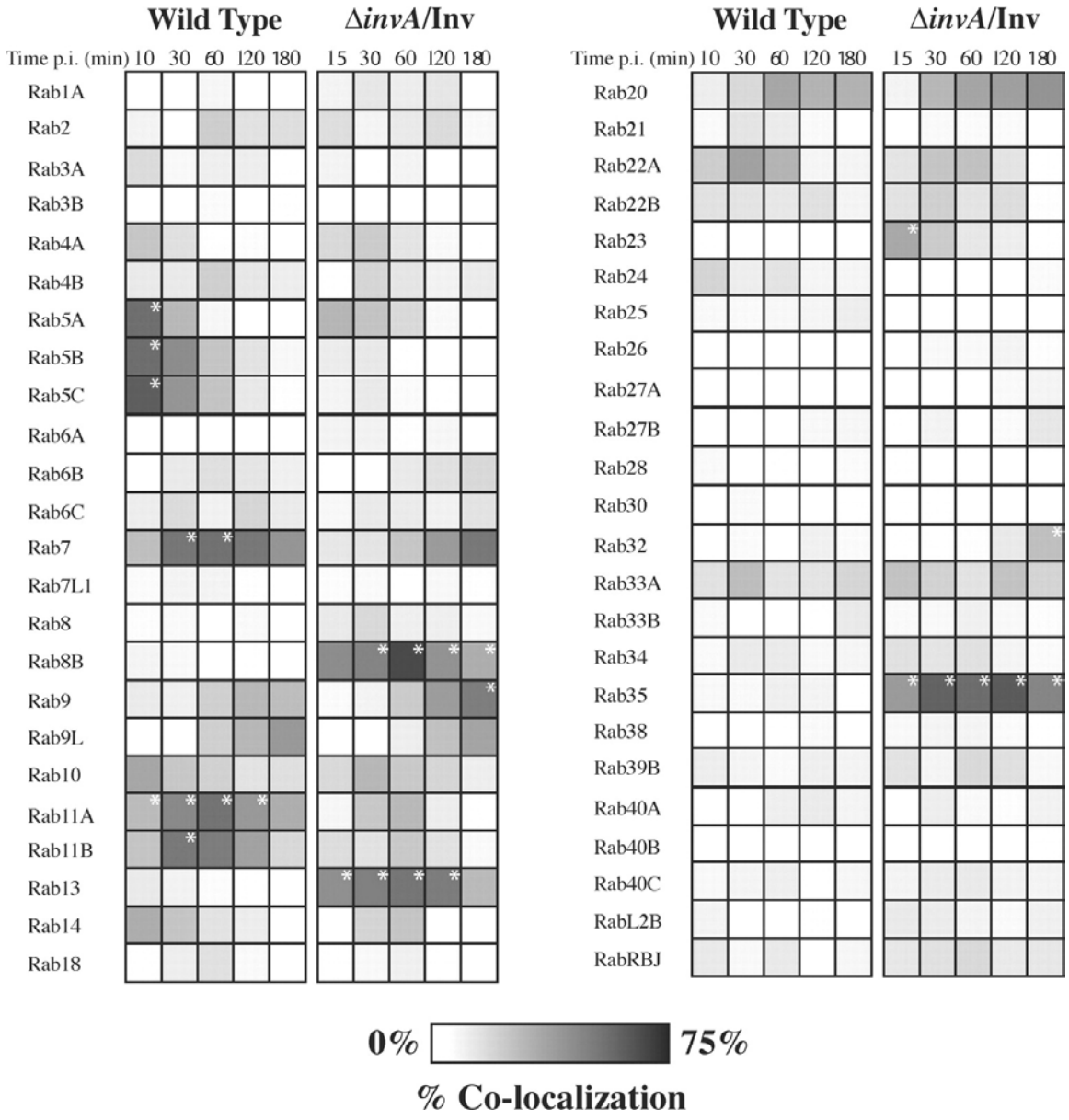

Fig. 1-2

Reprinted from [51]. Rab GTPase localization on wild-type and Δ*invA*/Inv *S.* Typhimurium vacuoles. InvA is a component of the SPI-1 TTSS. A mutant is deficient for secretion and non-invasive. Exprssion of the *invasin* (*inv*) locus from *Y. pseudotuberculosis* allowed the bacteria to enter the cell via an alternate mechanism, but they were targeted to late endosomes and unable to replicate. Wild-type SCVs and Δ*invA*/Inv S. Typhimurium model phagosomes were enumerated for their association with 48 Rab GTPases at the indicated times. The scale represents 0 to 75% of vacuoles colocalizing with the Rab GTPase as indicated by degree of shading.

recruits the dynein-dynactin motor complex through Rab7 interacting lysosomal protein (RILP). The functions of the other markers are unknown, but they are thought to help stabilize the vacuole. Additionally, the mannose-6-phosphate receptor, a late endosomal marker, is excluded from the SCV. The final stages of SCV maturation are characterized by vacuole associated actin polymerization (VAP) and *Salmonella* induced filaments (SIF), membrane tubules that radiate throughout the cell (reviewed in [6]). SIF and VAP function are unknown but they could be associated with cell-to-cell spread, nutrient acquisition, antigen presentation, vesicle fusion, or avoidance of anti-microbial mechanisms.

SCV biogenesis is effector driven, and in some cases effector roles have been characterized. Two SPI-1 effectors (SopB and SopD) and eleven SPI-1/2 or SPI-2 effectors (SptP, SifA, SifB, SseJ, SseF, SseG, PipB, PipB2, SopD2, SpvB, and SteC) are recruited to the SCV. Of these only *pipB* and *sifB* mutants lack virulence phenotypes. The phenotypes of the other effectors vary considerably. Please refer to Fig. 1-3 adapted from [49] as a visual aid for the following sections.

SPI-1 effector SopB and the SPI-1/2 effector SptP associate with the SCV

The SPI-1 effector SopB affects internalization as well as SCV biogenesis. After translocation the effector initially localizes to the host plasma membrane and increases the efficiency of uptake as previously described. SopB is then monoubiquitinated at nine different lysine residues. This relocalizes SopB to the nascent SCV where it recruits Vps34 and Rab5. Both SopB and Vps34 are phoshpoinositide phosphatases and are thought to enrich the SCV with PI3P [52]. SptP, on the other hand, encodes a C-terminal tyrosine phosphatase activity that dephosphorylates the AAA+ ATPase valosin-containing protein (VCP/p97) [53]. VCP participates in various cellular pathways including membrane fusion, protein folding/unfolding, proteolysis-dependent transcriptional control, and protein degradation [54]. It is required for the SIF phenotype and promotes bacterial replication within the host cell, but the precise mechanism is not known [53].

SPI-2 effectors SifA and SseJ

SifA was the first SPI-2 effector discovered, and it plays a central role in intracellular replication in both epithelial cells and macrophages [55]. SifA is necessary for the formation of *Salmonella* induced filamentous vesicles after which it is named

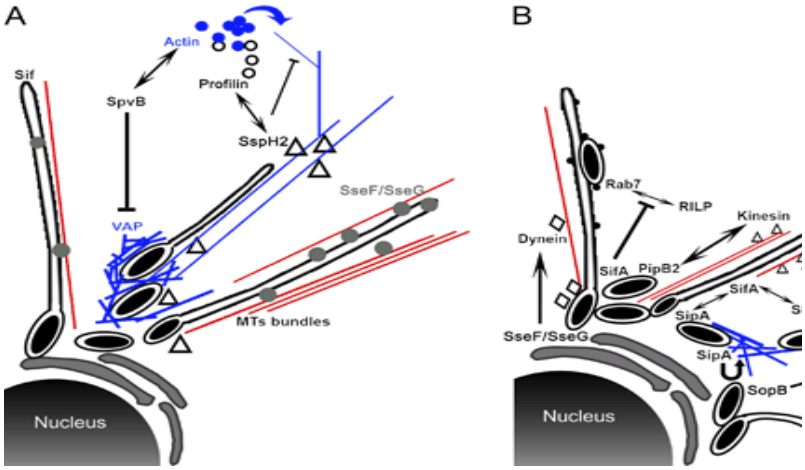

Fig. 1-3

Adapted from [49]. Modulation of host cell machinery during bacterial growth. Several hours after invasion, SCVs localize to a perinuclear region associated with the Golgi network. The bacteria establish a 'nest' and modify host cell machinery using a variety of secreted virulence factors. A) Alterations of the host cytoskeleton. B) Bacterial factors that regulate actin and microtubule motors to control SCV positioning. MTs, microtubules.

[55,56]. The *sifA* gene is located in the pot operon for polyamine transport, but it does not appear to be co-regulated with these genes. SifA contains a C-terminal CaaX motif that is prenylated by PGGT-1. This modification promotes association with the SCV in the same way as Rabs [57]. The C-terminal domain is a GAP mimic that is characterized by a WxxxE motif. The target of this activity is RhoA, an SCV associated protein that coordinates actin rearrangements [58-60]. SifA kinesin interacting protein (SKIP) interacts with the effector's N-terminus. SKIP is a tubulin binding protein required for SIF formation, and it attaches the SCV to microtubules. The SifA-SKIP complex also interacts with Rab7. This prevents Rab7 interaction with RILP, prevents dynein recruitment, and manipulates the movement of the SCV [60].

The SseJ effector is expressed at high levels following *Salmonella* internalization and is found on the cytoplasmic face of the SCV. Purified SseJ has deacylase and acyltransferase activity *in vitr*o, and SseJ catalytic-triad mutants that reduce deacylase activity are attenuated for virulence in mice, indicating that SseJ enzymatic activity contributes to intracellular replication in host tissues [61]. SseJ is thought to alter the composition of the SCV membrane by enriching it with cholesterol [62]. Interestingly, SseJ forms a complex with RhoA , SifA, and SKIP [60]. SseJ may counteract some of the effects of SifA because a *sifA* mutant escapes from the SCV whereas a *sifA sseJ* double mutant does not [63]. Furthermore, co-expression of SseJ and SifA from a mammalian vector results in filamentous vesicles similar to those observed during *Salmonella* infection [60].

SPI-2 effectors SseF, SseG, PipB2, and SopD2

The other SPI-2 effectors mentioned above have different SCV associated phenotypes. SseF and SseG form a complex and are required for virulence, but no activity has been ascribed to them. Along with SifA they direct the SCV to the perinuclear/Golgi region of the cell by an unknown mechanism. SseF contains three transmembrane domains suggesting that it may be inserted directly in the vesicular membrane. [3,52,64,65]. PipB and PipB2 are related effectors that associate with detergent resistant lipid rafts on the SCV and at similar vesicular membranes elsewhere in the cell [66]. PipB is not required for virulence, whereas PipB2 extends SIF vesicles during intracellular replication and relocates late endosomes/lysosomes from a

perinuclear location to the cell periphery [67]. SIF extension may occur by direct interaction between PipB2 and kinesin [68]. Interestingly, ectopic expression of PipB2 overcomes dominant active mutations in Rab7 and Rab34 that position vesicles near the microtubule organizing center suggesting that PipB2 acts downstream of these two Rabs [67]. SopD2 shares 47% identity with the SPI-1 effector SopD. SopD2 is required for virulence as a mutant is impaired in SIF formation [69]. Like many SPI-2 effectors, the precise function of SopD2 is unknown.

SPI-2 effectors SpvB and SteC

Depending upon cell type, *Salmonella* begins replication about 2-6 hours after infection. Actin accumulates around the SCV (VAP phenotype) by a process requiring SpvB and SteC although a mutation in either of these effectors is still virulent. SpvB ADP-ribosylates actin and depolymerizes actin filaments when expressed in cultured epithelial cells [70]. SteC is a kinase and has homology to the human kinase Raf-1. SteC kinase activity causes extensive rearrangement to the F-actin cytoskeleton in both transfected and infected fibroblasts [71].

Replication within the spleen

The SCV progressively fills with bacteria until they appear as large cytoplasmic holes filled with bacteria, but infection of neighboring, non-infected cells is not well understood. Detailed studies using specific sequence tags have examined the systemic spread of virulent *Salmonella* bacteria within the spleen. It was observed that an individual bacterium developed into a small, localized colony of infected cells suggesting that adjacent cells take up bacterial projeny once the original infected cell died. The bacteria then spread to areas distant from the initial colony suggesting that there may be an additional mechanism of dissemination, perhaps by carriage within phagocytic cells [72]. Not all interactions between *Salmonella* and phagocytic cells are successful as about 5-10% of infecting bacteria are non-replicating, found in tight vesicles, and cannot form colinies is re-isolated. These bacteria may be inactivated by DNA damage that specifically introduces a cross-link between the Watson and Crick strands of DNA. Such damage is not efficiently repaired in bacteria even though they remain metabolically active ([73]; D. Holden, pers. Comm.).

Infected epithelial and phagocytic cells undergo apoptosis and pyroptosis, respectively

Salmonella infected epithelial cells undergo apoptosis 12-18 hours after bacterial entry. Apoptosis is characterized by cytoplasmic and nuclear condensation, DNA cleavage, and maintenance of an intact plasma membrane. Caspases 8, 9, and 3 mediate apoptosis and are activated in response to ligation of cell surface death receptors. Conversely, infected macrophages undergo a different program of host cell death called pyroptosis. Pyroptosis is mediated by the caspase-1-dependent formation of membrane pores which causes loss of ionic equilibrium, water influx, swelling and osmotic lysis. Caspase-1 also triggers DNA cleavage and the release of pro-inflammatory cytokines IL-1β and IL-18. In this case the inflammasome is activated by flagellin release to the cytoplasm and stimulation of the NOD like receptor IPAF (reviewed in [74]). From a teleological standpoint cells may prefer death rather than infection as death removes an replicative niche.

Following infection, the cell can be considered to be at an unstable equilibrium where it survives and mounts an active inflammatory response or undergoes cell death [75,76]. There is little doubt that critical determinants of *Salmonella* pathogenesis reduce the expression of pro-inflammatory pathways that would lead to cell death however mutations with this phenotype have not yet been identified. What is clear is that *Salmonella* manipulates particular aspects of both the innate and adaptive immune systems to its advantage.

Salmonella manipulates particular aspects of innate and adaptive immunity

NF-κB is targeted by multiple *Salmonella* effectors

Many SPI-1 effectors are pro-inflammatory, and those phenotypes were described earlier. Importantly, they induce chemokine and cytokine secretion that recruit professional phagocytes, which serve as reservoirs for *Salmonella* replication. However, at least two SPI-1 effectors possess anti-inflammatory phenotypes. First, SptP GAP activity antagonizes the pro-inflammatory GEF mimicry of SipA, SopE, and SopE2 [28].

Second, SopB activates Akt1 which may prevent apoptosis of epithelial cells following infection (reviewed in [77]).

Central to many inflammatory responses is NF-κB, a protein complex that controls the transcription of many genes necessary for the inflammatory response. It is activated in response to stress, cytokines, and bacterial antigens among others (reviewed in [78]). Not surprisingly, four *Salmonella* effectors are known to inhibit NF-κB activation: AvrA, SseL, SspH1, and SrfH (SseI). AvrA is secreted by both SPI-1 and SPI-2 TTSS [29], and it deubiquitinates and stabilizes IκBα and β-catenin in epithelial cells. This activates β-catenin while inhibiting NF-κB activation and apoptosis [79]. AvrA also has acetyltransferase activity towards MAPK kinases MKK4 and MKK7, which potently inhibit JNK signaling and apoptosis [80]. AvrA is highly conserved among Gram negative pathogens, and it was first identified as an anti-virulence factor in the plant pathogen *Pseudomonas syringae*. Plants directly recognize this effector by a receptor similar to mammalian NLR. Recognition stimulates the plant to drop an infected leaf [81]. SspH1 is secreted by both the SPI-1 and SPI-2 TTSS. SspH1 is a ubiquitin ligase of PKN1[82], a protein kinase involved in the NF-κB pathway that is activated upon cell infection. However, SspH1 activity is not thought to cause PKN1 degradation because the interaction between SspH1 and PKN1 in mammalian cells leads to activation of the kinase and subsequent inhibition of NF-κB signaling [83]. SseL and SrfH are both secreted by the SPI-2 TTSS. SseL suppresses Iκ-Bα activation and degradation by deubiquitinating it before it can be degraded by the proteosome, a mechanism strikingly similar to AvrA. In fact, mice infected with an *sseL* mutant mount stronger inflammatory responses than those infected with the parent strain [84]. This difference in response may have important consequences for vaccine design because immune responses can be tailored by the presence or absence of effectors that modulate inflammation. Finally, SrfH inhibits NF-κB signaling downstream of NOD1 and NOD2, but the mechanism is not understood (D. Philpott, pers. Comm).

Major histocompatibility complex (MHC)

Salmonella alters antigen presentation pathways by multiple mechanisms. The classical MHC class I pathway of antigen processing and presentation is present in nearly all cell types. Foreign protein in the cell cytoplasm is degraded to peptides in the

proteosome, transported to the ER via TAP, loaded onto MHC-I, and then transported to the cell surface. *Salmonella* inhibits MHC-1 presentation in infected intestinal epithelial cells but not macrophages. The precise mechanism is not known, but non-infected cells were capable of MHC-I antigen presentation suggesting that this was an active process [85].

The MHC class II pathway is present in only a few specialized cell types: macrophages, B cells, and dendritic cells. Peptides presented by MHC-II molecules are derived from extracellular proteins. As a result, peptide loading occurs by a different mechanism. Extracellular proteins are endocytosed, traficked to lysozomes, and processed to peptides by cathepsin. MHC-II is loaded with invariant chain in the ER, traffics to vesicles containing antigen, antigen replaces the MHC-II invariant chain, and the complex traffics to the cellular membrane [86]. Following *Salmonella* infection there is a reduction in MHC-II surface expression that is concomitant with SPI-2 dependent ubiquitination of MHC II molecules. This post-translational modification led to removal of mature, peptide loaded αβ dimers from the cell surface and affected all class II isotypes similarly [87]. Furthermore, class II antigen processing and presentation is down regulated by the SCV itself because it is a privileged site that avoids trafficking to MHC-II compartments (reviewed in [88]).

Effectors that specifically interfere with MHC presentation have not been characterized, but a screen for effectors that inhibited MHC-1 and MHC-2 antigen presentation identified SifA, SspH2, SlrP, PipB2, and SopD2, whereas SseF and SseG contributed to a lesser extent to this phenotype [89]. Since many of these effectors are required for efficient SCV biogenesis, it's unclear how they could directly interfere with antigen presentation. Some of them may have been selected because of intracellular growth defects.

Dendritic, T, and B cells

Clearance of a *Salmonella* infection requires CD4 and CD8 T cells and B cells. An adaptive immune response to injected antigens or *Listeria* can typically be observed after about 4-7 days in the mouse and perhaps 7-10 days in humans. In contrast, the T cell response from *Salmonella* infection is delayed or weak [12]. Manipulation of antigen

presentation does not solely account for these observations because *Salmonella* targets multiple arms of the adaptive immune response as described below.

Three signals are necessary for optimal stimulation of T cells - engagement of the T cell receptor and co-receptor and cytokines that determine the outcome of T cell differentiation. Cytokines are produced as a consequence of PAMP-receptor interaction: TLR, NLR, and others. Cytokines act in both an autocrine and paracrine fashion ensuring that infection will activate antigen presenting cells (APC). Dendritic cells (DC) are the initial APC of the immune system and possess the unique ability to stimulate naïve T-cells directly. DC express a variety of cytokines that aid in tailoring the immune response to the infecting pathogen, and multiple DC subsets further refine the response [86]. To mount an effective adaptive immune response, *Salmonella* proteins must be processed and presented by DC to naïve T cells in secondary lymphoid organs. It has recently been shown that *Salmonella* kills a subset of DC ($CD8alpha^{+}$), which may create a more favorable environment for *Salmonella* to persist. The mechanism by which DC are targeted is not yet known [90].

T cells are distinguished by two specific surface glycoproteins, CD4 and CD8, that recognize antigen presented by MHC-II and MHC-I, respectively. Following the initial activation and replication phase, $CD8^{+}$ cells become cytolytic T lymphocytes (CTL). They act to kill cells infected with virus or intracellular pathogens if they present antigen on MHC-I molecules. Conversely, $CD4^{+}$ helper T cells are composed of at least five, specialized sub-classes that respond in different ways to infection [86]. At least two of these sub-classes are important during *Salmonella* infection, Th1 and Th17. Clearance of *S*. Typhimurium requires a Th1 response for phagocyte and T cell activation. Naïve CD4 T cells develop into Th1 cells in response to IL-12 and they secrete IFN-γ as an effector cytokine. In mice clearance requires production of IFN-γ by Th1 cells (12, 13). Similarly, human patients with genetic deficiencies in IFN-γ and IL-12 receptor signaling, or receiving anti-IL-12 therapy, display increased susceptibility to *Salmonella* infection (14, 15, 16), indicating that Th1 responses are necessary for clearance, if not sufficient, in human salmonellosis. Th17 have a different function. Th17 cells associate with the skin and GI tract and are positioned to attack bacteria and fungi at those locations by secreting defensins and IL-17, a cytokine that recruits neutrophils and T cells. SIV infection in

rhesus macaques depletes Th17 cell populations. Not surprisingly, co-infection with *Salmonella* resulted in a lower inflammatory response in the bowel and increased dissemination of bacteria [91]. These findings suggest that Th17 cells are required for an appropriate inflammatory response. It also provides insight on why *Salmonella* infection is a leading cause of death in HIV infected people in sub-Saharan Africa as these individuals likely have similar, weakened immune responses.

Two different approaches have been used to study how *Salmonella* infection impacts T cell activation and replication – *in vitro* and *in vivo*. *In vitro* studies showed that T cells failed to replicate upon contact with infected cells. When infected APC were exogenously loaded with ova peptide, ova-specific T cells still failed to replicate [92]. As a result, *Salmonella* infection of an APC may have prevented T cell activation. In a different set of experiments, *Salmonella* was co-cultured with T cells. An unidentified *Salmonella* protein was secreted into the media and down-regulated expression of the T cell receptor ß-chain, suggesting that extracellular bacteria prevented T cell activation by an alternative mechanism [93]. The *in vivo* approach in mice produced a different set of results. Injection of live or heat killed *Salmonella* resulted in immediate activation of *Salmonella* specific CD4 T cells, as judged by CD69 expression. However, in mice infected with live *Salmonella*, the activated T cells were lost after a few days suggesting that they were depleted as a consequence of infection. Therefore, these CD4 cells were unable to enter the memory pool or become effector cells. CD4 depletion was independent of T cell antigen specificity but required the SPI-2 TTSS [94] (McSorley Pers. Comm.). Since this observation was dependent upon SPI-2, we speculate that a SPI-2 effector may explain these results.

In contrast to T cells and dendritic cells, B cells are not known to be selectively culled by *Salmonella*. B cells take up antigen via cell membrane immunoglobin molecules, process them onto MHC-II molecules, and present them to CD4 T cells. In turn the T cell stimulates the B cell to become a mature, antibody secreting plasma cell [86]. The strongest antibody responses are to lipopolysaccharide, flagella, cell surface proteins such as porins, and other proteins expressed at high levels [95](McSorley, pers. Comm.).

Research objectives

Clearly, there is a lack of understanding in the *Salmonella* field regarding the mechanisms of many secreted effectors. Moreover, in some cases there are phenotypes for which SPI-2 type III secretion is required but the associated effector is not known. Further research into *Salmonella* pathogenesis will undoubtedly lead us into new and unexpected directions. My thesis addresses these two major questions as follows. My first topic was to define a more specific mechanism for the rapid septicemia phenotype while my second task was the identification of novel effectors.

Chapter 2

Salmonella Typhimurium Disseminates within its Host by Manipulating the Motility of Infected Cells

Micah J. Worley, George S. Niemann, Kaoru Geddes, and Fred Heffron

Contributions to this manuscript

Yeast two-hybrid assays

Rapid septicemia experiments

Department of Microbiology and Immunology, Oregon Health and Science University, Portland, OR

Published in PNAS November 2006, vol. 103, no. 47, pp. 17915-17920

Abstract

The mammalian host has a number of innate immune mechanisms designed to limit the spread of infection, yet many bacteria, including *Salmonella*, can cause systemic disease. *Salmonella typhimurium*-infected phagocytes traverse the gastrointestinal (GI) epithelium and enter the bloodstream within minutes after ingestion, thereby spreading throughout its host. Here, we provide a cellular and molecular basis for this phenomenon. We demonstrate that *S. typhimurium* manipulates the migratory properties of infected GI phagocytes with a type III secretion system. We show that one secreted effector, SrfH, interacts with the host protein TRIP6, a member of the zyxin family of adaptor proteins that regulate motility. SrfH promotes phagocyte motility *in vitro* and accelerates the systemic spread of infection away from the lumen of the intestine in the mouse. This is a previously uncharacterized mechanism by which an intracellular pathogen overcomes host defenses designed to immobilize infected cells.

Introduction

Numerous intracellular pathogens must breach epithelial barriers, navigate the lymphatic system, and travel considerable distances to reach their preferred sites of replication within a host. For enteric pathogens, in addition to the physical barrier that the gastrointestinal (GI) epithelium provides, microbes must also contend with a brush border, a thick mucus coat, an acidic environment, peristalsis, antimicrobial peptides, cell turnover, and endogenous flora. GI phagocytes can serve as vehicles for microbial dissemination into deeper tissue: they readily engulf microbes and can traverse epithelial barriers and inadvertently shield pathogens from other components of the immune system. However, when phagocytes internalize Gram-negative bacteria, their LPS binds Toll-like receptor 4, triggering the release of macrophage migration inhibition factor and other cytokines that strongly inhibits their motility [96,97]. Additionally, the best-characterized route for tissue phagocytes to reach the bloodstream is through the lymphatic system, and recirculation normally requires between 12 and 20 h [98-100]. Thus, it is remarkable that *Salmonella* Typhimurium- and *Salmonella* Typhi-infected phagocytes can enter the bloodstream within as little as 15 min after ingestion [9,10].

S. Typhimurium penetrates to deeper tissue through two different pathways. In one route, the bacteria access systemic tissue by the lymphatic system and the Peyer's patches. In the second pathway, phagocytes are believed to carry intestinal bacteria directly into the bloodstream without passing through the Peyer's patches [9,10,101-103]. After ingestion, bacteria reach systemic organs in <15 min in this pathway vs. ~24 h by the lymphatic system [9]. The bacteria are carried within CD18-expressing cells thought to be monocytes [104]. Movement of bacteria-infected cells requires not only stimulation of cell motility but also inhibition of the inflammatory pathways that would normally block this motility [105]. Thyroid receptor interacting protein 6 (TRIP6; ref. [106]) is an adaptor protein that binds components of the Rac signaling pathway, critical for cell motility, and the NF-κB inflammatory pathways [107-111]. Thus, *Salmonella* effector interaction with TRIP6 might alter both the inflammatory response to infection as well as the motility of an infected cell, as described below.

Salmonella enterica virulence is mediated in part by the passage of proteins to the host through one or more type III secretion systems [112]. Few of the type III secreted

proteins have been characterized with respect to their mechanism of action. In this work, we describe how one such effector, SrfH, alters cell motility. This is a new and unexpected function for a type III secretion system, suggesting that *Salmonella*, and perhaps other intracellular pathogens, direct their course of infection by controlling the migratory properties of the host cells harboring them.

Results

SrfH is a secreted type III effector that binds the LIM (Named for Lin-11, Isl-1, and Mec-3) domains of TRIP6

We recently identified *srfH/sseI* (SsrB regulated factor H/*Salmonella* secreted effector I), a chromosomal gene associated with SPI-2 whose expression is induced nearly 100-fold inside macrophages [113,114]. SrfH shares no homology with any database entries outside of its N-terminal sequence and possesses no conserved catalytic motifs, suggesting a unique function for the protein. We confirmed a report [115] that SrfH is secreted by SPI-2 across the vacuolar membrane after invasion [29]; however, it plays no role in promoting intracellular proliferation rendering its function enigmatic (data not shown) [113].

To delineate SrfH's role within infected host cells, we used *srfH* as the “bait” in a yeast two-hybrid screen of a human cDNA library. Of approximately one million yeast transformants screened, only two contained host peptides that interacted significantly with SrfH, both of which contained LIM domain fragments of TRIP6 (Fig. 2-1A). Despite their similarities, SrfH does not interact with other members of this adaptor family (Fig. 2-1B).

To support the relevance of the SrfH/TRIP6 binding, we conducted additional experiments. Transient transfection of RAW264.7 cells with a hybrid SrfH-GFP protein shows localization to the membrane and to focal adhesions. When these same cells are stained with anti-TRIP6 antibody, they show >90% colocalization of the two proteins within macrophages (Fig. 2-2 Upper). Transfection with a mammalian vector expressing GFP alone does not show colocalization with TRIP6 (Fig. 2-2 Lower). As shown in Fig. 2-2 lower left, staining with anti-TRIP6 antibody exhibits a characteristic punctate pattern that is diffusely spread across the cytoplasm, similar to staining observed in previous studies [110]. After SrfH transfection, TRIP6 relocalizes to the cellular cytoskeleton (Fig. 2-2. Upper). It is noteworthy that cells transfected with a mammalian vector expressing SrfH show ruffling patterns consistent with those seen after stimulation of the Rac signaling pathway (Fig. 2-2) [116], which is the major signal transduction pathway activated in cellular movement. In summary, the *Salmonella* secreted effector SrfH and

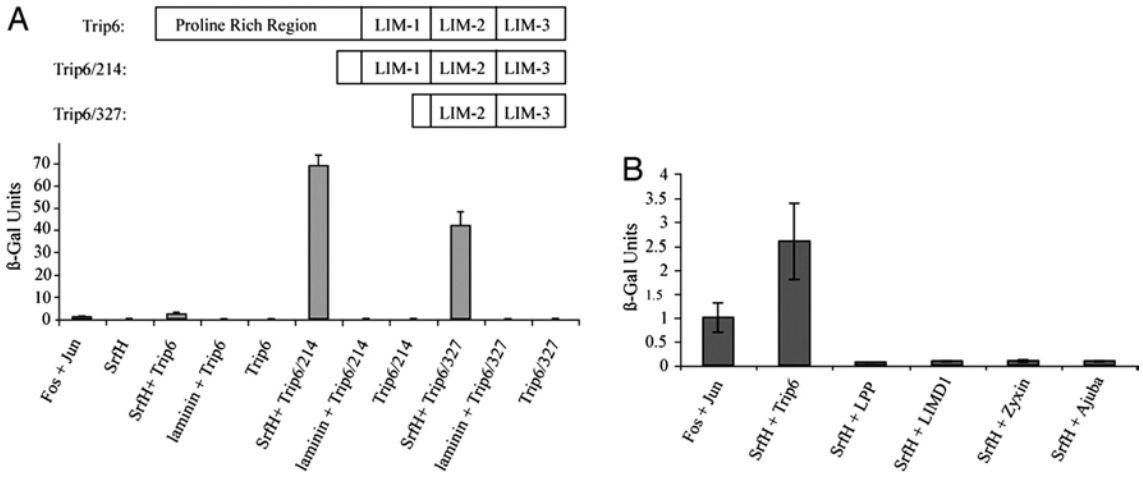

Fig. 2-1

Salmonella SrfH binds the adaptor protein TRIP6 in a yeast two-hybrid assay. (A) Yeast two-hybrid screen for SrfH interacting proteins. β-Gal assays were carried out on the indicated yeast cells. The level of β-gal expression is a measure of the strength of the binding. Fos + Jun are the c-Fos and c-Jun interacting partners used as a positive control. Laminin interaction is the negative nonspecific control. The TRIP6 fragments first identified contain the C-terminal LIM domains of TRIP6 starting from the amino acids indicated and thus contain either two or three LIM domains. Additional controls are shown. (B) SrfH interactions with LIM domain proteins. SrfH does not interact with any of the other zyxin family members in the yeast two-hybrid assay. Error bars in Figs. 1–6 represent the standard error of the mean.

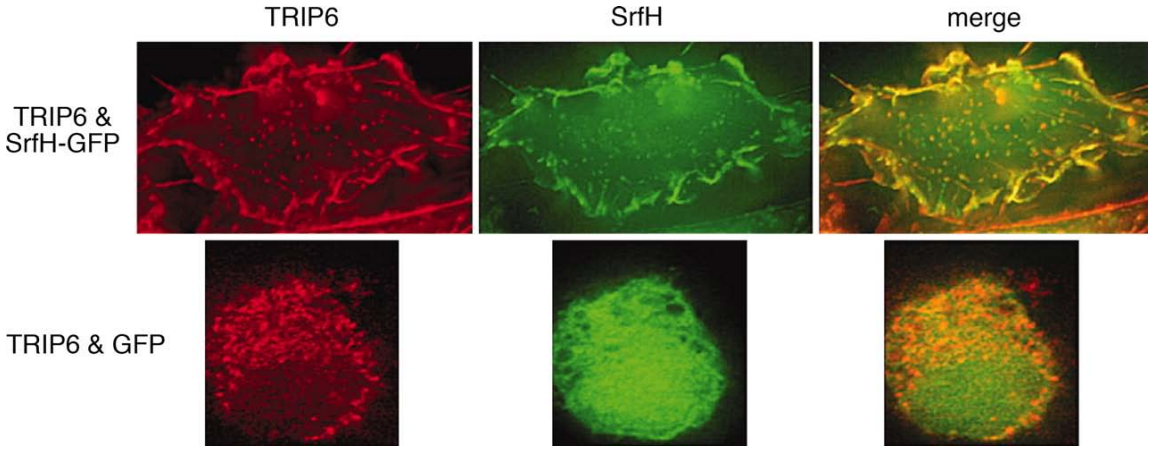

Fig. 2-2

Evidence for SrfH/TRIP6 interaction. (Upper) Micrograph of RAW264.7 macrophages transfected with srfH-GFP and then analyzed to determine whether SrfH and TRIP6 colocalize. TRIP6 is stained with Texas red-labeled anti-TRIP6 antibody, whereas GFP is present as a translational fusion with SrfH. (Lower) Cells transfected with the same mammalian vector but expressing GFP alone and stained as in Upper for TRIP6.

mammalian adaptor protein TRIP6 interact; however, because there are >250 LIM-domain-containing proteins, we cannot rule out interaction with additional proteins. Further experiments that describe the nature of the TRIP6/SrfH interaction in detail will be published separately.

SrfH stimulates phagocyte migration

Given that TRIP6 is an adaptor in a pathway that can stimulate cellular motility and that knockdown as well as overproduction of TRIP6 alters cellular motility [109-111], we hypothesized that SrfH promotes the motility of infected phagocytes. To test this possibility, RAW264.7 macrophage-like cells and JAWS dendritic-like cells (both are $CD18^{+}$) were infected with either wild-type *S.* Typhimurium 14028s or an isogenic *srfH* mutant at a multiplicity of infection of 0.1 [114]. After the initial infection period, all extracellular bacteria were removed by washing and treatment with gentamicin [117]. The ability of the infected macrophages to chemotax was determined in a modified Boyden chamber (Chemotax System; Neuro Probe, Gaithersburg, MD). Boyden chambers are composed of two compartments separated by a hydrophobic filter that contains small holes. Macrophages are cultured in the top compartment, and various macrophage chemoattractants may be placed in the bottom compartment. The number of cfus reaching the bottom compartment was used to measure macrophage migration. The gentamicin-containing media in the bottom compartment were shown to be free of viable extracellular bacteria. We found that significantly more macrophages or dendritic cells infected with wild-type *S.* Typhimurium migrated than these same cells types infected with an isogenic *srfH* mutant (Fig. 2-3A and B). Furthermore, SrfH expression in trans complemented a *srfH* mutant phenotype (Fig. 2-3A). Taken together with the results of the previous studies, these data indicated a role for SrfH in promoting the motility of infected cells, which may be a direct consequence of SrfH's interaction with TRIP6. However, these findings do not exclude the possibility that SrfH affects the motility of infected macrophages through an indirect mechanism requiring expression of additional effectors.

To establish whether SrfH was sufficient for increased macrophage motility, we expressed SrfH within the macrophage cytosol in the absence of any other bacterial components and assayed for induction of macrophage motility. Separate populations of

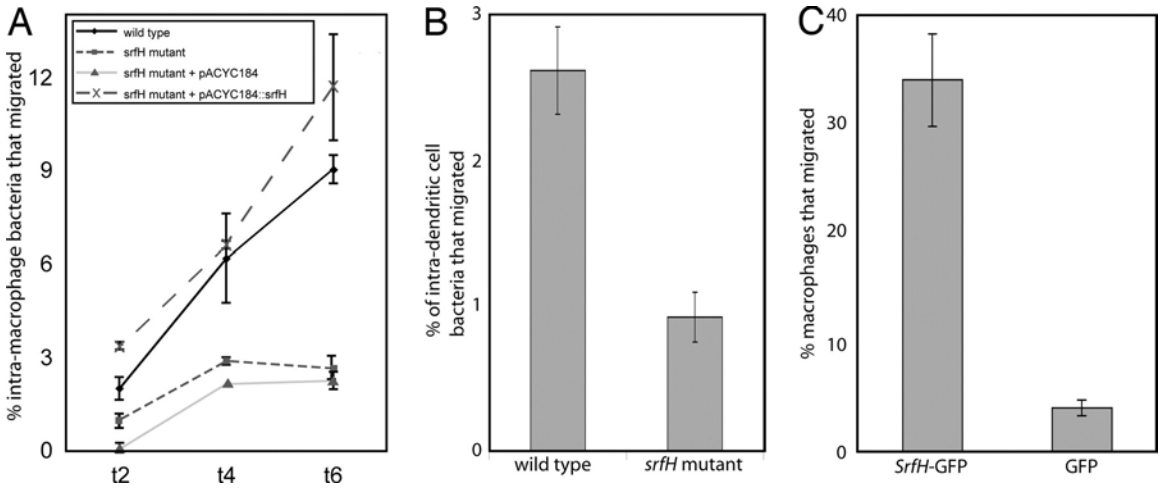

Fig. 2-3

Measurement of infected cell migration in a Boyden chamber. (A) Washed bacteria were used to infect RAW264.7 bacteria at a multiplicity of infection of 0.1–0.2, treated for 1 h with 100 μgm/ml gentamicin to kill extracellular bacteria, and placed in the top well of the Boyden chamber. At the times indicated, the cells in the bottom reservoir were lysed and the number of infected cells that migrated determined by plating and counting cfus. In the experiments shown, heat-treated Salmonella was used as a chemoattractant. Gentamicin (at 10 μg/ml) was used throughout the experiment to kill any released bacteria. Cell migration of infected RAW264.7 cells was stimulated by infection with srfH + *Salmonella* but not srfH −. SrfH, supplied in trans, complemented a srfH mutation. (B) Similar experiments were carried out by using the JAWS dendritic cell line with very similar results. The 6-hr time point is shown. (C) SrfH alone stimulates cell motility. RAW264.7 macrophages were transfected with a mammalian vector expressing SrfH-GFP or GFP alone. Six hours later, cells were removed and the number of fluorescent cells in the bottom reservoir counted in the microscope.

macrophages were transfected with either a plasmid expressing SrfH-GFP or a plasmid expressing GFP alone. More macrophages expressing SrfH-GFP migrated than the group expressing only GFP (Fig. 2-3C).

SrfH has no effect on host-cell movement in the absence of TRIP6

We next assessed the degree to which the *srfH* phenotype depends on TRIP6 expression. It was established that TRIP6 levels could be greatly reduced when the corresponding transcripts were targeted with small interfering RNA (siRNA). Macrophages were transfected with either nonsilencing or silencing TRIP6 siRNA. Subsequently, the cells were infected with either the *srfH* mutant or the wild-type *Salmonella* strain. When TRIP6 expression was blocked with siRNA, macrophages harboring either type of bacteria migrated almost identically (Fig. 2-4B). In contrast, when macrophages were transfected with nonsilencing siRNA, SrfH conferred an ~5-fold increase in macrophage motility, similar to what was observed in Fig. 2-3. Overall, the results of this experiment suggest that SrfH manipulates macrophage motility by interacting directly with the adaptor protein TRIP6. The finding that blocking TRIP6 expression resulted in increased cell motility is in agreement with others [111]. We hypothesize that TRIP6 inhibits cell migration and that the binding of SrfH to TRIP6 blocks this inhibition.

***S.* Typhimurium travels directly from the GI tract to the bloodstream within $CD18^+$ phagocytes**

Because SrfH is able to promote macrophage movement *in vitro*, we hypothesized that in an infection model, SrfH expression would correlate with a rapid appearance of *S.* Typhimurium-infected phagocytes in the bloodstream in a mouse infection [9,10]. During short time periods, *S.* Typhimurium travels from the murine lumen of the intestine into the bloodstream within GI phagocytes [9]. In $CD18^-$ mice, phagocytes cannot efficiently traverse the GI epithelium [9,118,119]. CD18 is an integrin specific to immune system cells that facilitates leukocyte transmigration and is present on the professional phagocytic cells: neutrophils, macrophages, and dendritic cells. Ten $CD18^-$ mice were inoculated with 1×10^9 *S.* Typhimurium by gavage. Thirty minutes postinfection, we did not recover any viable bacteria from their peripheral blood (Fig. 2-5A). This was not because of increased killing of intracellular bacteria, because CD18-deficient

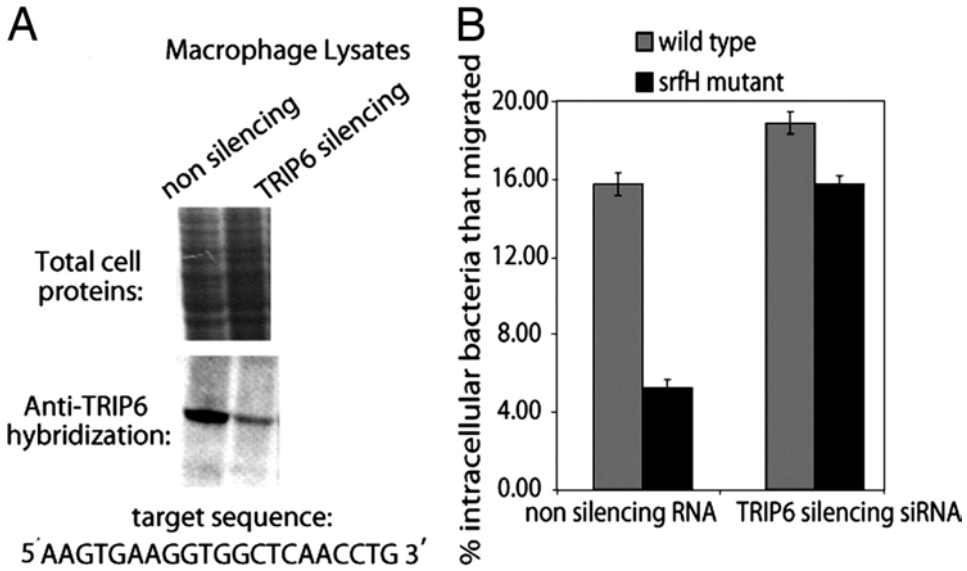

Fig. 2-4

Reducing the expression of TRIP6 by siRNA reduces the effect of SrfH on cell motility. (A) (Upper) Total proteins expressed by RAW264.7 treated with siRNA (Right) or an irrelevant siRNA (Left). (Lower) Western hybridization of the same gel probed with anti-TRIP6 antibody. TRIP6 expression was reduced by >95% with siRNA. (B) TRIP6 was required for SrfH to affect cell motility. Left-hand bars compare cell migration when RAW264.7 cells were treated with randomized control siRNA. Right-hand bars compare cell migration when RAW264.7 cells were treated with TRIP6 siRNA. RAW264.7 cells treated with TRIP6 siRNA show no difference in cell migration ± srfH.

macrophages are less microbiocidal to *S.* Typhimurium than are congenic control macrophages [9,104]. Thus, it was concluded that *S.* Typhimurium travels from the GI tract to the bloodstream exclusively inside of $CD18^+$ phagocytes in the short time frame used in this study. This finding allowed us to examine how various bacterial mutations may impact the migration of these cells.

SrfH accelerates entry of *S.* Typhimurium to the bloodstream

To determine whether SrfH accelerates the rate at which infected phagocytes travel from the lumen of the intestine into the bloodstream, we introduced either wild-type *S.* Typhimurium or the *srfH* mutant into mice by oral gavage (1×10^9). Thirty minutes after inoculation, an average of five times more wild-type *S.* Typhimurium than *srfH* mutants were recovered from the bloodstream (Fig. 2-5A). When the *srfH* mutation was complemented by SrfH expression in *trans* from a multicopy plasmid, the complemented mutant showed an even higher level of bacteria than that seen with wild-type *S.* Typhimurium (Fig. 2-5A). Each of these experiments was carried out with groups of five mice on seven separate occasions. In a dissemination assay with a *Salmonella* strain defective in all SPI-2-dependent type III secretion (*ssaK*::*cm*), no mutant bacteria were recovered in 18 of 25 mice intragastrically infected with the *ssaK* mutant. Thus, the phenotype of a complete knockout of the SPI-2 type III secretion systems is much stronger than the *srfH* mutation alone, which suggests that additional effectors are used during the course of infection in the mouse.

To establish whether the accelerated bacteremia resulted in accelerated colonization of internal organs, we assayed the number of bacteria in the spleen and liver, preferred sites for *Salmonella* replication, 24 h after oral inoculation. At 24 h, SrfH increased the rate at which *S.* Typhimurium colonized both the liver and spleen by an order of magnitude (Fig. 2-5B). The rapidity with which mouse infection was observed was surprising given the fact that previous studies suggested that expression of SPI-II and its effectors is delayed for hours *in vitro* (see ref. [120] for discussion). This conundrum has been resolved by direct assays for SPI-2 expression within ligated mouse ileal loops, which demonstrated rapid expression in the gut [120]. In fact, constitutive expression of SrfH did result in increased bacteremia after gavage. Thus, SrfH expression may limit the level of infection (Fig. 2-5A). In summary, after *Salmonella* Typhimurium 14028 oral

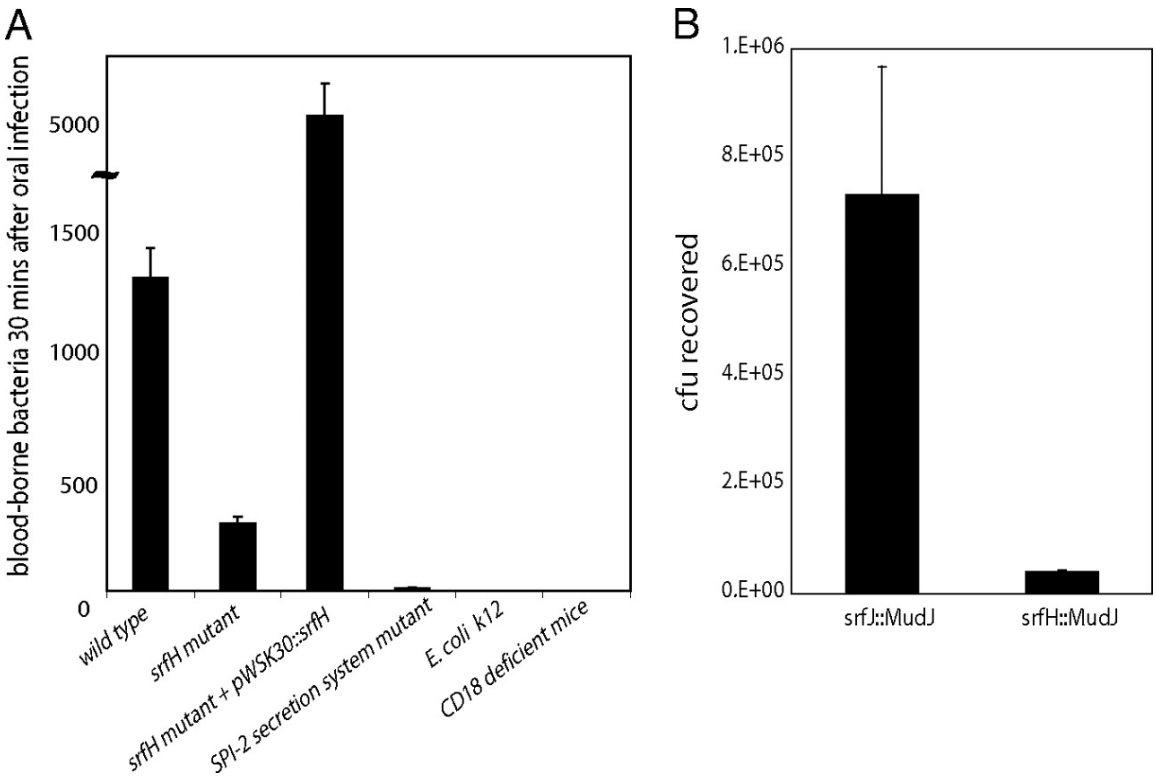

Fig. 2-5

Salmonella septicemia is observed 30 min. after oral infection of the mouse. (A) The number of bacteria recovered by cardiac puncture 30 min after oral infection with 1×10^9 bacteria of the strains indicated. The first two bars show that five times more wild-type *S.* Typhimurium was recovered than in an isogenic srfH mutant. The results shown are for BALB/c mice, and the error bars represent the standard error of the mean. The third bar shows the number of bacteria recovered for SrfH expression in trans from a multicopy plasmid. The y axis is discontinuous, so that the phenotypes could be displayed on the same graph. The fourth bar represents bacteria recovered for a SPI-2 type III secretion mutant (ssaK::cm). As a control, mice were inoculated with E. coli K12 at 10 times the dose used with *S.* Typhimurium, and no bacteria were recovered from the bloodstream. The last bar shows that no wild-type bacteria were recovered from $CD18^-$ mice inoculated with 1×10^9 bacteria. (B) The number of bacteria recovered from the spleen and liver 24 h after oral infection with either a srfH mutant or an arbitrary MudJ insertion that does not affect virulence (srfJ; ref. 41). Wild-type *S.* Typhimurium 14028 gave the same numbers as the srfJ mutation that is shown. A MudJ insertion is displayed based on concern that bacteriophage Mu might alter the phenotype of *Salmonella*.

infection of mice, at least one organism in one million inoculated traveled to the bloodstream within minutes.

As further verification that the bacteria are present within cells in the bloodstream, we performed FACS analysis of infected white blood cells isolated from *Salmonella*::GFP orally infected mice (Fig. 2-6). Most of the bacteria were present within monocytes (GR-1^+/CD11b^+), corroborating earlier observations [104], and the number of infected cells closely paralleled the number of cfu recovered in the previous experiment (Fig. 2-5A).

Bacteria are not killed in transit to the bloodstream

One concern we had at the outset was that the reduced numbers of mutant bacteria that reach the bloodstream was a consequence of bacterial death in transit and not a difference in infected cell motility. To investigate this possibility, we developed a more sensitive PCR assay for the presence of live or dead bacteria. The assay is based on incorporating a high copy number plasmid into the bacteria to provide a PCR template that is not readily degraded and can be easily detected. In our assay, we purified plasmid DNA from infected mouse blood, relying on its structure as a closed circular molecule, and then used the purified plasmid DNA to template PCR. In control experiments, we could detect even a single heat-killed bacterium in 1 ml of blood (data not shown). No bacteria were recovered by plating or PCR in dissemination experiments with *Escherichia coli* K12, a nonpathogenic relative of *S.* Typhimurium. To determine whether *ssaK* mutant bacteria were being killed during the short time period of this assay, we repeated the more sensitive PCR experiments. We could not detect live or dead bacteria within the bloodstreams of 10 additional mice that were inoculated with 1×10^{10} SPI-2 secretion mutant bacteria, 10 times the original inoculum used. Therefore, the earlier recovery of a few bloodstream bacteria in 7 of 24 mice inoculated with the type III secretion systems structural mutant was likely the result of abrasion by the gavage needle. To summarize, we verified that phagocytes did not kill *ssaK* mutants in transit (data not shown). Because SPI-2 genes mediate neither GI tract survival (data not shown) nor adherence and uptake by phagocytic cells (data not shown), the results imply that SPI-2 secretes additional effectors that manipulate cellular motility.

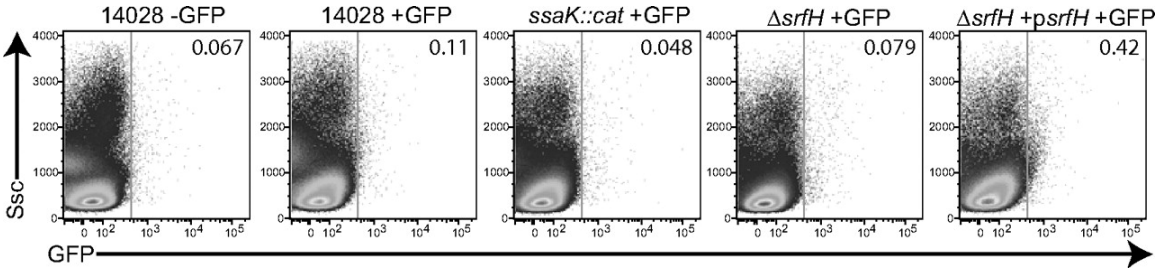

Fig. 2-6

Blood from mice orally infected with 1×10^9 CFU of GFP expressing *Salmonella* analyzed by FACS. GFP fluorescence vs. side scatter is shown in the scatter plots. Mice were inoculated IG with the *Salmonella* strain indicated above each image, and the percentage of GFP positive cells found in the bloodstream 30 min post inoculation is indicated in the upper right corner of each plot. Results are shown for pooled blood from three mice. An LSRII (Becton Dickinson) FACS analysis machine equipped with a 488-nm laser was used to detect GFP-expressing bacteria in infected peripheral blood cells. FACS data were analyzed by using FlowJo software (Tree Star).

Discussion

Our results show that SrfH is responsible for accelerating the movement of infected $CD18^+$ cells from the lumen of the intestine to the liver and spleen, which are the preferred sites for *Salmonella* replication. Partial experimental support for a direct interaction between SrfH and TRIP6 is provided but will be considered in detail in a later publication. Results from the Boyden chamber assays show that SrfH expression in infected cells is both necessary and sufficient for an increase in macrophage and dendritic cell motility. Most important, infection of mice with wild-type *Salmonella*, but not the *srfH* mutant, resulted in the presence of infected cells in the bloodstream within minutes. These bacteria are carried exclusively within $CD18^+$ cells: in mice lacking these cells, bacteremia takes place by a different route and is delayed many hours. *SrfH* does not affect bacterial adherence, cell invasion, survival within the intestine, or replication within macrophages, dendritic cells, or epithelial cells (data not shown and ref. [114]. Our data support the hypothesis that SrfH alters the motility of infected cells by its interaction with TRIP6.

TRIP6 functions in both inflammatory and cell motility pathways

TRIP6 is an adaptor that interacts with components of inflammatory pathways as well as the Rac pathway for cell motility [108-111,116]. Professional phagocytic cells chemotax toward infecting microbes, limiting the spread of infection by destroying the invading microbe and initiating the adaptive immune response. They are directed along a concentration gradient of bacterial products but stop at the site of infection. This must require a complex interaction between the Toll-like receptor pathways and the Rac cell motility pathway [111]. In the macrophage-like cell we have studied, reducing expression of TRIP6 stimulates motility of the infected cells, thus TRIP6 must be acting as a brake to inhibit infected cells from disseminating, and SrfH, in effect, removes the brake (our results; ref. [111]).

Antigen sampling and bacterial infection

Numerous intracellular pathogens can traverse epithelial barriers and disseminate within hosts with surprising speed. Accordingly, it has long been speculated that phagocytes might inadvertently spread such pathogens as part of a host-specified antigen-sampling pathway [9,121]. However, our results suggest that *S.* Typhimurium uses the

SPI-2 encoded type III secretion systems to stimulate infected GI phagocytes to carry them across the epithelium. This allows *Salmonella* to bypass the lymphatic system and penetrate the bloodstream, thereby accelerating the colonization of internal organs. This study provides one of the first descriptions of a virulence mechanism in which a pathogen directly alters the motility of infected host cells for its own benefit.

A common virulence strategy

The manipulation and subversion of host cell motility is a virulence strategy likely to be used by other intracellular pathogens aside from *S.* Typhimurium. Because such pathogens must traverse the host integuments and move within the host to reach their preferred site(s) of replication, the manipulation and subversion of host cell motility is a virulence strategy likely to be used by other intracellular pathogens aside from *S.* Typhimurium. Thus, it is not surprising that *Yersinia enterocolitica* and Vaccinia virus alter the motility of infected cells [101-103,122]. For these pathogens, the proteins responsible have not yet been identified. However, such observations suggest that numerous infectious microbes subvert phagocytes as vehicles for their own intrahost dissemination. Thus, it is surprising that *srfH* shows a very limited distribution within *S. enterica* given the fact that many strains of *Salmonella* have the ability to disseminate rapidly within mice and humans and to reach the bloodstream within minutes after oral infection [10]. It is therefore likely that there will be additional genes identified encoding proteins with similar function but not necessarily sequence homology.

The immediate consequence of the presence of intracellular bacteria is to block the motility of infected cells by release of cytokines such as migration inhibition factor (MIF)[123,124]. MIF is also proinflammatory and a pivotal regulator of innate immunity (reviewed in ref. [125]). It follows that a mechanism to overcome this component of the innate immune system must be an essential virulence determinant of pathogens that cause systemic infection. The underlying microbial machinery may provide a new generation of antimicrobial targets as well as tools for delineating the molecular mechanisms responsible for cell movement.

Materials and methods

Bacterial strains, constructs, and media

S. Typhimurium 14028s and derivatives as well as cultured RAW264.7 macrophages from American Type Culture Collection were used throughout this study. Bacteria and tissue culture cells were grown as described [126]. An SPI-2 structural mutant was created by disrupting the chromosomal *ssaK* allele, as described [114]. For *in vitro* motility assays, complemented derivatives of 14028s *srfH*::MudJ (MJW704; ref. [114]) were generated. The *srfH* ORF and 65 bp of upstream sequence were PCR amplified, cloned into pWKS30 [127], and electroporated into MJW704. For transfection experiments, *srfH* was cloned into the eukaryotic expression vectors, pEGFP-N1.

General methods

All molecular biology and genetic manipulations were performed with established protocols [128,129]. Transfections were performed with Effectene for mammalian vectors and with HiPerFect for siRNA (Qiagen, Valencia, CA). Higher concentrations than specified by the manufacturer were necessary for macrophage transfection but did not appear to affect the viability of the transfected cells. Intramacrophage survival/growth assays were performed at an multiplicity of infection of ≤1 [130]. TRIP6 was identified as the binding partner for SrfH with the Hybrid Hunter yeast two-hybrid kit (Invitrogen, Carlsbad, CA), according to the manufacturer's instructions, using a commercial prey bank derived from HeLa cells (Invitrogen). β-Gal assays were performed on cultures grown overnight with rigorous shaking at 30°C according to the assay conditions provided with the Invitrogen kit.

Microscopy

Samples were fixed in 4% formaldehyde, permeabilized, and stained with a native TRIP6 antibody and an anti-mouse secondary conjugated to Texas red (Molecular Probes, Eugene, OR). SrfH-GFP 3D colocalization analysis was performed with the Applied Precision (Marlborough, U.K.) Deltavision image restoration system. Deconvolution using the iterative constrained algorithm of Sedat and coworkers [131] and image processing were performed on an SGI Octane workstation. Colocalization analysis was performed with the CoolLocalizer algorithm (CytoLight, Ann Arbor, MI), on sets of 99 z

sections captured from representative macrophages expressing both GFP and Texas red.

***In vitro* motility assays**

Macrophages were infected with bacteria grown to saturation and washed three times with PBS at a multiplicity of infection of 0.1–0.2. Bacteria were centrifuged onto the monolayers and incubated for 1 hr. Infected monolayers were then washed four times, for 5 min each wash. The extracellular bacteria were killed with a 1-hr incubation in DMEM supplemented with 100 μg/ml gentamicin [126]. The monolayers were washed as before and collected in 1.0 ml of DMEM containing 10 μg/ml gentamicin and 50 μl of this suspension added to the top of a 12-μM pore chemotaxis plate from the Chemotax system (Neuro Probe, Gaithersburg, MD). In some experiments, heat-treated *S.* Typhimurium (90°C for 10 min) from a saturated overnight culture (diluted 1,000-fold in DMEM augmented with 10 μg/ml gentamicin) was used as a chemoattractant (30 μl of this mixture in the bottom reservoir). Counting macrophages with a hemocytometer as well as counting bacteria after macrophage lysis determined migration. Transfection studies were performed similarly, except background migration was determined with mock-transfected macrophages and subtracted from the values presented.

Animal experiments

Four-week-old female BALB/c mice were used in all animal experiments except for those concerning CD18. For these, 8-week-old female C57BL/6J Itgb2 and C57BL/6J Itgb2$^{tm1/Bay}$ mice were used [119]. Mice were orally inoculated by gavage with 1×10^9 or 1×10^{10} bacteria. Thirty minutes after inoculation, mice were anesthetized and peripheral blood obtained by cardiac puncture. Host cells were lysed with 1% Triton and bacteria recovered on MacConkey agar plates. Bacteria were confirmed to be *S.* Typhimurium by their growth and appearance on MacConkey agar, and sensitivity to bacteriophage P22 and, where appropriate, by resistance to antibiotics. Bacterial survival within the GI tract and the ability of bacterial strains to colonize the spleen and liver were performed as described [132].

PCR and RT-PCR

pBluescript, which has a copy number of >300 per cell, was electroporated into the various strains to serve as a sensitive target that would allow us to detect the presence of dead bacteria in the bloodstream. The PCR primers are 5′-

CAAGGCGAGTTACATGATCCC and 5′-ACTGCGGCCAACTTACTTCTG. On two independent occasions, five mice for each strain tested were infected with ~1×10^{10} bacteria and, 30 min later, total blood was collected and combined. Any plasmid DNA present was purified with plasmid DNA isolation columns (Qiagen), and the total eluates were used as templates in standard PCRs. All strains were tested side by side, with the same primers.

siRNA studies

Macrophages were transfected with the TRIP6-specific siRNA construct shown in Fig. 2-4 or a randomized sequence containing the same base composition (Qiagen), washed 24 h later, and then incubated for an additional 24 h. At this time, the macrophages were infected with bacteria, and the motility assay was performed as previously described.

FACS analysis

Mice were inoculated IG with 10^8 bacteria. Thirty minutes after inoculation, mice were anesthetized, and cardiac punctures were performed. Blood samples from three mice were pooled, red blood cells lysed, and white blood cells collected by using a lympholyte gradient (Cedarlane Laboratories, Burlington, NC) and passed through a 70-μm cell filter (Falcon, Colorado Springs, CO). Cells were resuspended in PBS containing 2% FBS and 0.1% sodium azide, then analyzed by FACS. A LSRII (Becton Dickinson, Franklin Lakes, NJ) FACS machine equipped with a 488-nm laser was used to detect GFP fluorescence (>500,000 cells were analyzed per sample using FlowJo software; Tree Star, Ashland, OR).

Acknowledgments

We are indebted to Dr. Kim Saunders for invaluable help with animal experiments. We are grateful to Dr. Mary Beckerle and Dr. Richard Klemke for providing us with encouragement and insight, and to Dr. Mary Beckerle for providing the anti-TRIP6 antibody. We are also indebted to Rebecca Tempel and Jean Gustin for help with this manuscript.

Chapter 3

Analysis of the Interaction between the *Salmonella* Secreted Effector SrfH and the Mammalian Target TRIP6

George S. Niemann[1], Yun-Ju Lai[2], Micah Worley[3], Fang-Tsyr Lin[2], Ujwal Shinde[4], Fred Heffron[1]

Contributions to this work

Yeast two-hybrid assays

Identification and characterization of SrfH point mutants

Src activation experiments

[1]Department of Microbiology and Immunology, Oregon Health and Science University, Portland, OR

[2]Department of Cell Biology, University of Alabama at Birmingham, Birmingham, AL

[3]Department of Biology, University of Louisville, Louisville, KY

[4]Department of Biochemistry, Oregon Health and Science University, Portland, OR

Abstract

Following oral infection *Salmonella* can rapidly disseminate from the intestinal lumen to the bloodstream by carriage in $CD18^{+}$ white blood cells. This process is dependent on the *Salmonella* secreted type III effector SrfH (SseI). The mammalian adaptor protein, thyroid hormone receptor interacting protein 6 (TRIP6), interacts with SrfH and may contribute to this phenotype. In response to lysophosphatidic acid (LPA), TRIP6 forms a complex with lysophosphatidic acid receptor 2 (LPA_2) and c-Src. This signaling complex is known to stimulate cell motility via c-Src phosphorylation of TRIP6 Y55, and we therefore tested the possibility that SrfH uses this pathway to promote rapid septicemia. To understand how the SrfH-TRIP6 interaction could modulate motility, we identified SrfH point mutants that no longer interacted with TRIP6 in a yeast two-hybrid assay but retained type III secretion and stability within macrophages. When mice were orally infected, the wild type but not the mutant bacteria rapidly disseminated to the bloodstream. To better understand the SrfH-TRIP6 interaction, we constructed a model partly based on published crystal structures of related proteins. The model predicts that the first 25 amino acids of SrfH likely play an important role in the TRIP6 interaction, and it describes how the SrfH point mutants may have destabilized TRIP6 binding. We then determined that SrfH forms a complex with both TRIP6 and c-Src, however SrfH had a modest impact upon c-Src activation and did not stimulate TRIP6 phosphorylation at Y55. These results suggest that SrfH may promote host cell migration and rapid septicemia via a mechanism that differs from the documented LPA-TRIP6 model.

Introduction

Salmonella enterica serovar Typhimurium (*S.* Typhimurium) is a common cause of diarrhea in the United States with more than 1 million cases estimated to occur each year. *S.* Typhimurium is an enteric pathogen that causes self-limiting gastroenteritis in humans and a systemic, typhoid like disease in mice [133]. Systemic *Salmonella* infection is characterized by colonization of the spleen, liver, and lymph nodes and requires the type III secretion system encoded within *Salmonella* pathogenicity island 2 (SPI-2). After oral ingestion *Salmonella* gains access to the bloodstream via two mechanisms. In the first mechanism, which requires about 24 hours, the bacteria destroy the M cells of the Peyer's patches, are engulfed by phagocytic cells, and use the lymphatics to colonize the spleen and liver [9,104,134]. In the second more rapid mechanism, *Salmonella* are carried directly to the bloodstream within monocytes [9-11].

Salmonella virulence is in part mediated by type III secretion of effector proteins from the bacterial cytoplasm to the eukaryotic cell. There are over 30 identified effectors in *Salmonella* although the list is still thought to be incomplete [2,135,136]. Effector proteins mediate host cell entry and facilitate an intracellular lifestyle. For example, effectors SopE and SopE2 function as guanine exchange factors (GEF) for Rac and CD42 and lead to actin rearrangements, localized membrane ruffling, and macropinocytosis (rev. in [22,23]). SifA, SseF, SseG, SopD2, and PipB2 associate with the *Salmonella* containing vacuole, induce tubular lysosomes called SIFs, and alter vesicular trafficking [52,89]. AvrA and SseL, two other type III secreted effectors, inhibit inflammatory pathways [80,84,137].

A recent publication suggests that the SPI-2 secreted effector, SrfH (also known as SseI), is at least partially responsible for rapid septicemia observed following oral infection [11]. In support of this the authors demonstrated that RAW264.7 macrophages migrated in a Boyden chamber when infected with the wild type but not Δ*srfH* mutant bacteria. When mice were orally infected with *Salmonella*, FACS sorting demonstrated that bacteria expressing wild type SrfH but not the Δ*srfH* mutant could be found in the bloodstream within $CD18^{+}$ cells within 1 hour [11]. SrfH encodes an N-terminal sequence of about 140 amino acids that defines a family of *Salmonella* effectors including: SspH1, SspH2, SseJ, SlrP, SifA, and SifB [113,138]. SifA interacts with the

mammalian protein SKIP (SifA and kinesin interacting protein) through its N-terminus [139] and encodes a C-terminal GEF domain that is required for SIF formation [59,60]. SspH1, SspH2, and SlrP are ubiquitin ligases [140]. Rather than target specific host proteins for degradation, this class of effectors appears to modulate the activities of their mammalian targets. SspH1 ubiquitinates PKN1 [82], a serine/threonine protein kinase that activates upon cell infection and is involved in NF-κB inflammatory pathways [83]. SlrP ubiquitinates thioredoxin-1 (Trx), a small reduction/oxidation regulatory protein [141]. The mammalian target of SspH2 is not yet known.

Yeast two-hybrid screening identified host TRIP6 (thyroid hormone receptor interacting protein 6) as a mammalian target of SrfH [11]. TRIP6 is an adaptor protein in a subfamily of LIM domain proteins that includes Zyxin, Ajuba, and lipoma preferred partner (LPP) [142-144]. TRIP6 possesses both nuclear export and import signals and has three C-terminal LIM domains [145]. TRIP6 functions as an adaptor protein in numerous cell-signaling cascades such as cell motility, innate immunity, and inflammation [108,109,145,146], but it is also dysregulated in some metastatic cancers [147]. TRIP6 can form protein complexes with a variety of proteins including lysophosphatidic acid receptor 2 (LPA_2), c-Src, $p130^{Cas}$, Crk, receptor interacting protein 2 (RIP2), interleukin 1 receptor (IL-1R), TNF receptor associated factor 2 (TRAF2), toll like receptors 1 and 2 (TLR1 and TLR2), nucleotide-binding oligomerization domain 1 (NOD1), and glucocorticoid receptor (GR) [108-110,146].

One of the best-characterized motility pathways involving TRIP6 occurs in response to lysophosphatidic acid (LPA) [110]. LPA treatment of ovarian cancer (SKOV-3) cells caused c-Src phosphorłylation of TRIP6 at residue Y55, cell rounding, and actin rearrangements characteristic of cell migration. A TRIP6 Y55F mutation inhibited cell migration towards LPA [109]. Cell migration is a coordinated process involving the assembly and disassembly of focal adhesions [148]. Focal adhesions are large, dynamic, macromolecular complexes that relay both extra and intracellular signals. TRIP6 localizes at focal adhesions, but in response to LPA it dissociates from them and interacts with c-Src, $p130^{Cas}$, and Crk [109]. LPA is also known to modulate cell adhesion and motility through a Rho dependent, integrin mediated signaling pathway [149-154]. Since TRIP6 and SrfH have a demonstrable role in cell motility, understanding that interaction

and its impact on signaling are essential for dissecting how *Salmonella* causes rapid septicemia after oral infection.

Within the last decade computational approaches have made it possible to predict how two proteins interact. For example, protein-protein interactions can be modeled by dividing their surfaces into patches containing critical shapes. An algorithm then matches shapes between the two proteins to resolve an interface [155]. When there is a lack of structural data, it's also possible to predict a protein's 3D structure using comparative and *ab initio* modeling. Comparative modeling exploits the fact that two proteins fold similarly if they share as little as 25% sequence identity [156]. Alternatively, the *ab initio* technique is an emerging computational method that helps overcome the scarcity of high-resolution structural data by utilizing the physical properties of a protein's primary sequence to predict its 3D structure. *Ab initio* methods model all of the energetics involved in the folding process and then statistically finds the lowest energy system, generally through the use of first principles [157-159]. Although the process becomes exponentially more complex as the length of the protein increases, it is nonetheless a very useful tool that can be coupled with homology modeling to make useful predictions about critical binding domains and regions that are absent from X-ray structures.

In our previous characterization of the SrfH-TRIP6 interaction we found that TRIP6 related proteins Zyxin, LPP, and Ajuba did not interact with SrfH in a yeast two-hybrid assay. We then demonstrated that siRNA knockdown of TRIP6 eliminated the difference in motility between RAW264.7 macrophages infected with wild type and Δ*srfH* mutant bacteria [11]. Taken together these experiments suggested a specific protein-protein complex between SrfH, TRIP6, and potentially other proteins. In this paper we define the SrfH-TRIP6 binding domains in more detail and show that this interaction may be required for the rapid septicemia phenotype. Furthermore, we demonstrate that SrfH is part of a complex containing the proto-oncogene c-Src, a protein that has been previously related to cell motility. SrfH expression in mammalian cells activated c-Src, however, SrfH did not affect TRIP6 Y55 phosphorylation, suggesting that SrfH may signal through a pathway distinct from the published models.

Results

Primary structures of TRIP6 and SrfH

The TRIP6 N-terminus possesses a nuclear export signal (NES), and the C-termiuns contains three, sequential LIM domains (Fig. 3-1A) [109]. TRIP6 also possesses several undefined domains. The N-terminus is proline rich and directly interacts with the SH3 domain of c-Src. Nuclear localization sequences are also present in the N and C-terminal halves of TRIP6, but their sequences have not been delineated [145]. The first 140 amino acids of SrfH possess sequence homology with six other effectors: SspH2, SspH1, SlrP, SseJ, SifA, and SifB (Fig. 3-1B) [113,138]. The C-terminal 141-323 amino acids have significant homology to a putative insect toxin in *Photorhabdus asymbiotica*, an enteric symbiote of nematodes [160]. Additional functional motifs or homology are not present in the database (Fig. 3-2B).

Mapping the sequences necessary for SrfH-TRIP6 interaction

When cloned into the appropriate vectors (see Materials and Methods) the TRIP6 LIM domains give a positive yeast two-hybrid assay with SrfH (Fig. 3-2A). To gain a better understanding of this interaction, we mapped the binding domains of SrfH and TRIP6 by constructing a series of deletions and assaying the interaction as above. These results show that SrfH required TRIP6 LIM domains 2 and 3 for an interaction (Fig. 3-2A). Conversely, the SrfH N-terminal 140 amino acids gave a positive two-hybrid result with TRIP6 (Fig. 3-2B). Because the SrfH N-terminus shares sequence homology with six other type III effectors (Fig. 3-1B), we tested three of them for an interaction with TRIP6. We found that SlrP, SspH2 (the most closely related SrfH homolog as shown in Fig. 3-1B), and SseJ did not interact with TRIP6 (Fig. 3-2C) although they were expressed at levels comparable to SrfH in *Saccharomyces cereviseae* (data not shown). In summary the SrfH N-terminus interacted with the second and third LIM domains of TRIP6. The interaction was specific despite N-terminal sequence homology with other effector proteins.

The main criticism of yeast two-hybrid is the possibility of false positive and negative data [128]. To address this issue we hypothesized that abrogation of the

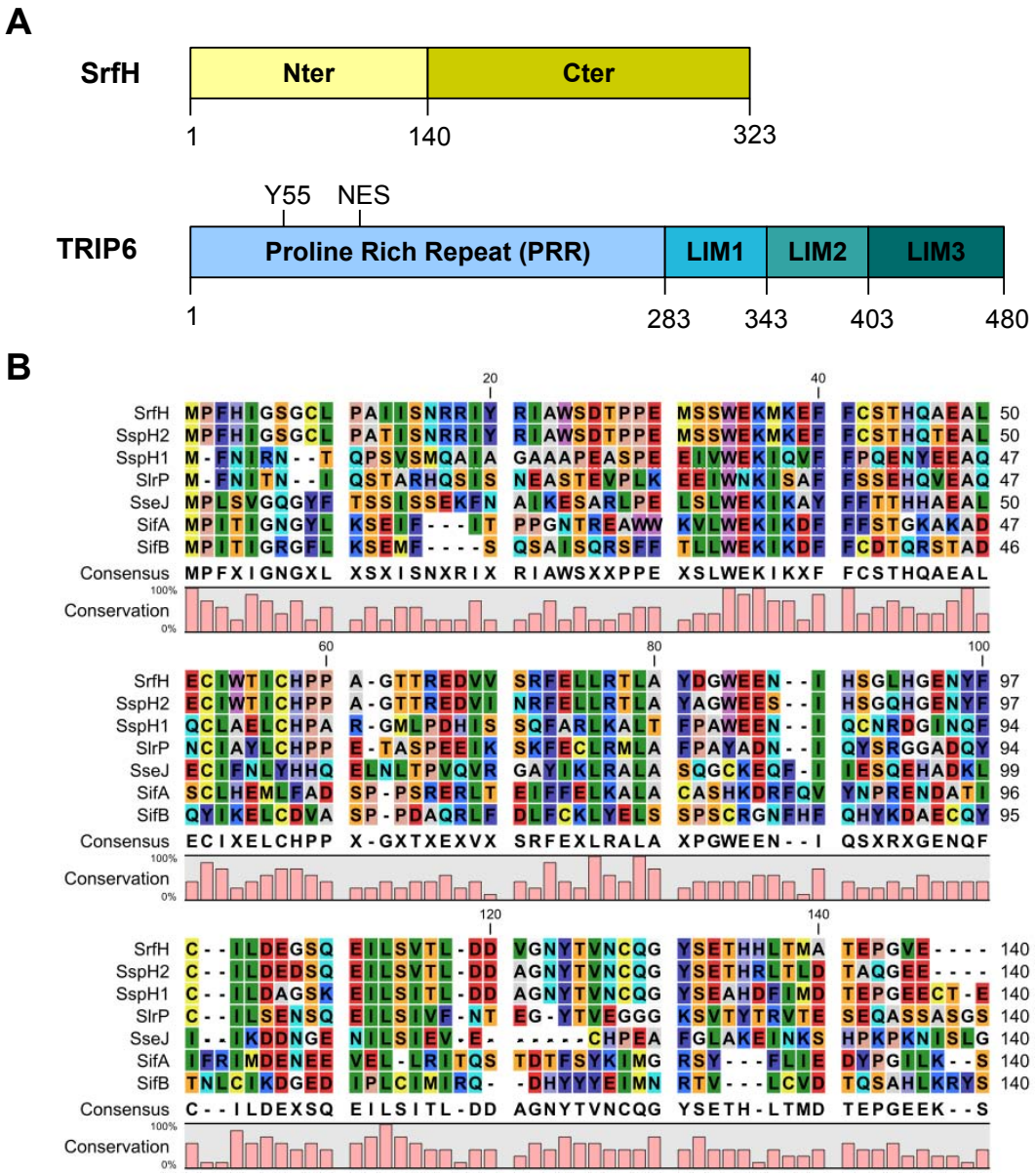

Fig. 3-1

Primary structures of SrfH and TRIP6. (A) The N-terminal domain of SrfH has homology to multiple effector proteins characterized by the WE/NKI/MXXFF motif. The C-terminal domain has homology to a putative insect toxin annotated in *P. asymbiotica*. TRIP6 has an N-terminal proline rich repeat (PRR) followed by three C-terminal LIM domains. The PRR possesses a nuclear export signal (NES) at residues 100-107 and is phosphorylated by c-Src at residue Y55. (B) N-terminal clustal alignment of the WE/NKI/MXXFF family of secreted effectors.

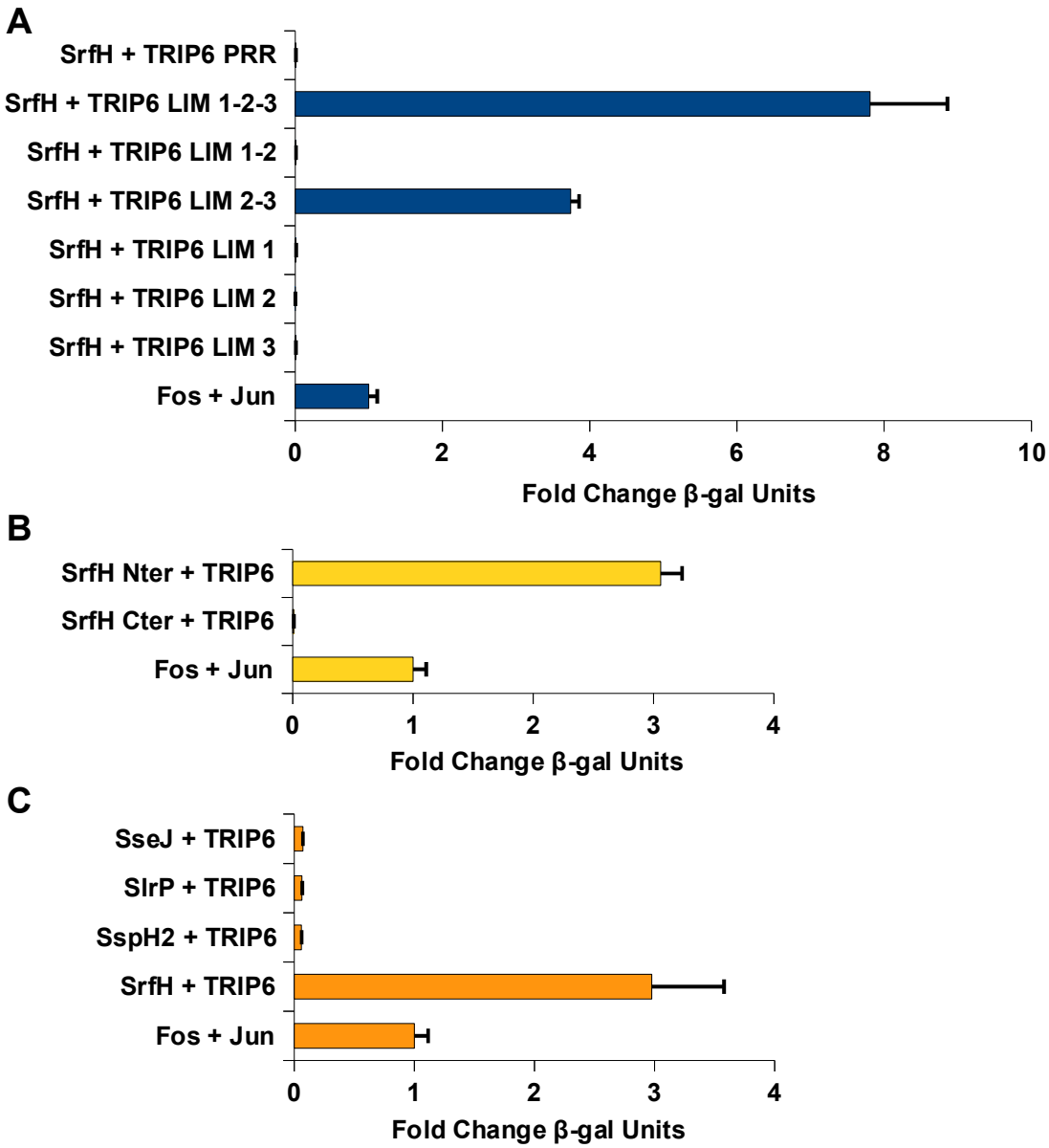

Fig. 3-2

Yeast two-hybrid analysis of SrfH-TRIP6 interaction. (A) SrfH interacts with the 2nd and 3rd LIM domains of TRIP6. (B) N-terminal domain of SrfH interacts with TRIP6. (C) WE/NKI/MXXFF effectors SseJ, SlrP, and SspH2 do not interact with TRIP6.

SrfH-TRIP6 interaction should attenuate the rapid septicemia phenotype (Fig. 3-3A). Since point mutants are often used to validate protein-protein interactions [161-163], we used the approach described in Fig. 3-3B to test our hypothesis.

Construction and analysis of point mutants that abrogated the SrfH-TRIP6 interaction

To further validate the binding between SrfH and TRIP6 we mutated *srfH* by error prone PCR, cloned the resulting mutant copies into an expression vector (pHybLexZeo) to create a library, and performed a blue/white yeast two-hybrid screen for SrfH clones that no longer bound to TRIP6. We selected 25 white colonies and performed colony PCR to generate *srfH* products for DNA sequencing. Roughly half of the mutations were frameshifts or premature stop codons, and four clones encoded multiple point mutations. Five clones contained a single SrfH point mutation (I22N, L10P, D114A, H45Y, and V68E) and were attenuated for TRIP6 interaction in a two-hybrid assay (Fig. 3-4A). SrfH point mutants I22N, D114A, H45Y, and V68E were attenuated 38, 5, 2, and 26 fold, respectively. No interaction between SrfH L10P and TRIP6 could be detected. Based on these results we tested SrfH I22N, L10P, and V68E for secretion. We constructed translational fusions to the calmodulin dependent *B. pertussis* adenylate cyclase (CyaA') and assayed cAMP levels from infected J774 macrophage cells. Of these three mutants, SrfH L10P and I22N were secreted normally. SrfH V68E cAMP concentration was 11 fold lower than wild type SrfH, suggesting that this mutation affected either protein stability or secretion, and it was not investigated further (Fig. 3-4B). Subsequent analyses focused on SrfH L10P and I22N since these mutants were secreted normally and were attenuated for TRIP6 interaction in a two-hybrid assay.

Western hybridization further verified the secretion data. SrfH was HA tagged on the C-terminus and cloned into a low copy number plasmid under the control of its native promoter. Cells were subsequently infected with *Salmonella* expressing wild type and mutant copies of SrfH, incubated six hours, and fractionated to separate bacteria from the host cytoplasm containing secreted SrfH. Secretion was detected by Western hybridization using *ssaK*::*cat* as a negative control (Fig. 3-4C). As can be seen all three proteins were secreted, but SrfH L10P was secreted ~two fold less efficiently when compared to the wild type and I22N mutant (Fig. 3-4C). Using the SrfH-cya secretion

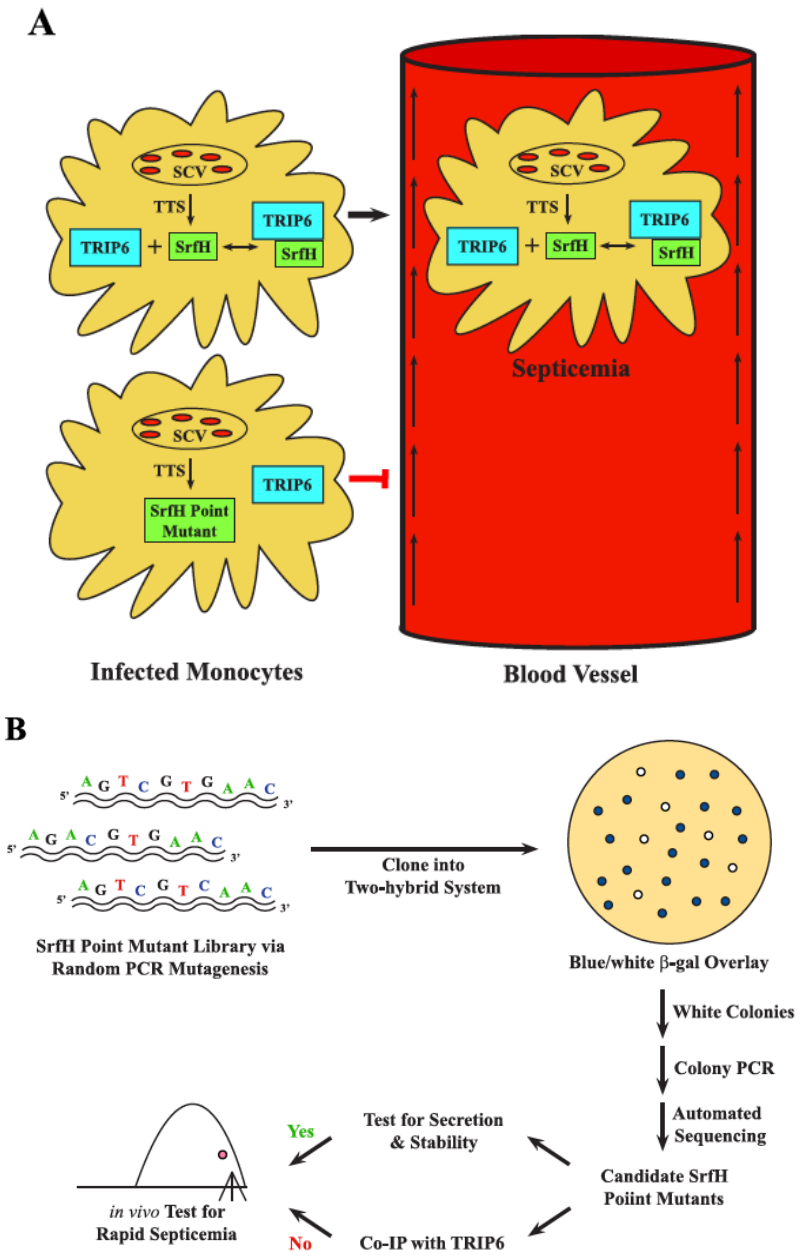

Fig. 3-3

Validating the SrfH-TRIP6 interaction. (A) Model of SrfH-TRIP6 mediated septicemia. *Salmonella* are carried within circulating $CD18^{+}$ cells. SrfH is secreted into cells. Abrogation of the SrfH-TRIP6 interaction should negatively affect septicemia. (B) Testing the SrfH-TRIP6 septicemia model. Briefly, generate random SrfH point mutants by PCR mutagenesis. Clone the mutant library into a two-hybrid system, perform a -gal overlay, and select white colonies indicative of a negative TRIP6 interaction. Verify the presence of a single point mutation by automated sequencing then test for secretion, protein stability, and attenuated TRIP6 interaction by Co-IP. Point mutants that met these criteria were used to infect mice to assess the role of the SrfH-TRIP6 interaction in rapid septicemia.

assay the clones all showed similar levels of activity in the target cells (Fig. 3-4B).

We then attempted to co-immunoprecipitate SrfH and TRIP6 from infected RAW264.7 macrophages, but our attempts were unsuccessful presumably due to low TRIP6 expression levels or because the association was transient (pers. Comm. F. Lin). Since RAW264.7 cells were not amenable to transfection, we verified the interaction in a different cell type. HEK293T cells were transiently transfected with eukaryotic expression vectors that co-expressed TRIP6 with wild type SrfH or the SrfH point mutants. For transfection experiments, SrfH was codon optimized for mammalian expression and cloned into the pIRES-eGFP plasmid with a C-terminal HA tag. Interestingly, plasmids encoding the SrfH point mutants transfected at a two fold lower efficiency when compared to the wild type allele (Fig. 3-4D), suggesting that over-expression of the point mutants but not the wild type SrfH affected cellular viability. As can be observed in Fig. 3-4D, wild type SrfH co-immunoprecipitated with TRIP6, whereas SrfH I22N was attenuated, and L10P did not co-precipitate at all. In total the results show that the native SrfH and the two mutants were stably expressed and secreted into mammalian cells. Consistent with the two-hybrid results, SrfH I22N interacted with TRIP6 but not at all in the case of L10P.

We next used the mutant derivatives of SrfH to test if the TRIP6 interaction was necessary for rapid septicemia. Four to six week old Balb/C mice were infected IG with 10^9 bacteria expressing wild type SrfH, SrfH L10P, and SrfH I22N. Thirty minutes post infection blood was collected via cardiac puncture, blood cells were lysed, and the number of bacteria determined. Wild type bacteria were present at 1,375 CFU/mL of blood. Mice infected with *Salmonella* expressing SrfH L10P and I22N had <75 CFU/mL, concentrations comparable to the Δ*srfH* control (Fig. 3-4E). Therefore, SrfH-TRIP6 interaction may be required for the rapid septicemia phenotype, but these findings do not explain how the SrfH point mutants abrogated the TRIP6 interaction.

Constrained *ab initio* modeling

To better understand how the SrfH point mutants affected interaction with TRIP6, we hypothesized that structural differences might account for our observations because SrfH residues L10 and I22 are conserved among some, but not all related effector proteins (Fig. 3-5A). In fact, the N-terminal 140 amino acids of SspH2 and SrfH share

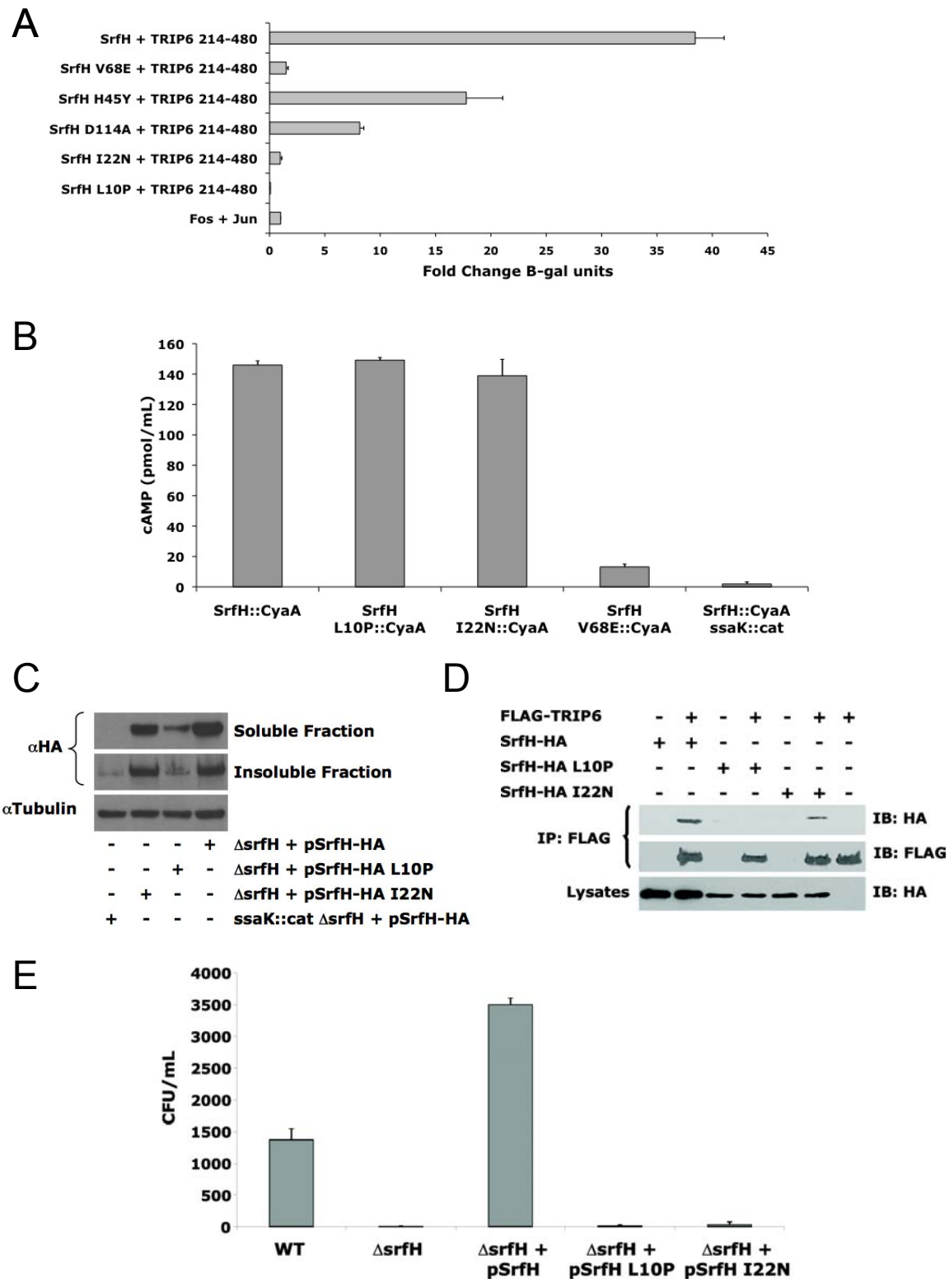
A
SrfH + TRIP6 214-480
SrfH V68E + TRIP6 214-480
SrfH H45Y + TRIP6 214-480
SrfH D114A + TRIP6 214-480
SrfH I22N + TRIP6 214-480
SrfH L10P + TRIP6 214-480
Fos + Jun
0 5 10 15 20 25 30 35 40 45
Fold Change B-gal units
B
cAMP (pmol/mL)
0 20 40 60 80 100 120 140 160
SrfH::CyaA
SrfH L10P::CyaA
SrfH I22N::CyaA
SrfH V68E::CyaA
SrfH::CyaA ssaK::cat
C
αHA
Soluble Fraction
Insoluble Fraction
αTubulin
- - - + ΔsrfH + pSrfH-HA
- - + - ΔsrfH + pSrfH-HA L10P
- + - - ΔsrfH + pSrfH-HA I22N
+ - - - ssaK::cat ΔsrfH + pSrfH-HA
D
FLAG-TRIP6 - + - + - + +
SrfH-HA + + - - - - -
SrfH-HA L10P - - + + - - -
SrfH-HA I22N - - - - + + -
IP: FLAG
IB: HA
IB: FLAG
Lysates
IB: HA
E
CFU/mL
0 500 1000 1500 2000 2500 3000 3500 4000
WT
ΔsrfH
ΔsrfH + pSrfH
ΔsrfH + pSrfH L10P
ΔsrfH + pSrfH I22N

Fig. 3-4

Evidence for SrfH interaction with TRIP6 *in vitro* and *in vivo*. (A) Yeast two-hybrid analysis of the SrfH point mutants with TRIP6. (B) Adenylate cyclase secretion assay. J774 macrophages were infected with Salmonella expressing SrfH or the SrfH point mutants (L10P, I22N, V68E) fused to the adenylate cyclase gene (CyaA) from *B. pertussis*. Secretion of the SrfH::CyaA fusions was assessed by cAMP ELISA. For the negative control we assessed SrfH::CyaA secretion in an ssaK::cat background, a functional SPI2 secretion mutant. (C) SrfH L10P and I22N are stably expressed and secreted into RAW264.7 macrophages. RAW264.7 macropohages were infected as described above but lysed in buffer containing Triton X-100. *Salmonella* are resistant to lysis by Triton X-100. Thus, cell associated bacteria and cellular debris were pelleted into the insoluble fraction and secreted protein retained in the soluble fraction. Samples were resolved by SDS-PAGE and analyzed by Western hybridization. (D) Co-immunoprecipitation of SrfH with TRIP6. FLAG-TRIP6 was co-expressed with SrfH-HA or one of the SrfH point mutants (L10P or I22N) in HEK293T cells. FLAG-TRIP6 was immunoprecipitated, resolved by SDS-PAGE, and probed for SrfH-HA. The bottom panel shows the expression of WT or mutants of SrfH-HA in the whole cell lysates. (E) SrfH L10P and I22N affect rapid septicemia. Balb/C mice were IG infected with 10^9 bacteria. 30 minutes post-infection mice were anesthetized and blood was harvested by cardiac puncture. Blood cells were lysed and bacteria enumerated on LB agar.

89% identity (Fig. 3-1B), yet SspH2 did not interact with TRIP6 in a yeast two-hybrid assay (Fig. 3-2C). A 3D structural model of the SrfH N-terminus was generated as described in Materials and Methods using both the comparative and *ab initio* methods. The predicted SrfH structure was easily fitted to the SifA crystal structure [60], and these two effectors appear to possess a core domain that is characterized by a β-sheet flanked by three helices (Fig. 3-5B). At the primary sequence level the core domain initiates at the WE/NKI/MXXFF motif, which is found in all seven related effectors. Thus, the core domain may be a conserved structural feature (Fig. 3-5B). We next used our model to assess how SrfH might interact with TRIP6. Based on NMR structures the TRIP6 LIM domains exhibit a helix followed by two partial β-sheets (http://dx.doi.org/10.2210/pdb2dlo/pdb). Recognition of TRIP6 by SrfH likely occurs through a network of hydrogen bonds and van der Waals contacts as predicted by Patchdock. The one salient difference between the predicted SrfH structure and that of SifA is that we used *ab initio* modeling to include the first 25 amino acids in our analyses. This region is absent from the SifA structure and is likely due to low resolution of the diffraction pattern, often a result of a highly flexible region that may not adopt a defined conformation. The effect of the two point mutants can be seen in the model as they attenuate the interaction. SrfH L10P should disrupt alpha helix 1 (Fig. 3-5C) as proline is a well established helix disruptor [164]. SrfH I22N resides within helix 2 and is predicted to diminish helix elasticity because asparagine residues have lower helical properties when compared to isoleucine, empirical concepts derived through experimental studies on protein and peptide structures [165]. Thus, SrfH I22N may affect conformational changes associated with TRIP6 binding, albeit not as strongly as L10P (Fig. 3-5C). Because of the N-terminal homology between effectors, we then used our model to gain insight into how SrfH may interact with TRIP6. SspH2, the closest SrfH homologue, differs by only a single amino acid within the N-terminal 25 amino acids (I13T). As can be seen, an I13T substitution may alter TRIP6 binding by affecting hydrophobic packing or by disrupting helix 1 similar to SrfH L10P (Fig. 3-5C), findings that are consistent with our two-hybrid data (Fig. 3-2C). Based upon these observations, sequence variation within the N-terminal 25 amino acids is likely a major determinant of target specificity. In summary, our predictive model may explain how SrfH interacts with

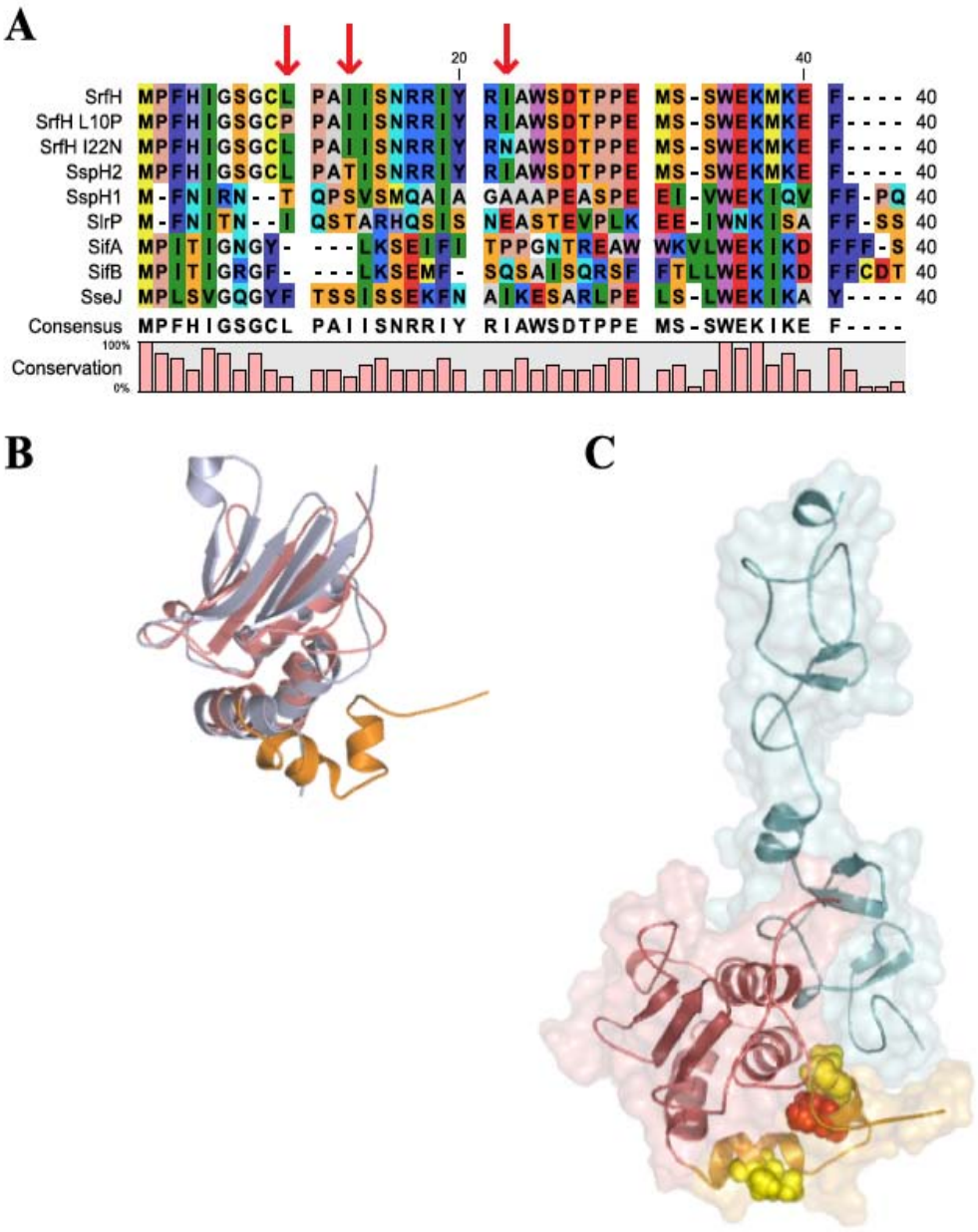

Fig. 3-5

Constrained *ab intio* modeling of the SrfH-TRIP6 interaction. (A) Clustal alignment of the SrfH point mutants with the WE/NKI/MXFF family of secreted effectors. (B) N-terminal overlay of the SifA crystal structure with the SrfH model. Magenta: SifA core domain. Blue: SrfH core domain. Orange: SrfH N-terminal 25 amino acids. (C) Structural modeling of the SrfH N-terminus with the 2nd and 3rd LIM domains of TRIP6. Turquoise: TRIP6 2nd and 3rd LIM domains. Magenta: SrfH core domain. Orange: SrfH N-terminal 25 amino acids. Yellow residues: L10 and I22. Red residue: I13.

TRIP6, and it suggests how closely related effector proteins may bind different host targets as both SifA [60] and SrfH have been shown to do. However, these observations do not explain how SrfH promotes cell motility. We address this in the next section using the constructs described above.

SrfH, TRIP6 and c-Src form a complex

One piece of information that relates TRIP6 to motility, and by inference SrfH, is work showing that LPA mediates cell motility through TRIP6 [110]. LPA is a potent chemoattractant and ligand for the G protein-coupled LPA_2 receptor. In response to LPA, the C-terminus of LPA_2 receptor interacts with TRIP6 promoting a protein complex that contains TRIP6, c-Src, $p130^{Cas}$, and Crk. TRIP6 is phosphorylated at Y55 by c-Src and motility is mediated by $p130^{Cas}$ and Crk, two proteins that act as a molecular switch for the Rho/Rac motility pathway [109,110]. The importance of c-Src in metastasis, cell differentiation, and motility has been demonstrated in numerous studies [166]. We therefore first investigated if SrfH participates in a multi-protein complex containing both TRIP6 and c-Src. We assessed this possibility by transiently transfecting HEK293T cells with plasmids expressing FLAG-SrfH, HA-c-Src, and Myc-TRIP6 as described in Fig. 3-6A. SrfH co-immunoprecipitated both c-Src and TRIP6, demonstrating that SrfH associates with both proteins. An important aspect of this experiment is that it was done in the presence of serum, which is an ample source of LPA [167,168]. LPA stimulates $p130^{Cas}$ and Crk interaction with TRIP6 and c-Src [109]. Our data suggest that SrfH, TRIP6, and c-Src form a steady state complex occurs independent of LPA.

SrfH expression has a modest impact upon the activation a Src family kinase (SFK)

Because SrfH, TRIP6, and c-Src formed a protein complex, we then asked if SrfH expression affects Src activation. c-Src is one member of the SFK family that includes c-Lck, Fyn, Hck, Yes, Lyn, and Abl. Many of these kinases have redundant functions, which can make it difficult to relate a phenotype to a specific protein. They have molecular weights between 50-65 kDa and are tightly regulated via similar mechanisms, presumably due to their potential for neoplastic transformation. SFK activity is controlled using tyrosine phosphorylation at two sites with opposing effects. Using c-Src as an example, phosphorylation of SrcY416 in the activation loop of the kinase domain up-regulates enzyme activity. Phosphorylation of Y527 in the carboxy-terminal tail

renders the enzyme less active [166,169]. Using an antibody that recognizes phosphorylated SrcY416, and therefore activated enzyme, we assessed Src activation following expression of SrfH and TRIP6 in mammalian cells. We chose not to use infected cells because we wished to avoid secondary signaling events associated with the innate immune response and other secreted effectors. As mentioned previously, RAW264.7 cells transfect poorly, so HEK293T cells were transiently transfected with mammalian expression vectors encoding SrfH-HA, Myc-TRIP6, or both (see Fig. 3-6B). The following day, cells were serum starved. As a positive control we activated c-Src by addition of 10% FBS. We separated proteins by SDS-PAGE and used Western hybridization to identify SrfH, TRIP6, c-Src, and activated Src kinase. Our results show that SrfH activated an endogenous Src kinase independent of FBS stimulation. The level of activation was 0.5 fold over background. The monoclonal antibody employed and all similar antibodies recognizes all activated Src kinases and thus SrfH may have activated another member of the family. However, when the blot was re-probed with a monoclonal antibody that was specific for c-Src, the two antibodies recognized the same molecular mass protein, suggesting that SrfH acted upon endogenously expressed c-Src and not another family member (Fig. 3-6B). Thus, SrfH may alter a c-Src signaling pathway, but the level of activation was below that seen in many metastatic cancers [170-173].

SrfH expression does not affect TRIP6 tyrosine phosphorylation

Phosphorylation of TRIP6 Y55 by c-Src is required for LPA induced cell migration [109]. Since SrfH interacts with TRIP6 and c-Src, we hypothesized that SrfH may affect TRIP6 tyrosine phosphorylation. To test this hypothesis we transiently transfected HEK293T cells with plasmids expressing FLAG-TRIP6 and SrfH-HA (see Fig. 3-6C). The following day cells were treated with sodium orthovanadate to inhibit tyrosine phosphatase activity. FLAG-TRIP6 was pulled down, resolved by SDS-PAGE, and samples were probed with a pan-antibody that recognizes phosphorylated tyrosine residues. SrfH did not affect TRIP6 tyrosine phosphorylation (Fig. 3-6C). Therefore, SrfH and LPA induced cell motility may occur via different mechanisms. However, it is also possible that there were changes to TRIP6 phosphorylation that we did not detect. For example, TRIP6 can be phosphorylated at S92 in response to epidermal growth factor (EGF) [174]. Efforts are underway to determine if SrfH affects TRIP6 post-translational

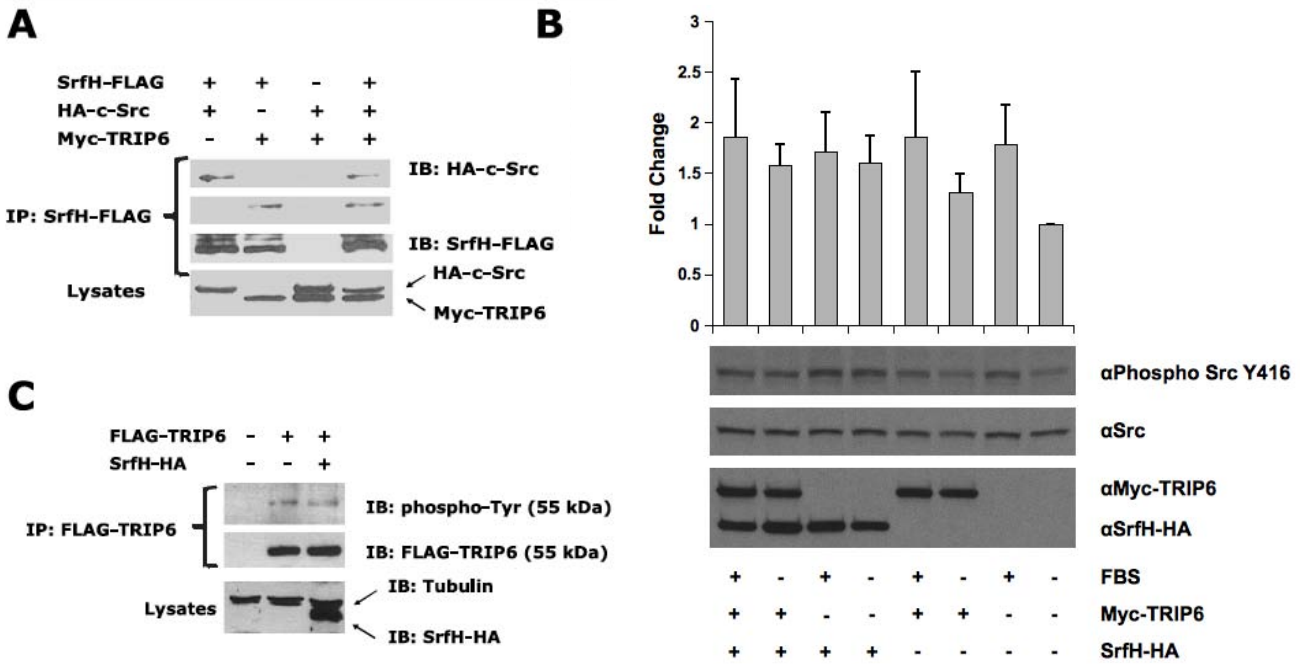

Fig. 3-6

SrfH effects upon c-Src signaling. (A) SrfH, TRIP6, and c-Src form a complex. SrfH-FLAG, Myc-TRIP6, and HA-c-Src were co-expressed in HEK293T cells. SrfH-FLAG was immunoprecipitated, resolved by SDS-PAGE, and probed for HA-c-Src and Myc-TRIP6. The bottom panel shows the expression of Myc-TRIP6 and HA-c-Src in whole cell lysates. (B) SrfH expression activates a Src family kinase. SrfH-HA and Myc-TRIP6 were co-expressed as indicated in HEK293T cells. To activate c-Src cells were treated with 10% FBS for 10 min. Samples were resolved by SDS-PAGE, and activation of an SFK was assessed by immunoblot using an antibody that recognizes phosphorylated SrcY416. The bottom panels show expression of SrfH-HA, Myc-TRIP6, and endogenous c-Src. (C) SrfH expression does not affect TRIP6 tyrosine phosphorylation. FLAG-TRIP6 and SrfH-HA were co-expressed as indicated in HEK293T cells. Cells were treated with 1 mM $NaVO_4$ to inhibit tyrosine phosphatase activity. FLAG-TRIP6 was immunoprecipitated, samples were resolved by SDS-PAGE, and then probed with a pan-phosphotyrosine antibody. Bottom panels show the expression of TRIP6 and SrfH.

modification. In summary these results suggest that SrfH modulates cell motility via a mechanism that differs from the LPA-TRIP6 paradigm.

Discussion

We characterized the interaction between the *Salmonella* effector SrfH and host TRIP6 in an effort to better understand how these proteins might facilitate rapid septicemia. The N-terminus of SrfH interacted with the 2nd and 3rd LIM domains of TRIP6. We then used a genetic approach to establish a direct interaction between SrfH and TRIP6. We identified two mutations, located within the amino terminal 25 amino acids of SrfH that were attenuated for TRIP6 interaction. Most importantly, cells infected with these mutants did not cause rapid septicemia in the mouse model unlike the parent strain. One caveat to these results is that the point mutants were secreted at lower levels with respect to the wild type protein, suggesting that there may have been dose dependent effects. However, the SrfH point mutants possessed full enzymatic activity when fused to a CyaA' reporter, indicating that they retained functionality independent of the TRIP6 binding domain. Since LPA stimulates c-Src phosphorylation of TRIP6 Y55 and cell motility, we next tested SrfH for an effect on this signaling cascade. We found that SrfH formed a multi-protein complex with both TRIP6 and c-Src. Unlike LPA mediated cell motility, SrfH expression activated an SFK in HEK293T cells only 0.5 fold and did not affect TRIP6 tyrosine phosphorylation, suggesting that LPA and SrfH mediate cell motility through different signaling pathways.

An alternative SrfH binding partner

McLaughlin et al. [175] recently published an alternative mammalian binding partner for SrfH. They found that SrfH interacted with IQGAP1, a regulator of the host cytoskeleton and cell migration. The authors convincingly demonstrated that SrfH interacted with IQGAP1 in primary bone marrow derived macrophages (BMDM) but not RAW 264.7 cells. Additionally, the motility of *Salmonella* infected BMDM was affected in a SrfH dependent manner. Specifically, SrfH directed motility away from heat killed *Salmonella* in a Boyden chamber, and the *srfH* mutant colonized the spleen and liver of infected mice less efficiently than the wild type bacteria [175]. While these results contradict some of the findings described in Chapters 2 and 3, our basic hypothesis that SrfH modulated cell motility was confirmed.

We now have evidence which suggests that a single amino acid substitution in SrfH may account for the different host binding partners. Out of 110 natural *Salmonella*

isolates, all but five encode an aspartic acid at SrfH position 103. The remaining five encode a glycine, and no other polymorphisms were observed suggesting that a functional SrfH is required for pathogenicity. When SrfH 103D and 103G were analyzed for two-hybrid interaction with TRIP6, only SrfH 103G interacted (pers. Comm. M. Worley). McLaughlin et al. [175] used *Salmonella* SL1344 which encodes SrfH 103D, whereas we used *Salmonella* 14028 encoding SrfH 103G. Thus, we have a plausible explanation for the different binding partners, but it remains to be demonstrated if the polymorphism affects IQGAP1 interaction and if SrfH 103G interacts with TRIP6 in BMDM. These experiments are currently in progress.

SrfH may have C-terminal activity

A SrfH C178A mutation impaired *Salmonella* colonization of the liver and spleen [175]. While a structural role for C178 cannot be ruled out, this is evidence for C-terminal activity. Anecdotal evidence further supports this hypothesis. Enzymatic activities have been attributed to the C-termini of four different effectors in the WE/NKI/MXXFF family. The SifA C-terminus is a Rho GTPase GEF [60] while the C-termini of SspH1, SspH2, and SlrP are E3 ubiquitin ligases [140,141].

SrfH may activate c-Src via TRIP6

Perhaps the most direct way of ascertaining c-Src's role in rapid septicemia is by testing a c-Src null mouse line following *Salmonella* infection. Since SrfH has a modest impact upon SFK activation in HEK293T cells (Fig. 3-6B), this may be the case and it will be necessary to dissect the mechanism by which this occurs. For example, the SrfH C-terminus might be a kinase that directly phosphorylates c-Src. Alternatively, SrfH might increase SFK activation by dephosphorylating Y527, the inhibitory c-Src tyrosine phosphate [166]. c-Src also possesses two auto-inhibitory domains that fold around its kinase domain to suppress its function [169]. SrfH may be a competitive inhibitor of one or both of these auto-inhibitory domains, thereby causing SFK activation. While these possibilities are being tested, the fact that SrfH forms a complex with c-Src does not suggest a direct interaction. Indeed, TRIP6 contains an N-terminal proline-rich region that directly interacts with the SH3 domain of c-Src [109].

SrfH may signal through multiple pathways

Rho family GTPases like RhoA, Rac1, and Cdc42 are downstream mediators of cell

motility that coordinate cell matrix adhesions. Rac1 and Cdc42 facilitate actin polymerization and membrane protrusions. RhoA antagonizes Rac1 and Cdc42 activities. During cell motility these functions are coordinated to promote directionality [151]. Therefore, SrfH may promote signaling through a Rho family GTPase, but defining these pathways may be complicated by TRIP6's role as an adaptor in other signaling cascades. In fact, TRIP6 over-expression exacerbates NF-κB activation by TNF, IL-1, TLR2 and Nod1 [146]. Thus, the SrfH-TRIP6 interaction may interfere with both NF-κB and SFK signaling.

In conclusion *Salmonella* SrfH interacted with host TRIP6 and c-Src and the association may be required for rapid septicemia following IG infection of a mouse. Additional testing will determine if SFK signaling mediates this phenotype.

Methods

Cell Culture

Bacteria were grown at 37°C in Luria-Bertani (LB) broth. 100 mg/mL carbenicillin, 30 mg/mL chloramphenicol, and 60 mg/mL kanamycin was added as required for maintenance of plasmids. Low-salt LB containing 25 mg/mL zeocin was used when growing bacteria containing this marker. Yeast were grown at 30°C in YC media lacking tryphtophan but supplemented with 300 mg/mL zeocin to maintain prey and bait plasmids, respectively. Eukaryotic cell lines were cultured at 37°C in the presence of 5% CO2 using Dulbecco's modified Eagle's medium (DMEM) supplemented with 10% fetal bovine serum (FBS), 4.5 g/L D-glucose, 2 mM L-glutamine, 1 mM nonessential amino acids, 0.075% sodium bicarbonate, and 110 mg/L sodium pyruvate.

Strains and plasmids

Primers used for strain construction and cloning reactions are listed in Table 3-1. A non-polar, in frame *srfH* deletion was generated by λ red recombination using the pKD4 template. Following P22 transduction the kanamycin marker was resolved [176]. For yeast two-hybrid assays murine TRIP6 was PCR amplified with flanking 5' *Eco*RI and 3' *Xho*I sites for directional cloning into pYESTrp2. *srfH*, *slrP*, *sspH2*, and *sseJ* constructs were PCR amplified with 5' *Eco*RI/*Sac*I and 3' *Xho*I/*Pst*I sites for directional cloning into pHybLexZeo. For liquid β-gal assays effector fusions in the pHybLexZeo plasmid were transformed into *S. cerevisiae* expressing full length prey TRIP6 (pTRIP6). The Diversity Random PCR Mutagenesis Kit (Clontech) was used to obtain the SrfH point mutant library. Briefly, the forward and reverse pHybLexZeo sequencing primers were used to PCR amplify *srfH* nucleotide residues 1-450 using template pGSN001 and condition 4 from the manufacturer's manual. The resulting PCR products were cloned into pCR2.1-TOPO to generate a library which was subsequently purified, digested with *Eco*RI and *Xho*I, sub-cloned back into similarly digested pHybLexZeo, and transformed into *S. cerevisiae* harboring pTRIP6/214 for X-gal screening. For over-expression in eukaryotic cells, human codon optimized *srfH* (H*srfH*) was purchased from Blue Heron Biotechnology.

Hs*rfH* sequence:

ATGCCATTCCACATAGGTTCTGGATGCCTGCCAGCAATCATTAGCAA
CAGACGAATATACCGAATAGCATGGTCAGACACCCCCCCCGAAATG
TCATCCTGGGAAAAAATGAAAGAGTTTTTTTGTTCTACCCACCAAG
CCGAAGCCCTTGAATGTATCTGGACAATCTGCCACCCACCTGCCGG
TACCACGAGAGAAGATGTTGTTTCTAGATTTGAACTGCTGAGAACA
CTTGCATATGATGGATGGGAAGAAAACATACACTCCGGTCTGCATG
GAGAGAATTATTTCTGTATTTTGGACGAGGGAAGCCAAGAGATTCT
GAGCGTTACTTTGGACGATGTAGGTAATTATACAGTAAACTGCCAG
GGCTACAGTGAGACCCACCATCTGACAATGGCTACCGAACCCGGT
GTTGAAAGAACTGATATCACTTATAACCTTACTTCAGACATTGACGC
AGCCGCATACCTTGAAGAACTCAAACAAAATCCCATTATTAATAAC
AAGATTATGAACCCTGTTGGCCAGTGCGAGAGCTTGATGACACCAG
TATCCAATTTCATGAACGAGAAAGGCTTTGATAATATTAGATACCGA
GGCATATTTATTTGGGACAAACCTACAGAAGAAATCCCCACAAACC
ATTTCGCAGTCGTCGGGAACAAAGAAGGCAAGGATTACGTGTTTGA
TGTTTCTGCCCACCAATTTGAGAACAGAGGAATGAGCAACCTTAAC
GGCCCCCTGATCCTGTCCGCCGATGAATGGGTTTGCAAGTACCGAA
TGGCAACTAGAAGAAAATTGATTTACTATACTGATTTTTCAAATTCT
TCCATCGCAGCAAATGCTTATGATGCACTTCCACGCGAACTGGAGT
CAGAGAGTATGGCAGGAAAGGTTTTCGTGACATCCCCCCGCTGGTT
CAACACGTTTAAAAAACAAAAATATTCATTGATAGGTAAGATGTAA

Hs*rfH* was PCR amplified with a C-terminal HA or FLAG tag flanked by 5' *Eco*RI and 3' *Bam*HI sites for directional cloning into pIRES2-eGFP. For expression in expression in bacterial cells, *srfH* was PCR amplified from pMJW1810 with its native promoter, a C-terminal HA tag, and flanking 5' *Xba*I and 3' *Xho*I sites for directional cloning into similarly digested pWSK29. For cAMP secretion assays pMJW1810 and control backgrounds were previously described [29]. SrfH point mutants used for secretion and co-IP experiments were generated with the Quick Change Site Directed Mutagenesis kit (Stratagene) according to the manufacturer's instructions. FLAG-TRIP6, Myc-TRIP6,

and HA-c-Src were previously described [110]. A complete list of strains and plasmids is provided in Table 3-2.

Table 3-1. Primers used in this study.

ID	Orientation	5'-Sequence-3'	Description
1	Forward	CGGACAGATACTATATGTAAATTTATAAAGGTTTTTTGTTGTGTAGGCTGGAGCTGCTTC	14028 Δ*srfH*
2	Reverse	CGGATTGACAGGGTTCTGACAGACGTCCTCCACGGTGCGCCATATGAATATCCTCCTTAG	
3	Forward	TGAGCTCCGCACAGATATAACTTACAAC	pGSN001
4	Reverse	GCTCGAGTTACATTTTACCTATTAAGG	
5	Forward	TGAGCTCCGCACAGATATAACTTACAAC	pGSN002
6	Reverse	TCTCGAGTTATTCCACTCCCGGTTCTGTTGCC	
7	Forward	TAGGGAATTCATGTTTAATATTACTAATATAC	pGSN003
8	Reverse	CTGCCTGCAGCTATCGCCAGTAGGCGCTCATG	
9	Forward	GTTTGAATTCATGCCCTTTCATATTGGAAGC	pGSN004
10	Reverse	ACCTCTCGAGTCAGTTACGACGCCACTGAAC	
11	Forward	GGAGGAATTCATGCCATTGAGTGTTGGAC	pGSN005
12	Reverse	CGATCTCGAGTTATTCAGTGGAATAATGATG	
13	Forward	GGAATTCTGATGTCCGGGCCCACCTGGCTT	pGSN006
14	Reverse	ACCGCTCGAGTTACTCCCCACTGGGAGGGTGGC	
15	Forward	CCTCGAATTCGGGAGTACTTTGGTCGGTGTGGTG	pGSN007
16	Reverse	TAGCTCGAGTCAACAATCAGTGGTGACAG	
17	Forward	CCTCGAATTCGGGAGTACTTTGGTCGGTGTGGTG	pGSN008
18	Reverse	GTGGCTCGAGTTACCTGTGGAAATCTTCAATGC	
19	Forward	AGCTGAATTCTGGCCACCCTGGAGAAATGTTCC	pGSN009
20	Reverse	TAGCTCGAGTCAACAATCAGTGGTGACAG	

21	Forward	CCTCGAATTCGGGAGTACTTTGGTCGGTGTGGTG	pGSN010
22	Reverse	ATTTCTCGAGTTAGGCCACATAGCAGCTCTC	
23	Forward	AGCTGAATTCTGGCCACCCTGGAGAAATGTTCC	pGSN011
24	Reverse	GTGGCTCGAGTTACCTGTGGAAATCTTCAATGC	
25	Forward	GATTGAATTCGGAAATTTGCCCCACGATGCTCAG	pGSN012
26	Reverse	TAGCTCGAGTCAACAATCAGTGGTGACAG	
27	Forward	AGGGCTGGCGGTTGGGGTTATTCGC	pHybLexZeo sequencing primers
28	Reverse	GAGTCACTTTAAAATTTGTATACAC	
29	Forward	ATTGGAAGCGGATGTCCTCCCGCCATCATCAG	SrfH L10P site directed mutagenesis: pGSN0018, pGSN0025
30	Reverse	ACTGATGATGGCGGGAGGACATCCGCTTCC	
31	Forward	CGCCGCATTTATCGTAATGCCTGGTCTGATACC	SrfH I22N site directed mutagenesis: pGSN0019, pGSN0026
32	Reverse	GGTATCAGACCAGGCATTACGATAAATGCGGCG	
33	Forward	ACGACGCGGGAGGATGAGGTCAGCAGATTTG	SrfH V68E site directed mutagenesis: pGSN0020
34	Reverse	TTCAAATCTGCTGACCTCATCCTCCCGCGTCG	
35	Forward	AGAATTCGCCACCATGCCATTCCACATAGGTTCTGGATGCCTG	pJG001
36	Reverse	TTGGATCCTTAAGCGTAATCTGGAACATCGTATGGGTAGCTGCCCATCTTACCTATCAATGAATA	
37	Forward	CATAGGTTCTGGATGCCCGCCAGCAATCATTAGC	HsrfH L10P site directed mutagenesis: pGSN0021
38	Reverse	GCTAATGATTGCTGGCGGGCATCCAGAACCTATG	
39	Forward	CAACAGACGAATATACCGAAACGCATGGTCAGACACCC	HsrfH I22N site directed mutagenesis: pGSN0022
40	Reverse	GGGTGTCTGACCATGCGTTTCGGTATATTCGTCTGTTG	
41	Forward	CTTCGAATTCGCCACCATGCCATTCCACATAGGTTCTGGATGCCTG	pGSN0023

42	Reverse	GCTTGGATCCTTACTTGTCATCGTCATCCTT GTAGTCCATCTTACCTATCAATGAATA	
43	Forward	CGCTCTAGAACTAGTGGATC	pGSN0024
44	Reverse	CGCCTCGAGTTATTAAGCGTAATCTGGAAC ATCGTATGGGTAGCTGCCCGAGCCCATTTTA CCTATTAAGGAATA	

Table 3-2. Strains/plasmids used in this study.

Category	**Strain/ Plasmid**	**Genotype/Description**	**Reference/ Source**
S. Typhimurium	14028	Wild type strain	ATCC
	JG110R	Δ*srfH*	This study
	MJW1301	*ssaK*::*cat*	[29]
	GSN1000	Δ*srfH ssaK*::*cat*	This study
S. cerevisiae	L40	*MATa his3Δ200 trp1-901 leu2-3112 ade2 LYS2::(4lexAop-HIS3)URA3::(8lexAop-lacZ) GAL4*	Invitrogen
Mammalian Cells	J774	Monocyte/macrophage	ATCC
	RAW264.7	Macrophage	ATCC
	HEK293T	Epithelial	ATCC
Plasmids	pKD4	λ red recombination	[176]
	pHybLexZeo	Yeast two-hybrid vector for bait protein	Invitrogen
	pYESTrp2	Yeast two-hybrid vector for prey protein	Invitrogen
	pHybLexZeo-Fos	Positive control bait plasmid	Invitrogen
	pYESTrp2-Jun	Positive control prey plasmid	Invitrogen
	pMJW1828	SrfH, pHybLexZeo derivative	[11]
	pGSN0001	SrfH Nter, pHybLexZeo derivative	This study
	pGSN0002	SrfH Cter, pHybLexZeo derivative	This study
	pGSN0003	SlrP, pHybLexZeo derivative	This study

	pGSN0004	SspH2, pHybLexZeo derivative	This study
	pGSN0005	SseJ, pHybLexZeo derivative	This study
	pTRIP6	TRIP6 1-480, pYESTrp2 derivative	[11]
	pTRIP6/214	TRIP6 214-480, pYESTrp2 derivative	[11]
	pGSN0003	TRIP6 PRR, pYESTrp2 derivative	This study
	pGSN0004	TRIP6 LIM 1-2-3, pYESTrp2 derivative	This study
	pGSN0005	TRIP6 LIM 1-2, pYESTrp2 derivative	This study
	pGSN0006	TRIP6 LIM 2-3, pYESTrp2 derivative	This study
	pGSN0007	TRIP6 LIM 1, pYESTrp2 derivative	This study
	pGSN0008	TRIP6 LIM 2, pYESTrp2 derivative	This study
	pGSN0009	TRIP6 LIM 3, pYESTrp2 derivative	This study
	pCR2.1-TOPO	General cloning vector	Invitrogen
	pGSN0010	SrfH L10P, pGSN001 derivative	This study
	pGSN0011	SrfH I22N, pGSN001 derivative	This study
	pGSN0012	SrfH D114A, pGSN001 derivative	This study
	pGSN0013	SrfH H45Y, pGSN001 derivative	This study
	pGSN0014	SrfH V68E, pGSN001 derivative	This study
	pWSK29	Prokaryotic expression vector	[127]
	pMJW1810	SrfH::CyaA, pWSK29 derivative	[29]
	pGSN0015	SrfH L10P::CyaA, pMJW1810 derivative	This study
	pGSN0016	SrfH I22N::CyaA, pMJW1810 derivative	This study
	pGSN0017	SrfH V68E::CyaA, pMJW1810 derivative	This study
	pIRES2-eGFP	Eukaryotic expression vector	Clontech
	pHsrfH	Human codon optimized srfH	Blue Heron

		(HsrfH)	
	pJG001	HsrfH-HA, pIRES2-eGFP derivative	This study
	pGSN0018	HsrfH L10P-HA, pJG001 derivative	This study
	pGSN0019	HsrfH I22N-HA, pJG001 derivative	This study
	pcDNA-FLAG-TRIP6	FLAG-TRIP6	[110]
	pGSN0020	HsrfH-FLAG, pIRES2-eGFP derivative	This study
	pCMV-Myc-TRIP6	Myc-TRIP6	[110]
	pCMV-HA-Src	HA-Src	[110]
	pGSN0021	SrfH-HA, pMJW1810/pWSK29 derivative	This study
	pGSN0022	SrfH L10P-HA, pGSN0021 derivative	This study
	pGSN0023	SrfH I22N-HA, pGSN0021 derivative	This study

Yeast two-hybrid assays

β-galactosidase assays were performed according to the Hybrid Hunter Manual (Invitrogen) and Current Protocols in Molecular Biology [128]. Sample data was normalized to the Fos + Jun control set to a value of one. Yeast X-gal overlay assays were performed according to the online protocol of the Herskowitz lab (http://biochemistry.ucsf.edu/labs/herskowitz/xgalagar.html).

SrfH secretion assays

For CyaA' secretion assays, J774 macrophages were infected and analyzed for cAMP levels as previously described [29]. To evaluate secretion by Western hybridization, RAW264.7 macrophages were infected at an input MOI = 500 in a 6 well dish. This is equivalent to 5-10 bacteria per infected cell. 30 minutes post infection, cells were washed in PBS, and extracellular bacteria were killed by the addition of DMEM containing 100 mg/mL gentamycin (Gibco). One hour later, cells were washed again, and the media was replaced with DMEM containing 10 mg/mL gentamycin. 6 hours post infection cells were scraped into ice cold PBS and pelleted at 500 × g for 5 minutes.

Pelleted cells were lysed on ice for 30 minutes with 1.1% Triton X-100, 10% glycerol, 150 mM NaCl, 50 mM HEPES pH 7.4, 1 mM EGTA, 1 mM EDTA, 0.1 mM PMSF, 10 mM NaF, 10 mM $Na_4P_2O_7$, 1 mM $NaVO_4$, and Roche protease inhibitor cocktail without EDTA. The lysate was centrifuged to separate the samples into insoluble and soluble fractions. Samples were resolved by SDS-PAGE and analyzed by immunoblot using aHA (Covance, 1:1,000) and aTubulin (Calbiochem, 1:5,000) antibodies.

Co-immunoprecipitation (co-IP)

For co-IP experiments, HEK293T cells were transiently transfected with mammalian expression vectors encoding TRIP6, SrfH, or c-Src as described in the text. When required cells were treated with 1 mM $NaVO_4$ for 2 hrs to inhibit tyrosine phosphorylation. Cells were lysed as described above, sonicated for 10 sec, and centrifuged 10 min 16,000 × g. The soluble fraction was immunoprecipitated for FLAG-TRIP6 using anti-FLAG M2 monoclonal antibody-conjugated agarose beads (Sigma). Samples were resolved by SDS-PAGE and analyzed by immunoblot using aHA (Santa Cruz Biotechnology, 1:1000), aFLAG (Sigma, 1:1,000), aMyc (Santa Cruz, 1:2000), or aPhosphotyrosine (PY20H, Santa Cruz, 1:1000) antibodies.

Murine infection studies

6-8 week old female BALB/c mice were purchased from Jackson Laboratories (Bar Harbor, ME). All experiments were performed in accordance with Animal Care and Use Committee guidelines. Septicemia studies were performed as previously described [11].

Src kinase activation

HEK293T cells were transiently transfected with plasmids expressing SrfH-HA and Myc-TRIP6. Cells were serum starved in DMEM containing 0.1% fatty acid free BSA overnight. The following days cells were treated with 10% fetal bovin serum (FBS) for 10 minutes to stimulate Src activation. The reaction was stopped by an ice cold PBS wash, and the cells were lysed as described above. Samples were resolved by SDS-PAGE and assessed by immunoblot using aHA (Santa Cruz, 1:1,000), aMyc (Santa Cruz, 1:1000), anti-c-Src (Santa Cruz, 1:1,000), and phospho Src family (Y416) antibodies (Cell Signaling, 1:1,000).

Modeling and docking analysis

The SifA crystal structure [60]was used to generate a homology model of SrfH residues 26-140 (Modeller version 9v6). Constrained *ab initio* modeling was then applied to predict the tertiary structure of residues 1-140. Briefly, SrfH 1-140 fragments were generated from the standard Rosetta fragment server, and ten thousand independent structures were created using structural constraints calculated from the SrfH homology model. The N-termini were extracted using the MMTSB tool set and were subjected to a clustering analysis using distance constraints. The centers of the three largest clusters were chosen as the three best models, defined as having the lowest standard deviation of the mean among positions of C atoms of all residues to all other simulations in a cluster. The N-terminus 1-30 was then superimposed on SrfH by using residues 26-30 as anchors. Residues 1-25 were extracted, ligated to the SrfH homology model, and then energy minimized using CHARMM force fields. Since the centers of the top three N-terminal models showed remarkable structural similarity, we used the top cluster as our preferred model. Homology models of LIM2 and LIM3 (Modeller version 9v6) were then docked with our preferred SrfH model using Patchdock (http://bioinfo3d.cs.tau.ac.il/PatchDock) and the hits were refined using FireDock (http://bioinfo3d.cs.tau.ac.il/FireDock).

Acknowledgments

We acknowledge Jennifer Niemann, Lidia Crosa, Hyunchin Yoon, and Kaoru Geddes for technical assistance and revision of this manuscript. This work was supported by NIH R21 grant EB000985 to F.H, NIH RO1 grant CA100848 to F.-T. Lin, and NSF award 0746589 to U.S.

Chapter 4

Identification of New Secreted Effectors in *Salmonella enterica* Serovar Typhimurium

Kaoru Geddes, Micah Worley, George Niemann, and Fred Heffron

Contributions to this work

Construction and development of Cycler transposon

CyaA' screens and the identification of novel effectors

Department of Microbiology and Immunology, Oregon Health and Science University, Portland, OR

Published in Infection and Immunity, October 2005, vol. 73, no. 10, pp. 6260-6271

Abstract

A common theme in bacterial pathogenesis is the secretion of bacterial products that modify cellular functions to overcome host defenses. Gram-negative bacterial pathogens use type III secretion systems (TTSSs) to inject effector proteins into host cells. The genes encoding the structural components of the type III secretion apparatus are conserved among bacterial species and can be identified by sequence homology. In contrast, the sequences of secreted effector proteins are less conserved and are therefore difficult to identify. A strategy was developed to identify virulence factors secreted by Salmonella enterica serovar Typhimurium into the host cell cytoplasm. We constructed a transposon, which we refer to as mini-Tn5-cycler, to generate translational fusions between Salmonella chromosomal genes and a fragment of the calmodulin-dependent adenylate cyclase gene derived from Bordetella pertussis (cyaA'). In-frame fusions to bacterial proteins that are secreted into the eukaryotic cell cytoplasm were identified by high levels of cyclic AMP in infected cells. The assay was sufficiently sensitive that a single secreted fusion could be identified among several hundred that were not secreted. This approach identified three new effectors as well as seven that have been previously characterized. A deletion of one of the new effectors, steA (Salmonella translocated effector A), attenuated virulence. In addition, SteA localizes to the trans-Golgi network in both transfected and infected cells. This approach has identified new secreted effector proteins in Salmonella and will likely be useful for other organisms, even those in which genetic manipulation is more difficult.

Introduction

Pathogenic bacteria interact with host cells to create unique niches for replication and dissemination. Bacterial pathogens modify their host cells via the expression of exotoxins, proteases, and several other factors that are required for virulence. To alter the host cell, bacterial virulence factors must reach a host target. The ability of bacterial proteins to gain access to the host cell cytoplasm is often a critical step in pathogenesis. There are several defined mechanisms by which this secretion and subsequent uptake can take place. Bacterial proteins can be auto-transported, they can pass through the general secretory pathway, or most important from the standpoint of virulence, they can be secreted by one of several specialized mechanisms found in pathogenic bacteria. Many gram-negative bacterial pathogens encode type III secretion systems (TTSSs), syringe-like macromolecular complexes, to directly inject proteins into the host cell [112,177-179]. The structural genes encoding the TTSS "needle complex" are conserved among bacterial pathogens and appear to have been acquired through horizontal gene transfer. This high degree of homology has facilitated their identification through genome sequencing and analysis. In contrast, the secreted effector proteins (EPs) are often species specific, lack a consensus secretion signal, and have been difficult to identify.

Salmonella enterica serovar Typhimurium encodes two TTSSs on separate pathogenicity islands. *Salmonella* pathogenicity island 1 (SPI-1) encodes a TTSS that is responsible for mediating the intestinal phase of *Salmonella* infection [22,180]. The SPI-1 TTSS is highly expressed during late log phase in media that are relatively rich and contain high levels of salt, conditions that are thought to simulate the environment in the small intestine [181]. SopE, SipA, SptP, and AvrA are effector proteins secreted via the SPI-1 TTSS, and they promote the invasion of epithelial cells and enhance inflammation [22,45,180,182-184].

A second TTSS, encoded by *Salmonella* pathogenicity island 2 (SPI-2), is essential for the systemic phase of infection [136]. This secretion system is expressed under nutrient-starved conditions (including low magnesium and low pH) that may mimic the intracellular environment encountered by *Salmonella* [185-188]. The expression of the structural components of the secretion apparatus and many of its secreted proteins is controlled by a two-component regulatory system encoded within

SPI-2 by the *ssrA/B* genes [113,114,189-191]. Many phenotypes in infected cells have been associated with this TTSS. These phenotypes include delayed macrophage cytotoxicity, avoidance of oxidative burst, and altered inducible nitric oxide synthase (iNOS) localization [126,136,192,193]. However, the secreted virulence factors responsible for producing these phenotypes have yet to be identified. Further elucidation of EPs in *S. enterica* serovar Typhimurium may reveal the mechanisms responsible for these and other phenotypes.

An extremely useful technique has been developed to investigate the secretion of EPs. Sory et al. used the amino-terminal adenylate cyclase domain of the hemolysin/adenylate cyclase toxin (CyaA) from *Bordetella pertussis* as a tool to demonstrate type III secretion of EPs in *Yersinia enterocolitica* [194,195]. The adenylate cyclase domain is contained within the first 400 amino acids of CyaA and is called CyaA'. CyaA' activity is entirely dependent on host cell calmodulin and is thus inactive within the bacterial cell. Adenylate cyclase activity is therefore only observed when CyaA' is translocated into host cells as part of a translational fusion to a secreted EP. The secretion of fusion proteins can thereby be easily monitored by measuring the levels of cyclic AMP (cAMP) in infected cells.

For this study, we adapted the reporter system developed by Sory et al. [195] for use in the construction of a EZ::TN (Epicenter)[196]-derived transposon called mini-Tn*5*-cycler. Mini-Tn*5*-cycler mutagenesis was used to introduce translational fusions to CyaA', thereby identifying secreted effectors by assaying cAMP levels in infected cells. The technique is sensitive because the assay detects secreted fusions even if they constitute <0.5% of the bacteria used to infect cells. The method is versatile, requiring only electroporation of a transposon/transposase complex into the target organism and no other genetic manipulation. Using this method, we identified three previously uncharacterized *S. enterica* serovar Typhimurium secreted effectors. One of these localizes to the *trans*-Golgi network (TGN) and is required for the colonization of mouse spleens following intraperitoneal infection.

Results

Construction of mini-Tn*5*-cycler transposon

The mini-Tn*5*-cycler transposon (Fig. 4-1A) is a modified EZ::TN (Epicenter)-based transposon. One advantage of this transposon is that stable transposon/transposase complexes can be prepared that can then be introduced to recipient bacteria by direct transformation of chemically competent or electrocompetent bacteria [196]. The transposition reaction requires magnesium ions supplied from the recipient cell cytoplasm to complete the reaction, resulting in insertions in the recipient DNA. Alternatively, the complete reaction may be carried out in vitro, and the recombinant DNA can then be introduced directly into the desired bacterium. This last method of transposition allows for the generation of DNA insertions within genes of bacteria that are not usually amenable to such genetic manipulation, and this procedure can be further extended to yeast and mammalian cells. Thus, this construct can be utilized in many pathogenic organisms, making it an important tool for the identification of secreted virulence factors. The basis for the identification of secreted *Salmonella* virulence factors is that the mini-Tn*5*-cycler transposon contains a promoterless *cyaA*' gene, oriented to allow the construction of translational fusions with external genes.

Functional analysis of mini-Tn*5*-cycler mutagenesis

To confirm that mini-Tn*5*-cycler transposition could result in functional *cyaA*' gene fusions, *srfH* (also called *sseI*), an *S. enterica* serovar Typhimurium gene encoding an effector secreted by the SPI-2 TTSS [113,114,197], was cloned into a suicide vector and mutagenized with mini-Tn*5*-cycler in vitro (Fig. 4-2B). An in-frame chromosomal *srfH*::*mini-Tn5-cycler* allele was created. This strain was used to infect J774 macrophages under growth conditions in which the SPI-1 TTSS is repressed and the SPI-2 TTSS is induced [126]. The level of cAMP in the infected cells was then measured by ELISA. Using an input MOI of ~1, which results in <5% of cells being infected, we observed a >30-fold increase in host cell cAMP over the background levels when J774 macrophages were infected with *srfH::mini-Tn5-cycler* (Fig. 4-1C). Background levels of cAMP were detected in cells infected with either WT 14028s or a strain expressing a β-galactosidase-*cyaA*' (p*lacZ-cyaA*') in-frame fusion from a low-copy-number vector (Fig. 4-1C). Approximately 160-fold higher levels of cAMP were observed if a *srfH-cyaA*' fusion was

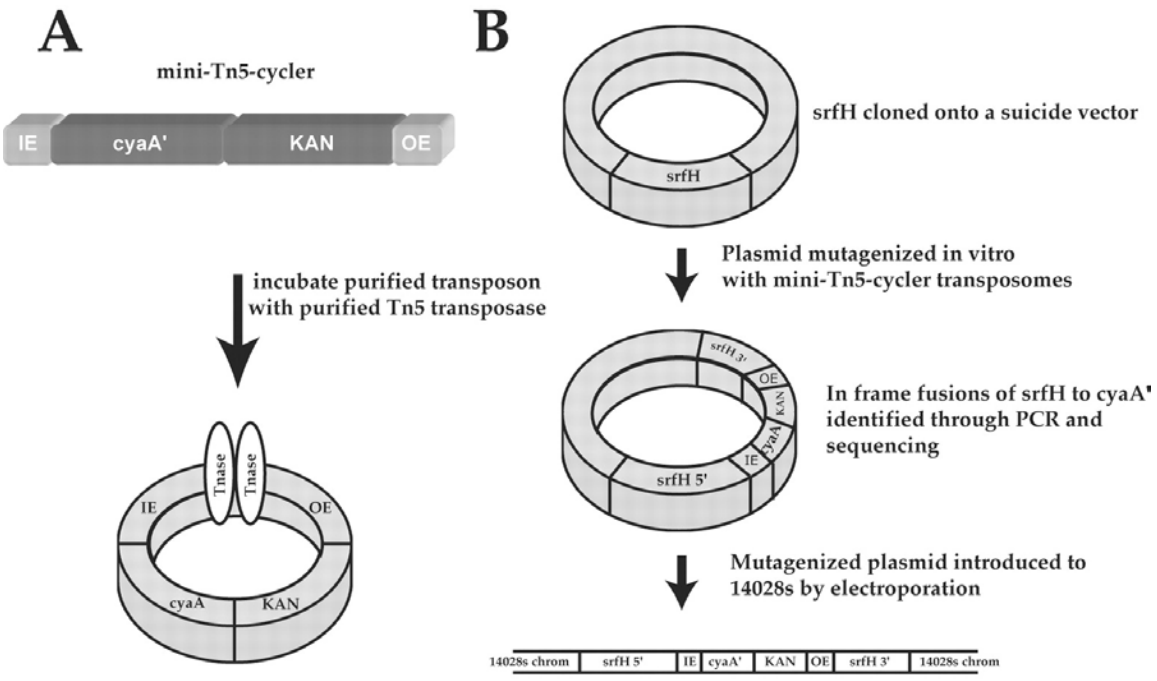

Kanamycin resistant colonies following electroporation either have an integrated plasmid with two copies of srfH after a single crossover or have a single copy of srfH with a cyaA' fusion after a double cross over, as shown above. Double crossovers were identified by PCR

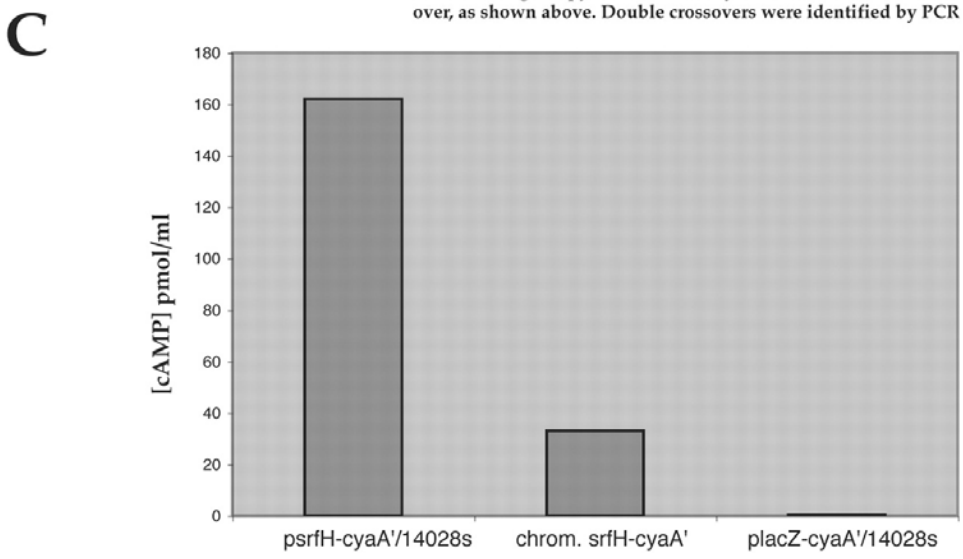

FIG. 4-1

Schematic representation of the mini-Tn5-cycler transposon (A) and mutagenesis of srfH (B). IE and OE are the modified Tn5 transposon ends (also called mosaic ends). cyaA' is the promoterless 400 amino acids of the amino terminus of cyaA from *Bordetella bronchiseptica*. KAN represents the Tn903 aminoglycoside phosphotransferase. To test our system, *srfH* was cloned into pBluescript (B). The purified plasmid was mutagenized in vitro using mini-Tn5-cycler transposon/transposase complexes (transposons) by the addition of 5 mM magnesium. Plasmids containing insertions were selected on LB-kanamycin plates, and in-frame insertions in *srfH* were identified by PCR and sequencing. An in-frame fusion of *srfH-cyaA*' at the codon encoding amino acid 145 was then cloned into the suicide vector pKas32. The suicide vector containing an in-frame insertion of mini-Tn5-cycler was then electroporated into 14028s. Crossover events were selected on LB-kanamycin, and a double crossover was identified by PCR. (C) Secretion by srfH::mini-Tn5-cycler. Stationary-phase cultures of srfH::mini-Tn5-cycler, a mutant expressing a fusion from a low-copy-number plasmid (psrfH-cyaA'), or a mutant expressing a fusion of CyaA' to the β-galactosidase alpha peptide (placZ-cyaA') were used to infect J774 macrophages for 8 h at an MOI of ~1. Infected cells were lysed with 0.1 M HCl, and the concentration of cAMP (pmol/ml) in the lysates was measured by ELISA.

expressed from a low-copy-number plasmid vector (p*srfH-cyaA*') (Fig. 4-1C). Secretion of the SrfH-CyaA' fusion protein did not appear to significantly increase the level of macrophage cell death during the course of an 8-h assay (data not shown). We wished to establish if a mixed infection containing a minority of the hybrid fusion-expressing bacteria and a majority of bacteria that do not express *cyaA*' could be used. This would allow us to screen large pools of mutagenized bacteria rather than having to screen the bacteria one by one, which is an impossible task. For control experiments, we used a mixed infection containing *srfH*::*mini-Tn5-cycler* at various ratios with the parent strain. The dilution of *srfH*::*mini-Tn5-cycler* with a 200-fold excess of wild-type 14028s cells still resulted in a 10-fold increase in cAMP levels in infected J774 cells (data not shown). These results demonstrate that a single in-frame fusion to a secreted EP can be detected among 200 proteins that do not express *cyaA*'. To make the assay even more sensitive, we tried varying the input MOI and found that even an MOI of 500 bacteria per cell was tolerated and further increased the detected cAMP levels.

Library construction and analysis

The strategy used to identify secreted effectors is shown in Fig. 4-2. Mini-Tn*5*-cycler transposon/transposase complexes were electroporated into *S. enterica* serovar Typhimurium strain 14028s to create libraries containing approximately 5,000 independent insertions. These bacteria were mixed together, the number of bacteria was determined by measuring the optical density, and the bacteria were then diluted into wells of a 96-well microtiter dish so that the wells contained pools of 50 to 100 bacteria. These pools were either grown overnight to stationary phase and used to infect J774 macrophages for 8 to 10 h at an input MOI of ~250 or grown to logarithmic phase and used to infect HeLa cells for 2 h at an input MOI of ~150. Following infection, cells were lysed with 0.1 M HCl, and the concentration of intracellular cAMP was determined. The bacteria corresponding to any well showing at least a 10-fold increase in cAMP above background levels were replated for the isolation of individual colonies. From these colonies, smaller and smaller pools were constructed until individual positive clones were obtained. The transposon in each positive clone was P22 transduced to a new background, retested, and processed for DNA sequencing to identify the transposon-*Salmonella*-chromosome junction.

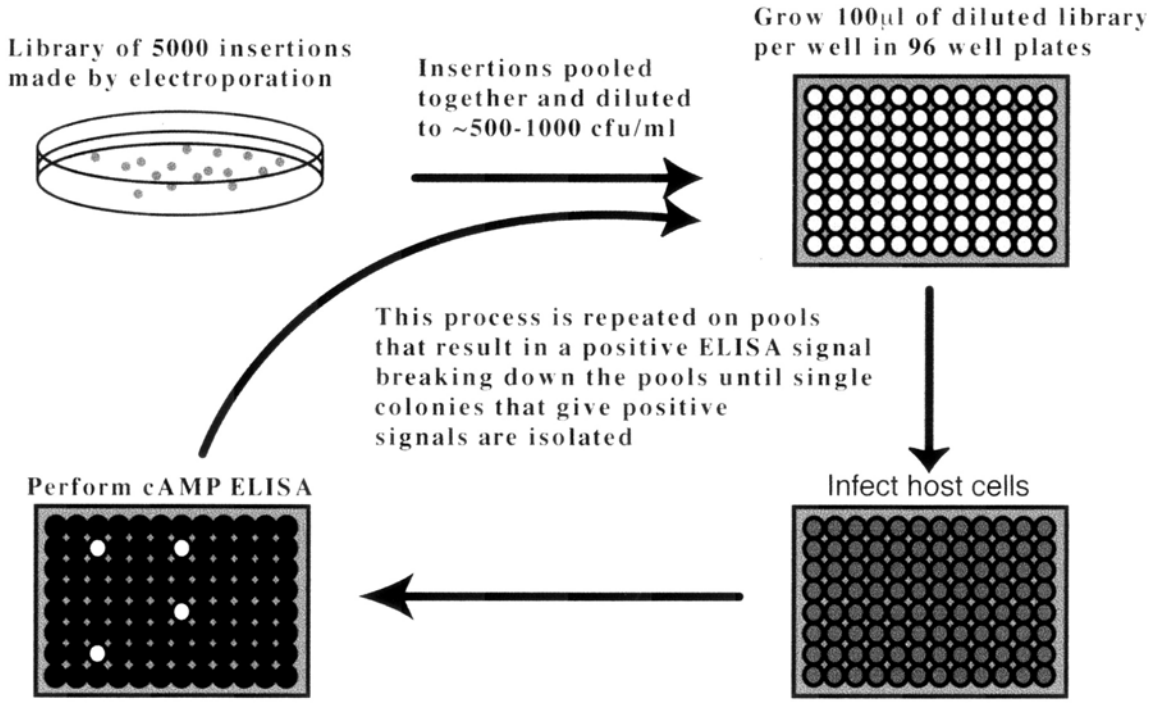

FIG. 4-2

Strategy for identifying effectors. Libraries of approximately 5,000 insertions were generated by electroporating mini-Tn5-cycler transposon/transposase complexes into either 14028s or a ΔslrP derivative. These colonies were diluted in LB broth to approximately 500 to 1,000 bacteria/ml (based on optical density readings at 600 nm), and 100-µl aliquots of the diluted library were grown to either stationary phase or late log phase. These cultures were then used to infect J774 cells or HeLa cells seeded in 96-well plates. After 8 to 10 h of infection for J774 cells or 2 h for HeLa cells, the medium was removed, and 0.1 M HCl was added to lyse the cells. The level of cAMP in each well was then measured using an ELISA. Any pool from which infected cells showed at least 10 times higher levels of cAMP than the background level was isolated and screened further by repooling into smaller groups (10 or 1) until individual bacteria containing the cognate CyaA' fusion were obtained.

Six libraries were generated from independent electroporation reactions containing a total of ~30,000 insertions. The majority of these were screened for *cyaA*' secretion in infected J774 macrophages. After screening these insertions, we identified a total of 23 positive signals, of which 17 were fusions to the known secreted effector *slrP*. Sequence analysis demonstrated that all *slrP* insertions had occurred at the same nucleotide position, although at least five of these were independent isolates. This suggested the presence of a Tn*5* transpositional "hot spot." To avoid this hot spot, six additional libraries, each containing approximately 5,000 insertions, were constructed in a Δ*slrP* background. Sixteen positive fusions were identified from a screen of 25,000 insertions in this Δ*slrP* background. In addition to our screens with the J774 macrophage cell line, a single library of 5,000 insertions in the Δ*slrP* background was screened in HeLa cells. Three clones were identified from this pool. Each contained a *cyaA*' fusion to *sipA*, which encodes a previously characterized effector [198]. Sequence analysis of each of these *sipA* insertions demonstrated that they were identical and likely to be siblings. In summary, for every 5,000 mini-Tn*5*-cycler insertions screened, three or four positive fusions were identified.

In total, we isolated 42 positive clones, each of which contained an in-frame insertion in either a gene encoding a known EP or an ORF encoding a protein of unknown function. Following DNA sequencing of all 42 clones, we found fusions to 10 different ORFs, of which 7 had been previously identified to encode secreted effectors. Three of the fusions were to unknown ORFs that presumably encode new effectors. Table 4-1 lists the genes isolated in our screen, along with a short description of each gene's reported function, the number of times each gene was isolated, and the number of unique insertion sites and independent isolates. The genes identified were *sipA* [198], *slrP* [113,199], *pipB2* [66], *sptP* [200], *sseJ* [201], *srfH* [114,188], *avrA* [182,202], and *Salmonella enterica* serovar Typhimurium LT2 reference numbers STM1583, STM1629, and STM1698 [203]. We refer to these last genes as *Salmonella* translocated effectors (*ste*) *steA* (STM1583), *steB* (STM1629), and *steC* (STM1698). Interestingly, there were five unique insertions in *pipB2* and four unique insertions in *steC* (Table 4-1).

Table 4-1. List of genes isolated in screens.

Gene	No. of times isolated	No. of unique insertion sites	No. of independent isolates	Known/predicted function of gene product	Reference(s)
slrP	17	1	5	Type III secreted protein involved in murine virulence	[199]
pipB2	8	5	5	Type III secreted protein, SsrB regulated	[66]
steC (STM1698)	5	4	5	Putative inner membrane protein, SsrB regulated	[203], Rue and Heffron (unpublished)
sipA[b]	3	1	1	Type III secreted protein-neutrophil migration, inflammation, actin polymerization	[45,183,184]
sseJ	2	2	2	Type III secreted protein, SsrB regulated	[113]
steA (STM1583)	2	1	1	Putative cytoplasmic protein	[203]
srfH	2	1	1	Type III secreted protein, affects macrophage motility, SsrB regulated	[114,188], M. Worley and F. Heffron (unpublished)
sptP	1	1	1	Type III secreted protein with phosphatase activity	[200]
steB (STM1629)	1	1	1	Putative dipicolinate reductase	[203]
avrA	1	1	1	Type III secreted protein, NFB localization	[182]

[a] Genes were isolated by mini-Tn*5*-cycler mutagenesis and ELISA of J774 cells or HeLa cells

[b] Identified from infection of HeLa cells.

An intact TTSS is required for secretion of the newly identified EP

The fact that seven of the identified genes encode known effectors strongly suggested that our approach was working, but it was necessary to confirm that the newly identified ORFs were also secreted via a type III secretion apparatus. For these experiments, we utilized both genetic mutants defective in needle complex assembly and growth conditions that either induce or repress expression of the two *Salmonella* type III secretion systems. Each fusion was transduced into both an *invA*::*cat* mutation that

renders the bacteria defective for SPI-1 TTSS-dependent secretion and an *ssaK*::*cat* mutant defective for SPI-2 TTSS-dependent secretion. The 10 unique mini-Tn*5*-cycler fusions were tested under conditions that allow expression of the SPI-1 TTSS [204]. Strains harboring *cyaA*' fusions were grown to late log phase and used to infect J774 macrophage-like cells for 1 h. As shown in Fig. 4-3A, there was a significant increase in cAMP for J774 cells infected with the SipA-, SptP-, AvrA-, SlrP-, SteA-, and SteB-CyaA' fusions. The secretion of these fusions was dependent on an intact SPI-1- but not SPI-2-encoded TTSS. Secretion of the remaining four fusions (SseJ, SrfH, PipB2, and SteC) could not be detected under SPI-1-inducing conditions (Fig. 4-3A). Similar results were observed following infection of HeLa cells (data not shown).

Next, strains harboring each *cyaA*' fusion in either a WT, *invA*::*cat*, or *ssaK*::*cat* background were grown to stationary phase in order to repress SPI-1 and induce SPI-2 expression. These cultures were used to infect J774 macrophages for 8 h at an input MOI of ~250. As shown in Fig. 4-3B, with the exception of SipA-CyaA', every fusion that we tested resulted in a significant increase in host cell cAMP which was dependent on an intact SPI-2 TTSS. Similar results were found when we infected the dendritic cell line JAWS II (data not shown).

We focused on the characterization of the three newly identified secreted effectors. We constructed *cyaA*' fusions to full-length copies of *steA*, *steB*, and *steC* to rule out aberrant secretion by the flagella or some as yet uncharacterized mechanism. As before, we tested the full-length CyaA' fusions to SteA, SteB, and SteC in either the WT, *invA*::*cat*, or *ssaK*::*cat* background for secretion into infected host cells. The same conditions were used as before to induce either the SPI-1 TTSS or the SPI-2 TTSS, and the secretion profiles of the full-length fusion proteins were found to be identical to those of the original fusions (Fig. 4-4).

***steA* is required for efficient colonization of mouse spleens**

To determine if *steA*, *steB*, or *steC* plays a role in a mouse infection model, competitive infections were performed. Deletions of *steA*, *steB*, and *steC* were generated using the λ-red recombination system [176], and the competitive index of each strain was determined (Table 4-2). Neither the Δ*steB* nor Δ*steC* strain had a competitive index statistically different from that of the control wild-type strain. However, the Δ*steA* strain

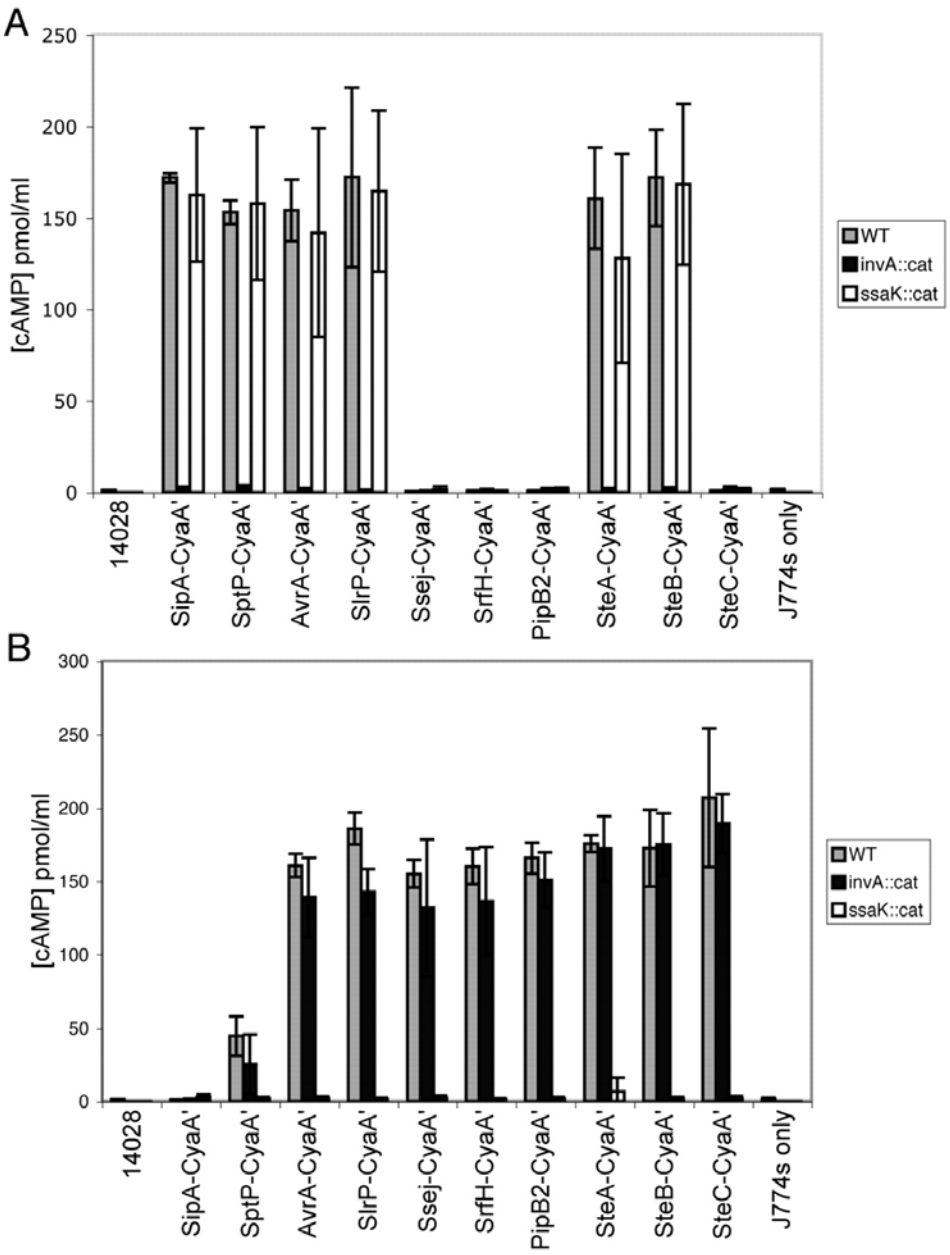

FIG. 4-3

SPI-1 TTSS (A)- and SPI-2 TTSS (B)-dependent secretion of CyaA' fusions into J774 macrophages. Levels of cAMP were measured within the macrophage-like cell line J774 following infection with the 10 cyaA' fusions listed in Table 2. Three different backgrounds were used for this experiment. These were WT (gray bars), *invA*::*cat* (black bars), and *ssaK*::*cat* (white bars). Bacteria were grown to late log phase and used to infect J774 cells at an input MOI of ~50 for 1 hour (A) or were grown to stationary phase and used to infect J774 cells for 8 h at an input MOI of ~250 (B). The cells were then lysed with 0.1 M HCl, and an ELISA (Assay Designs) was used to quantitate the cAMP levels. The cAMP concentration (in pmol/ml) was measured in triplicate samples, and the error bars represent 1 standard error of the mean.

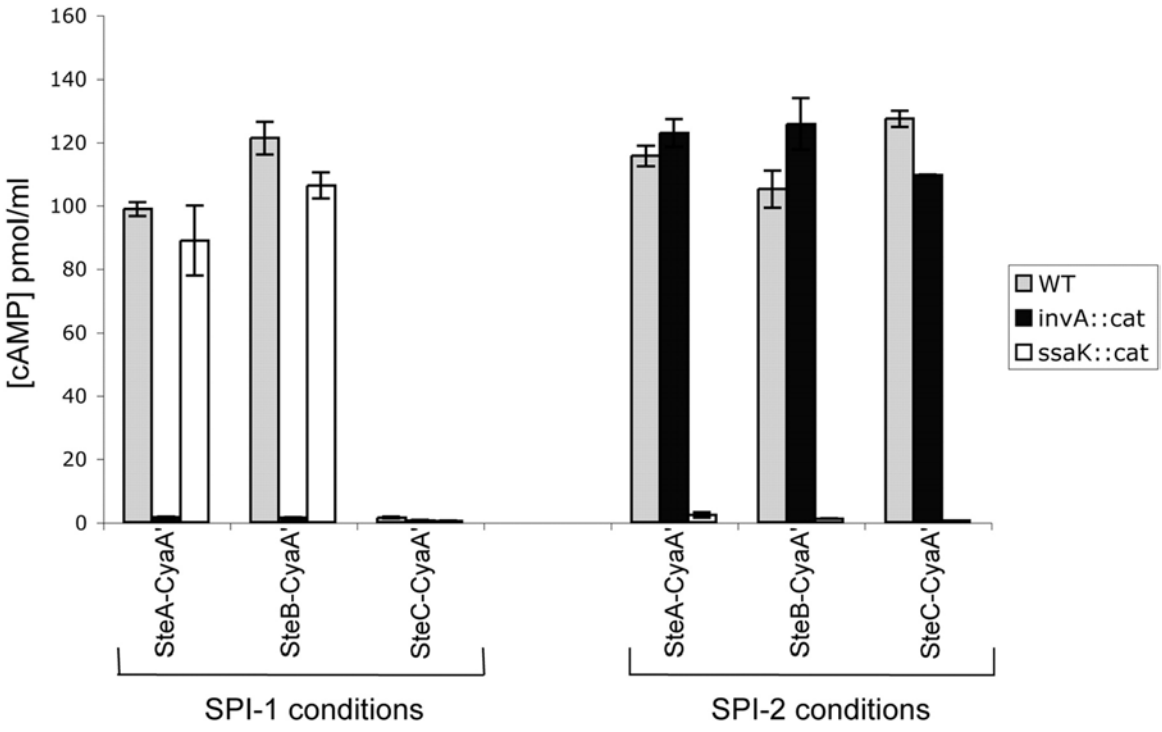

FIG. 4-4

SPI-1 TTSS- and SPI-2 TTSS-dependent secretion of full-length CyaA' fusions. Levels of cAMP were measured within the macrophage-like cell line J774 following infection with SteA-CyaA', SteB-CyaA', and SteC-CyaA'. Three different backgrounds were used for this experiment. These were WT (gray bars), *invA*::*cat* (black bars), and *ssaK*::*cat* (white bars). Bacteria were grown to late log phase and used to infect J774 cells at an input MOI of ~50 for 1 hour (SPI-1 conditions) or were grown to stationary phase and used to infect J774 cells for 8 h at an input MOI of ~250 (SPI-2 conditions). The cells were then lysed with 0.1 M HCl, and an ELISA (Assay Designs) was used to quantitate the cAMP levels. The cAMP concentration (in pmol/ml) was measured in triplicate samples, and the error bars represent 1 standard error of the mean.

had an approximately threefold competitive disadvantage for mouse spleen colonization. Expressing *steA* from its native promoter in a low-copy-number vector (p*steA*) complemented this competitive defect.

Table 4-2. Competitive infections using Δ*steA*, Δ*steB*, Δ*steC*, and *steA* complemented strains[a]

Genotype	Median CI	No. of mice	*P* value
14028s	1.026	10	>0.05
Δ*steA*	0.306	10	<0.05
p*steA*/Δ*steA*	1.261	10	>0.05
Δ*steC*	2.497	10	>0.05
Δ*steB*	1.071	10	>0.05

[a] All strains were competed against MA6054. BALB/c mice were injected intraperitoneally, and then spleens were harvested and recovered CFUs were used to determine the CI as described in Materials and Methods. Student's *t* test was used for statistical analysis of the data, and the resulting *P* values are shown.

SteA localizes to the Golgi network in host epithelial cells

Because of its potential role as a virulence factor, we further characterized *steA*. HeLa cells were transfected with an expression vector expressing either EGFP alone or a translational fusion of SteA to EGFP. As shown in Fig. 4-5, cells transfected with the EGFP expression vector alone displayed uniform fluorescence throughout the cell. In contrast, EGFP fluorescence was concentrated in perinuclear regions in cells transfected with a plasmid expressing the SteA-EGFP fusion protein. To further define this perinuclear compartment, transfected cells were costained with Bodipy-TR-ceramide, a dye that targets the Golgi network. In Fig. 4-5C, SteA-EGFP is shown to extensively colocalize with Bodipy-TR-ceramide. This suggests that SteA localizes to the TGN when it is expressed in host cells.

The subcellular localization of SteA translocated by the bacteria was also investigated. SteA-HA/14028s, a double-HA-tagged SteA fusion-expressing strain, was

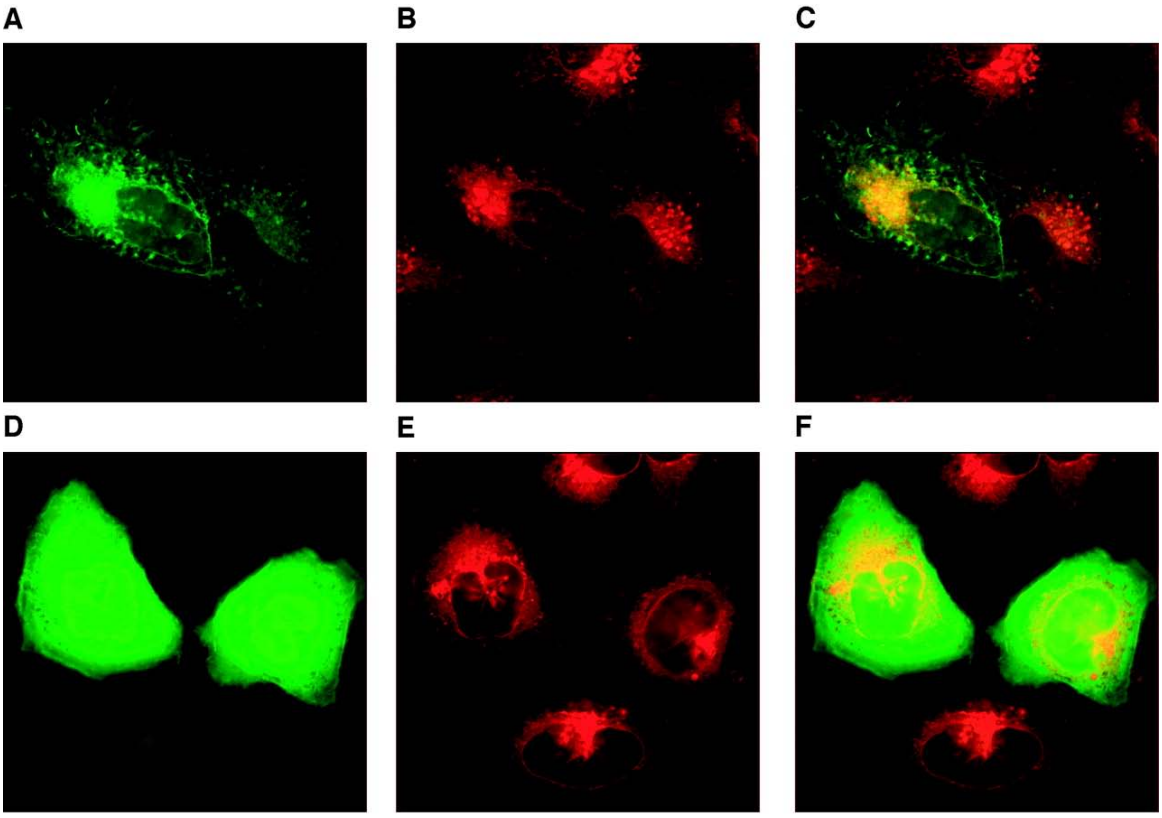

FIG. 4-5

A SteA-eGFP fusion expressed in HeLa cells colocalizes with the TGN. HeLa cells were transfected for 24 h with pEGFP (bottom panels) or pSteA-EGFP (top panels), and Bodipy-TR-ceramide (red) was used to stain the TGN. The images shown are 0.2-µm z sections captured using deconvolution microscopy. EGFP fluorescence images are shown in panels A and D, and Bodipy-TR-ceramide fluorescence images are shown in panels B and E. Panels C and F show mergers of panels A and B and panels D and E, respectively. In panels C and F, the areas where EGFP and Bodipy-TR-ceramide fluorescence overlap are yellow.

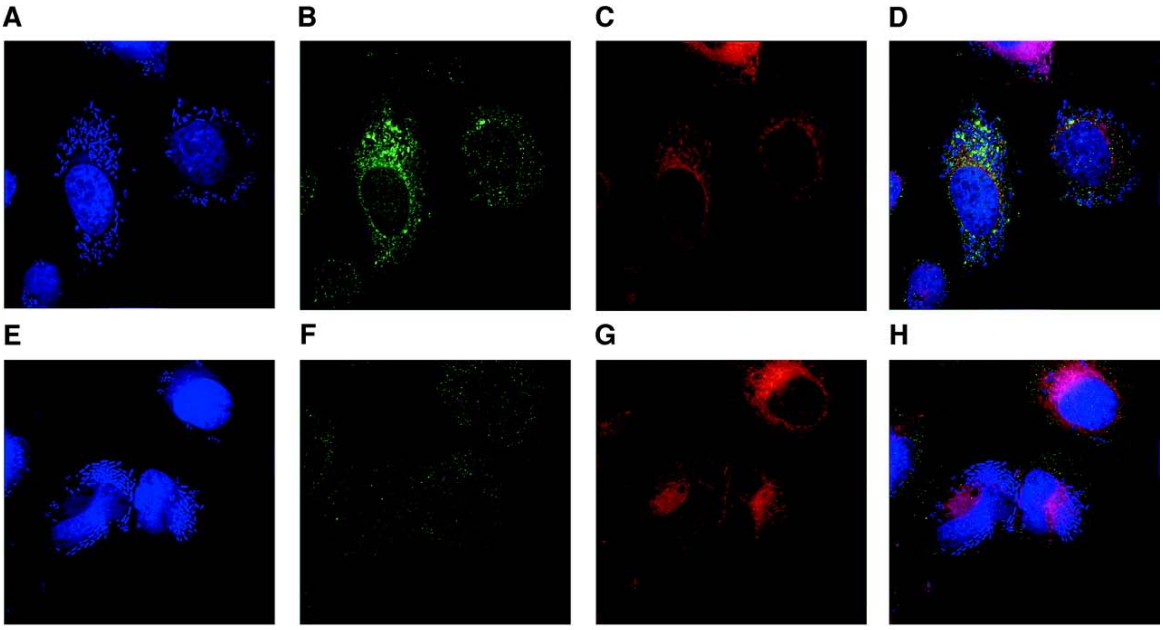

FIG. 4-6

Secreted SteA colocalizes with the TGN in infected HeLa cells. HeLa cells were infected with SteA-HA/14028s (top panels) or with WT 14028s (bottom panels) for 4 hours at an MOI of 100 under SPI-1-inducing conditions. HA-specific antibodies were used to visualize HA-tagged SteA (green). Bodipy-TR-ceramide (red) was used to stain the TGN, and the DNA stain DRAQ5 (blue) was used to visualize host cell nuclei and bacteria. DRAQ5 fluorescence images are shown in panels A and E, HA tag-specific fluorescence images are shown in panels B and F, and Bodipy-TR-ceramide fluorescence images are shown in panels C and G. Panels D and H show mergers of the images from panels A to C and E to G, respectively.

used to infect HeLa cells for 4 hours under SPI-1-inducing conditions. Alexa Fluor 488-conjugated antibodies were used to visualize SteA-HA by fluorescence microscopy, and Bodipy-TR-ceramide was again used to visualize the TGN. In many infected cells, little to no SteA-HA-specific fluorescence was seen, possibly due to low expression levels of SteA. In addition, most of the SteA-HA-specific fluorescence that was observed was found only in proximity to bacteria in infected cells. However, in a few isolated cells containing large numbers of bacteria, broader SteA-HA-specific staining could be seen (Fig. 4-6B). In these cases, it was possible to see SteA-specific staining that was not directly adjacent to bacteria. As shown in Fig. 4-6D, in a cell with extensive SteA-HA-specific staining, SteA-HA colocalized with Bodipy-TR-ceramide. This staining was specific, as it was never observed in cells infected with WT 14028s (Fig. 4-6F). These data, along with the data from transfected cells, strongly suggest that secreted SteA localizes to the TGN.

Discussion

This report describes a novel strategy for the identification of secreted effector proteins. In this work, three previously unidentified effectors, SteA, SteB, and SteC, were found. Using a competitive infection model, we show that one of these effectors, SteA, is required for *Salmonella* to colonize the mouse spleen. SteA was also shown to localize to the *trans*-Golgi network within both transfected and infected epithelial cells. Evidence of the power of this approach is demonstrated by the identification of seven known secreted effectors in the same screen.

At least four strategies have been used to identify secreted EPs in *Salmonella* and other pathogens. Guttman et al. described a de novo method of screening using wilting of plant leaves as an easily observed phenotype. However, their method is limited to certain plant pathogens such as *Pseudomonas syringae* [201]. Luo and Isberg used selection and screening to identify type IV secreted proteins in *Legionella pneumophila* [205]. Their method requires the identification of secreted proteins based on interbacterial transfer and thus could not be applied to the type III secreted effectors we have found. Tu et al. constructed a mini-Tn*5cyaA*' transposon similar to ours but identified only surface-exposed proteins in *Bordetella bronchiseptica* [206]. Our mini-Tn*5*-cycler screen employed a more sensitive enzymatic assay and relied on the infected host cell to supply calmodulin. In our assay, we only identified translocated effectors, as evidenced by the fact that an intact secretion apparatus was required for each of the 10 EPs found. Of the 60,000 mutants we screened, 42 produced detectable adenylate cyclase activity in infected cells, and each encoded an in-frame fusion to a secreted effector protein.

We wondered if it is possible to calculate the total number of effectors encoded by *Salmonella* based on the sample we examined. Assuming that insertion is random, there are several other factors that will reduce the chance of identifying any given effector. First, there is a one-in-six chance of an insertion occurring in the correct orientation and reading frame of any given gene. Second, the target area must be only a portion of a given gene because sequences that are essential for secretion or binding to a chaperone will be excluded. Third, however sensitive the assay is, the level of expression must be above a given threshold of detection. These caveats make it difficult to extrapolate from the number of effectors identified in our screen but do imply that there are many as yet

undetected effectors. In addition, we have only examined specific conditions and cell types. More EPs might be identified if other cell types are used and if the infection time is varied. For example, SseK2, a recently identified effector in *S. enterica* serovar Typhimurium, is secreted only after 21 h of infection [207]. SseK2 and possibly other effectors secreted at later time points would only have been detected if we had lengthened the infection time. One additional limitation that we observed stemmed from the existence of transpositional hot spots resulting in the repeated isolation of mini-Tn*5*-cycler fusions to *slrP*. In fact, many of the identified genes were only found after the deletion of *slrP*. Presumably, a systematic deletion of effectors that are uncovered in the screen could be used to detect additional new genes. Additionally, some genes encoding EPs are simply not amenable to mini-Tn*5*-cycler mutagenesis, including any that are targeted to vesicles that do not contain calmodulin as well as those with extremely small targets for transposition.

Our technique can be used to identify secreted type III EPs from a wide range of pathogens and possibly proteins secreted by other mechanisms. CyaA' has been used to demonstrate type IV secretion [208], and in *B. pertussis*, CyaA is secreted via a type I secretion system [209]. Finally, there are many genetically intractable organisms for which the isolation of a large number of transposon insertions is simply not possible, even by electroporation of transposon complexes. In these cases, it may be possible to express a gene library from a plasmid in a genetically tractable host that also expresses the complete structural apparatus for secretion, thereby making it amenable to mini-Tn*5*-cycler mutagenesis.

Three new secreted EPs were identified in the screen, namely, SteA, SteB, and SteC. The genes encoding all three of these proteins have low GC contents (*steA* GC content, 43%; *steB* GC content, 41.9%; and *steC* GC content, 38%), suggesting horizontal acquisition, which is common for virulence-associated genes. The Δ*steA* strain was found to have a competitive defect in colonization of the mouse spleen, whereas *steB* and *steC* did not appear to play a significant role in this model. This competitive defect suggests that *steA* is required either for passage of the bacteria from the peritoneal cavity into the spleen, for survival and replication within host cells, or for avoiding host immune defenses.

Interestingly, SteA localizes to the Golgi network in transfected and infected HeLa cells. SseG, another EP in *S. enterica* serovar Typhimurium, has also been shown to localize to the Golgi network [210]. The presence of SseG was found to be important for the association of *Salmonella*-containing vacuoles with the Golgi network. Furthermore, the association of *Salmonella*-containing vacuoles with the Golgi network was required for normal bacterial replication within HeLa cells. We are investigating whether SteA plays a similar role to that of SseG in infected cells. The coding sequence of *steA* is 94% conserved in *Salmonella enterica* serovar Typhi strains TY2 and CT18 and 95% conserved in *Salmonella enterica* serovar Paratyphi strain ATCC 9150. This conservation suggests that *steA* may be important for virulence in human infections as well. In a recent paper by Morgan et al., STM1698 (the ORF encoding SteC) was identified as the gene for a colonization factor specific for the chick infection model [211]. The coding sequence of *steC* is 93% conserved in *Salmonella enterica* serovar Paratyphi strain ATCC 9150 and *Salmonella enterica* serovar Typhi strains TY2 and CT18, again suggesting a possible role in human infection. Of the three newly described proteins, only SteB has significant homology to a bacterial protein from a different species: it shares 40% amino acid identity to a protein in the tropical pathogen *Chromobacterium violaceum*. This pathogen is found in water and soil throughout tropical South America and causes septicemia with metastatic abscesses with a 64% fatality rate. *C. violaceum* contains genes encoding a TTSS, suggesting that the homology may be meaningful [212]. SteB (STM1629) is encoded in a genetic island in close proximity to the gene for another secreted protein, SseJ (STM1631). STM1630, the ORF immediately downstream of *steB*, is required for virulence in both the calf and chick infection models [211].

Interestingly, five of the EPs identified were secreted by both the SPI-1 and SPI-2 TTSSs (SptP, SlrP, AvrA, SteA, and SteB), whereas SipA was observed to be secreted only via the SPI-1 TTSS. Since these five proteins are secreted by both TTSSs, they may function in both the intestinal and systemic phases of infection. Four of the identified proteins, SseJ, SrfH, PipB2, and SteC, were only secreted via the SPI-2 TTSS. These results raise two possibilities that are not exclusive, either that these effectors are only expressed under one condition or that they cannot be secreted through the alternative needle complex. The expression of all four of these genes is regulated by SsrB

([113,114]; J. Rue and F. Heffron, unpublished data). These data suggest that proteins secreted exclusively by the SPI-2 TTSS are regulated by SsrB, while proteins secreted by both the SPI-1 and SPI-2 TTSSs are regulated by an unknown mechanism. The observed secretion patterns may be a result of a SPI-1 or SPI-2 TTSS-specific signal in the RNA messages or amino acid sequences of these proteins. Alternatively, TTSS specificity may be determined by either the regulation of expression of the EPs themselves or the regulation of expression of the chaperones required for their secretion.

While the mini-Tn*5*-cycler transposon may allow the identification of a large number of new EPs, identifying these proteins is only the first step in the further study of EPs. Many years have been spent studying secreted bacterial EPs, but the functions of only a few have been fully elucidated. Several more *S. enterica* serovar Typhimurium EPs are thought to exist because the cognate EPs for many observed pathogenic phenotypes remain a mystery. This report provides the initial step in expanding our knowledge of the repertoire of secreted EPs in *Salmonella* and potentially many other bacterial pathogens.

Materials and methods

Bacterial strains, tissue culture, and growth conditions

The strains and plasmids used for this study are listed in Table 4-3. *Salmonella enterica* serovar Typhimurium strain 14028s was used as the wild-type (WT) strain. Bacteria were grown at 37°C in Luria-Bertani broth (LB). Kanamycin was used at 60 μg ml^{-1}. Chloramphenicol was used at 30 μg ml^{-1}. Carbenicillin was used at 100 μg ml^{-1}. Tetracycline was used at 20 μg ml^{-1}. HeLa cells and J774 macrophages were obtained from the American Type Culture Collection. Cells were maintained in Dulbecco's modified Eagle medium (DMEM) supplemented with 10% fetal calf serum, sodium pyruvate, and nonessential amino acids and grown at 37°C with 5% CO_2. All P22 transductions were performed as previously described [129]. Transductants were streaked for isolation on LB agar containing 10 mM EGTA and then confirmed for smooth lipopolysaccharide and lack of pseudolysogeny by cross-streaking transductants against P22 on Evan's blue uranine plates.

Table 4-3. Strains and plasmids used for this study.

Strain or plasmid	**Genotype**	**Source or reference**
Strains		
14028s	WT S. enterica serovar typhimurium	ATCC
HH100	14028s steC::mini-Tn5-cycler fusion at amino acid 447	This work
HH101, 104	14028s steA::mini-Tn5-cycler fusion at amino acid 174	This work
HH102, 105, 106, 109, 110, 111-114, 116-123, 126	14028s slrP::mini-Tn5-cycler fusion at amino acid 123	This work
HH107	14028s steC::mini-Tn5-cycler fusion at amino acid 428	This work
HH108	14028s pipB2::mini-Tn5-cycler fusion at amino acid 176	This work
HH115	14028s sptP::mini-Tn5-cycler fusion at amino acid 307	This work

HH124, 125	14028s pipB2::mini-Tn5-cycler fusion at amino acid 305	This work
HH127	14028s pipB2::mini-Tn5-cycler fusion at amino acid 165	This work
HH128, 131	14028s srfH::mini-Tn5-cycler fusion at amino acid 149	This work
HH129	14028s steC::mini-Tn5-cycler fusion at amino acid 448	This work
HH130	14028s steC::mini-Tn5-cycler fusion at amino acid 369	This work
HH132	14028s steB::mini-Tn5-cycler fusion at amino acid 137	This work
HH133, 134	14028s pipB2::mini-Tn5-cycler fusion at amino acid 241	This work
HH135, 138	14028s pipB2::mini-Tn5-cycler fusion at amino acid 145	This work
HH136	14028s sseJ::mini-Tn5-cycler fusion at amino acid 168	This work
HH137	14028s avrA::mini-Tn5-cycler fusion at amino acid 252	This work
HH139	14028s sseJ::mini-Tn5-cycler fusion at amino acid 368	This work
HH140, 141, 142	14028s sipA::mini-Tn5-cycler fusion at amino acid 511	This work
HH200	MJW1835 steC::mini-Tn5-cycler fusion at amino acid 447	This work
HH201	MJW1835 steA::mini-Tn5-cycler fusion at amino acid 174	This work
HH202	MJW1835 slrP::mini-Tn5-cycler fusion at amino acid 123	This work
HH208	MJW1835 pipB2::mini-Tn5-cycler fusion at amino acid 176	This work
HH215	MJW1835 sptP::mini-Tn5-cycler fusion at amino acid 307	This work
HH228	MJW1835 srfH::mini-Tn5-cycler fusion at amino acid 149	This work
HH232	MJW1835 steB::mini-Tn5-cycler fusion at amino acid 137	This work

HH237	MJW1835 avrA::mini-Tn5-cycler fusion at amino acid 252	This work
HH239	MJW1835 sseJ::mini-Tn5-cycler fusion at amino acid 368	This work
HH240	MJW1835 sipA::mini-Tn5-cycler fusion at amino acid 511	This work
HH300	MJW1301 steC::mini-Tn5-cycler fusion at amino acid 447	This work
HH301	MJW1301 steA::mini-Tn5-cycler fusion at amino acid 174	This work
HH302	MJW1301 slrP::mini-Tn5-cycler fusion at amino acid 123	This work
HH308	MJW1301 pipB2::mini-Tn5-cycler fusion at amino acid 176	This work
HH315	MJW1301 sptP::mini-Tn5-cycler fusion at amino acid 307	This work
HH328	MJW1301 srfH::mini-Tn5-cycler fusion at amino acid 149	This work
HH332	MJW1301 steB::mini-Tn5-cycler fusion at amino acid 137	This work
HH337	MJW1301 avrA::mini-Tn5-cycler fusion at amino acid 252	This work
HH339	MJW1301 sseJ::mini-Tn5-cycler fusion at amino acid 368	This work
HH340	MJW1301 sipA::mini-Tn5-cycler fusion at amino acid 511	This work
MA6054	14028s ara-907 araD 901::MudJ	[213]
MJW1883	14028s srfH::mini-Tn5-cycler chromosomal srfH-cyaA' fusion at amino acid 145	This work
MJW1301	14028s ssaK::cat	This work
MJW1835	14028s invA::cat	This work
ΔslrP	14028s ΔslrP	This work
ΔsteA	14028s ΔsteA::kan	This work

ΔsteB	14028s ΔsteB::kan	This work
ΔsteC	14028s ΔsteC::kan	This work
SteA-HA/14028s	14028s with chromosomal double-HA-tagged SteA	This work
Plasmids		
pMJW1753	pWSK29 + cyaA'	This work
pMJW1791	pMJW1753 + lacZ (placZ-cyaA')	This work
pMJW1810	pMJW1753 + srfH (psrfH-cyaA')	This work
pMini-Tn5-cycler	pCRScript + mini-Tn5-cycler	This work
pEGFP-N1	EGFP transfection vector	Clontech
pSteA-EGFP	pEGFP-N1 + steA	This work
psteA	pWKS30 + steA	This work
pNFB15	Template vector for making double HA tag with a kanamycin resistance cassette	Lionello Bossi

Construction of *S. enterica* serovar Typhimurium mutant strains

An *ssaK*::*cat* (MJW1301) strain was constructed by first cloning the *ssaK* open reading frame (ORF) using PCR and then introducing a chloramphenicol resistance cassette into the SepI site of the gene. This construct was moved into the suicide vector pKAS32 [214], and then the disrupted *ssaK* gene was reintroduced into strain 14028s as previously described [114]. The construction of *invA*::*cat* is described elsewhere [126] and was transduced from SR-11 x 3014 into 14028s using P22 phage, resulting in strain MJW1835. Δ*slrP*, Δ*steA*, Δ*steB*, and Δ*steC* strains were constructed using the λ-red PCR-based gene deletion method [176] and were verified by PCR. All PCR primer sequences can be obtained upon request.

Construction of mini-Tn*5*-cycler transposon and mutagenesis using mini-Tn*5*-cycler transposomes

The mini-Tn*5*-cycler transposon was constructed from the DICE II transposon [215]. pDICE II was digested with EcoRI and XbaI and religated. A BamHI site downstream of the kanamycin cassette was then removed using a Quick Change site-directed mutagenesis kit (Stratagene). The *cyaA*' gene was PCR amplified from pMJW1753 and then cloned into the NdeI and BamHI sites. The resulting plasmid, pCycler, contains the completed mini-Tn*5*-cycler transposon. Mini-Tn*5*-cycler transposon/transposase complexes were prepared as previously described [196]. Transposon/transposase complexes were electroporated into *Salmonella* using the following electroporation conditions. Overnight cultures of *Salmonella* were diluted 1:100 in LB and grown at 37°C for 3 h with aeration. The culture was then pelleted and washed three times with ice-cold deionized water. Following the washes, the pellet was resuspended in 1/500 the original culture volume in ice-cold 10% glycerol. One to 3 µl of transposon/transposase complex was added to 70 µl of electrocompetent cells, which were transferred into 1-mm-gap electroporation cuvettes (BTX). For electroporation, an Electro Cell manipulator 600 (BTX) was used with the following settings: resistance, 2.5 kV; capacitance timing, 25 µF; resistance timing, 129 Ω; and charging voltage, 1.70 kV.

Creation of *srfH-cyaA', steA-cyaA', steB-cyaA',* and *steC-cyaA'* fusions

The *srfH* ORF was PCR amplified and cloned into pBluescript. This construct was mutagenized with the transposon in vitro, and in-frame fusions to *srfH* were identified by PCR and sequencing. In vitro mutagenesis of *srfH* was performed using an EZ::TN kit (Epicenter). The in-frame fusion was then cloned into the suicide vector pKAS32 and used for allelic exchange, as previously described [214], to generate the chrom-*srfH-cyaA*' strain MJW1883. To generate pMJW1753, *cyaA*' (bp 4 to 1233) was PCR amplified from a clinical isolate of *B. pertussis* and cloned into pWSK29 [127] under *lacp* control, with a GGG 5' extension to recreate the SmaI site. Cloning into this site creates a glycine linker. The *srfH* ORF and promoter were PCR amplified and cloned into the SmaI site of pMJW1753 to generate p*srfH-cyaA*'. As a control, *cyaA*' was fused to the carboxy-terminal end of the ß-galactosidase alpha peptide, generating p*lacZ-cyaA*'. The full-length *steA-cyaA*', *steB-cyaA*', and *steC-cyaA*' fusions were generated using the λ-red

recombination system [176]. To generate PCR products for recombination, forward primers contained 40 bp from the carboxy terminus of the gene being targeted at the 5' end plus the sequence 5'-CTGTCTCTTATACACATCTCA-3', and reverse primers contained 40 bp downstream of the gene being targeted plus the sequence 5'-CTGTCTCTTATACACATCTGGT-3'. Primers containing overhanging 5' sequences specific for *steA*, *steB*, and *steC* were then used to amplify the mini-Tn*5*-cycler transposon using PCR. The PCR products were digested with DpnI, dialyzed, and then electroporated into 14028s/pKD46.

Screening for translocated proteins

Libraries of ~5,000 mini-Tn*5*-cycler insertions were made. Libraries were diluted in LB to approximately 500 to 1,000 CFU/ml based on optical density readings at 600 nm. One hundred microliters of diluted library was grown in each well of a 96-well plate. Each well was then used to infect J774 cells (using SPI-2 conditions) or HeLa cells (using SPI-1 conditions) seeded in 96-well plates. If infection resulted in at least a 10-fold increase in cAMP levels, then the pool of mini-Tn*5*-cycler insertions from the 96-well plate was diluted and plated to isolate individual colonies. One hundred fifty to 300 colonies (three times the original pool size) were isolated using toothpicks, patched, and numbered. Numbered colonies were grouped into pools of 10 and then used to reinfect J774 or HeLa cells. If infection resulted in increased cAMP, then the colonies from that group of 10 mini-Tn*5*-cycler insertions were retested individually. Individual colonies with adenylate cyclase activity were transduced using P22 and then retested. Isolates that maintained adenylate cyclase activity following transduction were processed for sequencing.

Bacterial infection of cultured cells and ELISAs

Unless otherwise stated, J774 or HeLa cells were plated in 96-well plates at ~2 x 10^4 cells/well and incubated overnight at 37°C with 5% CO_2. For the infection of J774 cells under SPI-2 conditions, stationary-phase bacteria were added at a multiplicity of infection (MOI) of 250. Bacteria were centrifuged onto the cell monolayer at 200 x *g* for 5 min and then incubated at 37°C with 5% CO_2 for 1 h. The cell culture was then washed twice with phosphate-buffered saline (PBS), DMEM supplemented with 100 μg ml^{-1}

gentamicin was added, and the culture was incubated for another hour. After 1 h, the culture was washed twice with PBS, overlaid with DMEM containing 10 μg ml^{-1} gentamicin, and incubated for another 7 to 9 h. For SPI-1-dependent infections of J774 and HeLa cells, stationary-phase cultures of 14028s were diluted 1:33 in LB and grown with aeration at 37°C for 3 h. Bacteria were then added to J774 cells at an MOI of 50, centrifuged onto the monolayer at 200 x *g* for 5 min, and incubated for 1 h. HeLa cells were infected at an MOI of 150, centrifuged at 200 x *g* for 5 min, and incubated for 1.5 to 2 h. Following infections, cells were washed once with PBS and then lysed with 0.1 M HCl. The level of cAMP in the lysates was determined using a direct cAMP enzyme-linked immunosorbent assay (ELISA) kit (Assay Designs) according to the manufacturer's instructions. In all cases, the MOI refers to the amount of bacteria initially added to host cells. The actual number of bacteria entering host cells was between 1 and 5% of the initial inoculum.

Sequencing of mini-Tn*5*-cycler insertion sites and sequence analysis

Chromosomal DNA was prepared from isolated mini-Tn*5*-cycler mutants as previously described [128]. Chromosomal DNA was digested with EcoRI and cloned into the EcoRI site of pACYC184. Plasmids containing chromosomal inserts were electroporated into GeneHogs competent cells (Invitrogen), and insertions harboring chromosomal fragments with mini-Tn*5*-cycler were selected on LB agar supplemented with kanamycin. Plasmids from kanamycin-resistant colonies were then purified using a QIAprep spin miniprep kit (QIAGEN). The DNA sequence of the fusion junction was obtained using the primer 5' GTTGACCAGGCGGAACATCAATGTG 3', which is complementary to bp 166 to 190 of the 5' end of mini-Tn*5*-cycler. Sequence analysis was performed using MacVector 7.1.1 software and the NCBI BLAST server at http://www.ncbi.nlm.nih.gov/BLAST/.

Competitive infection studies

Competitive infections were based on a protocol described by Ho et al. [213]. Each strain was grown overnight in LB at 37°C with aeration. The bacteria were pelleted, resuspended in PBS, and diluted in PBS to approximately 2,000 to 20,000 CFU/ml. Each test strain was mixed 1:1 with the reference strain MA6054, and 100 μl of the mixture was injected intraperitoneally into 6- to 8-week-old female BALB/c mice. Three days

after injection, the mice were sacrificed, and their spleens were harvested and homogenized. Spleen suspensions were diluted and plated on LB plates containing X-Gal (5-bromo-4-chloro-3-indolyl-ß-D-galactopyranoside; 40 µg/ml) and arabinose (1 mM). The reference strain MA6054 has arabinose-inducible β-galactosidase activity and can be easily distinguished from the test strains when plated on LB agar with X-Gal and arabinose. The competitive index (CI) was then calculated using the following equation: (percentage of test strain recovered/percentage of reference strain recovered)/(percentage of test strain inoculated/percentage of reference strain inoculated). Student's *t* test was performed to analyze the CIs. Complementation of Δ*steA* was achieved by cloning the entire *steA* ORF and 62 bp upstream of the start codon into the low-copy-number expression vector pWKS30. The resulting plasmid, p*steA*, was electroporated into the Δ*steA* strain.

Expression of SteA-EGFP and SteA-HA in HeLa cells and visualization by microscopy

To make SteA-enhanced green fluorescent protein (SteA-EGFP), *steA* was PCR amplified and cloned into pEGFP-N1 (Clontech). The resulting plasmid, pSteA-EGFP, and pEGFP-N1 were purified using a QIAGEN EndoFree Maxi kit. HeLa cells were grown to ~25 to 50% confluency on Lab-Tek II chambered cover glass (Nalge Nunc International) and were transfected for 24 h using FuGENE 6 transfection reagent (Roche). Bodipy-TR-ceramide (Molecular Probes) was used to stain the Golgi network in live cells following the manufacturer's recommendations. A chromosomal SteA-hemagglutinin (SteA-HA) fusion was constructed using the λ-red recombination system as described by Uzzau et al. [216]. To make a double-HA-tagged SteA, the plasmid pNFB15 (received from Lionello Bossi) was used as a template for PCR using the following primer pair: 5' CGACATAAAAGCTCGCTACCATAACTATTTGGACAATTATTATCCGTATGATGTGCCGGA 3' and 5' CTGATTTCTAACAAAACTGGCTAAACATAAACGCTTTTTACACCTGCAGATCATCGAGCT 3'. The PCR product generated from these primers was introduced into 14028s/pKD46 via electroporation, and transformants were selected on LB agar containing kanamycin. The SteA-HA fusion was verified by PCR and Western blotting.

SPI-1 conditions (described above) were used to infect confluent HeLa cells on cover glass in six-well plates with SteA-HA-expressing 14028s and WT 14028s, using an MOI of 100. Bacteria were centrifuged onto the cell monolayer, and the infection was allowed to proceed at 37°C for 20 min. After this incubation, the cells were washed three times with PBS, and DMEM supplemented with 100 μg ml^{-1} gentamicin was added for 1 hour and then replaced with DMEM supplemented with 10 μg ml^{-1} gentamicin for the remainder of the 4-hour infection. Bodipy-TR-ceramide (Molecular Probes) was used to stain the TGN, and then the cells were fixed in 4% paraformaldehyde for 20 min. A mouse anti-HA monoclonal antibody (Covance) was used at a 1:100 dilution, and an Alexa Fluor 488-conjugated goat anti-mouse (Molecular Probes) secondary antibody was used at a 1:1,000 dilution. The DNA stain DRAQ5 (Alexis Biochemicals) was used at a 1:1,000 dilution to visualize host cell nuclei and bacteria. A 60x oil-immersion, 1.4-numerical-aperture objective lens was used along with standard filter sets for EGFP and Alexa Fluor 488 (488 nm), Texas Red (568 nm), and DRAQ5 (685 nm) visualization. Z sections (0.2 μm) were captured at a resolution of 1,024 by 1,024 pixels. Images were acquired by Aurelie Snyder of the OHSU-MMI Research Core Facility (http://www.ohsu.edu/core) with an Applied Precision DeltaVision image restoration system. This includes an API chassis with a precision motorized XYZ stage, a Nikon TE200 inverted fluorescence microscope with standard filter sets, halogen illumination with an API light homogenizer, a CH350L camera (500 kHz, 12-bit, 2 Mp, KAF 1400 GL, 1,317 x 1,035, liquid cooled), and DeltaVision software. Deconvolution using the iterative constrained algorithm of Sedat and Agard and additional image processing were performed on an SGI Octane workstation. Images were processed for deconvolution using Softworx (Applied Precision) image processing software.

Acknowledgments

We thank the members of the Heffron and So labs, who contributed invaluable advice and aided in revision of the manuscript. We also thank Lionello Bossi for strain MA6054, plasmid pNFB15, and helpful suggestions. We acknowledge Aurelie Schneider for performing microscopy. We are very grateful to Joanne Rue for sharing *ssrB* regulon microarray data. This work was supported by NIH grants ROI A1 022933 and ROI A1 037201.

Chapter 5

Proteomic Identification of Novel Secreted Virulence Factors from *Salmonella enterica* serovar Typhimurium

George Niemann[1]*, Roslyn N. Brown[2]*, Jean Gustin[1], Afke Stufkens[1], Afshan Kidwai[1], Jie Li[1], Jason McDermott[3], Heather M. Brewer[4], Athena Schepmoes[4], Richard D. Smith[3], Joshua N. Adkins[3], and Fred Heffron[1]

Contributions to this study

- Experimental design
- Sample preparation for proteomic analysis
- Western hybridization
- Growth curves
- Animal studies

[1]Department of Microbiology and Immunology, Oregon Health and Science University, Portland, OR

[2]Biological Sciences Division Pacific Northwest National Laboratory, Richland, WA

[3]Computational Biology and Bioinformatics, Pacific Northwest National Laboratory, Richland, WA

[4]Environmental Molecular Sciences Laboratory, Pacific Northwest National Laboratory, Richland, WA

Abstract

Salmonella enterica serovar Typhimurium is an intracellular pathogen and a leading cause of acute gastroenteritis in the world. Two, type-III secretion systems (TTSS) are necessary for virulence. The secretion systems are encoded in Salmonella pathogenicity islands 1 and 2 (SPI-1 and SPI-2) and function to deliver effector proteins to host cell cytoplasm. While many effectors have been identified and at least partially characterized, the full repertoire has not been cataloged. Here, we used mass spectrometry to identify effector proteins secreted into acidic, minimal medium, conditions that promote expression of both the SPI-2 TTSS and its effectors. The secretomes of the wild type 14028 parent strain and mutants missing essential (*ssaK*) and regulatory components (*ssaL*) of the SPI-2 secretion apparatus were compared. We identified 75% of the known type III effector repertoire. Excluding translocon components, 95% of these known effectors were secreted at higher levels in the *ssaL* mutant, demonstrating that SsaL regulates SPI-2 type III secretion. We selected 15 novel candidates and tested each one for secretion into animal cells. Secretion was assessed by constructing translational fusions to the calmodulin dependent adenylate cyclase of *Bortedella pertussis*, infection of J774 macrophages, followed by ELISA to measure cAMP levels from infected cells. From this we identified six new type III effectors and two effectors secreted independent of either TTSS. Non-polar deletions were constructed and assessed for virulence in intraperitoneally infected SvJ/129 mice. Two of these mutants were more lethal than the wild type parent strain, suggesting that some effectors function to attenuate virulence, and that TTS is not the exclusive mechanism by which an effector gains access the host cell cytoplasm during infection.

Introduction

Salmonella is a leading cause of morbidity and mortality in the developing world due to dehydration and untreated sepsis [217-219]. *Salmonella* actively secretes effector proteins into the host cell cytoplasm to disarm defensive mechanisms and to provide an intracellular, replicative niche. Many of these effectors are delivered by one of two type III secretion systems (TTSS), which are encoded on *Salmonella* pathogenicity islands (SPI-1 and SPI-2) (reviewed in [135]). The SPI-1 TTSS facilitates host cell entry and inflammation, whereas SPI-2 mediates intracellular survival [191,220]. Both SPI-1 and SPI-2 are required in a mouse model of persistent infection [221]. Over 30 TTSS effectors have been identified to date, [2,4,6,49,221], but the list is thought to be an underestimate of the true effector repertoire because there are virulence phenotypes dependent on TTS but which lack an associated effector protein [90,94].

Recent proteomic studies in *Escherichia coli* O157:H7 identified over 31 new type III effectors. This study took advantage of a *sepL* mutant that secreted effector proteins into media [222]. *E. coli* SepL localizes to the bacterial cytosol and membrane, and it interacts with Tir [223], an effector that inserts into the host cytoplasmic membrane and functions as a receptor for the bacterial protein intimin [224]. The SepL-Tir complex is thought to occlude secretion until the translocon (host membrane pore) is assembled. This ensures that Tir is secreted first and coordinates effector release. In a *sepL* mutant this system is dysregulated and effectors are secreted into media [225]. Because *Salmonella ssaL* is a homolog of *E. coli sepL*, we hypothesized that an *ssaL* mutation may have a similar phenotype in *Salmonella*.

The SPI-2 encoded type III secretion system and its many effectors are directly regulated by the two-component regulatory system SsrAB and the MarR type regulator SlyA [114,226,227]. These regulators are induced by low pH and limiting amounts of phosphate, magnesium, and iron [186-188]. The *Salmonella*-containing vacuole (SCV) can be partially mimicked *in vitro* using a semi-defined low-phosphate, low-magnesium medium (LPM) [228]. While LPM has been used to evaluate the secretion of specific SPI-2 effectors [229,230], the LPM secretome has not been analyzed as we describe here.

Discovery of the proteins secreted into LPM medium utilized an enrichment strategy based on solid phase, reverse phase chromatography resin. The captured proteins

and peptides were identified utilizing liquid chromatography-coupled tandem mass spectrometry-based proteomics. We employed a recently developed algorithm that classifies possible type III secreted proteins [231] to aid in interpreting the results and select candidates for validation. The combined experimental and machine learning approach provided an excellent strategy to successfully identify novel type III secreted proteins and may prove useful for the large number of Gram negative pathogens that contain type III secretion systems where the effectors are not known or even partially studied.

Results

Rationale for strains used in this study

We used three different isogenic *Salmonella* strains in this work: 14028, a 14028 derivative containing a non-polar deletion of the *ssaL* gene (Δ*ssaL*), and mutation in an essential component of the secretion apparatus (*ssaK*::*cat*). To each of these three isogenic strains we added a C-terminal, HA-tagged copy of SseJ and the pBAD*ssrB* plasmid. SseJ::HA allowed us to monitor secretion of a SPI-2 effector by Western hybridization. pBAD*ssrB* encodes an arabinose-inducible copy of *ssrB* and was used in a previous study that identified many SsrB regulated genes [114]. SsrB over-expression likely causes self-activation, a phenotype that has been previously demonstrated for the PhoP two component regulator [232]. Because SsrB positively regulates genes encoded within the SPI-2 pathogenicity island and virulence factors spread throughout the chromosome [114,187], we compared secretion under conditions that induced SsrB via growth in minimal acidic medium to conditions in which SsrB was over-expressed by pBAD.

Salmonella growth in mLPM

LPM is a semi-defined growth medium that is suitable for the secretion of effector proteins [186,188,228-230]. This medium contains 0.1% acid hydrolyzed casein that could have resulted in the addition of unwanted peptides and was thus omitted from the recipe. We found that induction of pBAD*ssrB* with 0.2% arabinose inhibited bacterial growth, presumably due to high-level SsrB expression and its activities upon the SPI-2 regulon (Fig. 5-1).

Assessing sample quality by Western hybridization

Samples were prepared as described in Fig. 5-2. Briefly, 500 mL cultures were grown for four, eight, or sixteen hours in mLPM ± 0.2% arabinose. Bacteria were first pelleted by centrifugation, and the supernatant was filter sterilized using a low protein affinity membrane. At each time point we used Western hybridization to evaluate the cell pellet and an aliquot of the supernatant for levels of intracellular and secreted SseJ::HA, respectively. In samples grown without arabinose, SseJ was detected in the supernatant at eight and sixteen hours, but not at four hours. Secretion of SseJ::HA was observed only in the *ssaL* mutant and was not observed in the parental strain nor the *ssaK* mutant

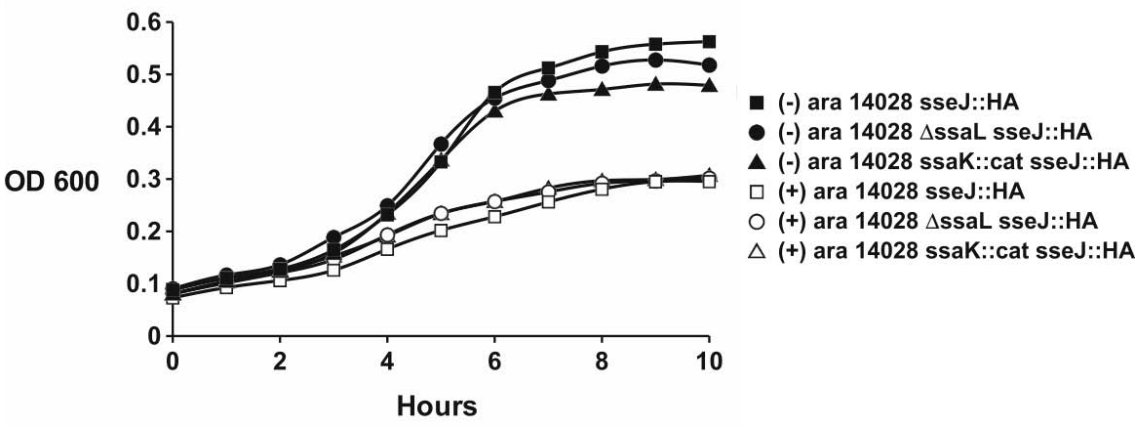

Fig. 5-1

mLPM growth curves. mLPM is a defined, low phosphate, low magnesium medium buffered to pH 5.8. Bacterial strains were normalized to a starting OD_{600}= 0.1 and grown in mLPM ± 0.2% arabinose. Arabinose was added to over-express SsrB from the pBAD*ssrB* plasmid. The difference in growth rates between the induced and non-induced samples was significant ($P<0.05$).

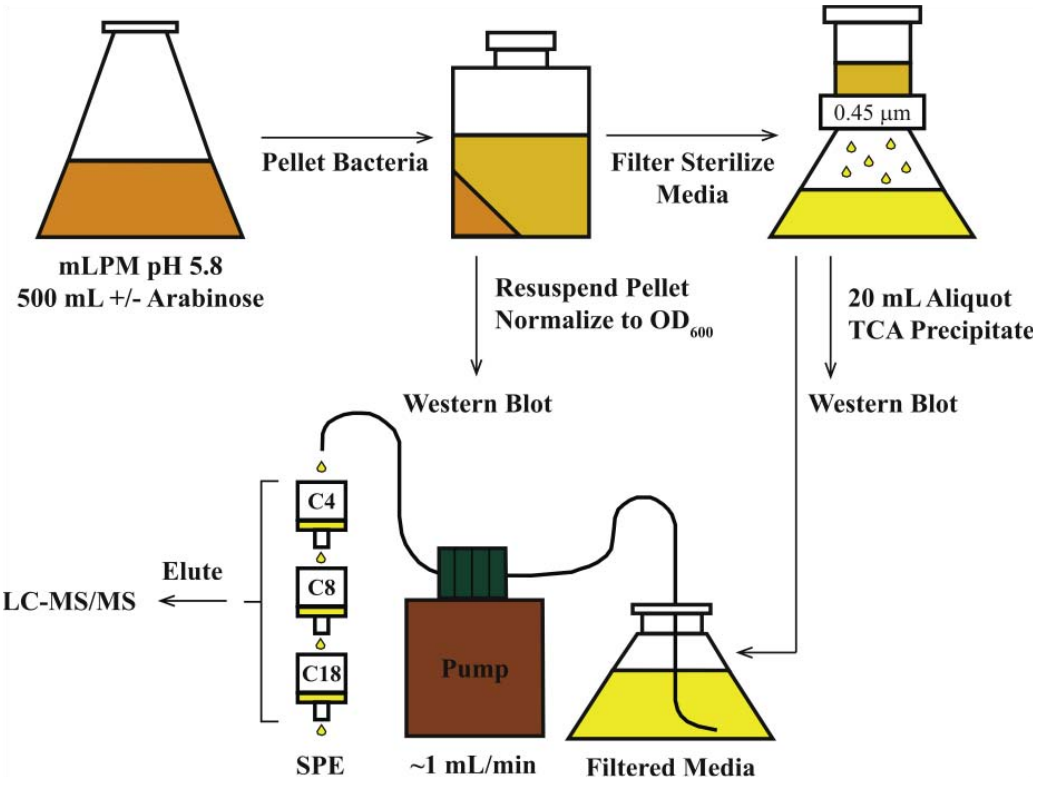

Fig. 5-2

Sample preparation for LC-MS/MS analysis. 500 mL mLPM culture volumes were grown for 4, 8, or 16 hours. Bacteria were pelleted and the supernatant was filter sterilized. The bacterial pellet and an aliquot of filter-sterilized media were analyzed by Western blot to evaluate sample quality; SseJ secretion and retention of an intracellular protein, DnaK, in the cell pellet. The remaining media was then pumped through serial C4, C8, and C18 solid phase extraction resins (SPE). Samples were eluted and then analyzed by LC-MS/MS.

(Fig. 5-3). When pBAD*ssrB* was induced with arabinose, SseJ secretion was also dependent upon the *ssaL* deletion, but secretion was observed at four hours but not at eight or sixteen hours. LC-MS/MS analysis provided some insight on the different SseJ secretion profiles and is discussed in more detail below. We also probed for the cytoplasmic protein DnaK to ensure that the pelleted cells but not the supernatant contained this protein. DnaK was not observed in any of the secreted fractions. Its detection was limited exclusively to the cell pellets (Fig. 5-3), suggesting that the bacteria maintained cell integrity throughout the course of the experiment.

Our data also demonstrated that intracellular SseJ levels decreased over time in *ssaL* encoding strains, but not the *ssaL* mutant. This result suggests that SsaL may regulate SseJ transcription and/or translation in addition to occluding the secretion apparatus. Further experiments are necessary to determine how this repression takes place and if it affects other secreted effectors as well.

Characterization of the SPI-2 T3SS secretome by LC-MS/MS

Wild-type, Δ*ssaL*, and *ssaK* mutant bacteria were grown as described above (see Fig. 5-2). Filtered culture supernatants were applied to serial C4, C8, and C18 solid phase extraction (SPE) columns. After elution the protein concentrations were measured, and we estimated the total protein concentration in culture supernatants to be ~3 μg/mL.

Peptide identifications were made using SEQEST analysis of raw spectra [233]. After peptide quality filters were applied, we performed a semi-quantitative measure of protein abundance by summing the total number of mass spectra (peptides) corresponding to a particular protein. This approach, known as spectral counting, is widely used in the proteomics community [234-238]. SEQEST analysis of 72 LC-MS/MS runs yielded approximately 1,400 unique, filter-passing peptides that mapped to 414 proteins (data not shown). To increase the probability of detecting novel secreted proteins, we did not establish a minimum number of unique peptide identifications per protein. However, higher confidence was assigned to 204 proteins that were identified by two or more unique peptides. As an alternative to spectral counting, we also used the accurate mass and elution time (AMT) tag approach [239-241]. AMT improves granularity (level of detail) and reduces under-sampling for relative abundance measurements. Using less restrictive filtering criteria than spectral counting, a total of

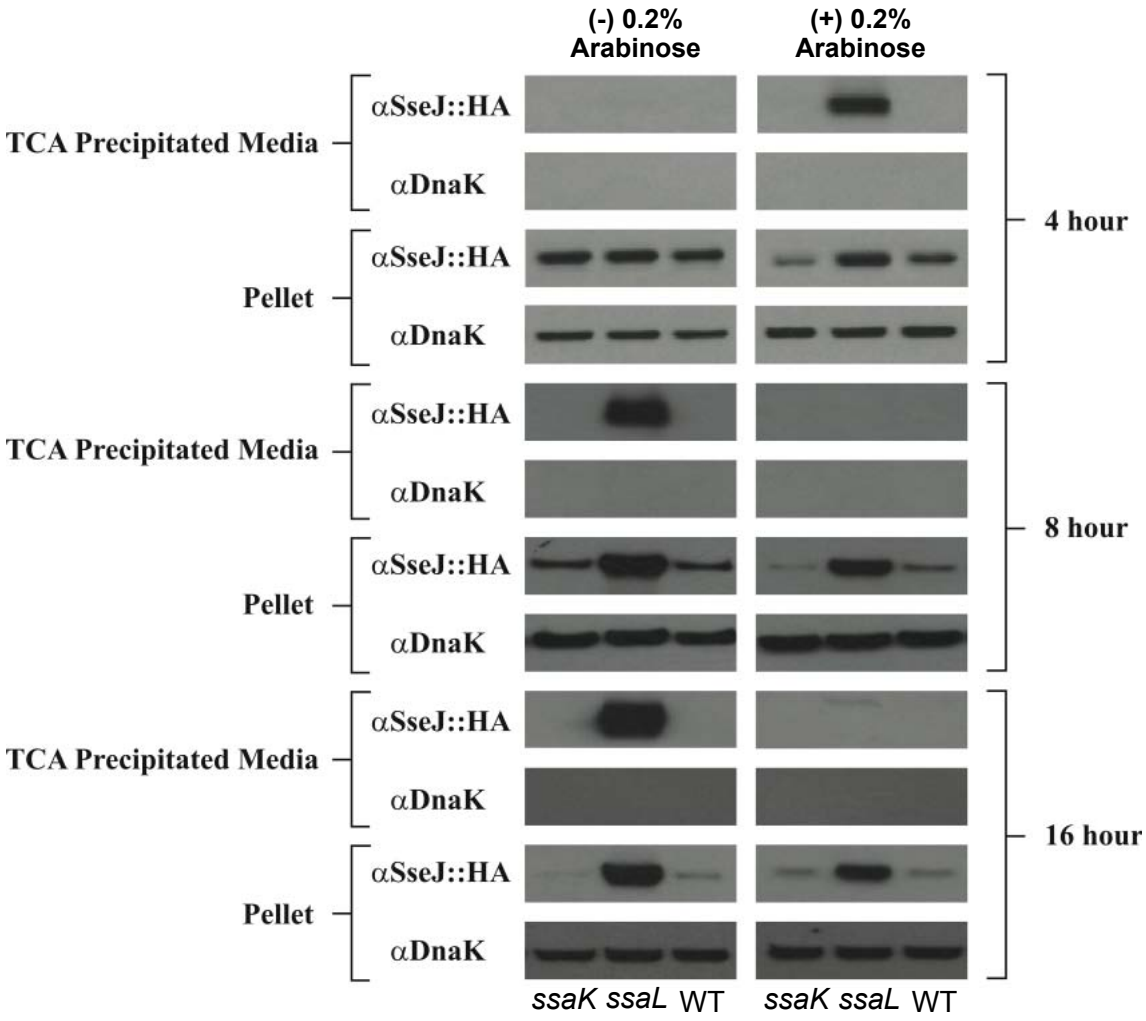

Fig. 5-3

Western hybridization of secretome samples. At each time point (4, 8, or 16 hrs) the bacterial pellet (~1 x 10^7 CFU) and 20 mL of filter sterilized TCA precipitated media were analyzed by Western blot against SseJ::HA and DnaK. Cell pellet and TCA precipitated media demonstrate cellular expression and effector secretion, respectively.

529 putative proteins were detected, of which 431were identified by two or more unique peptides.

Despite these differences, the relative protein expression patterns between the AMT tag and spectral counting methods were in general agreement (raw and processed results can be found at SysBEP.org). Due to the lower complexity of the *Salmonella* secretome samples relative to a typical cellular proteome, the AMT approach was useful for selecting some candidates for additional evaluation, but the spectral count data is presented because of its broader use in the proteomics community.

SseJ and DnaK peptide identifications

The mass spectrometry-based results agreed well with Western blots in Fig. 5-3. Under the non-induced growth condition, 122 SseJ peptides were detected in the *ssaL* mutant, whereas zero SseJ peptides were observed in the wild type and *ssaK* mutant. DnaK was observed only as a single filter-passing peptide in the wild type at the sixteen hour time-point, suggesting that there was some cell death or cytoplasmic leakage, though a single peptide observation is not strong evidence (Table 5-1). When SsrB was induced by arabinose induction, SseJ peptides matched the Western blot in Fig. 5-3 only at the four hour time-point. At the eight and sixteen hour time-points, the LC-MS/MS detected SseJ peptides in the arabinose-induced *ssaL* mutant, but no secreted SseJ was observed by Western Blot in these samples. These findings suggest that at later time points SseJ was secreted and subsequently degraded in response to SsrB over-expression. We hypothesize that degradation occurred because of a *Salmonella* encoded trypsin like protease because we found that the secretome samples contained a similar proportion of tryptic or partially tryptic peptides with or without trypsin digestion (18.8% and 18.2% of unfiltered peptides, respectively). The protease has not been identified and could be an outer membrane, periplasmic protein, or secreted effector.

Table 5-1. Spectral counts (peptide observations) of SseJ and DnaK observed in the secretome of strains grown +/- 0.2% arabinose.

		- Arabinose			+ Arabinose		
Protein	**Time (h)**	**WT**	***ssaL***	***ssaK***	**WT**	***ssaL***	***ssaK***
SseJ	4	0	1	0	0	13	0
	8	0	27	0	0	33	0
	16	0	28	0	0	20	0
DnaK	4	0	0	0	0	0	0
	8	0	0	0	0	0	0
	16	1	0	0	0	0	0

Detection of known Type III secreted effectors

15 known SPI-2 effectors (PipB, PipB2, SifA, SifB, SopD2, SseB, SseC, SseD, SseG, SrfH, SseJ, SseK2, SseL, SspH2, and SteC) and five additional effectors secreted by both SPI-1 and SPI-2 T3SSs were observed (AvrA, SpvC, GogB, SlrP, SteA, and SteB) (Fig. 5-4). Surprisingly, six SPI-1 effector proteins were also identified (SipA, SopB, SopD, SipC, SipD, and SipB) (Fig. 5-4). This occurred despite the culture conditions that were designed to inhibit expression of SPI-1 genes [114,187,188].

All known SPI-2 TTS effectors were biased for secretion in the *ssaL* mutant with the exception of the translocon proteins, SseBCD, which were secreted only in the wild type background. The latter result suggests that SsaL is necessary for secretion of proteins that form the pore in the eukaryotic membrane (Fig. 5-4), a finding that agrees with Coombes, et al [228] showing that SsaL was required for the expression and secretion of SseBCD. On the other hand, five components of the SPI-2 secretion apparatus (SsaC, SsaG, SsaI, SsaK, and SsaT) were detected in the *ssaK* mutant (data not shown). Thus, the presence of SPI-2 apparatus proteins was independent of SsaK. Surprisingly, SPI-1 effectors SipA and SopD were observed exclusively in the *ssaL* mutant (Fig. 5-4), exhibiting a secretion profile similar to SPI-2 effectors. This result may suggest regulatory interaction between the two secretion systems. Secretion of the other SPI-1 effectors was independent of the SPI-2 secretion apparatus (Fig. 5-4). SipBCD, which

Locus	Protein Description	Gene	SIEVE
STM1091	Inositol polyphosphate phosphatase	sopB	2.32
STM2882	Binds and stabilizes F-actin	sipA	1.76
STM2945	Membrane fission and macropinosome formation	sopD	2.18
STM0800	E3 ubiquitin ligase of thioredoxin	slrP	1.64
STM2865	Deubiquitinase of IκBα and β-catenin	avrA	2.27
STM2584	Leucine rich protein, unknown activity	gogB	2.24
PSLT038	Phosphothreonine lyase of MAPKs	spvC	2.37
STM1629	Required for full virulence, unknown activity	steB	2.93
STM1583	Putative dipicolinate reductase	steA	2.62
STM1698	Serine/threonine kinase required for VAP	steC	1.24
STM2780	Recruits kinesin-1 to the SCV	pipB2	0.98
STM0972	Contributes to SIF formation	sopD2	2.81
STM1631	Glyerophospholipid:cholesterol acetyltransferase	sseJ	2.45
STM2287	Deubuitinates IκBα	sseL	1.63
STM2241	E3 ubiquitin ligase, host target unknown	sspH2	1.14
STM1051	Modulates macrophage motility	srfH	2.64
STM1088	Targeted to detergent resistant rafts on SCV	pipB	2.64
STM1602	Targeted to the SCV and SIFs	sifB	2.52
STM1224	GEF mimic, inhibits Rab9 interaction with SKIP	sifA	2.44
STM1405	Contributes to SIF formation	sseG	2.14
STM2137	Unknown activity and role in virulence	sseK2	2.50
STM2883	SPI-1 TTSS needle tip	sipD	2.52
STM2885	SPI-1 TTSS translocon component	sipB	1.79
STM2884	SPI-1 TTSS translocon component	sipC	2.41
STM1401	SPI-2 TTSS translocon component	sseD	1.93
STM1398	SPI-2 TTSS needle tip	sseB	2.22
STM1400	SPI-2 TTSS translocon component	sseC	2.54

Fig. 5-4

Known TTSS effectors and translocon components. Heat map representation of known TTSS efffectors and translocon proteins identified in the secretome. Total counts of peptides for each protein (spectral counts) were used for relative quantitation. Proteins were binned by their association with the SPI-1 or SPI-2 translocon and TTSS. SopD has characteristics in common with SPI-2 secreted proteins [37,38] and is sometimes reported as secreted via both secretion systems [9,39]. Columns indicate the strain in which secreted proteins were observed. Abundance values were clustered by Hierarchical clustering. Known TTSS effectors, but not translocon components, were primarily observed in the *ssaL m*utant.

form the SPI-1 TTSS translocon, were only observed in the *ssaK* mutant, and SopB was observed exclusively in the wild type background.

Patterns of protein secretion

Proteins detected in the filtered culture supernatants were divided into several broad categories based on strain, time, and SsrB induction. To determine if a protein had a strain bias, spectral counts were summed and clustered by Z-scores (range -1.15 to +1.15). The Z-score allows comparison across data sets and represents the divergence of an experimental result from the mean divided by standard deviation. We limit the following results to those 204 proteins identified by two or more unique peptides. The following analysis was aided by previous work describing the most abundant *Salmonella* proteins expressed under a variety of growth conditions [234]. We also employed the SVM-based Identification and Evaluation of Virulence Effectors (SIEVE) method of predicting TTSS effectors (Fig. 5-4 and 5-8) [231]. Since a positive SIEVE score is suggestive of secretion, this algorithm was used to evaluate distinct protein populations within the secretome.

(i) *ssaL* bias

Twenty-six percent (53) of all observed proteins were expressed more highly (≥ two fold) in the *ssaL* mutant than in the parental strain (Fig. 5-5). Only three proteins were among the 200 most expressed in *Salmonella*. In general these proteins were not significantly different from the rest of the secretome or genome in terms of molecular mass, but they had significantly higher SIEVE scores than the rest of the secretome (mean 0.36 vs. 0.04, $P = 0.007$) and the genome (mean 0.36 vs. 0, $P = 6 \times 10^{-5}$) suggesting that a significant proportion of these proteins may be secreted. In terms of subcellular localization, 18% of *ssaL*-biased proteins were predicted by the PSORTb algorithm [242] to be cytoplasmic, compared to 26% for the rest of the secretome ($P = 0.07$, χ^2) and 35% for the genome ($P = 0.0001$, χ^2). Conversely, the *ssaL*-biased subset was enriched in predicted periplasmic proteins when compared to the secretome and genome (Table 5-2). Of the 53 *ssaL*-biased proteins, 80% were absent in the *ssaK* mutant, and an additional four proteins had only a single filter-passing peptide observed in the *ssaK* control. With 90% of the proteins having zero or one peptide detected in the *ssaK* mutant, the *ssaL*-biased subset likely contained novel secreted effectors.

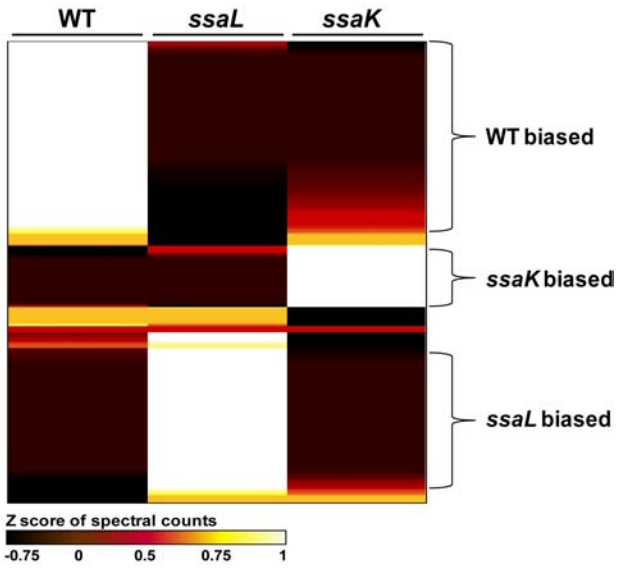

Fig. 5-5

Strain biases in secretion. Heat map representation of spectral counting (protein abundance) Z scores calculated for each strain. Hierarchical clustering was used to determine the primary strain in which each secreted protein was observed. Proteins falling outside the indicated strain biased regions were considered to be non strain-specific.

(ii) WT bias

Seventy-four of 204 proteins were observed at their highest levels in the secretome of the parental, wild type strain. Of these ~75% had either zero or one peptide identification in the *ssaK* mutant (n = 89 and 21 proteins, respectively). As mentioned previously, the WT biased subset included the SPI-2 translocon components SseBCD. Unlike proteins in the *ssa*L group which had a molecular mass distribution similar to the genome, the WT-biased subset was enriched for small cytoplasmic proteins and ribosomal subunits with molecular weights less than 20 kDa (55% compared to 28% for the genome) (Fig. 5-6). Notably, 25% of the WT-biased proteins were among the top 200 most highly expressed *Salmonella* proteins observed under similar growth conditions (Table 5-2). Thus, the WT-biased group was enriched for small, abundant cellular proteins. Moreover, the WT-biased subset had a mean SIEVE score of 0.24, indicating a low probability of secretion. In summary, the WT subset was not as selective as the *ssaL*-biased group; however, it is puzzling that a specific subset of small, molecular weight proteins predominated in the secretome samples.

(ii) ssaK bias

Only three proteins were observed preferentially in the ssaK mutant background. If we include proteins for which there was only a single MS identification, there was an overall enrichment in proteins with molecular weights above the genome median of 30 kDa (67% in *ssaK*-biased, 41% in secretome, 48% in genome). The *ssaK*-biased group was low in abundant cellular proteins (Table 5-2), suggesting that their presence in the secretome was not an artifact due to cell lysis. Additionally, this group was enriched for outer membrane proteins (11%, vs. 2% in genome, $P = 2 \times 10^{-5}$, χ^2). The *ssaK* biased subset had a low mean SIEVE score (0.04) indicating a lower probability of secretion.

(iii) No strain differences observed

Seventy four proteins were observed at nearly equal levels in all strain backgrounds, and 78% of this group had two or more peptide identifications in the *ssaK* mutant. Notably, we also identified components of the SPI-2 T3SS apparatus (SsaC, SsaG, and SsaI) and three proteins that form the SPI-1 translocon (SipB, SipC, and SipD) (Fig. 5-4). It should be kept in mind that the secretome was prepared from bacteria grown under SPI-2 inducing culture conditions. This subset was also enriched for

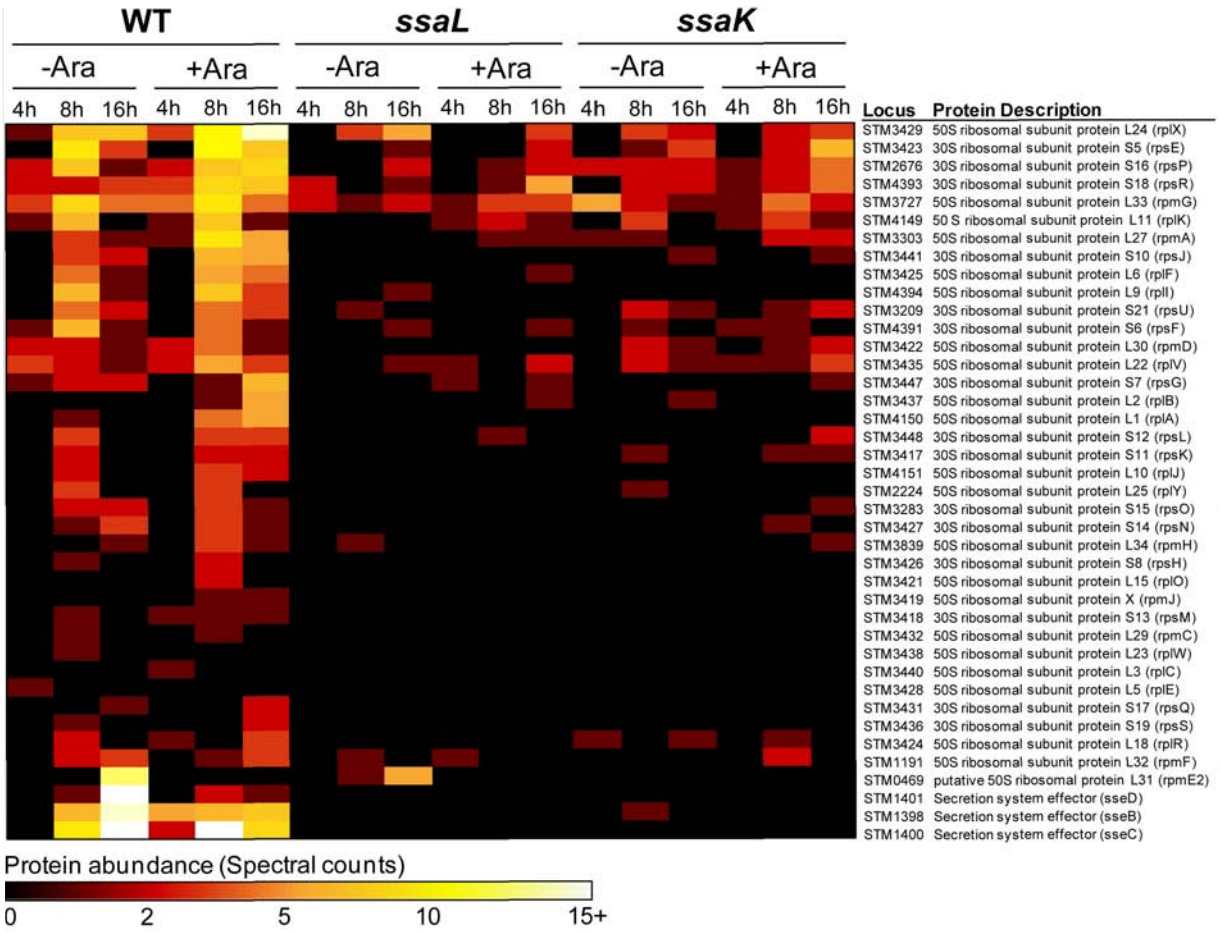

Fig. 5-6

Translocon and ribosome-related group of secreted proteins. Heat map representation of proteins belonging to the SPI-2 TTSS translocon or ribosomal subunits. Columns indicate the incubation time, presence (+Ara) or absence (-Ara) of arabinose during growth, and strain used. Hierarchical clustering of spectral count values revealed that the ribosome-related group showed trends similar to the SPI-2 TTSS translocon proteins.

abundant cellular proteins (n = 25) and for proteins with predicted signal sequences (Table 5-2) [242], suggesting that outer membrane, inner membrane, and periplasmic proteins were prevalent. The mean SIEVE score was 0.11, indicating a lower probability of secretion. We confirmed observations made by Komoriya et al. showing that flagellins (FliC and FljB) were abundant in *Salmonella* culture supernatants [243]. This group was notable for the presence of SrfN, PagC, PagD, PagK, and the PagK homolog, of which PagC, PagD, and SrfN have been shown to be required for virulence [244-246]. Taken together these observations suggest that some virulence factors gain access to culture supernatants independent of TTS.

Table 5-2. Properties of proteins in strain-biased groups.

Property	**WT bias**	***ssaL* bias**	***ssaK* bias**	**No bias**	**Secretome**	**Genome**
mean MW, kDa	27.25	35.54	41.05	29.03	31.64	34.62
mean SIEVE score	-0.24	0.36	-0.04	0.11	0.04	0.00
# in top 200[a]	37 (25%)	6 (5%)	3 (7%)	25 (26%)	72 (17%)	200 (4%)
mean pep count	2.35	3.51	1.07	6.24	3.46	na
# with >1 pep	74	53	3	74	204	na
total proteins	149	122	46	97	414	4527
Subcellular location[b]						
Cytoplasm	53	22	19	14	108	1591
Inner membrane	14	13	4	4	35	861
Periplasm	6	17	3	13	39	146
Outer memrane	2	2	5	10	19	89
Extracellular	1	4	0	4	9	35
Unknown	73	61	15	51	200	1805

[a] Previously observed in *Salmonella* proteomic studies

[b] Predicted using the PSORTb algorithm

(iv) Time-dependent and SsrB-induced secretion

When the secretome was analyzed as a whole, there were time and SsrB-related patterns of secretion that varied between the wild type, Δ*ssaL*, and *ssaK* mutant backgrounds. Most proteins had greater abundances at eight hours than at four hours (Fig. 5-7). A minority of proteins continued to increase for sixteen hours. In the *ssaL* mutant grown without arabinose, 50% of the observed proteins were detected at higher levels at eight hours than at four hours, and 53% were observed at higher levels at sixteen compared to eight hours (data not shown). Induction of SsrB in the *ssaL* mutant correlated with an increase in the number of proteins identified (207 vs. 170) and an increase in peptide counts at eight hours, followed by a decline at sixteen hours (Fig. 5-7). Interestingly, in the arabinose-induced *ssaL* mutant, 38 proteins were observed almost exclusively at the sixteen hour time-point. Nearly all of these proteins were annotated as outer membrane or periplasmic proteins, and, therefore, were unlikely to be secreted by a TTSS (Fig. 5-7). Thus, under SPI-2 inducing growth conditions and SsrB arabinose induction, some periplasmic and outer membrane proteins were present in the culture supernatants.

Selection of candidate secreted proteins

Based on the secretion patterns exhibited by known SPI-2 T3SS effectors and translocon components we developed a set of criteria to select for novel type III effectors: detection in Δ*ssaL* or WT backgrounds, low/no detection in the *ssaK* mutant, and a positive SIEVE score (Fig. 5-8). 15 candidate proteins were identified (Fig. 5-8), four of which (SpvD, GtgE, PipA, and STM2139) were predicted to be secreted by the sequence-based computational method of Arnold et al. [247].

Confirmation of novel secreted proteins

To determine if candidate effectors were secreted into host cells, we constructed *cyaA'* fusions to each open reading frame [29,195]. Following infection under SPI-1 and SPI-2 inducing conditions, cAMP levels were measured within the J774 macrophage-like cell line. We identified three novel proteins secreted by the SPI-2 TTSS (STM1026 [GtgA], STM3762 [CigR], and STM2139), three secreted by both SPI-1 and SPI-2 TTSSs (PSLT037 [SpvD], STM1055 [GtgE], STM2585), and two secreted independent of the SPI-1 and SPI-2 TTSSs (STM0359 and STM1478 [YdgH]) (Fig. 5-8).

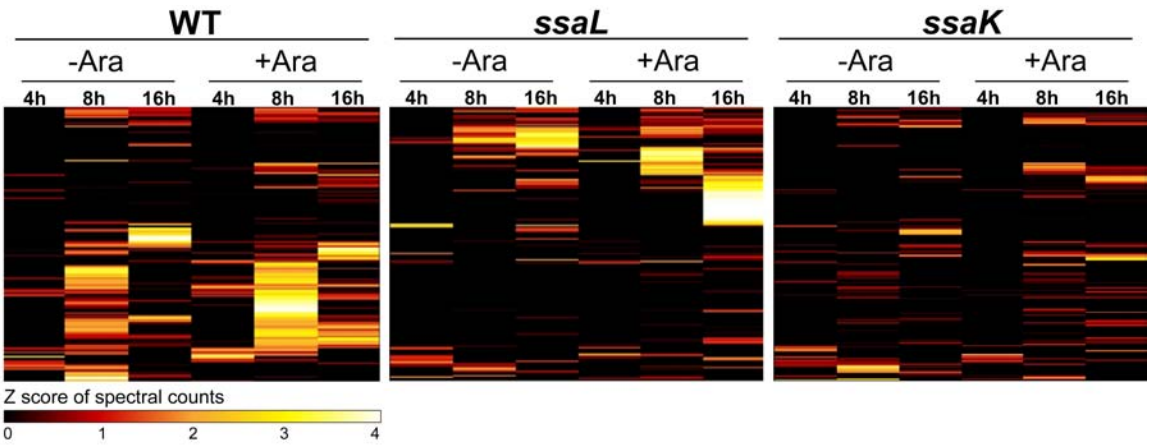

Fig. 5-7

Time- and *ssrB*-dependent patterns of secretion. Heat maps showing Z scores of protein abundance (spectral counts) at different culture incubation times and with (+Ara) or without (-Ara) arabinose induction of *ssrB*. Hierarchical clustering was done for each strain separately.

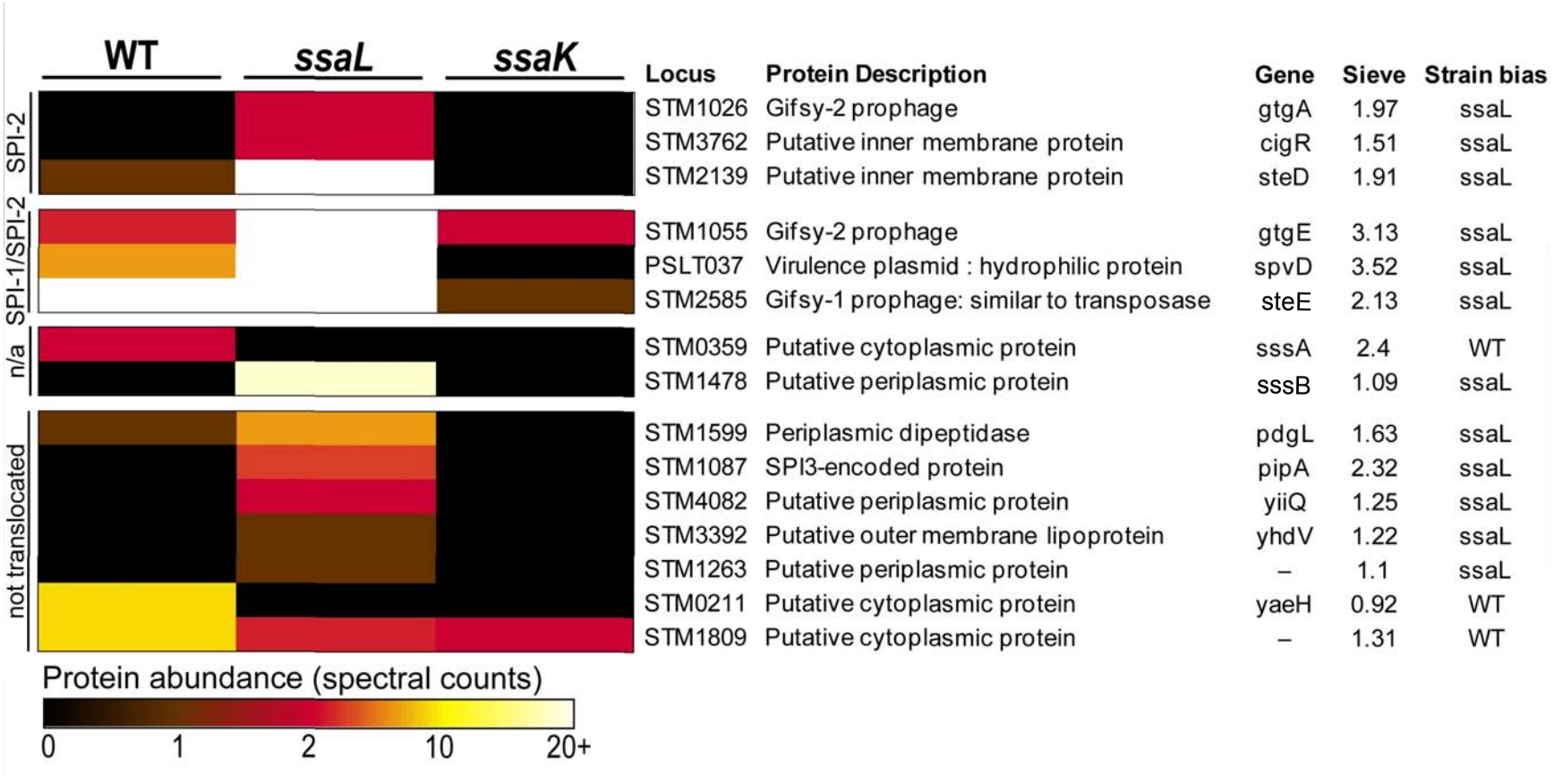

Locus	Protein Description	Gene	Sieve	Strain bias
STM1026	Gifsy-2 prophage	gtgA	1.97	ssaL
STM3762	Putative inner membrane protein	cigR	1.51	ssaL
STM2139	Putative inner membrane protein	steD	1.91	ssaL
STM1055	Gifsy-2 prophage	gtgE	3.13	ssaL
PSLT037	Virulence plasmid : hydrophilic protein	spvD	3.52	ssaL
STM2585	Gifsy-1 prophage: similar to transposase	steE	2.13	ssaL
STM0359	Putative cytoplasmic protein	sssA	2.4	WT
STM1478	Putative periplasmic protein	sssB	1.09	ssaL
STM1599	Periplasmic dipeptidase	pdgL	1.63	ssaL
STM1087	SPI3-encoded protein	pipA	2.32	ssaL
STM4082	Putative periplasmic protein	yiiQ	1.25	ssaL
STM3392	Putative outer membrane lipoprotein	yhdV	1.22	ssaL
STM1263	Putative periplasmic protein	–	1.1	ssaL
STM0211	Putative cytoplasmic protein	yaeH	0.92	WT
STM1809	Putative cytoplasmic protein	–	1.31	WT

Fig 5-8

Candidates tested for secretion into host cells. Three criteria were used to select candidates low/no spectral counts (peptide observations) in the *ssaK* mutant, a positive SIEVE score, and ≥1 spectral counts in the *ssaL* mutant or WT backgrounds. Heat map represent total spectral counts for proteins in each strain. Proteins with spectral counts of 1 were identified by multiple mass tags (peptides) via the AMT approach.

We propose the designations SteD (SPI-2 effector D), SteE, SsaA (*Salmonella* secreted substrate A), and SssB for STM2139, STM2585, STM0359, and STM1478, respectively. Of the remaining eleven candidates, no secretion into host cells was observed under SPI-1 or SPI-2 inducing conditions. There are several reports suggesting that secretion may be cell or tissue specific [248,249]. Thus, some of the non-confirmed candidates may be secreted into cell types that were not tested and additional testing is required to verify the negative results. Nevertheless, nearly 50% of the 15 candidates were confirmed as secreted substrates. Notably, there was a higher rate of confirmation for the *ssaL*-biased proteins (64%) than for the WT-biased proteins (20%), an observation that supports the function of SsaL in regulating secretion. These experiments also demonstrated that candidate proteins with a SIEVE score above 1.5 had an 89% probability of being secreted.

Chromosomal location and virulence phenotypes of novel secreted proteins

spvD is located on the *Salmonella* virulence plasmid, and most of the other loci reside within pathogenicity islands such as Gifsy-2 (*gtgA* and *gtgE*), Gifsy-3 (*steE*), and SPI-3 (*cigR*) (Fig. 5-8), suggesting that these secreted proteins were horizontally acquired. On the other hand, *steD*, *sssA*, and *sssB* do not appear to be located in a pathogenicity island, suggesting more ancient origins. Curiously, SssA and SssB were secreted independent of SPI-I and SPI-2 TTSSs and only under SPI-1 inducing conditions (data not shown). SssB has a domain that is conserved in numerous members of the Enterobacteriaceae family (DUF1471). SssA is unique in that it is only 33 amino acids in length and is the smallest effector reported to date. We theorize that these two proteins may be secreted by an alternative, evolutionarily conserved system(s). Because SssB and SssA were secreted into host cells exclusively under SPI-1 inducing conditions, they may be involved in cell invasion.

Some of these novel effectors have been characterized in the literature. *spvD* is absent from some pathogenic *Salmonella* strains, and is not required for virulence in subcutaneously infected mice [250,251]. Conversely, a *gtgE* mutant is attenuated seven fold for spleen colonization of intra-peritoneally (IP) infected mice [213]. Virulence phenotypes have not been reported for the other six novel secreted proteins. To evaluate the role of these putative effectors in a persistence model of infection, non-polar deletions

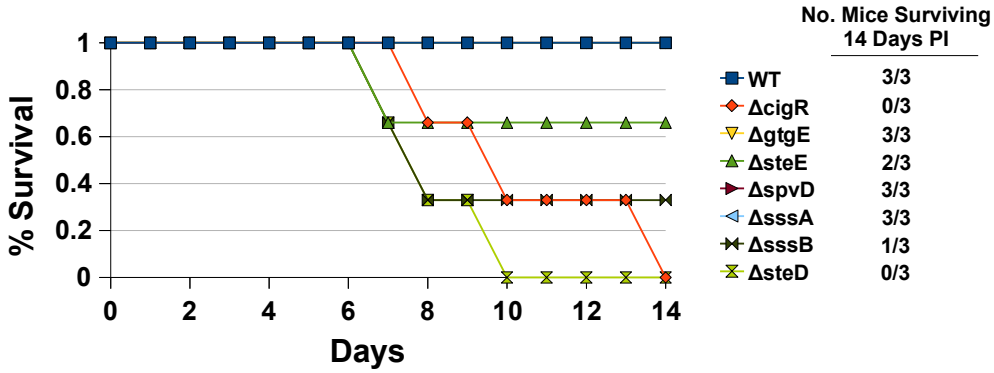

Fig. 5-9

Virulence in IP infected SVJ/129 mice. Mice were infected with 10^4 CFU of the indicated bacterial strains and monitored over a 14 day period.

were constructed as described in Materials and Methods and used to infect 129/SVJ mice IP. 129/SVJ mice express natural resistance-associated macrophage protein 1 (NRAMP1), a transporter of divalent cations expressed in myeloid cells that affects susceptibility to *Salmonella* and other intracellular pathogens. In 129/SvJ mice a persistent *Salmonella* infection lasts for weeks [8,252]. To evaluate virulence 129/SvJ mice were infected IP with 10^4 bacteria and monitored for fourteen days. We had difficulty resolving the gtgA mutant, so this construct was not investigated. The wild type, *gtgE*, *spvD*, and *sssA* mutants did not affect murine survival (Fig. 5-9). These results are consistent with the previously reported phenotypes for GtgE and SpvD. However, mice infected with *cigR* and *steD* mutants were more susceptible to infection, demonstrating a hyper-virulence phenotype (Fig. 5-9). For the *sssB* and *steE* mutants, 1/3 and 2/3 mice survived, respectively. The *sseB* and *steE* mutants may be hyper-virulent, but their phenotypes were more subtle as only some of the mice succumbed to infection (Fig. 5-9).

Discussion

We used global proteomic profiling to investigate the secretome of *S.* Typhimurium wild-type, Δ*ssaL*, and *ssaK* mutants under SPI-2-inducing conditions. Among 15 candidates, we report eight as novel secreted substrates that are translocated into host macrophages, some of which were required for full virulence in mice. By over-expressing SsrB, many effectors had increased secretion or were secreted into media at earlier time-points. However, only one effector, SifB, was exclusively secreted under this condition, suggesting that over-expression of the SPI-2 regulon did not have a dramatic effect upon secretion into media.

SsaL is an ortholog of SepL and is implicated in the hierarchical switch between translocator and effector secretion in enterohemorrhagic *E. coli* (EHEC) and enteropathogenic *E. coli* (EPEC) [253,254]. *sepL* mutants have been exploited for the global identification of TTS effectors due to the secretion of effector proteins into culture media [222,253]. In agreement with this function, our results show that an *ssaL* mutant of *S.* Typhimurium 14028 exhibited a similar secretion phenotype. As evidence of this our proteomic analysis identified 20 known type III effectors (Fig. 5-4) and seven novel proteins (GtgA, CigR, SteD, SpvD, GtgE, SteE, and SssB) (Fig. 5-8) secreted more strongly in the *ssaL* mutant than in the wild type or a SPI-2 functional mutant.

Additional phenotypes have been reported for an *ssaL* mutant of *S.* Typhimurium SL1344. Coombes and co-workers observed that SsaL was required for expression and *in vitro* secretion of translocon components (SseB and SseD) and of effectors encoded within SPI-2 (SseG and SseF), but was dispensable for effectors encoded outside SPI-2, specifically PipB, SseL and SopD2 [228,229]. In our hands, SseF, PipB, SseL and SopD2 were all detected in culture supernatants from the *ssaL* mutant (Fig. 5-4). This discrepancy may be related to differences in the strains or media used or in the growth phase of the bacteria. Interestingly, *ssaM* (SPI-2 gene immediately downstream of *ssaL*) and *spiC* mutants of *S.* Typhimurium also exhibit altered secretion phenotypes as both mutants secrete SseJ and PipB effectors into LPM, but fail to secrete translocon components SseB, SseC, and SseD [255,256]. SpiC and SsaM have also been shown to interact inside the bacterial cell and are hypothesized to coordinate the timing of type III secretion by blocking secretion of effectors until the translocon components form a pore

in the host membrane [255]. Because SsaL appears to have a similar function, it will be interesting to determine how SsaL regulates secretion and if it is part of a complex with SsaM and SpiC.

In an earlier attempt to identify secreted *Salmonella* proteins, bacteria were grown in rich media (LB), supernatants were analyzed by 1-D SDS-PAGE, and proteins were identified by amino acid sequencing. This study found ten proteins secreted by wild-type SJW1103: the SPI-1 TTSS needle (InvJ), two translocon components (SipB and SipC), and one SPI-1 effector (SipA) while the other proteins were of flagellar origin, dominated by FliC (flagellin) [243]. Our analysis also identified peptides corresponding to these proteins and confirmed that FliC was one of the most abundant secreted proteins (data not shown). While FliC is a substrate of the flagellar secretion system, it can also be secreted into the host cytosol by the SPI-1 TTSS [257].

The secretome data further suggest that *Salmonella* secretes a subset of effector proteins into host cells independent of TTS as SssA and SssB fell into this category. SssA and SssB may be secreted by different mechanisms such as type V secretion [258] or by an alternative pathway as is being investigated. The secretome likely contained OMV because OmpA and TolC, both known to be present in OMV [259], were identified in this study. Additionally, the secretome contained cytoplasmic, periplasmic, and outer membrane proteins consistent with OMV content [260-265]. Finally, filtered culture supernatants, as described in our protein extraction protocol (Fig. 5-2), are the starting material in OMV purification strategies [259,260,266]. Our lab is actively pursuing these possibilities as SrfN, PagC, PagD, PagK, and the PagK homolog were identified in this study and are likely secreted in OMV. Those findings are discussed in more detail in the Discussion of this thesis.

The present study raised several exciting implications. Deletion of *cigR* and *steD* increased *Salmonella* virulence in 129/SvJ mice. Each encodes a secreted protein suggesting that hyper-virulence was a consequence of their effects upon the infected cell. Hyper-virulence has been reported for *Salmonella* ZirTS, a two component secretion system. A *zirT* mutant colonized the intestine and liver of orally infected SvJ/129 mice more efficiently than the wild type parent strain [267]. Efforts are underway to determine if the hyper-virulence phenotypes we observed resulted from increased bacterial burdens.

Corroborating these findings, the same genes have been identified by negative selection as ones that increase virulence [20,268]. There are other reports that demonstrate *Salmonella* down regulates intracellular replication (rev. in [269]). Specifically *Salmonella* does not replicate in fibroblasts and is quiescent in this cell type, but mutations in *phoPQ* were found to increase intracellular replication. Intracellular *Salmonella* lives within a vacuole that depends on at least eight secreted effectors. In epithelial cells escape from the vacuole results in rapid intracellular replication and is perhaps what is being observed here. *Salmonella* infects multiple cell types during infection, and this is something that will need to be examined.

We identified a secreted peptide of only 33 amino acids, SssA. It is too small to encode an enzymatic activity, possesses no sequence similarity to cytokines or chemokines, and is unstructured in the NMR. However, the target of the peptide may be of great interest. It is also interesting that conserved unknown proteins can be secreted and required for virulence such as SssB (YdgH). Application of global proteomics allowed identification of several type III effectors however the most important implication may be the identification of new secretory pathways for virulence factors.

Materials and methods

Strains and plasmids

Bacterial strains and plasmids are listed in Table 5-3. All experiments were done with *Salmonella enterica* serovar Typhimurium (ATCC 14028). Briefly, λ red recombination [176] was used to construct gene deletions and the *sseJ*::HA strains. Deletions were constructed using PCR products derived from primers listed in Table 5-4 and the pKD4 template. All constructs were transduced with bacteriophage P22, and resolved to create in frame, non-polar deletions. 14028 *ssaK*::*cat* and 14028 *invA*::*cat* were previously described [29]. 14028 *sseJ*::HA was derived from a PCR product using primers 3 and 4 with the pNFB15 template (received from Lionello Bossi). This generated a C-terminal, double HA-tagged SseJ followed by a non-resolvable kanamycin marker. This gene was P22 transduced into 14028, Δ*ssaL*, and *ssaK*::*cat* strains so that they each expressed a chromosomal copy of *sseJ*::HA under the control of its native promoter. 14028 *sseJ*::HA, 14028 Δ*ssaL sseJ*::HA, and 14028 *ssaK*::*cat sseJ*::HA were then transformed with the pBAD*ssrB* plasmid [114] to generate the strains used for proteomic analysis. For CyaA' secretion assays, candidate effectors were PCR amplified from 14028 chromosomal DNA using primer sets described in Table 5-4. Each PCR product was designed to anneal ~20 bp upstream of the start codon so as to encode the putative RBS. Flanking 5' *Xba*I and 3' *Pvu*II or *EcoR*V restriction sites were added to enable directional cloning into pMJW1753 [29] cut with *Xba*I and *Sma*I. Transcription was driven by the constitutive *lac* promoter in *Salmonella*. *cyaA'* fusions were verified by automated sequencing and plasmids were transformed into 14028, 14028 *ssaK*::*cat,* and 14028 *invA*::*cat* backgrounds. Expression was confirmed by Western hybridization against CyaA' (Santa Cruz, 1:1000).

Table 5-3. Strains and plasmids used in this study.

Category	**Strain/ Plasmid**	**Genotype/Description**	**Reference/Source**
S. Typhimurium	14028	Wild type	ATCC
	JG122.1	*sseJ*::HA	This study
	FH1001	Δ*ssaL*	This study

	MJW1301	*ssaK*::*cat*	[29]
	MJW1835	*invA*::*cat*	[29]
	GSN3000	Δ*ssaL sseJ*::HA	This study
	GSN3001	ssaK::cat sseJ::HA	This study
	GSN3002	*sseJ*::HA + pBAD*ssrB*	This study
	GSN3003	Δ*ssaL sseJ*::HA + pBAD*ssrB*	This study
	GSN3004	*ssaK*::*cat sseJ*::HA + pBAD*ssrB*	This study
	AK001	Δ*spvD*	This study
	AK002	Δ*gtgE*	This study
	AK003	Δ*steE*	This study
	AK004	Δ*steD*	This study
	AK005	Δ*cigR*	This study
	AK006	Δ*sssB*	This study
	AK007	Δ*sssA*	This study
Plasmids	pKD4	λ red recombination template	[176]
	pNFB15	λ red 2X HA tag	Lionello Bossi
	pBAD*ssrB*	Arabinose inducible SsrB expression	[114]
	pMJW1753	CyaA' fusions, pWSK29 derivative	[29]
	HH128	SrfH::CyaA, SPI-2 positive control	[29]
	HH228	SrfH::CyaA, MJW1835 derivative	[29]
	HH328	SrfH::CyaA, MJW1301 derivative	[29]
	HH140	SipA::CyaA, SPI-1 positive control	[29]
	HH240	SipA::CyaA, MJW1835 derivative	[29]
	HH340	SipA::CyaA, MJW1301 derivative	[29]

	pGSN2001	pSLT037::CyaA', pMJW1753 derivative	This study
	pGSN2002	pSTM0211::CyaA', pMJW1753 derivative	This study
	pGSN2003	pSTM0359::CyaA', pMJW1753 derivative	This study
	pGSN2004	pSTM1026::CyaA', pMJW1753 derivative	This study
	pGSN2005	pSTM1055::CyaA', pMJW1753 derivative	This study
	pGSN2006	pSTM1087::CyaA', pMJW1753 derivative	This study
	pGSN2007	pSTM1121::CyaA', pMJW1753 derivative	This study
	pGSN2008	pSTM1263::CyaA', pMJW1753 derivative	This study
	pGSN2009	pSTM1478::CyaA', pMJW1753 derivative	This study
	pGSN2010	pSTM1513::CyaA', pMJW1753 derivative	This study
	pGSN2011	pSTM1599::CyaA', pMJW1753 derivative	This study
	pGSN2012	pSTM1809::CyaA', pMJW1753 derivative	This study
	pGSN2013	pSTM2139::CyaA', pMJW1753 derivative	This study
	pGSN2014	pSTM2585::CyaA', pMJW1753 derivative	This study
	pGSN2015	pSTM2610::CyaA', pMJW1753 derivative	This study
	pGSN2016	pSTM3392::CyaA', pMJW1753 derivative	This study
	pGSN2017	pSTM3762::CyaA', pMJW1753 derivative	This study
	pGSN2018	pSTM3799::CyaA', pMJW1753 derivative	This study
	pGSN2019	pSTM4082::CyaA', pMJW1753 derivative	This study

Table 5-4. Primers used in this study.

ID	**Orientation**	**5'-Sequence-3'**	**Description**
1	Forward	ATGGTGAAGATAAAAGAGGTAGCGATGAATATTAAAATTGTGTAGGCTGGAGCTGCTTC	14028 Δ*ssaL*

2	Reverse	TATTGAAAGCCAGGTATCAGAATAAA ACCTGATTTATCTTCATATGAATATCC TCCTTAG	
3	Forward	TGTTTTGTAATATGCATTTTATTGAGG TAGTGTAACTATGATTCCGGGGATCC GTCGACC	14028 Δ*spvD*
4	Reverse	ATATTTAAAAAAGTTATCAATCGTGT TTTTCATCATAAGCGTGTAGGCTGGA GCTGCTCC	
5	Forward	AATTACATTAACAAAATTACTATTCG GCGAGTATATTATGATTCCGGGGATC CGTCGACC	14028 Δ*gtgE*
6	Reverse	TGGTAAAGGTTAACTATCATAAAATG GTACACCAGTCTTTGTGTAGGCTGGA GCTGCTCC	
7	Forward	TTAAAAACTACTGCATGTAAAAGGG TCTCCTCTTGTTGTGATTCCGGGGAT CCGTCGACC	14028 Δ*steE*
8	Reverse	TTTATAACGCTTTGTTTTATTCATCCG GGAAAACCTCTGCGTGTAGGCTGGA GCTGCTCC	
9	Forward	CATAAACATAAACAGGCATGTGCATG AAGAGGTTTATATGATTCCGGGGATC CGTCGACC	14028 Δ*steD*
10	Reverse	TGCTGTGTTTGCTCATTTATGGCCAG GCTGGCCGGGTTCTGTGTAGGCTGG AGCTGCTCC	
11	Forward	CTATTTTCATGGTATCCCACATCAGA AGGGCAATATCATGATTCCGGGGATC CGTCGACC	14028 Δ*cigR*
12	Reverse	CTGGTGGGATAGGCTCTTAATCAAAT ACGCCATTAATAATGTGTAGGCTGGA GCTGCTCC	
13	Forward	CCAGTACCTGGTTTGCGCAAGGCGA AGGATTATTTTTATGATTCCGGGGATC CGTCGACC	14028 Δ*ydgH*
14	Reverse	GATGGCGACGCGCGCCTTATTTATAG AGGTCGGCGCTGATGTGTAGGCTGG AGCTGCTCC	
15	Forward	GATATTGCCAAGTGAATGTAACTAAG GGAGACATGTTATGATTCCGGGGATC CGTCGACC	14028 Δ*sssA*
16	Reverse	GGAATATCCAGATAAATTACGATTTTT TTTGCGGCTGGCTGTGTAGGCTGGA GCTGCTCC	

17	Forward	AATGTTAGAAAGTTTTATAGCTCATC ATTATTCCACTGAAGGCAGCTATCCG TATGATGTGCCGGA	14028 *sseJ*::HA
18	Reverse	AGCTGTGTTTTGCTCAAGGCGTACC GCAGCCGATGGAACTCACCTGCAGA TCATCGAGCT	
19	Forward	TGTTTTGTAATATGCATTTTATTGAGG TAGTGTAACTATGATTCCGGGGATCC GTCGACC	14028 Δ*spvD*
20	Reverse	ATATTTAAAAAAGTTATCAATCGTGT TTTTCATCATAAGCGTGTAGGCTGGA GCTGCTCC	
21	Forward	AATTACATTAACAAAATTACTATTCG GCGAGTATATTATGATTCCGGGGATC CGTCGACC	14028 Δ*gtgE*
22	Reverse	TGGTAAAGGTTAACTATCATAAAATG GTACACCAGTCTTTGTGTAGGCTGGA GCTGCTCC	
23	Forward	TTAAAAACTACTGCATGTAAAAGGG TCTCCTCTTGTTGTGATTCCGGGGAT CCGTCGACC	14028 Δ*steE*
24	Reverse	TTTATAACGCTTTGTTTTATTCATCCG GGAAAACCTCTGCGTGTAGGCTGGA GCTGCTCC	
25	Forward	CATAAACATAAACAGGCATGTGCATG AAGAGGTTTATATGATTCCGGGGATC CGTCGACC	14028 Δ*steD*
26	Reverse	TGCTGTGTTTGCTCATTTATGGCCAG GCTGGCCGGGTTCTGTGTAGGCTGG AGCTGCTCC	
27	Forward	CTATTTTCATGGTATCCCACATCAGA AGGGCAATATCATGATTCCGGGGATC CGTCGACC	14028 Δ*cigR*
28	Reverse	CTGGTGGGATAGGCTCTTAATCAAAT ACGCCATTAATAATGTGTAGGCTGGA GCTGCTCC	
29	Forward	CCAGTACCTGGTTTGCGCAAGGCGA AGGATTATTTTTATGATTCCGGGGATC CGTCGACC	14028 Δ*sssB*
30	Reverse	GATGGCGACGCGCGCCTTATTTATAG AGGTCGGCGCTGATGTGTAGGCTGG AGCTGCTCC	
31	Forward	GATATTGCCAAGTGAATGTAACTAAG GGAGACATGTTATGATTCCGGGGATC CGTCGACC	14028 Δ*sssA*

32	Reverse	GGAATATCCAGATAAATTACGATTTTTTTTGCGGCTGGCTGTGTAGGCTGGAGCTGCTCC	
33	Forward	TGGTCTAGATTTATTGAGGTAGTGTAACT	pGSN2001 (PSLT037::CyaA')
34	Reverse	CGCCAGCTGATCGTGTTTTTCATCATAAG	
35	Forward	TGGTCTAGAGTGTGATGAAGGATACCGCT	pGSN2002 (STM0211::CyaA')
36	Reverse	CGCCAGCTGCTTACGGGTAAGCTTGTCCA	
37	Forward	TGGTCTAGAACTAAGGGAGACATGTTATG	pGSN2003 (STM0359::CyaA')
38	Reverse	CGCCAGCTGCGATTTTTTTTGCGGCTGGC	
39	Forward	TGGTCTAGAATAAAGCCAGGCTGGAACCA	pGSN2004 (STM1026::CyaA')
40	Reverse	CGCCAGCTGATTACTAAATTCGTAGGCGA	
41	Forward	TGGTCTAGATACTATTCGGCGAGTATATT	pGSN2005 (STM1055::CyaA')
42	Reverse	CGCCAGCTGTAAAATGGTACACCAGTCTT	
43	Forward	TGGTCTAGATAGTCAGGAAATAAGAAGTTATGCTTCCGGT	pGSN2006 (STM1087::CyaA')
44	Reverse	CGCCAGCTGTTTATTGAAGATGTAGACCATTCTGGGAGG	
45	Forward	TGGTCTAGATATGACGGAGGTCAGTAATG	pGSN2007 (STM1121::CyaA')
46	Reverse	CGCCAGCTGGCTATTACGGTTACTGCTTT	
47	Forward	TGGTCTAGAATGAGGGTAACGTTTTGGTG	pGSN2008 (STM1263::CyaA')
48	Reverse	CGCCAGCTGATGATGTAGCATTTCGTCAA	
49	Forward	TGGTCTAGACAAGGCGAAGGATTATTTTTATGAAGCTTA	pGSN2009 (STM1478::CyaA')
50	Reverse	CGCCAGCTGTTTATAGAGGTCGGCGCTGATGGTGATGTT	
51	Forward	TGGTCTAGAATCATGAGGATTATATTATG	pGSN2010 (STM1513::CyaA')
52	Reverse	CGCCAGCTGATTGCCGGATTTCCGTCCAC	
53	Forward	TGGTCTAGAACTCTCGCGAGGTGTAACAT	pGSN2011 (STM1599::CyaA')

54	Reverse	CGCGATATCGGGTCTCTGCTTAACGGGAA	
55	Forward	TGGTCTAGAGAGTTCAAAGGAGGAAATCA	pGSN2012 (STM1809::CyaA')
56	Reverse	CGCCAGCTGGAGTAGTTTAATTTTAACGT	
57	Forward	TGGTCTAGAATGTGCATGAAGAGGTTTAT	pGSN2013 (STM2139::CyaA')
58	Reverse	CGCCAGCTGTGGCCAGGCTGGCCGGGTTC	
59	Forward	TGGTCTAGAAAGGGTCTCCTCTTGTTGTG	pGSN2014 (STM2585::CyaA')
60	Reverse	CGCCAGCTGTTCATCCGGGAAAACCTCTG	
61	Forward	TGGTCTAGAGACTGAGGGTCTTACATATG	pGSN2015 (STM2610::CyaA')
62	Reverse	CGCGATATCTTTTATCTGAATATTGACGC	
63	Forward	TGGTCTAGAATTAATGAGGTAACACCATG	pGSN2016 (STM3392::CyaA')
64	Reverse	CGCCAGCTGTTTAGAAAGCGCAATGATAC	
65	Forward	TGGTCTAGACACATCAGAAGGGCAATATC	pGSN2017 (STM3762::CyaA')
66	Reverse	CGCCAGCTGATCAAATACGCCATTAATAA	
67	Forward	TGGTCTAGAGCTAAATACGTGCTATCACC	pGSN2018 (STM3799::CyaA')
68	Reverse	CGCCAGCTGTGGGATTGCTGATCCTGGCG	
69	Forward	TGGTCTAGACCTAACGAAAGGTAAGATTG	pGSN2019 (STM4082::CyaA')
70	Reverse	CGCCAGCTGATTCGCCCCTTCCAGATTTT	

mLPM

mLPM contained 5 mM KCl, 7.5 mM $(NH_4)_2SO_4$, 0.5 mM K_2SO_4, 0.3% (v/v) glycerol, 0.00001% thiamine, 0.5 μM ferric citrate, 8 μM $MgCl_2$, 337 μM PO_4^{3-}, and 80 mM MES free acid adjusted to pH 5.8 with NaOH.

Secretome sample preparation

Bacteria were grown overnight in 50 mL LB. The following day bacteria were washed three times in mLPM and then diluted 1:10 to a final volume of 500 mL. We

then added 100 μg/mL carbenicillin to select for inoculated bacteria and one tablet of protease inhibitor cocktail without EDTA (Roche) to inhibit protein degradation. At four, eight, or sixteen hour time points the media was centrifuged 10 min 5,000 × g to pellet the bacteria. Spent media was filtered through a 0.45 μM Durapore filter assembly (Millipore) and then pumped at ~1 mL/min overnight at 4°C through serial 6 mL columns containing 50 mg of C4, C8, and C18 SPE resins (Strata and Supelco). Prior to loading the samples SPE columns were conditioned with 100% methanol followed by 0.1% TFA. After sample processing, SPE columns were washed with 95:5 H_2O:acetonitrile (ACN), 0.1% TFA and stored at -20°C until they were eluted with 80:20 ACN:H_2O, 0.1% TFA. Eluted samples were concentrated by speed-vac, quick frozen in liquid nitrogen, and stored at -80°C until needed. Protein concentration was assessed by BCA protein assay (Pierce). When required, tryptic digests were performed as previously described [234,235].

Capillary LC-MS/MS analysis

The high-performance liquid chromatography (HPLC) system and method used for capillary liquid chromatography have been described in detail elsewhere [234,270]. MS analysis was performed using an LTQ-Orbitrap mass spectrometer (Thermo Fisher Scientific, San Jose, CA) with electrospray ionization. The HPLC column was coupled to the mass spectrometer using an in-house manufactured interface. The heated capillary temperature and spray voltage were 200°C and 2.2kV, respectively. Data acquisition began 20 min after the sample was injected and continued for 100 min over a m/z range of 400–2000. For each cycle, the 6 most abundant ions from MS analysis were selected for MS/MS analysis, using a collision energy setting of 35 eV. A dynamic exclusion time of 60 s was used to discriminate against previously analyzed ions. Each sample was injected in duplicate.

Data analysis

Peptides were identified by using SEQUEST™ to search the mass spectra from 180 LC-MS/MS analyses. These searches were performed using the annotated *S.* Typhimurium FASTA data file, containing 4,550 protein sequences provided by The Institute for Genomic Research (www.tigr.org/, September 19, 2004, Stanford University), a standard parameter file with no modifications to amino acid residues and a

mass error window of 3 m/z units for precursor mass and 0 m/z units for fragmentation mass. The searches were allowed for all possible peptide termini, i.e. not limited by tryptic terminus state. These results were filtered using criteria established by Washburn et al. [271] and a statistical approach to estimate the accuracy of peptide identifications [272], with a score of at least 0.9 used to increase confidence in identified peptides. Peptides that mapped to multiple proteins (redundant peptides) were removed. An estimate of the false positive rate was obtained by searching against a reversed FASTA database, as described elsewhere [273]. A calculated false discovery rate of 2% was determined by using the combined filtering rules. The number of peptide observations from each protein (spectral count) was used as a rough measure of relative abundance. Multiple charge states of a single peptide were considered as individual observations as were the same peptides detected in different mass spectral analyses. Similar approaches for quantitation have been described previously [234,235,274]. Peptide identifications were summed across technical replicates and were analyzed separately for the eluents of the C4, C8, and C18 SPE columns. The results of the C4 and C8 columns were similar, and C18 columns yields were sparse to null. Therefore, results from the C4 and C8 column eluents were combined, and C18 eluents were not used in subsequent analyses.

As a complementary approach to increase the sensitivity of peptide detection and as a secondary method of relative peptide quantification, the accurate mass and elution time (AMT) tag approach [239,240,275] was used. For this method, a reference database containing accurate peptide masses and normalized LC elution times was built from 72 LC-MS/MS (tandem MS) runs. C18 SPE column data were excluded from the AMT database due to the paucity of peptides observed. The corresponding peptide sequences were determined using SEQUEST. Peptide masses and elution times observed in the high-resolution MS spectra were then matched to the reference database for peptide validation and identification. Quantitation was based on measuring mass spectral peak intensity of each peptide. This approach to proteomics research is enabled by published and unpublished in-group developed tools, which are available for download at omics.pnl.gov. Quantitation was based on measuring mass spectral peak intensity. The software program DAnTE [276] was used to perform the abundance roll-up procedure to convert peptide information into protein information, allowing relative protein

abundances to be inferred. Statistical analyses were done using Microsoft Excel and SigmaPlot 11.0. Hierarchical clustering and construction of heat maps were done using OmniViz 6.0.

Growth curves

Bacteria were grown overnight in LB. The following day bacteria were washed three times in mLPM and then inoculated into a final volume of 20 mL at a starting OD_{600} ≈ 0.1. We then added 100 μg/mL carbenicillin and protease inhibitor cocktail without EDTA (Roche) to simulate the conditions used for proteomic analysis. OD_{600} was measured at hourly intervals.

Western hybridization

To evaluate cellular expression, pelleted bacteria from above were suspended in PBS and the OD_{600} was measured. Samples were suspended in Laemli sample buffer, and a volume corresponding to an OD_{600} = 0.01 (~1×10^5 bacteria) was resolved by SDS-PAGE. To evaluate secretion a 20 mL aliquot of spent, filter-sterilized media was taken from each of the samples described above. Protein was precipitated overnight at 4°C in 20% TCA. The following day samples were centrifuged at 12,000 × g for 30 minutes and pellet was re-suspended in 1 mL 20% TCA. Samples were transferred to an eppendorf tube and centrifuged at 16,000 × g for 30 minutes. The pellet was washed two times in ice-cold acetone, placed on a 95°C heat block to evaporate solvent, and then suspended in Laemli sample buffer. If a sample turned yellow, acidity was neutralized by adding 1M Tris pH 9 until the sample turned blue. Media samples were normalized to the pellet OD_{600} and resolved by SDS-PAGE. Western hybridization using antibodies targeting DnaK (Assay Design, 1:10,000) and the HA tag of SseJ (Covance, 1:1,000) were used to detect intracellular and secreted proteins.

CyaA' secretion assays

CyaA' secretion assays were performed as previously described [29]. Three biological replicates were performed for each CyaA' fusion (data not shown).

Murine infection studies

6-8 week old female 129/SvJ mice were purchased from Jackson Laboratories (Bar Harbor, ME). All experiments were performed in accordance with Animal Care and Use Committee guidelines. Briefly, bacteria were grown overnight in LB broth and the

following day were washed three times in PBS. For each strain 10^4 bacteria were used to infect mice IP in triplicate. Mice were monitored for two weeks post infection.

Acknowledgements

We are grateful to Jennifer Niemann, Karl Weitz, Therese Clauss, Angela Norbeck, and Megan Burnett, for contributions to this work. Support for this work was provided by the National Institute of Allergy and Infectious Diseases NIH/DHHS through interagency agreement Y1-A1-8401-01 and by grant NIH/NIAID A1022933-22A1 to F.H. Significant portions of this work were performed in the Environmental Molecular Science Laboratory, a United States Department of Energy (DOE) national scientific user facility at Pacific Northwest National Laboratory (PNNL) in Richland, WA. PNNL is operated for the DOE by Battelle Memorial Institute under contract DE-AC05-76RLO-1830. This work used instrumentation and capabilities developed under support from the National Center for Research Resources (Grant RR 018522 to RDS) and the DOE's Office of Biological and Environmental Research.

Chapter 6

General Discussion

Summary

This discussion is partitioned into three sections. The first section critiques our findings regarding the rapid septicemia phenotype. In particular, we focus upon the SrfH-TRIP6 interaction and additional experiments that could improve our model. The second section addresses the screens we employed for novel secreted effectors. Particular emphasis is placed on our proteomic analysis of culture supernatants because this study diverged into multiple areas of research. The last topic discusses our preliminary findings on a third research project that is provided here as supplemental information. In this set of experiments we attempted to dissect the minimum signal required for TTS. Our data suggests that the mRNA is a determinant of the SPI-2 TTS signal, specifically the ribosome binding site (RBS).

Rapid septicemia phenotype

Overview of the SrfH-TRIP6 interaction

Generally, the host binding partners and activities of SPI-1 effectors are better understood than their SPI-2 counterparts. As a result, much of the biology concerning SPI-2 type III effectors and their roles during infection remains unknown. Micah Worley, a previous member of the laboratory, determined that the SPI-2 effector SrfH interacts with host TRIP6 to stimulate cell motility. My own work has been to test this model and to identify the signaling pathway involved.

Elucidating an effector's molecular mechanism is decidedly more problematic than a phenotype. Primary sequence alignments against mammalian genes possess little value because many *Salmonella* effectors are examples of convergent evolution although this has been successful for other pathogens such as *Legionella pneumophila* [277]. However, there are a few exceptions within *Salmonella*. For example, SteC has been shown to be a serine/threonine kinase via its homology with Raf-1 [71], and some effectors possess small motifs that can be identified by specialized BLAST searches. For example, SipA and SipB, are GEF mimics identifiable by a WxxxE motif [59]. Much of the insight regarding effector activities has been based upon observable phenotypes from infected host cells. Actin rearrangements associated with bacterial uptake or the SCV are

classic examples. More recently X-ray crystallography and NMR structural analyses have been used to dissect function because many effectors have been shown to be structural homologs of eukaryotic signaling molecules. As a result of these efforts, *Salmonella* effectors are now known to possess a diverse array of activities. For example, SopA, SlrP, SspH1, and SspH2 are ubiquitin ligases, some of which have been shown to ubiquitinate host proteins [140,141,278]. GEF mimicry also appears to be a common strategy as both SopE and SopE2 possess this activity within the host cell [279]. Conversely, SptP is a GAP mimic that antagonizes the GEF activities of SopE and SopE2 [28]. Other effectors modify membranes. SseJ associates with SCV and acetylates cholesterol [62], and SopB is an inositol phosphatase that acts upon host cell membrane phospholipids [280,281]. A more complete list describing the activities, host binding partners, and phenotypes of all known secreted effectors is provided in Table A-1 which is adapted from the recent review by McGhie et al. [2].

Critique of the SrfH-TRIP6 data

We repeated the SrfH-TRIP6 interaction using two-hybrid, Co-IP, *in silico*, and *in vivo* analyses. Most importantly, SrfH point mutants that abrogated the TRIP6 interaction in a two-hybrid assay were blocked from causing rapid septicemia, suggesting the interaction was crucial to the phenotype. Several of these observations appear to be irrefutable based on the fact that three laboratories have observed rapid septicemia following oral infection. Furthermore, relocalization of TRIP6 by SrfH has been observed by more than one laboratory. The strong interaction between SrfH and TRIP6 LIM domains also appears specific as five other LIM domain containing proteins do no interact with SrfH. Beyond these observations nothing is certain at this stage of the investigation. First, the *ab inito* model described above requires greater validation because it is not reliable without analyzing additional mutants. For example, there is a tryptophan at position 24 in the SrfH N-terminus which appears to be buried in a hydrophobic core. Changing this to a charged residue (eg Lys, Arg, Asp or Glu) might affect the N-terminal structure while changing it to a polar residue (eg Phe or Tyr) may not. Moreover, our model predicted that the closely related effector SspH2 does not interact with TRIP6 because of a single threonine substitution at position 13. All of these observations require testing. Binding experiments using these SrfH point mutants are in

progress. Secondly, our data did not define a molecular mechanism by which SrfH modulates cell motility. Although SrfH forms a complex with both c-Src and TRIP6 and activates a Src kinase in HEK293T cells, TRIP6 Y55 phosphorylation was not observed. Since this is the only known TRIP6 modification that results in increased cell motility, we cannot claim that SrfH modulates cell motility via c-Src and TRIP6, however, the experiments above do suggest that c-Src activation might occur via a TRIP6 scaffold. Purified c-Src phosphorylates TRIP6 Y55 *in vitro* [109], and the addition of purified SrfH might change the kinetics. We have been able to Co-IP SrfH and TRIP6 only when the two proteins are overexpressed in HEK293T cells but unable to Co-IP SrfH and TRIP6 from RAW 264.7 macrophages, which is worrysome. The Boyden chamber motility assays have never been reproducible from one day to the next suggesting an unidentified variable. It is well known that these assays are difficult to perform and that the results depend on the manufacturere of the Boyden chamber. The most reproducible assay has always been oral infection of mice which is fortunate because it is the preferred assay of reviewers. One pitfall to this assay is that is not possible to alter conditions in the infected cell such as siRNA knock down of TRIP6. Some of these issues may be resolved by using primary cells such as bone marrow derived macrophages (BMDM). Additionally, our dissection of the SrfH motility mechanism was complicated by a second phenotype. As described below, SrfH manipulates inflammatory pathways that may be required for cell motility, but, on the other hand, it may be the simplest functional assay.

IQGAP1 was recently identified as an alternative SrfH binding partner [175]. Much like TRIP6, IQGAP1 is a ubiquitous adaptor protein that coordinates multiple signal transduction networks including those for cell motility. IQGAP1 interacts with components of the cytoskeleton, cell adhesion molecules, and with signaling molecules that regulate cell morphology and motility. IQGAP1 effects on motility are thought to occur via interactions with Cdc42 and Rac1, but it is also known to interact with and is phosphorylated by c-Src [282]. As previously discussed in Chapter 3, SrfH has a naturally occurring amino acid polymorphism at position 103. Preliminary data from M. Worley suggests that SrfH 103G targets TRIP6, whereas SrfH 103D targets IQGAP1. If true, the fact that SrfH targets two different adaptor proteins that coordinate similar cellular processes is exciting and would be an important facet of this work when the

structure of SrfH has been determined. It will be interesting to determine if the two SrfH variants have cell type or tissue specific phenotypes.

SrfH down regulates NF-κB signaling

TRIP6 has been show to interact with several components of the innate immune system including NOD1, IL-1R, TLR2, TNFR Tollip, IRAK1, and TRAF6. TRIP6 has also been shown to interact with RIP2, an adaptor protein required for NF-κB signaling. Interestingly, RIP2 also binds to the TRIP6 LIM domains, but that association has not been clearly defined [146]. Since TRIP6 is required for disparate steps in innate immune signaling, we initiated a collaboration with Dana Philpott's laboratory to determine if SrfH expression affects NF-κB signaling. For this experiment HEK293T cells were co-transfected with SrfH and a NF-κB luciferase reporter. When cells were treated with NOD1 and NOD2 ligands, but not TNFα or IL-1, SrfH expression decreased NF-kB signaling in a dose dependent manner (Fig. A-1). Additional experiments are needed to verify that SrfH signals through TRIP6 to down regulate inflammation although it has already been shown that TRIP6 over expression increased NF-κB signaling in response to activation by TNFα, IL-1, TRL2, and Nod1 [146]. RNA-interference against TRIP6 ablated this phenotype demonstrating a requirement for TRIP6 [146]. We predict that co-expression of SrfH may decrease NF-κB activation by TRIP6. If true, SrfH may down regulate inflammation by directly preventing protein interactions required for NF-kB signaling perhaps via the LIM domains already demonstrated to be necessary for RIP2 interaction [146].

Evidence for SrfH activity

We demonstrated that the SrfH N-terminus interacted with the TRIP6 LIM domains and proposed various possibilities for how this could lead to rapid septicemia as described above, but what precisely does the SrfH C-terminus do? SrfH does not affect cell invasion or intracellular replication [11], steady state levels of TRIP6 (data not shown), nor TRIP6 tyrosine phosphorylation (Fig. 3-6C). However, we now have additional evidence suggesting that SrfH possesses an activity. BMDM were infected overnight with *Salmonella* over expressing SrfH, SrfH L10P, and SrfH I22N. A *srfH* null mutant, SPI-2 mutant and wild type bacteria were tested as controls. Phase contrast images of the infected cells were taken. Cells infected with the SrfH L10P mutant were

strikingly different morphologically, displaying fewer refractile cells than those infected with the other strains (Fig. A-2). Since SrfH L10P does not interact with TRIP6, these results might suggest indiscriminate activity resulting from the lack of TRIP6 interaction. We did not observe this phenotype with the SrfH I22N mutant, but this is not surprising considering that I22N mutation did not completely abolish TRIP6 interaction.

HBH tandem affinity tag

To determine how SrfH-TRIP6 facilitates rapid septicemia, we need a better understanding of the protein interactions in which SrfH participates. Our lab recently co-developed a His-Biotin-His (HBH) tandem affinity tag that is well-suited for this application. Following mild formaldehyde cross-linking, the HBH tag was designed for the purification of protein complexes under fully denaturing conditions and is compatible with both mass spectrometry and SDS-PAGE analysis. Since *Salmonella* can secrete effector::HBH fusions into RAW264.7 macrophages (data not shown), we are planning to analyze lysates from infected cells containing secreted SrfH::HBH in BMDM from BALB/c mice, RAW264.7 cells, and dendritic cells also from BALB/c mice. Given our data and the sensitivity of this approach, it is possible that TRIP6, IQGAP1, and c-Src will co-purify with SrfH::HBH. Furthermore, mass spectrometry may reveal a post-translational modification that is indicative of SrfH activity such as serine or threonine phosphorylation of TRIP6. Many effectors are known to interact with multiple host proteins, for example AvrA, SptP, and SifA[28,53,60,79,80,283,284]. Thus, it is certainly possible that SrfH interacts with both IQGAP1 and TRIP6. SspH2::HBH will be tested as a negative control because of its N-terminal homology with SrfH and because it did not interact with TRIP6 in a two-hyrbid assay. SspH2 is an E3 ubiquitin ligase [140], but its host target(s) is unknown and may be defined in the same experiment.

Modular organization of effector proteins

As mentioned previously, the N-terminus of SrfH is conserved with six other type III effector proteins, and a comparison of their primary sequences is provided in Fig. A-3. The N-termini of this effector family appear to mediate host protein interactions. For example, the N-terminus of SifA interactes with host SKIP. The C-termini, on the other hand, appear to have catalytic activities. For example, the SifA C-terminus is a GEF for RhoA [60]. Interestingly, SspH1, SspH2, and SlrP each possess an internal leucine rich

repeat (LRR) followed by a C-terminal ubiquitin ligase domain (Fig. A-3). Since the SspH1 LRR domain interacts with PKN1 [83] and PKN1 is ubiquitinated by this effector [82], the LRR domain likely recognizes substrate for ubiquitination by the C-terminus. SlrP ubiquitinates thioredoxin [141], but the binding domains have not been defined. Thus, the activity of each of these proteins appears to be encoded in the C-terminus while the N-terminus and LRR domains are less defined. These examples also illustrate that modular organization is a common theme among many type III effectors. *Salmonella* effectors show as much complexity as many eukaryotic proteins because they contain multiple protein binding domains and possess different enzymatic activities. In the longer run we will construct a tandem affinity tagged version of each of these effectors, infect cells, treat with formaldehyde, and define interacting partners following purification and mass spectrometric analysis. It's also possible that some effectors lack an enzymatic activity and serve as adaptor proteins that alter mammalian protein complexes, but no effectors have been reported with this characteristic to date.

Screens for novel effectors

Shortcomings of genetic screens

CyaA' secretion assays have been adopted by many members of the research community as a way to identify or corroborate secretion to the eukaryotic cell. Although this is a sensitive method for the evaluation of individual effectors, our screen for effector::CyaA' fusions by transposon mutagenesis had several shortcomings. In particular, the screen was prone to insertion hotspots and was biased for the identification of effectors secreted at high levels. In total we identified three novel and seven previously characterized effector proteins. The effector repertoire is much larger for the reasons described in my Research Objectives. As a result, I set out to find a more comprehensive system for effector identification which was the basis for the secretome work in Chapter 5.

Proteomics based approaches

Mass spectrometry has the implicit advantage of extremely high sensitivity and is an ideal instrument for evaluating the *Salmonella* secretome. We would like to identify

all *Salmonella* proteins secreted into eukaryotic cells *in vivo*, but this is not currently possible because the technology cannot selectively identify the effector repertoire from the tens of thousands mammalian proteins. *In vitro* based methods avoid this pitfall and have proven to be powerful tools for evaluating the type III secretome of pathogenic *E. coli* and now *S.* Typhimurium. Critical to this approach are *in vitro* growth conditions, a mutant that promotes effector secretion, and a control that is deficient for secretion. We employed an *ssaL* mutant to promote effector secretion, but *ssaM* and *spiC* mutants could also be used as described below.

Secretion through SPI-2 TTSS is regulated by SsaL, SsaM, and SpiC

Unpublished work by Holden and coworkers has shown that SsaL, SsaM, and SpiC form an intracellular complex that blocks SPI-2 secretion until the secretion apparatus is fully assembled. The complex is thought to act as a pH sensor that blocks secretion until the needle protrudes through the host membrane. When the complex detects a pH shift from the acidic environment of the SCV to the neutral pH of the host cytosol, the complex disassociates, permitting passage of effectors through the secretory apparatus (3rd ASM Conference on *Salmonella*, 2009). In line with the proposal that all three proteins form a complex that guards the TTSS from premature secretion, *ssaM* and *spiC* mutants secrete the SseJ effector into LPM media [255,256], suggesting that all three regulators possess similar secretion phenotypes *in vitro*. Thus, proteomic analysis of culture supernatants following a pH shift may identify additional SPI-2 secreted effectors.

Secretion regulators like SsaL, SpiC, and SsaM generally lack primary sequence homology between species suggesting that environmental signals that trigger type III secretion depends on the niche occupied by a particular pathogen. However, many TTSSs are horizontally acquired pathogenicity islands, so functionally analogous regulators should be encoded within them. Sequence analysis has recently identified a conserved domain now known as the HrpJ domain that is conserved in both SsaL, SepL and other type III systems (Pfam ID: PF07201). The HrpJ domain is approximately 200 residues long, but its precise function is unknown. However, in all cases where a mutant was tested, virulence was attenuated [228,254,285,286], suggesting that this protein family may function similarly between species. Interestingly, the SPI-1 protein InvE possesses

an HrpJ domain and is required for the invasion of cultured epithelail cells [285]. Therefore, InvE may function as a secretion regulator similar to SsaL, opening the door to anlayis of the SPI-1 secretome.

SsaL may be a negative regulator of effector expression

Western hybridization demonstrated that an *ssaL* mutant secreted SseJ into mLPM (Fig. 5-3). However, the pellet fraction shows that the *ssaL* mutant expressed approximately eight fold more SseJ at 16 hours than the wild type and *ssaK* mutant (Fig. 5-3). This phenotype was readily observable at eight hours, and based on these observations we hypothesize that SsaL may be a negative regulator of multiple effectors, but this remains to be demonstrated as does the level at which regulation takes place.

A growth defect that was not reported in the manuscript could be used to address that mechanism. The *ssaL* mutant showed an mLPM growth defect at neutral, but not at acidic pH (Fig. A-4). The growth defect was not a consequence of over secretion of effectors as is observed for *Yersinia* sp. in low calcium media because we did not observe SseJ secretion at neutral pH (Fig. A-5). This could be explained by dysregulation of effector expression without secretion or by SseJ degradation at neutral, but not acidic pH. To dissect SsaL regulation *Salmonella* mutants could be selected that survive at neutral pH. Because many of the networks regulating SPI-2 expression have been characterized, it should be possible to develop and test a model describing how SsaL down regulates effector expression.

Outer membrane vesicles (OMV)

We suspected the presence of OMV in the secretome for reasons described in Chapter 5. Briefly, two novel effectors, SssA and SssB were secreted independent of TTS, our sample preparations were similar to OMV purification strategies [259,260,266], and known OMV markers, TolC and OmpA , were identified [259]. We then hypothesized that *Salmonella* may use OMVs during infection because they are known to deliver toxins from *Vibrio, Helicobacter,* and *E. coli* species as well as hemolytic phospholipase from *Pseudomonas aeruginosa*, among others [64,287-289]. Based upon these observations we used the secretome data to identify OMV effector proteins.

Hyunjin Yoon, while working on a completely different project, found that SrfN was secreted into host cells independent of TTS. Since SrfN was also identified in the

secretome, we hypothesized that it may be secreted in OMV. SrfN is regulated by PhoPQ, a conserved two component virulence regulator present in many enteric bacteria [290]. Additionally, SrfN has a high SIEVE score. The SIEVE algorithm was intended to predict type III effectors, but it also accurately predicts secretion of other proteins, the reasons for which are not yet clear (pers. commun. J. McDermott). Using SIEVE score and PhoPQ regulation as criteria, she used the secretome data to quickly identify 12 candidates that could be secreted in OMV. CyaA' fusions were constructed, and she confirmed secretion of the following proteins into J774 macrophages: PagC, PagD, PagK, and PagK-H (Fig. A-6A). To establish an association with OMV, vesicle preparations were purified via centrifugation and probed by Western blotting using the OmpA outer membrane protein as a vesicle marker (Fig. A-6B). She also used fluroescence microscopy to visualize secretion within infected J774 macrophages. The OMV effectors had distributed, punctate secretion patterns within the cell (Fig. A-6C).

Some of the secreted OMV proteins have known virulence phenotypes. For example, PagC confers serum resistance which is required for bacteremia [246], and the *srfN* mutant colonizes the spleen and liver of IP infected BALB/c mice less efficiently than wild type bacteria (data not shown). Transposon insertions in *pagC* and *pagK* severely attenuated virulence in IP infected Balb/C mice [244], whereas a *pagD* mutant attenuated macrophage survival but not virulence in an acute infection model [245]. A phenotype has not been attributed to PagK-H. Because the positive CyaA' assays demonstrated access to the host cell cytoplasm we believe that these proteins serve as secreted effectors. Recently, it was shown that *P. aeruginosa* OMV fuse to lipid rafts in the host cell plasma membrane and are internalized by N-WASP-mediated actin trafficking [287]. All Gram negative bacteria produce OMV [291], so membrane fusion may be a conserved mechanism between species, but this remains to be demonstrated.

Reiter's syndrome

The secretome project may also provide some insight regarding Reiter's syndrome, a form of reactive arthritis that occurs in 6-30% of *Salmonella* infected individuals. Reiter's syndrome is associated with infections by other Gram negative pathogens such as *Chlamydia trachomatis*, *Shigella* spp., *Yersinia* spp., and *Campylobacter* spp. It manifests one to three weeks after infection as asymmetric

inflammation of the joints (e.g. knees, ankles, feet, and wrists). *Salmonella* antigens, but not bacteria, can be found in the synovial fluid and tissues. Reiter's syndrome is highly associated with specific MHC molecules especially HLA-B27. The simplest explanation for these observations is that a microbial derived antigen similar to a human peptide is presented by HLA-B27, breaks self-tolerance, and results in reactive arthritis. The secretome contained a large number of peptides corresponding to conserved proteins, for example ribosomes and heat shock proteins. These peptides were not intact proteins, but were apparently cleaved by a *Salmonella* encoded trypsin-like protease as the secretome contained a similar proportion of tryptic or partially tryptic peptides with or without trypsin digestion (18.8% and 18.2% of unfiltered peptides, respectively) (data not shown). Interestingly, a similar set of peptides was identified in a separate study that analyzed the proteome of *Salmonella* grown in acidic minial media [234], suggesting that this trypsin-like protease can function both intra- and extracellularly. We propose that these peptides are transported to host cells within OMV and that they are a causative agent of reactive arthritis that can follow *Salmonella*, *Campylobacter*, *Yersinia*, and *Shigella* infections. To test this we will purify OMV and determine their protein/peptide content by mass spectrometry. Second, we have access to serum from patients that suffered Reiter's syndrome following Gram negative infection as well as age/sex matched subjects from infected individuals that did not present with this condition. Western hybridization against OMV samples will determine if this secretion mechanism contributes to Reiter's syndrome.

TTS Signal

Background

The proteomic analysis described above was performed in collaboration with the Pacific Northwest National Laboratories (PNNL). Jason McDermott from PNNL was instrumental because of the SIEVE algorithm he developed. Since the SIEVE algorithm was used to predict type III effectors from annotated genomes [231], we attempted to use this algorithm to gain a better understanding of the TTS signal, which surprisingly is not well defined.

Opposing views in literature have demonstrated that the signal may be protein or mRNA encoded. *Yersinia* outer proteins (YOP) are the best understood effector model. The N-terminal 15 amino acids were inititially proposed as a secretion signal because this region is sufficient for secretion of reporter fusions [292]. However, the amino acid sequence lacks conservation between effectors. In fact, residues 2-8 of YopE can be substituted with an ampipathic series of serine/isoleucine repeats without affecting secretion although polymers of either isoleucine or serine blocked secretion [293]. When the N-terminal 15 amino acids of YopE, YopN, and YopQ were frameshifted after the translation start codon but with a compensatory suppressor mutation at the fusion site, secretion was not affected. More importantly, point mutations in the secretion signals of *yopE* and *yopQ* that altered the mRNA, but not the amino acid sequence, blocked secretion [294-296]. These contradictory results argue for both mRNA and amino acid sequences functioning as a secretion signal.

The luminal diameter of TTSSs range between 2-5 nm and are thus too narrow for passage of a folded protein [293]. It is possible to jam the type III apparatus and prevent secretion, but this has only been demonstrated using effector fusions to cytoplasmic proteins, for example β-galactosidase (LacZ) or dihydrofolate reductase (DHFR). DHFR is thought to fold so quickly that it irreversibly occludes the TTSS [297]. Some effectors are maintained in an unfolded state by chaperone proteins. The chaperone SicP with the effector SptP is one example [298], but it is not known how the chaperone-effector complex is recognized by the TTSS. The literature further suggests that some type III effector proteins, such as YopQ, can be translated concurrent with secretion [295,299,300], but this is a controversial mechanism. If this model is true then there must be specific RNA docking proteins and ribosomes at the secretion apparatus, but this has not been demonstrated.

The SPI-2 TTS signal is encoded upstream and downstream of mRNA start codon

We have designed a model system that provides insight on the *Salmonella* TTS signal and which can be adapted for dissecting the sequence requirements required for secretion. In an attempt to characterize the minimum signal required for *Salmonella* TTS, we used the SIEVE algorithm to predict consensus signals for effectors that go out through SPI-1, SPI-2, and both TTSSs (SPI-1/2) (Fig. A-7A). These 37 AA sequences

were fused to CyaA' and assessed for secretion with *Salmonella* infected J774 macrophages. Secretion occurred for all three derivatives, suggesting that the N-terminus does not play a role in directing an effector to a particular TTSS (Fig. A-7C). To our amazement, secretion required an RBS originating from an effector (SPI-1 = *sifA*, SPI-1/2 = *steA*, SPI-2 = *srfH*) (Fig. A-7C), but was inhibited when the effector was expressed from a phage RBS (Fig. A-7C). Since all constructs were cloned with ≤25 nucleotides upstream of the AUG (Fig. A-7B), these results indicate that an appropriate RBS is required for SPI-2 TTS. To determine if the RBS was sufficient for secretion, *sifA*, *srfH*, *steA*, and phage RBS were fused directly to *cyaA*' and tested. Only the SteA::CyaA' fusion was secreted (Fig. A-7D). Thus, sequences downstream of the AUG start codon influence secretion, suggesting that mRNA secondary structure may be another determinant of the secretion signal. Protein expression, as judged by Western hybridization, varied between the different constructs and is one caveat to these experiments (Fig. A-7C and Fig. A-7D). In some cases there was up to a 10 fold difference, but all of the constructs were expressed and, when secreted, had a robust cAMP response, suggesting that the assays were sensitive and accurate. Taken together, these results indicate that the SPI-2 TTS signal is mRNA encoded, but they do not explicitly refute a proteinaceous signal. Interestingly, none of these constructs were secreted under SPI-1 inducing conditions (data not shown) suggesting that other factors such as chaperones may be necessary for SPI-1 TTS. The minimalist approach we described will be used to determine if the RBS of all other type III effector is sufficient for secretion. Based upon these results we hope to formulate a testable model for the minimal sequences and mRNA structures necessary for secretion. Second we can add upstream or downstream sequences to ascertain how effectors are directed to the SPI-1 TTSS. Finally, computational analyses can be designed around these findings to further refine the SIEVE algorithm and to identify additional effectors.

Conclusions

Salmonella pathogenesis is effector driven and is a remarkable aspect of this microbe's biology. However, the research community's reliance on a limited number of models

makes effector phenotypes difficult to discern as they often share redundant activities and can interact with multiple proteins when overproduced in the mammalian cell. Future research will likely begin to evaluate when and where an effector is expressed and if its activity affects cell, tissues, and animal models differently. Continued study will undoubtedly define the pathways subverted during infection and identify many new therapeutic targets.

References

1. Galen JE, Pasetti MF, Tennant S, Ruiz-Olvera P, Sztein MB et al. (2009) Salmonella enterica serovar Typhi live vector vaccines finally come of age. Immunol Cell Biol 87: 400-412.
2. McGhie EJ, Brawn LC, Hume PJ, Humphreys D, Koronakis V (2009) *Salmonella* takes control: effector-driven manipulation of the host. Curr Opin Microbiol 12: 117-124.
3. Ramsden AE, Holden DW, Mota LJ (2007) Membrane dynamics and spatial distribution of Salmonella-containing vacuoles. Trends Microbiol 15: 516-524.
4. Thomas M, Holden DW (2009) Ubiquitination - a bacterial effector's ticket to ride. Cell Host Microbe 5: 309-311.
5. Santos RL, Raffatellu M, Bevins CL, Adams LG, Tukel C et al. (2009) Life in the inflamed intestine, Salmonella style. Trends Microbiol 17: 498-506.
6. Steele-Mortimer O (2008) The Salmonella-containing vacuole: moving with the times. Curr Opin Microbiol 11: 38-45.
7. Ohl ME, Miller SI (2001) Salmonella: a model for bacterial pathogenesis. Annu Rev Med 52: 259-274.
8. Monack DM, Bouley DM, Falkow S (2004) Salmonella typhimurium persists within macrophages in the mesenteric lymph nodes of chronically infected Nramp1+/+ mice and can be reactivated by IFNgamma neutralization. J Exp Med 199: 231-241.
9. Vazquez-Torres A, Jones-Carson J, Baumler AJ, Falkow S, Valdivia R et al. (1999) Extraintestinal dissemination of Salmonella by CD18-expressing phagocytes. Nature 401: 804-808.
10. GERICHTER CB (1960) The dissemination of Salmonella typhi, S. paratyphi A and S. paratyphi B through the organs of the white mouse by oral infection. J Hyg (Lond) 58: 307-319.
11. Worley MJ, Nieman GS, Geddes K, Heffron F (2006) Salmonella typhimurium disseminates within its host by manipulating the motility of infected cells. Proc Natl Acad Sci U S A 103: 17915-17920.
12. Mittrucker HW, Kaufmann SH (2000) Immune response to infection with Salmonella typhimurium in mice. J Leukoc Biol 67: 457-463.
13. Bambou JC, Giraud A, Menard S, Begue B, Rakotobe S et al. (2004) In vitro and ex vivo activation of the TLR5 signaling pathway in intestinal epithelial cells by a commensal Escherichia coli strain. J Biol Chem 279: 42984-42992.
14. Hapfelmeier S, Hardt WD (2005) A mouse model for S. typhimurium-induced enterocolitis. Trends Microbiol 13: 497-503.
15. Stecher B, Hapfelmeier S, Muller C, Kremer M, Stallmach T et al. (2004) Flagella and chemotaxis are required for efficient induction of Salmonella enterica serovar Typhimurium colitis in streptomycin-pretreated mice. Infect Immun 72: 4138-4150.
16. Liu J, Fujiwara TM, Buu NT, Sanchez FO, Cellier M et al. (1995) Identification of polymorphisms and sequence variants in the human homologue of the mouse natural resistance-associated macrophage protein gene. Am J Hum Genet 56: 845-853.

17. Vidal S, Tremblay ML, Govoni G, Gauthier S, Sebastiani G et al. (1995) The Ity/Lsh/Bcg locus: natural resistance to infection with intracellular parasites is abrogated by disruption of the Nramp1 gene. J Exp Med 182: 655-666.
18. Rodriguez-Morales O, Fernandez-Mora M, Hernandez-Lucas I, Vazquez A, Puente JL et al. (2006) Salmonella enterica serovar Typhimurium ompS1 and ompS2 mutants are attenuated for virulence in mice. Infect Immun 74: 1398-1402.
19. Jones BD, Ghori N, Falkow S (1994) Salmonella typhimurium initiates murine infection by penetrating and destroying the specialized epithelial M cells of the Peyer's patches. J Exp Med 180: 15-23.
20. Lawley TD, Chan K, Thompson LJ, Kim CC, Govoni GR et al. (2006) Genome-wide screen for Salmonella genes required for long-term systemic infection of the mouse. PLoS Pathog 2: e11.
21. Linehan SA, Rytkonen A, Yu XJ, Liu M, Holden DW (2005) SlyA regulates function of Salmonella pathogenicity island 2 (SPI-2) and expression of SPI-2-associated genes. Infect Immun 73: 4354-4362.
22. Zhou D, Galan J (2001) Salmonella entry into host cells: the work in concert of type III secreted effector proteins. Microbes Infect 3: 1293-1298.
23. Cain RJ, Hayward RD, Koronakis V (2008) Deciphering interplay between Salmonella invasion effectors. PLoS Pathog 4: e1000037.
24. Huang Z, Sutton SE, Wallenfang AJ, Orchard RC, Wu X et al. (2009) Structural insights into host GTPase isoform selection by a family of bacterial GEF mimics. Nat Struct Mol Biol 16: 853-860.
25. Buchwald G, Friebel A, Galan JE, Hardt WD, Wittinghofer A et al. (2002) Structural basis for the reversible activation of a Rho protein by the bacterial toxin SopE. EMBO J 21: 3286-3295.
26. Huang FC, Werne A, Li Q, Galyov EE, Walker WA et al. (2004) Cooperative interactions between flagellin and SopE2 in the epithelial interleukin-8 response to Salmonella enterica serovar typhimurium infection. Infect Immun 72: 5052-5062.
27. Molero C, Rodriguez-Escudero I, Aleman A, Rotger R, Molina M et al. (2009) Addressing the effects of Salmonella internalization in host cell signaling on a reverse-phase protein array. Proteomics 9: 3652-3665.
28. Fu Y, Galan JE (1999) A salmonella protein antagonizes Rac-1 and Cdc42 to mediate host-cell recovery after bacterial invasion. Nature 401: 293-297.
29. Geddes K, Worley M, Niemann G, Heffron F (2005) Identification of new secreted effectors in Salmonella enterica serovar Typhimurium. Infect Immun 73: 6260-6271.
30. Kubori T, Galan JE (2003) Temporal regulation of salmonella virulence effector function by proteasome-dependent protein degradation. Cell 115: 333-342.
31. Lin SL, Le TX, Cowen DS (2003) SptP, a Salmonella typhimurium type III-secreted protein, inhibits the mitogen-activated protein kinase pathway by inhibiting Raf activation. Cell Microbiol 5: 267-275.
32. Van Engelenburg SB, Palmer AE (2008) Quantification of real-time Salmonella effector type III secretion kinetics reveals differential secretion rates for SopE2 and SptP. Chem Biol 15: 619-628.

33. Schlumberger MC, Muller AJ, Ehrbar K, Winnen B, Duss I et al. (2005) Real-time imaging of type III secretion: Salmonella SipA injection into host cells. Proc Natl Acad Sci U S A 102: 12548-12553.
34. Hernandez LD, Hueffer K, Wenk MR, Galan JE (2004) Salmonella modulates vesicular traffic by altering phosphoinositide metabolism. Science 304: 1805-1807.
35. Patel JC, Galan JE (2006) Differential activation and function of Rho GTPases during Salmonella-host cell interactions. J Cell Biol 175: 453-463.
36. Dai S, Zhang Y, Weimbs T, Yaffe MB, Zhou D (2007) Bacteria-generated PtdIns(3)P recruits VAMP8 to facilitate phagocytosis. Traffic 8: 1365-1374.
37. Marcus SL, Wenk MR, Steele-Mortimer O, Finlay BB (2001) A synaptojanin-homologous region of Salmonella typhimurium SigD is essential for inositol phosphatase activity and Akt activation. FEBS Lett 494: 201-207.
38. Kuijl C, Savage ND, Marsman M, Tuin AW, Janssen L et al. (2007) Intracellular bacterial growth is controlled by a kinase network around PKB/AKT1. Nature 450: 725-730.
39. Hayward RD, Koronakis V (2002) Direct modulation of the host cell cytoskeleton by Salmonella actin-binding proteins. Trends Cell Biol 12: 15-20.
40. McGhie EJ, Hayward RD, Koronakis V (2004) Control of actin turnover by a salmonella invasion protein. Mol Cell 13: 497-510.
41. McGhie EJ, Hayward RD, Koronakis V (2001) Cooperation between actin-binding proteins of invasive Salmonella: SipA potentiates SipC nucleation and bundling of actin. EMBO J 20: 2131-2139.
42. Nikolaus T, Deiwick J, Rappl C, Freeman JA, Schroder W et al. (2001) SseBCD proteins are secreted by the type III secretion system of Salmonella pathogenicity island 2 and function as a translocon. J Bacteriol 183: 6036-6045.
43. Hayward RD, Koronakis V (1999) Direct nucleation and bundling of actin by the SipC protein of invasive Salmonella. EMBO J 18: 4926-4934.
44. Perrett CA, Jepson MA (2009) Regulation of Salmonella-induced membrane ruffling by SipA differs in strains lacking other effectors. Cell Microbiol 11: 475-487.
45. Silva M, Song C, Nadeau WJ, Matthews JB, McCormick BA (2004) Salmonella typhimurium SipA-induced neutrophil transepithelial migration: involvement of a PKC-alpha-dependent signal transduction pathway. Am J Physiol Gastrointest Liver Physiol 286: G1024-31.
46. Jones MA, Wood MW, Mullan PB, Watson PR, Wallis TS et al. (1998) Secreted effector proteins of Salmonella dublin act in concert to induce enteritis. Infect Immun 66: 5799-5804.
47. Bakowski MA, Cirulis JT, Brown NF, Finlay BB, Brumell JH (2007) SopD acts cooperatively with SopB during Salmonella enterica serovar Typhimurium invasion. Cell Microbiol 9: 2839-2855.
48. Drecktrah D, Knodler LA, Howe D, Steele-Mortimer O (2007) Salmonella trafficking is defined by continuous dynamic interactions with the endolysosomal system. Traffic 8: 212-225.
49. Bakowski MA, Braun V, Brumell JH (2008) Salmonella-containing vacuoles: directing traffic and nesting to grow. Traffic 9: 2022-2031.

50. Fang F, Vazquez-Torres A (2002) Salmonella selectively stops traffic. Trends Microbiol 10: 391-392.
51. Smith AC, Heo WD, Braun V, Jiang X, Macrae C et al. (2007) A network of Rab GTPases controls phagosome maturation and is modulated by Salmonella enterica serovar Typhimurium. J Cell Biol 176: 263-268.
52. Ramsden AE, Mota LJ, Munter S, Shorte SL, Holden DW (2007) The SPI-2 type III secretion system restricts motility of Salmonella-containing vacuoles. Cell Microbiol 9: 2517-2529.
53. Humphreys D, Hume PJ, Koronakis V (2009) The Salmonella effector SptP dephosphorylates host AAA+ ATPase VCP to promote development of its intracellular replicative niche. Cell Host Microbe 5: 225-233.
54. Ye Y (2006) Diverse functions with a common regulator: ubiquitin takes command of an AAA ATPase. J Struct Biol 156: 29-40.
55. Stein MA, Leung KY, Zwick M, Garcia-del Portillo F, Finlay BB (1996) Identification of a Salmonella virulence gene required for formation of filamentous structures containing lysosomal membrane glycoproteins within epithelial cells. Mol Microbiol 20: 151-164.
56. Brumell JH, Rosenberger CM, Gotto GT, Marcus SL, Finlay BB (2001) SifA permits survival and replication of Salmonella typhimurium in murine macrophages. Cell Microbiol 3: 75-84.
57. Reinicke AT, Hutchinson JL, Magee AI, Mastroeni P, Trowsdale J et al. (2005) A Salmonella typhimurium effector protein SifA is modified by host cell prenylation and S-acylation machinery. J Biol Chem 280: 14620-14627.
58. Alto NM, Dixon JE (2008) Analysis of Rho-GTPase mimicry by a family of bacterial type III effector proteins. Methods Enzymol 439: 131-143.
59. Alto NM, Shao F, Lazar CS, Brost RL, Chua G et al. (2006) Identification of a bacterial type III effector family with G protein mimicry functions. Cell 124: 133-145.
60. Ohlson MB, Huang Z, Alto NM, Blanc MP, Dixon JE et al. (2008) Structure and function of Salmonella SifA indicate that its interactions with SKIP, SseJ, and RhoA family GTPases induce endosomal tubulation. Cell Host Microbe 4: 434-446.
61. Freeman JA, Ohl ME, Miller SI (2003) The Salmonella enterica serovar typhimurium translocated effectors SseJ and SifB are targeted to the Salmonella-containing vacuole. Infect Immun 71: 418-427.
62. Nawabi P, Catron DM, Haldar K (2008) Esterification of cholesterol by a type III secretion effector during intracellular Salmonella infection. Mol Microbiol 68: 173-185.
63. Ruiz-Albert J, Yu XJ, Beuzon CR, Blakey AN, Galyov EE et al. (2002) Complementary activities of SseJ and SifA regulate dynamics of the Salmonella typhimurium vacuolar membrane. Mol Microbiol 44: 645-661.
64. Abrahams GL, Muller P, Hensel M (2006) Functional dissection of SseF, a type III effector protein involved in positioning the salmonella-containing vacuole. Traffic 7: 950-965.
65. Deiwick J, Salcedo SP, Boucrot E, Gilliland SM, Henry T et al. (2006) The translocated Salmonella effector proteins SseF and SseG interact and are required to establish an intracellular replication niche. Infect Immun 74: 6965-6972.

66. Knodler LA, Vallance BA, Hensel M, Jackel D, Finlay BB et al. (2003) Salmonella type III effectors PipB and PipB2 are targeted to detergent-resistant microdomains on internal host cell membranes. Mol Microbiol 49: 685-704.
67. Knodler LA, Steele-Mortimer O (2005) The Salmonella effector PipB2 affects late endosome/lysosome distribution to mediate Sif extension. Mol Biol Cell 16: 4108-4123.
68. Henry T, Couillault C, Rockenfeller P, Boucrot E, Dumont A et al. (2006) The Salmonella effector protein PipB2 is a linker for kinesin-1. Proc Natl Acad Sci U S A 103: 13497-13502.
69. Jiang X, Rossanese OW, Brown NF, Kujat-Choy S, Galan JE et al. (2004) The related effector proteins SopD and SopD2 from Salmonella enterica serovar Typhimurium contribute to virulence during systemic infection of mice. Mol Microbiol 54: 1186-1198.
70. Gotoh H, Okada N, Kim YG, Shiraishi K, Hirami N et al. (2003) Extracellular secretion of the virulence plasmid-encoded ADP-ribosyltransferase SpvB in Salmonella. Microb Pathog 34: 227-238.
71. Poh J, Odendall C, Spanos A, Boyle C, Liu M et al. (2008) SteC is a Salmonella kinase required for SPI-2-dependent F-actin remodelling. Cell Microbiol 10: 20-30.
72. Grant AJ, Restif O, McKinley TJ, Sheppard M, Maskell DJ et al. (2008) Modelling within-host spatiotemporal dynamics of invasive bacterial disease. PLoS Biol 6: e74.
73. Buchmeier NA, Heffron F (1991) Inhibition of macrophage phagosome-lysosome fusion by Salmonella typhimurium. Infect Immun 59: 2232-2238.
74. Fink SL, Cookson BT (2007) Pyroptosis and host cell death responses during Salmonella infection. Cell Microbiol 9: 2562-2570.
75. Bruey JM, Bruey-Sedano N, Luciano F, Zhai D, Balpai R et al. (2007) Bcl-2 and Bcl-XL regulate proinflammatory caspase-1 activation by interaction with NALP1. Cell 129: 45-56.
76. Micheau O, Tschopp J (2003) Induction of TNF receptor I-mediated apoptosis via two sequential signaling complexes. Cell 114: 181-190.
77. Layton AN, Galyov EE (2007) Salmonella-induced enteritis: molecular pathogenesis and therapeutic implications. Expert Rev Mol Med 9: 1-17.
78. Gilmore TD (2006) Introduction to NF-kappaB: players, pathways, perspectives. Oncogene 25: 6680-6684.
79. Ye Z, Petrof EO, Boone D, Claud EC, Sun J (2007) Salmonella effector AvrA regulation of colonic epithelial cell inflammation by deubiquitination. Am J Pathol 171: 882-892.
80. Jones RM, Wu H, Wentworth C, Luo L, Collier-Hyams L et al. (2008) Salmonella AvrA Coordinates Suppression of Host Immune and Apoptotic Defenses via JNK Pathway Blockade. Cell Host Microbe 3: 233-244.
81. Napoli C, Staskawicz B (1987) Molecular characterization and nucleic acid sequence of an avirulence gene from race 6 of Pseudomonas syringae pv. glycinea. J Bacteriol 169: 572-578.
82. Rohde JR, Breitkreutz A, Chenal A, Sansonetti PJ, Parsot C (2007) Type III secretion effectors of the IpaH family are E3 ubiquitin ligases. Cell Host Microbe 1: 77-83.

83. Haraga A, Miller SI (2006) A Salmonella type III secretion effector interacts with the mammalian serine/threonine protein kinase PKN1. Cell Microbiol 8: 837-846.
84. Le Negrate G, Faustin B, Welsh K, Loeffler M, Krajewska M et al. (2008) Salmonella secreted factor L deubiquitinase of Salmonella typhimurium inhibits NF-kappaB, suppresses IkappaBalpha ubiquitination and modulates innate immune responses. J Immunol 180: 5045-5056.
85. Harding CV, Pfeifer JD (1994) Antigen expressed by Salmonella typhimurium is processed for class I major histocompatibility complex presentation by macrophages but not infected epithelial cells. Immunology 83: 670-674.
86. Murphy KP, Travers P, Walport M, Janeway C (2008) Janeway's immunobiology. New York: Garland Science. xxi, 887 p.
87. Lapaque N, Hutchinson JL, Jones DC, Meresse S, Holden DW et al. (2009) Salmonella regulates polyubiquitination and surface expression of MHC class II antigens. Proc Natl Acad Sci U S A 106: 14052-14057.
88. Kaufmann SH, Schaible UE (2005) Antigen presentation and recognition in bacterial infections. Curr Opin Immunol 17: 79-87.
89. Halici S, Zenk SF, Jantsch J, Hensel M (2008) Functional analysis of the Salmonella pathogenicity island 2-mediated inhibition of antigen presentation in dendritic cells. Infect Immun 76: 4924-4933.
90. Sundquist M, Wick MJ (2009) Salmonella induces death of CD8alpha(+) dendritic cells but not CD11c(int)CD11b(+) inflammatory cells in vivo via MyD88 and TNFR1. J Leukoc Biol 85: 225-234.
91. Raffatellu M, Santos RL, Verhoeven DE, George MD, Wilson RP et al. (2008) Simian immunodeficiency virus-induced mucosal interleukin-17 deficiency promotes Salmonella dissemination from the gut. Nat Med 14: 421-428.
92. van der Velden AW, Copass MK, Starnbach MN (2005) Salmonella inhibit T cell proliferation by a direct, contact-dependent immunosuppressive effect. Proc Natl Acad Sci U S A 102: 17769-17774.
93. van der Velden AW, Dougherty JT, Starnbach MN (2008) Down-modulation of TCR expression by Salmonella enterica serovar Typhimurium. J Immunol 180: 5569-5574.
94. Srinivasan A, Nanton M, Griffin A, McSorley SJ (2009) Culling of activated CD4 T cells during typhoid is driven by Salmonella virulence genes. J Immunol 182: 7838-7845.
95. McSorley SJ, Jenkins MK (2000) Antibody is required for protection against virulent but not attenuated Salmonella enterica serovar typhimurium. Infect Immun 68: 3344-3348.
96. Calandra T, Bucala R (1997) Macrophage migration inhibitory factor (MIF): a glucocorticoid counter-regulator within the immune system. Crit Rev Immunol 17: 77-88.
97. Hermanowski-Vosatka A, Mundt SS, Ayala JM, Goyal S, Hanlon WA et al. (1999) Enzymatically inactive macrophage migration inhibitory factor inhibits monocyte chemotaxis and random migration. Biochemistry 38: 12841-12849.
98. MacPherson GG, Jenkins CD, Stein MJ, Edwards C (1995) Endotoxin-mediated dendritic cell release from the intestine. Characterization of released dendritic cells and TNF dependence. J Immunol 154: 1317-1322.

99. Rothkotter HJ, Pabst R, Bailey M (1999) Lymphocyte migration in the intestinal mucosa: entry, transit and emigration of lymphoid cells and the influence of antigen. Vet Immunol Immunopathol 72: 157-165.
100. Westermann J, Puskas Z, Pabst R (1988) Blood transit and recirculation kinetics of lymphocyte subsets in normal rats. Scand J Immunol 28: 203-210.
101. Autenrieth IB, Kempf V, Sprinz T, Preger S, Schnell A (1996) Defense mechanisms in Peyer's patches and mesenteric lymph nodes against Yersinia enterocolitica involve integrins and cytokines. Infect Immun 64: 1357-1368.
102. Marra A, Isberg RR (1997) Invasin-dependent and invasin-independent pathways for translocation of Yersinia pseudotuberculosis across the Peyer's patch intestinal epithelium. Infect Immun 65: 3412-3421.
103. Pepe JC, Miller VL (1993) Yersinia enterocolitica invasin: a primary role in the initiation of infection. Proc Natl Acad Sci U S A 90: 6473-6477.
104. Vazquez-Torres A, Fang FC (2000) Cellular routes of invasion by enteropathogens. Curr Opin Microbiol 3: 54-59.
105. Stupack DG, Cho SY, Klemke RL (2000) Molecular signaling mechanisms of cell migration and invasion. Immunol Res 21: 83-88.
106. Lee JW, Choi HS, Gyuris J, Brent R, Moore DD (1995) Two classes of proteins dependent on either the presence or absence of thyroid hormone for interaction with the thyroid hormone receptor. Mol Endocrinol 9: 243-254.
107. Kain KH, Klemke RL (2001) Inhibition of cell migration by Abl family tyrosine kinases through uncoupling of Crk-CAS complexes. J Biol Chem 276: 16185-16192.
108. Kassel O, Schneider S, Heilbock C, Litfin M, Gottlicher M et al. (2004) A nuclear isoform of the focal adhesion LIM-domain protein Trip6 integrates activating and repressing signals at AP-1- and NF-kappaB-regulated promoters. Genes Dev 18: 2518-2528.
109. Lai YJ, Chen CS, Lin WC, Lin FT (2005) c-Src-mediated phosphorylation of TRIP6 regulates its function in lysophosphatidic acid-induced cell migration. Mol Cell Biol 25: 5859-5868.
110. Xu J, Lai YJ, Lin WC, Lin FT (2004) TRIP6 enhances lysophosphatidic acid-induced cell migration by interacting with the lysophosphatidic acid 2 receptor. J Biol Chem 279: 10459-10468.
111. Yi J, Kloeker S, Jensen CC, Bockholt S, Honda H et al. (2002) Members of the Zyxin family of LIM proteins interact with members of the p130Cas family of signal transducers. J Biol Chem 277: 9580-9589.
112. Hueck CJ (1998) Type III protein secretion systems in bacterial pathogens of animals and plants. Microbiol Mol Biol Rev 62: 379-433.
113. Miao EA, Miller SI (2000) A conserved amino acid sequence directing intracellular type III secretion by Salmonella typhimurium. Proc Natl Acad Sci U S A 97: 7539-7544.
114. Worley MJ, Ching KH, Heffron F (2000) *Salmonella* SsrB activates a global regulon of horizontally acquired genes. Mol Microbiol 36: 749-761.
115. Miao EA, Brittnacher M, Haraga A, Jeng RL, Welch MD et al. (2003) Salmonella effectors translocated across the vacuolar membrane interact with the actin cytoskeleton. Mol Microbiol 48: 401-415.

116. Klemke RL, Leng J, Molander R, Brooks PC, Vuori K et al. (1998) CAS/Crk coupling serves as a "molecular switch" for induction of cell migration. J Cell Biol 140: 961-972.
117. Fields PI, Swanson RV, Haidaris CG, Heffron F (1986) Mutants of *Salmonella typhimurium* that cannot survive within the macrophage are avirulent. Proc Natl Acad Sci U S A 83: 5189-5193.
118. Li XC, Miyasaka M, Issekutz TB (1998) Blood monocyte migration to acute lung inflammation involves both CD11/CD18 and very late activation antigen-4-dependent and independent pathways. J Immunol 161: 6258-6264.
119. Wilson RW, Ballantyne CM, Smith CW, Montgomery C, Bradley A et al. (1993) Gene targeting yields a CD18-mutant mouse for study of inflammation. J Immunol 151: 1571-1578.
120. Brown NF, Vallance BA, Coombes BK, Valdez Y, Coburn BA et al. (2005) Salmonella pathogenicity island 2 is expressed prior to penetrating the intestine. PLoS Pathog 1: e32.
121. Rescigno M, Urbano M, Valzasina B, Francolini M, Rotta G et al. (2001) Dendritic cells express tight junction proteins and penetrate gut epithelial monolayers to sample bacteria. Nat Immunol 2: 361-367.
122. Sanderson CM, Way M, Smith GL (1998) Virus-induced cell motility. J Virol 72: 1235-1243.
123. Lue H, Kleemann R, Calandra T, Roger T, Bernhagen J (2002) Macrophage migration inhibitory factor (MIF): mechanisms of action and role in disease. Microbes Infect 4: 449-460.
124. Stavitsky AB, Xianli J (2002) In vitro and in vivo regulation by macrophage migration inhibitory factor (MIF) of expression of MHC-II, costimulatory, adhesion, receptor, and cytokine molecules. Cell Immunol 217: 95-104.
125. Roger T, Froidevaux C, Martin C, Calandra T (2003) Macrophage migration inhibitory factor (MIF) regulates host responses to endotoxin through modulation of Toll-like receptor 4 (TLR4). J Endotoxin Res 9: 119-123.
126. van der Velden AW, Lindgren SW, Worley MJ, Heffron F (2000) Salmonella pathogenicity island 1-independent induction of apoptosis in infected macrophages by Salmonella enterica serotype typhimurium. Infect Immun 68: 5702-5709.
127. Wang RF, Kushner SR (1991) Construction of versatile low-copy-number vectors for cloning, sequencing and gene expression in Escherichia coli. Gene 100: 195-199.
128. Ausubel FM, Brent R, Kingston RE, Moore DD, Seidman JG et al. K Struhl (1987-1997) Current protocols in molecular biology.
129. Maloy SR, Stewart VJ, Taylor R, Maloy SR Genetic Analysis of Pathogenic Bacteria: A Laboratory Manual, 1996. CSHL Press
130. Worley MJ, Stojiljkovic I, Heffron F (1998) The identification of exported proteins with gene fusions to invasin. Mol Microbiol 29: 1471-1480.
131. Hanser BM, Gustafsson MG, Agard DA, Sedat JW (2004) Phase-retrieved pupil functions in wide-field fluorescence microscopy. J Microsc 216: 32-48.
132. van der Velden AW, Baumler AJ, Tsolis RM, Heffron F (1998) Multiple fimbrial adhesins are required for full virulence of Salmonella typhimurium in mice. Infect Immun 66: 2803-2808.

133. Mead PS, Slutsker L, Griffin PM, Tauxe RV (1999) Food-related illness and death in the united states reply to dr. hedberg. Emerg Infect Dis 5: 841-842.
134. Tam MA, Rydstrom A, Sundquist M, Wick MJ (2008) Early cellular responses to Salmonella infection: dendritic cells, monocytes, and more. Immunol Rev 225: 140-162.
135. Hansen-Wester I, Hensel M (2001) *Salmonella* pathogenicity islands encoding type III secretion systems. Microbes Infect 3: 549-559.
136. Waterman SR, Holden DW (2003) Functions and effectors of the Salmonella pathogenicity island 2 type III secretion system. Cell Microbiol 5: 501-511.
137. Liao AP, Petrof EO, Kuppireddi S, Zhao Y, Xia Y et al. (2008) Salmonella type III effector AvrA stabilizes cell tight junctions to inhibit inflammation in intestinal epithelial cells. PLoS One 3: e2369.
138. Miao EA, Scherer CA, Tsolis RM, Kingsley RA, Adams LG et al. (1999) Salmonella typhimurium leucine-rich repeat proteins are targeted to the SPI1 and SPI2 type III secretion systems. Mol Microbiol 34: 850-864.
139. Boucrot E, Henry T, Borg JP, Gorvel JP, Meresse S (2005) The intracellular fate of Salmonella depends on the recruitment of kinesin. Science 308: 1174-1178.
140. Quezada CM, Hicks SW, Galan JE, Stebbins CE (2009) A family of Salmonella virulence factors functions as a distinct class of autoregulated E3 ubiquitin ligases. Proc Natl Acad Sci U S A 106: 4864-4869.
141. Bernal-Bayard J, Ramos-Morales F (2009) Salmonella type III secretion effector SlrP is an E3 ubiquitin ligase for mammalian thioredoxin. J Biol Chem 284: 27587-27595.
142. Petit MM, Mols R, Schoenmakers EF, Mandahl N, Van dV, W. J. (1996) LPP, the preferred fusion partner gene of HMGIC in lipomas, is a novel member of the LIM protein gene family. Genomics 36: 118-129.
143. Marie H, Pratt SJ, Betson M, Epple H, Kittler JT et al. (2003) The LIM protein Ajuba is recruited to cadherin-dependent cell junctions through an association with alpha-catenin. J Biol Chem 278: 1220-1228.
144. Hervy M, Hoffman L, Beckerle MC (2006) From the membrane to the nucleus and back again: bifunctional focal adhesion proteins. Curr Opin Cell Biol 18: 524-532.
145. Wang Y, Gilmore TD (2001) LIM domain protein Trip6 has a conserved nuclear export signal, nuclear targeting sequences, and multiple transactivation domains. Biochim Biophys Acta 1538: 260-272.
146. Li L, Bin LH, Li F, Liu Y, Chen D et al. (2005) TRIP6 is a RIP2-associated common signaling component of multiple NF-kappaB activation pathways. J Cell Sci TRIP6 is a RIP2-associated common signaling component of multiple NF-kappaB activation pathways 118: 555-563.
147. Chastre E, Abdessamad M, Kruglov A, Bruyneel E, Bracke M et al. (2009) TRIP6, a novel molecular partner of the MAGI-1 scaffolding molecule, promotes invasiveness. Faseb J 23: 916-928.
148. Webb DJ, Parsons JT, Horwitz AF (2002) Adhesion assembly, disassembly and turnover in migrating cells -- over and over and over again. Nat Cell Biol 4: E97-100.

149. Panetti TS, Magnusson MK, Peyruchaud O, Zhang Q, Cooke ME et al. (2001) Modulation of cell interactions with extracellular matrix by lysophosphatidic acid and sphingosine 1-phosphate. Prostaglandins 64: 93-106.
150. Sah VP, Seasholtz TM, Sagi SA, Brown JH (2000) The role of Rho in G protein-coupled receptor signal transduction. Annu Rev Pharmacol Toxicol 40: 459-489.
151. Huveneers S, Danen EH (2009) Adhesion signaling - crosstalk between integrins, Src and Rho. J Cell Sci 122: 1059-1069.
152. Kim M, Carman CV, Springer TA (2003) Bidirectional transmembrane signaling by cytoplasmic domain separation in integrins. Science 301: 1720-1725.
153. Plow EF, Haas TA, Zhang L, Loftus J, Smith JW (2000) Ligand binding to integrins. J Biol Chem 275: 21785-21788.
154. Vinogradova O, Velyvis A, Velyviene A, Hu B, Haas T et al. (2002) A structural mechanism of integrin alpha(IIb)beta(3) "inside-out" activation as regulated by its cytoplasmic face. Cell 110: 587-597.
155. Shatsky M, Dror O, Schneidman-Duhovny D, Nussinov R, Wolfson HJ (2004) BioInfo3D: a suite of tools for structural bioinformatics. Nucleic Acids Res 32: W503-7.
156. Eswar N, Webb B, Marti-Renom MA, Madhusudhan MS, Eramian D et al. (2007) Comparative protein structure modeling using MODELLER. Curr Protoc Protein Sci Chapter 2: Unit 2 9.
157. Hart GL, Blum V, Walorski MJ, Zunger A (2005) Evolutionary approach for determining first-principles hamiltonians. Nat Mater 4: 391-394.
158. Rohl CA, Strauss CE, Misura KM, Baker D (2004) Protein structure prediction using Rosetta. Methods Enzymol 383: 66-93.
159. Dill KA, Bromberg S, Yue K, Fiebig KM, Yee DP et al. (1995) Principles of protein folding--a perspective from simple exact models. Protein Sci 4: 561-602.
160. Wilkinson P, Waterfield NR, Crossman L, Corton C, Sanchez-Contreras M et al. (2009) Comparative genomics of the emerging human pathogen Photorhabdus asymbiotica with the insect pathogen Photorhabdus luminescens. BMC Genomics 10: 302.
161. Cayrol C, Cabrolier G, Ducommun B (1997) Use of the two-hybrid system to identify protein-protein interaction temperature-sensitive mutants: application to the CDK2/p21Cip1 interaction. Nucleic Acids Res 25: 3743-3744.
162. Moreira IS, Fernandes PA, Ramos MJ (2007) Hot spots--a review of the protein-protein interface determinant amino-acid residues. Proteins 68: 803-812.
163. Wells JA (1991) Systematic mutational analyses of protein-protein interfaces. Methods Enzymol 202: 390-411.
164. Nelson DL, Lehninger AL, Cox MM (2008) Lehninger principles of biochemistry. New York: W.H. Freeman. 1 v. (various pagings) p.
165. Pace CN, Scholtz JM (1998) A helix propensity scale based on experimental studies of peptides and proteins. Biophys J 75: 422-427.
166. Alper O, Bowden ET (2005) Novel insights into c-Src. Curr Pharm Des 11: 1119-1130.
167. Aoki J (2004) Mechanisms of lysophosphatidic acid production. Semin Cell Dev Biol 15: 477-489.

168. Tigyi G, Miledi R (1992) Lysophosphatidates bound to serum albumin activate membrane currents in Xenopus oocytes and neurite retraction in PC12 pheochromocytoma cells. J Biol Chem 267: 21360-21367.
169. Engen JR, Wales TE, Hochrein JM, Meyn MAr, Banu O, S et al. (2008) Structure and dynamic regulation of Src-family kinases. Cell Mol Life Sci 65: 3058-3073.
170. Irby RB, Yeatman TJ (2000) Role of Src expression and activation in human cancer. Oncogene 19: 5636-5642.
171. Cartwright CA, Coad CA, Egbert BM (1994) Elevated c-Src tyrosine kinase activity in premalignant epithelia of ulcerative colitis. J Clin Invest 93: 509-515.
172. Kumble S, Omary MB, Cartwright CA, Triadafilopoulos G (1997) Src activation in malignant and premalignant epithelia of Barrett's esophagus. Gastroenterology 112: 348-356.
173. Ottenhoff-Kalff AE, Rijksen G, van B, EA, Hennipman A, Michels AA et al. (1992) Characterization of protein tyrosine kinases from human breast cancer: involvement of the c-src oncogene product. Cancer Res 52: 4773-4778.
174. Olsen JV, Blagoev B, Gnad F, Macek B, Kumar C et al. (2006) Global, in vivo, and site-specific phosphorylation dynamics in signaling networks. Cell 127: 635-648.
175. McLaughlin LM, Govoni GR, Gerke C, Gopinath S, Peng K et al. (2009) The Salmonella SPI2 effector SseI mediates long-term systemic infection by modulating host cell migration. PLoS Pathog 5: e1000671.
176. Datsenko KA, Wanner BL (2000) One-step inactivation of chromosomal genes in *Escherichia coli* K-12 using PCR products. Proc Natl Acad Sci U S A 97: 6640-6645.
177. Cornelis GR, Van Gijsegem F (2000) Assembly and function of type III secretory systems. Annu Rev Microbiol 54: 735-774.
178. Galan JE, Collmer A (1999) Type III secretion machines: bacterial devices for protein delivery into host cells. Science 284: 1322-1328.
179. Winstanley C, Hart CA (2001) Type III secretion systems and pathogenicity islands. J Med Microbiol 50: 116-126.
180. Galan JE (2001) Salmonella interactions with host cells: type III secretion at work. Annu Rev Cell Dev Biol 17: 53-86.
181. Bajaj V, Lucas RL, Hwang C, Lee CA (1996) Co-ordinate regulation of Salmonella typhimurium invasion genes by environmental and regulatory factors is mediated by control of hilA expression. Mol Microbiol 22: 703-714.
182. Collier-Hyams LS, Zeng H, Sun J, Tomlinson AD, Bao ZQ et al. (2002) Cutting edge: Salmonella AvrA effector inhibits the key proinflammatory, anti-apoptotic NF-kappa B pathway. J Immunol 169: 2846-2850.
183. Galkin VE, Orlova A, VanLoock MS, Zhou D, Galan JE et al. (2002) The bacterial protein SipA polymerizes G-actin and mimics muscle nebulin. Nat Struct Biol 9: 518-521.
184. Zhang S, Santos RL, Tsolis RM, Stender S, Hardt WD et al. (2002) The Salmonella enterica serotype typhimurium effector proteins SipA, SopA, SopB, SopD, and SopE2 act in concert to induce diarrhea in calves. Infect Immun 70: 3843-3855.
185. Cirillo DM, Valdivia RH, Monack DM, Falkow S (1998) Macrophage-dependent induction of the Salmonella pathogenicity island 2 type III secretion system and its role in intracellular survival. Mol Microbiol 30: 175-188.

186. Deiwick J, Nikolaus T, Erdogan S, Hensel M (1999) Environmental regulation of *Salmonella* pathogenicity island 2 gene expression. Mol Microbiol 31: 1759-1773.
187. Lee AK, Detweiler CS, Falkow S (2000) OmpR regulates the two-component system SsrA-SsrB in *Salmonella* pathogenicity island 2. J Bacteriol 182: 771-781.
188. Miao EA, Freeman JA, Miller SI (2002) Transcription of the SsrAB regulon is repressed by alkaline pH and is independent of PhoPQ and magnesium concentration. J Bacteriol 184: 1493-1497.
189. Hensel M, Shea JE, Gleeson C, Jones MD, Dalton E et al. (1995) Simultaneous identification of bacterial virulence genes by negative selection. Science 269: 400-403.
190. Ochman H, Soncini FC, Solomon F, Groisman EA (1996) Identification of a pathogenicity island required for Salmonella survival in host cells. Proc Natl Acad Sci U S A 93: 7800-7804.
191. Shea JE, Hensel M, Gleeson C, Holden DW (1996) Identification of a virulence locus encoding a second type III secretion system in *Salmonella typhimurium*. Proc Natl Acad Sci U S A 93: 2593-2597.
192. Chakravortty D, Hansen-Wester I, Hensel M (2002) Salmonella pathogenicity island 2 mediates protection of intracellular Salmonella from reactive nitrogen intermediates. J Exp Med 195: 1155-1166.
193. Vazquez-Torres A, Xu Y, Jones-Carson J, Holden DW, Lucia SM et al. (2000) Salmonella pathogenicity island 2-dependent evasion of the phagocyte NADPH oxidase. Science 287: 1655-1658.
194. Ladant D, Ullmann A (1999) Bordatella pertussis adenylate cyclase: a toxin with multiple talents. Trends Microbiol 7: 172-176.
195. Sory MP, Boland A, Lambermont I, Cornelis GR (1995) Identification of the YopE and YopH domains required for secretion and internalization into the cytosol of macrophages, using the *cyaA* gene fusion approach. Proc Natl Acad Sci U S A 92: 11998-12002.
196. Goryshin IY, Jendrisak J, Hoffman LM, Meis R, Reznikoff WS (2000) Insertional transposon mutagenesis by electroporation of released Tn5 transposition complexes. Nat Biotechnol 18: 97-100.
197. Figueroa-Bossi N, Bossi L (1999) Inducible prophages contribute to Salmonella virulence in mice. Mol Microbiol 33: 167-176.
198. Kaniga K, Trollinger D, Galan JE (1995) Identification of two targets of the type III protein secretion system encoded by the inv and spa loci of Salmonella typhimurium that have homology to the Shigella IpaD and IpaA proteins. J Bacteriol 177: 7078-7085.
199. Tsolis RM, Townsend SM, Miao EA, Miller SI, Ficht TA et al. (1999) Identification of a putative Salmonella enterica serotype typhimurium host range factor with homology to IpaH and YopM by signature-tagged mutagenesis. Infect Immun 67: 6385-6393.
200. Kaniga K, Uralil J, Bliska JB, Galan JE (1996) A secreted protein tyrosine phosphatase with modular effector domains in the bacterial pathogen Salmonella typhimurium. Mol Microbiol 21: 633-641.

201. Guttman DS, Vinatzer BA, Sarkar SF, Ranall MV, Kettler G et al. (2002) A functional screen for the type III (Hrp) secretome of the plant pathogen Pseudomonas syringae. Science 295: 1722-1726.
202. Hardt WD, Galan JE (1997) A secreted Salmonella protein with homology to an avirulence determinant of plant pathogenic bacteria. Proc Natl Acad Sci U S A 94: 9887-9892.
203. McClelland M, Sanderson KE, Spieth J, Clifton SW, Latreille P et al. (2001) Complete genome sequence of Salmonella enterica serovar Typhimurium LT2. Nature 413: 852-856.
204. Steele-Mortimer O, Meresse S, Gorvel JP, Toh BH, Finlay BB (1999) Biogenesis of Salmonella typhimurium-containing vacuoles in epithelial cells involves interactions with the early endocytic pathway. Cell Microbiol 1: 33-49.
205. Luo ZQ, Isberg RR (2004) Multiple substrates of the Legionella pneumophila Dot/Icm system identified by interbacterial protein transfer. Proc Natl Acad Sci U S A 101: 841-846.
206. Tu X, Nisan I, Miller JF, Hanski E, Rosenshine I (2001) Construction of mini-Tn5cyaA' and its utilization for the identification of genes encoding surface-exposed and secreted proteins in Bordetella bronchiseptica. FEMS Microbiol Lett 205: 119-123.
207. Kujat Choy SL, Boyle EC, Gal-Mor O, Goode DL, Valdez Y et al. (2004) SseK1 and SseK2 are novel translocated proteins of Salmonella enterica serovar typhimurium. Infect Immun 72: 5115-5125.
208. Chen J, de Felipe KS, Clarke M, Lu H, Anderson OR et al. (2004) Legionella effectors that promote nonlytic release from protozoa. Science 303: 1358-1361.
209. Glaser P, Sakamoto H, Bellalou J, Ullmann A, Danchin A (1988) Secretion of cyclolysin, the calmodulin-sensitive adenylate cyclase-haemolysin bifunctional protein of Bordetella pertussis. EMBO J 7: 3997-4004.
210. Salcedo SP, Holden DW (2003) SseG, a virulence protein that targets Salmonella to the Golgi network. EMBO J 22: 5003-5014.
211. Morgan E, Campbell JD, Rowe SC, Bispham J, Stevens MP et al. (2004) Identification of host-specific colonization factors of Salmonella enterica serovar Typhimurium. Mol Microbiol 54: 994-1010.
212. (2003) The complete genome sequence of Chromobacterium violaceum reveals remarkable and exploitable bacterial adaptability. Proc Natl Acad Sci U S A 100: 11660-11665.
213. Ho TD, Figueroa-Bossi N, Wang M, Uzzau S, Bossi L et al. (2002) Identification of GtgE, a novel virulence factor encoded on the Gifsy-2 bacteriophage of Salmonella enterica serovar Typhimurium. J Bacteriol 184: 5234-5239.
214. Skorupski K, Taylor RK (1996) Positive selection vectors for allelic exchange. Gene 169: 47-52.
215. Ellefson D, van der Velden AW, Parker D, Heffron F (2000) Identification of bacterial class I accessible proteins by disseminated insertion of class I epitopes. Methods Enzymol 326: 516-527.
216. Uzzau S, Figueroa-Bossi N, Rubino S, Bossi L (2001) Epitope tagging of chromosomal genes in Salmonella. Proc Natl Acad Sci U S A 98: 15264-15269.

217. Graham SM (2002) Salmonellosis in children in developing and developed countries and populations. Curr Opin Infect Dis 15: 507-512.
218. Guerrant RL, Hughes JM, Lima NL, Crane J (1990) Diarrhea in developed and developing countries: magnitude, special settings, and etiologies. Rev Infect Dis 12 Suppl 1: S41-50.
219. Mermin JH, Villar R, Carpenter J, Roberts L, Samaridden A et al. (1999) A massive epidemic of multidrug-resistant typhoid fever in Tajikistan associated with consumption of municipal water. J Infect Dis 179: 1416-1422.
220. Ginocchio CC, Olmsted SB, Wells CL, Galan JE (1994) Contact with epithelial cells induces the formation of surface appendages on *Salmonella typhimurium*. Cell 76: 717-724.
221. Haraga A, Ohlson MB, Miller SI (2008) Salmonellae interplay with host cells. Nat Rev Microbiol 6: 53-66.
222. Tobe T, Beatson SA, Taniguchi H, Abe H, Bailey CM et al. (2006) An extensive repertoire of type III secretion effectors in Escherichia coli O157 and the role of lambdoid phages in their dissemination. Proc Natl Acad Sci U S A An extensive repertoire of type III secretion effectors in Escherichia coli O157 and the role of lambdoid phages in their dissemination 103: 14941-14946.
223. Wang D, Roe AJ, McAteer S, Shipston MJ, Gally DL (2008) Hierarchal type III secretion of translocators and effectors from *Escherichia coli* O157:H7 requires the carboxy terminus of SepL that binds to Tir. Mol Microbiol 69: 1499-1512.
224. Kenny B, DeVinney R, Stein M, Reinscheid DJ, Frey EA et al. (1997) Enteropathogenic *E. coli* (EPEC) transfers its receptor for intimate adherence into mammalian cells. Cell 91: 511-520.
225. Tree JJ, Wolfson EB, Wang D, Roe AJ, Gally DL (2009) Controlling injection: regulation of type III secretion in enterohaemorrhagic *Escherichia coli*. Trends Microbiol 17: 361-370.
226. Hensel M, Shea JE, Waterman SR, Mundy R, Nikolaus T et al. (1998) Genes encoding putative effector proteins of the type III secretion system of *Salmonella* pathogenicity island 2 are required for bacterial virulence and proliferation in macrophages. Mol Microbiol 30: 163-174.
227. Walthers D, Carroll RK, Navarre WW, Libby SJ, Fang FC et al. (2007) The response regulator SsrB activates expression of diverse *Salmonella* pathogenicity island 2 promoters and counters silencing by the nucleoid-associated protein H-NS. Mol Microbiol 65: 477-493.
228. Coombes BK, Brown NF, Valdez Y, Brumell JH, Finlay BB (2004) Expression and secretion of *Salmonella* pathogenicity island-2 virulence genes in response to acidification exhibit differential requirements of a functional type III secretion apparatus and SsaL. J Biol Chem 279: 49804-49815.
229. Coombes BK, Lowden MJ, Bishop JL, Wickham ME, Brown NF et al. (2007) SseL is a *Salmonella*-specific translocated effector integrated into the SsrB-controlled *Salmonella* pathogenicity island 2 type III secretion system. Infect Immun 75: 574-580.
230. Coombes BK, Wickham ME, Brown NF, Lemire S, Bossi L et al. (2005) Genetic and molecular analysis of GogB, a phage-encoded type III-secreted substrate in

Salmonella enterica serovar typhimurium with autonomous expression from its associated phage. J Mol Biol 348: 817-830.
231. Samudrala R, Heffron F, McDermott JE (2009) Accurate prediction of secreted substrates and identification of a conserved putative secretion signal for type III secretion systems. PLoS Pathog 5: e1000375.
232. Lejona S, Castelli ME, Cabeza ML, Kenney LJ, Garcia Vescovi E et al. (2004) PhoP can activate its target genes in a PhoQ-independent manner. J Bacteriol 186: 2476-2480.
233. Eng JK, Mccormack AL, Yates JR (1994) An Approach to Correlate Tandem Mass-Spectral Data of Peptides with Amino-Acid-Sequences in a Protein Database. Journal of the American Society for Mass Spectrometry 5: 976-989.
234. Adkins JN, Mottaz HM, Norbeck AD, Gustin JK, Rue J et al. (2006) Analysis of the *Salmonella typhimurium* proteome through environmental response toward infectious conditions. Mol Cell Proteomics 5: 1450-1461.
235. Ansong C, Yoon H, Norbeck AD, Gustin JK, McDermott JE et al. (2008) Proteomics analysis of the causative agent of typhoid fever. J Proteome Res 7: 546-557.
236. Gao J, Opiteck GJ, Friedrichs MS, Dongre AR, Hefta SA (2003) Changes in the protein expression of yeast as a function of carbon source. J Proteome Res 2: 643-649.
237. Hendrickson EL, Xia Q, Wang T, Leigh JA, Hackett M (2006) Comparison of spectral counting and metabolic stable isotope labeling for use with quantitative microbial proteomics. Analyst 131: 1335-1341.
238. Liu H, Sadygov RG, Yates JR, 3rd (2004) A model for random sampling and estimation of relative protein abundance in shotgun proteomics. Anal Chem 76: 4193-4201.
239. Smith RD, Anderson GA, Lipton MS, Masselon C, Pasa-Tolic L et al. (2002) The use of accurate mass tags for high-throughput microbial proteomics. OMICS 6: 61-90.
240. Smith RD, Anderson GA, Lipton MS, Pasa-Tolic L, Shen Y et al. (2002) An accurate mass tag strategy for quantitative and high-throughput proteome measurements. Proteomics 2: 513-523.
241. Zimmer JS, Monroe ME, Qian WJ, Smith RD (2006) Advances in proteomics data analysis and display using an accurate mass and time tag approach. Mass Spectrom Rev 25: 450-482.
242. Gardy JL, Laird MR, Chen F, Rey S, Walsh CJ et al. (2005) PSORTb v.2.0: expanded prediction of bacterial protein subcellular localization and insights gained from comparative proteome analysis. Bioinformatics 21: 617-623.
243. Komoriya K, Shibano N, Higano T, Azuma N, Yamaguchi S et al. (1999) Flagellar proteins and type III-exported virulence factors are the predominant proteins secreted into the culture media of Salmonella typhimurium. Mol Microbiol 34: 767-779.
244. Belden WJ, Miller SI (1994) Further characterization of the PhoP regulon: identification of new PhoP-activated virulence loci. Infect Immun 62: 5095-5101.

245. Gunn JS, Alpuche-Aranda CM, Loomis WP, Belden WJ, Miller SI (1995) Characterization of the *Salmonella typhimurium pagC/pagD* chromosomal region. J Bacteriol 177: 5040-5047.
246. Nishio M, Okada N, Miki T, Haneda T, Danbara H (2005) Identification of the outer-membrane protein PagC required for the serum resistance phenotype in *Salmonella enterica* serovar Choleraesuis. Microbiology 151: 863-873.
247. Arnold R, Brandmaier S, Kleine F, Tischler P, Heinz E et al. (2009) Sequence-based prediction of type III secreted proteins. PLoS Pathog 5: e1000376.
248. Geddes K, Cruz F, Heffron F (2007) Analysis of cells targeted by *Salmonella* type III secretion in vivo. PLoS Pathog 3: e196.
249. Gong H, Vu GP, Bai Y, Yang E, Liu F et al. (2009) Differential expression of *Salmonella* Type III secretion system factor InvJ, PrgJ, SipC, SipD, SopA, and SopB in cultures and in mice. Microbiology
250. Bauerfeind R, Barth S, Weiss R, Baljer G (2001) Prevalence of the *Salmonella* plasmid virulence gene "spvD" in *Salmonella* strains from animals. Dtsch Tierarztl Wochenschr 108: 243-245.
251. Matsui H, Bacot CM, Garlington WA, Doyle TJ, Roberts S et al. (2001) Virulence plasmid-borne *spvB* and *spvC* genes can replace the 90-kilobase plasmid in conferring virulence to *Salmonella enterica* serovar Typhimurium in subcutaneously inoculated mice. J Bacteriol 183: 4652-4658.
252. Cuellar-Mata P, Jabado N, Liu J, Furuya W, Finlay BB et al. (2002) Nramp1 modifies the fusion of Salmonella typhimurium-containing vacuoles with cellular endomembranes in macrophages. J Biol Chem 277: 2258-2265.
253. Deng W, Puente JL, Gruenheid S, Li Y, Vallance BA et al. (2004) Dissecting virulence: systematic and functional analyses of a pathogenicity island. Proc Natl Acad Sci U S A 101: 3597-3602.
254. Kresse AU, Beltrametti F, Muller A, Ebel F, Guzman CA (2000) Characterization of SepL of enterohemorrhagic *Escherichia coli*. J Bacteriol 182: 6490-6498.
255. Yu XJ, Liu M, Holden DW (2004) SsaM and SpiC interact and regulate secretion of Salmonella pathogenicity island 2 type III secretion system effectors and translocators. Mol Microbiol 54: 604-619.
256. Yu XJ, Ruiz-Albert J, Unsworth KE, Garvis S, Liu M et al. (2002) SpiC is required for secretion of Salmonella Pathogenicity Island 2 type III secretion system proteins. Cell Microbiol 4: 531-540.
257. Sun YH, Rolan HG, Tsolis RM (2007) Injection of flagellin into the host cell cytosol by *Salmonella enterica* serotype Typhimurium. J Biol Chem 282: 33897-33901.
258. Desvaux M, Parham NJ, Henderson IR (2004) The autotransporter secretion system. Res Microbiol 155: 53-60.
259. Wai SN, Lindmark B, Soderblom T, Takade A, Westermark M et al. (2003) Vesicle-mediated export and assembly of pore-forming oligomers of the enterobacterial ClyA cytotoxin. Cell 115: 25-35.
260. Deatherage BL, Lara JC, Bergsbaken T, Rassoulian Barrett SL, Lara S et al. (2009) Biogenesis of bacterial membrane vesicles. Mol Microbiol 72: 1395-1407.
261. Kuehn MJ, Kesty NC (2005) Bacterial outer membrane vesicles and the host-pathogen interaction. Genes Dev 19: 2645-2655.

262. Lee EY, Bang JY, Park GW, Choi DS, Kang JS et al. (2007) Global proteomic profiling of native outer membrane vesicles derived from *Escherichia coli*. Proteomics 7: 3143-3153.
263. Mashburn-Warren L, McLean RJ, Whiteley M (2008) Gram-negative outer membrane vesicles: beyond the cell surface. Geobiology 6: 214-219.
264. Vaughan TE, Skipp PJ, O'Connor CD, Hudson MJ, Vipond R et al. (2006) Proteomic analysis of *Neisseria lactamica* and *Neisseria meningitidis* outer membrane vesicle vaccine antigens. Vaccine 24: 5277-5293.
265. Vipond C, Suker J, Jones C, Tang C, Feavers IM et al. (2006) Proteomic analysis of a meningococcal outer membrane vesicle vaccine prepared from the group B strain NZ98/254. Proteomics 6: 3400-3413.
266. Kadurugamuwa JL, Beveridge TJ (1995) Virulence factors are released from *Pseudomonas aeruginosa* in association with membrane vesicles during normal growth and exposure to gentamicin: a novel mechanism of enzyme secretion. J Bacteriol 177: 3998-4008.
267. Gal-Mor O, Gibson DL, Baluta D, Vallance BA, Finlay BB (2008) A novel secretion pathway of Salmonella enterica acts as an antivirulence modulator during salmonellosis. PLoS Pathog 4: e1000036.
268. Chaudhuri RR, Peters SE, Pleasance SJ, Northen H, Willers C et al. (2009) Comprehensive identification of Salmonella enterica serovar typhimurium genes required for infection of BALB/c mice. PLoS Pathog 5: e1000529.
269. Garcia-del Portillo F, Nunez-Hernandez C, Eisman B, Ramos-Vivas J (2008) Growth control in the Salmonella-containing vacuole. Curr Opin Microbiol 11: 46-52.
270. Shen Y, Tolic N, Zhao R, Pasa-Tolic L, Li L et al. (2001) High-throughput proteomics using high-efficiency multiple-capillary liquid chromatography with on-line high-performance ESI FTICR mass spectrometry. Anal Chem 73: 3011-3021.
271. Washburn MP, Wolters D, Yates JR, 3rd (2001) Large-scale analysis of the yeast proteome by multidimensional protein identification technology. Nat Biotechnol 19: 242-247.
272. Keller A, Nesvizhskii AI, Kolker E, Aebersold R (2002) Empirical statistical model to estimate the accuracy of peptide identifications made by MS/MS and database search. Anal Chem 74: 5383-5392.
273. Peng J, Elias JE, Thoreen CC, Licklider LJ, Gygi SP (2003) Evaluation of multidimensional chromatography coupled with tandem mass spectrometry (LC/LC-MS/MS) for large-scale protein analysis: the yeast proteome. J Proteome Res 2: 43-50.
274. Adkins JN, Varnum SM, Auberry KJ, Moore RJ, Angell NH et al. (2002) Toward a human blood serum proteome: analysis by multidimensional separation coupled with mass spectrometry. Mol Cell Proteomics 1: 947-955.
275. Ansong C, Yoon H, Porwollik S, Mottaz-Brewer H, Petritis BO et al. (2009) Global systems-level analysis of Hfq and SmpB deletion mutants in *Salmonella*: implications for virulence and global protein translation. PLoS One 4: e4809.
276. Polpitiya AD, Qian WJ, Jaitly N, Petyuk VA, Adkins JN et al. (2008) DAnTE: a statistical tool for quantitative analysis of -omics data. Bioinformatics 24: 1556-1558.

277. Burstein D, Zusman T, Degtyar E, Viner R, Segal G et al. (2009) Genome-scale identification of Legionella pneumophila effectors using a machine learning approach. PLoS Pathog 5: e1000508.
278. Diao J, Zhang Y, Huibregtse JM, Zhou D, Chen J (2008) Crystal structure of SopA, a Salmonella effector protein mimicking a eukaryotic ubiquitin ligase. Nat Struct Mol Biol 15: 65-70.
279. Friebel A, Ilchmann H, Aepfelbacher M, Ehrbar K, Machleidt W et al. (2001) SopE and SopE2 from Salmonella typhimurium activate different sets of RhoGTPases of the host cell. J Biol Chem 276: 34035-34040.
280. Mallo GV, Espina M, Smith AC, Terebiznik MR, Aleman A et al. (2008) SopB promotes phosphatidylinositol 3-phosphate formation on Salmonella vacuoles by recruiting Rab5 and Vps34. J Cell Biol 182: 741-752.
281. Terebiznik MR, Vieira OV, Marcus SL, Slade A, Yip CM et al. (2002) Elimination of host cell PtdIns(4,5)P(2) by bacterial SigD promotes membrane fission during invasion by Salmonella. Nat Cell Biol 4: 766-773.
282. White CD, Brown MD, Sacks DB (2009) IQGAPs in cancer: a family of scaffold proteins underlying tumorigenesis. FEBS Lett 583: 1817-1824.
283. Jackson LK, Nawabi P, Hentea C, Roark EA, Haldar K (2008) The Salmonella virulence protein SifA is a G protein antagonist. Proc Natl Acad Sci U S A 105: 14141-14146.
284. Murli S, Watson RO, Galan JE (2001) Role of tyrosine kinases and the tyrosine phosphatase SptP in the interaction of Salmonella with host cells. Cell Microbiol 3: 795-810.
285. Ginocchio C, Pace J, Galan JE (1992) Identification and molecular characterization of a Salmonella typhimurium gene involved in triggering the internalization of salmonellae into cultured epithelial cells. Proc Natl Acad Sci U S A 89: 5976-5980.
286. Hirano SS, Charkowski AO, Collmer A, Willis DK, Upper CD (1999) Role of the Hrp type III protein secretion system in growth of Pseudomonas syringae pv. syringae B728a on host plants in the field. Proc Natl Acad Sci U S A 96: 9851-9856.
287. Bomberger JM, Maceachran DP, Coutermarsh BA, Ye S, O'Toole GA et al. (2009) Long-distance delivery of bacterial virulence factors by Pseudomonas aeruginosa outer membrane vesicles. PLoS Pathog 5: e1000382.
288. Ricci V, Chiozzi V, Necchi V, Oldani A, Romano M et al. (2005) Free-soluble and outer membrane vesicle-associated VacA from Helicobacter pylori: Two forms of release, a different activity. Biochem Biophys Res Commun 337: 173-178.
289. Soderblom T, Oxhamre C, Wai SN, Uhlen P, Aperia A et al. (2005) Effects of the Escherichia coli toxin cytolysin A on mucosal immunostimulation via epithelial Ca2+ signalling and Toll-like receptor 4. Cell Microbiol 7: 779-788.
290. Osborne SE, Walthers D, Tomljenovic AM, Mulder DT, Silphaduang U et al. (2009) Pathogenic adaptation of intracellular bacteria by rewiring a cis-regulatory input function. Proc Natl Acad Sci U S A Pathogenic adaptation of intracellular bacteria by rewiring a cis-regulatory input function 106: 3982-3987.
291. Beveridge TJ (1999) Structures of gram-negative cell walls and their derived membrane vesicles. J Bacteriol Structures of gram-negative cell walls and their derived membrane vesicles 181: 4725-4733.

292. Sory MP, Cornelis GR (1994) Translocation of a hybrid YopE-adenylate cyclase from *Yersinia enterocolitica* into HeLa cells. Mol Microbiol 14: 583-594.
293. Hill Gaston JS, Lillicrap MS (2003) Arthritis associated with enteric infection. Best Pract Res Clin Rheumatol 17: 219-239.
294. Anderson DM, Schneewind O (1997) A mRNA signal for the type III secretion of Yop proteins by Yersinia enterocolitica. Science 278: 1140-1143.
295. Anderson DM, Schneewind O (1999) Yersinia enterocolitica type III secretion: an mRNA signal that couples translation and secretion of YopQ. Mol Microbiol 31: 1139-1148.
296. Cheng LW, Kay O, Schneewind O (2001) Regulated secretion of YopN by the type III machinery of Yersinia enterocolitica. J Bacteriol 183: 5293-5301.
297. Sorg JA, Miller NC, Marketon MM, Schneewind O (2005) Rejection of impassable substrates by Yersinia type III secretion machines. J Bacteriol 187: 7090-7102.
298. Stebbins CE, Galan JE (2001) Maintenance of an unfolded polypeptide by a cognate chaperone in bacterial type III secretion. Nature 414: 77-81.
299. Anderson DM, Ramamurthi KS, Tam C, Schneewind O (2002) YopD and LcrH regulate expression of Yersinia enterocolitica YopQ by a posttranscriptional mechanism and bind to yopQ RNA. J Bacteriol 184: 1287-1295.
300. Feldman MF, Muller S, Wuest E, Cornelis GR (2002) SycE allows secretion of YopE-DHFR hybrids by the Yersinia enterocolitica type III Ysc system. Mol Microbiol 46: 1183-1197.
301. Boyle EC, Brown NF, Finlay BB (2006) Salmonella enterica serovar Typhimurium effectors SopB, SopE, SopE2 and SipA disrupt tight junction structure and function. Cell Microbiol 8: 1946-1957.
302. Brawn LC, Hayward RD, Koronakis V (2007) Salmonella SPI1 effector SipA persists after entry and cooperates with a SPI2 effector to regulate phagosome maturation and intracellular replication. Cell Host Microbe 1: 63-75.
303. Cain RJ, Hayward RD, Koronakis V (2004) The target cell plasma membrane is a critical interface for Salmonella cell entry effector-host interplay. Mol Microbiol 54: 887-904.
304. Lee CA, Silva M, Siber AM, Kelly AJ, Galyov E et al. (2000) A secreted Salmonella protein induces a proinflammatory response in epithelial cells, which promotes neutrophil migration. Proc Natl Acad Sci U S A 97: 12283-12288.
305. Lilic M, Galkin VE, Orlova A, VanLoock MS, Egelman EH et al. (2003) Salmonella SipA polymerizes actin by stapling filaments with nonglobular protein arms. Science 301: 1918-1921.
306. Popp D, Yamamoto A, Iwasa M, Nitanai Y, Maeda Y (2008) Single molecule polymerization, annealing and bundling dynamics of SipA induced actin filaments. Cell Motil Cytoskeleton 65: 165-177.
307. Raffatellu M, Wilson RP, Chessa D, Andrews-Polymenis H, Tran QT et al. (2005) SipA, SopA, SopB, SopD, and SopE2 contribute to Salmonella enterica serotype typhimurium invasion of epithelial cells. Infect Immun 73: 146-154.
308. Schlumberger MC, Kappeli R, Wetter M, Muller AJ, Misselwitz B et al. (2007) Two newly identified SipA domains (F1, F2) steer effector protein localization and contribute to Salmonella host cell manipulation. Mol Microbiol 65: 741-760.

309. Wall DM, Nadeau WJ, Pazos MA, Shi HN, Galyov EE et al. (2007) Identification of the Salmonella enterica serotype typhimurium SipA domain responsible for inducing neutrophil recruitment across the intestinal epithelium. Cell Microbiol 9: 2299-2313.
310. Winnen B, Schlumberger MC, Sturm A, Schupbach K, Siebenmann S et al. (2008) Hierarchical effector protein transport by the Salmonella Typhimurium SPI-1 type III secretion system. PLoS One 3: e2178.
311. Zhou D, Mooseker MS, Galan JE (1999) An invasion-associated Salmonella protein modulates the actin-bundling activity of plastin. Proc Natl Acad Sci U S A 96: 10176-10181.
312. Zhou D, Mooseker MS, Galan JE (1999) Role of the S. typhimurium actin-binding protein SipA in bacterial internalization. Science 283: 2092-2095.
313. Figueiredo JF, Lawhon SD, Gokulan K, Khare S, Raffatellu M et al. (2009) Salmonella enterica Typhimurium SipA induces CXC-chemokine expression through p38MAPK and JUN pathways. Microbes Infect 11: 302-310.
314. Hayward RD, Cain RJ, McGhie EJ, Phillips N, Garner MJ et al. (2005) Cholesterol binding by the bacterial type III translocon is essential for virulence effector delivery into mammalian cells. Mol Microbiol 56: 590-603.
315. Hernandez LD, Pypaert M, Flavell RA, Galan JE (2003) A Salmonella protein causes macrophage cell death by inducing autophagy. J Cell Biol 163: 1123-1131.
316. Hersh D, Monack DM, Smith MR, Ghori N, Falkow S et al. (1999) The Salmonella invasin SipB induces macrophage apoptosis by binding to caspase-1. Proc Natl Acad Sci U S A 96: 2396-2401.
317. Mueller CA, Broz P, Cornelis GR (2008) The type III secretion system tip complex and translocon. Mol Microbiol 68: 1085-1095.
318. Zhang Y, Higashide W, Dai S, Sherman DM, Zhou D (2005) Recognition and ubiquitination of Salmonella type III effector SopA by a ubiquitin E3 ligase, HsRMA1. J Biol Chem 280: 38682-38688.
319. Layton AN, Brown PJ, Galyov EE (2005) The Salmonella translocated effector SopA is targeted to the mitochondria of infected cells. J Bacteriol 187: 3565-3571.
320. Bujny MV, Ewels PA, Humphrey S, Attar N, Jepson MA et al. (2008) Sorting nexin-1 defines an early phase of Salmonella-containing vacuole-remodeling during Salmonella infection. J Cell Sci 121: 2027-2036.
321. Dukes JD, Lee H, Hagen R, Reaves BJ, Layton AN et al. (2006) The secreted Salmonella dublin phosphoinositide phosphatase, SopB, localizes to PtdIns(3)P-containing endosomes and perturbs normal endosome to lysosome trafficking. Biochem J 395: 239-247.
322. Mason D, Mallo GV, Terebiznik MR, Payrastre B, Finlay BB et al. (2007) Alteration of epithelial structure and function associated with PtdIns(4,5)P2 degradation by a bacterial phosphatase. J Gen Physiol 129: 267-283.
323. Norris FA, Wilson MP, Wallis TS, Galyov EE, Majerus PW (1998) SopB, a protein required for virulence of Salmonella dublin, is an inositol phosphate phosphatase. Proc Natl Acad Sci U S A 95: 14057-14059.
324. Patel JC, Galan JE (2005) Manipulation of the host actin cytoskeleton by Salmonella--all in the name of entry. Curr Opin Microbiol 8: 10-15.

325. Steele-Mortimer O, Knodler LA, Marcus SL, Scheid MP, Goh B et al. (2000) Activation of Akt/protein kinase B in epithelial cells by the Salmonella typhimurium effector sigD. J Biol Chem 275: 37718-37724.
326. Wasylnka JA, Bakowski MA, Szeto J, Ohlson MB, Trimble WS et al. (2008) Role for myosin II in regulating positioning of Salmonella-containing vacuoles and intracellular replication. Infect Immun 76: 2722-2735.
327. Zhou D, Chen LM, Hernandez L, Shears SB, Galan JE (2001) A Salmonella inositol polyphosphatase acts in conjunction with other bacterial effectors to promote host cell actin cytoskeleton rearrangements and bacterial internalization. Mol Microbiol 39: 248-259.
328. Patel JC, Hueffer K, Lam TT, Galan JE (2009) Diversification of a Salmonella virulence protein function by ubiquitin-dependent differential localization. Cell 137: 283-294.
329. Mukherjee K, Parashuraman S, Raje M, Mukhopadhyay A (2001) SopE acts as an Rab5-specific nucleotide exchange factor and recruits non-prenylated Rab5 on Salmonella-containing phagosomes to promote fusion with early endosomes. J Biol Chem 276: 23607-23615.
330. Bakshi CS, Singh VP, Wood MW, Jones PW, Wallis TS et al. (2000) Identification of SopE2, a Salmonella secreted protein which is highly homologous to SopE and involved in bacterial invasion of epithelial cells. J Bacteriol 182: 2341-2344.
331. Stender S, Friebel A, Linder S, Rohde M, Mirold S et al. (2000) Identification of SopE2 from Salmonella typhimurium, a conserved guanine nucleotide exchange factor for Cdc42 of the host cell. Mol Microbiol 36: 1206-1221.
332. Figueroa-Bossi N, Uzzau S, Maloriol D, Bossi L (2001) Variable assortment of prophages provides a transferable repertoire of pathogenic determinants in Salmonella. Mol Microbiol 39: 260-271.
333. Chen L, Wang H, Zhang J, Gu L, Huang N et al. (2008) Structural basis for the catalytic mechanism of phosphothreonine lyase. Nat Struct Mol Biol 15: 101-102.
334. Li H, Xu H, Zhou Y, Zhang J, Long C et al. (2007) The phosphothreonine lyase activity of a bacterial type III effector family. Science 315: 1000-1003.
335. Mazurkiewicz P, Thomas J, Thompson JA, Liu M, Arbibe L et al. (2008) SpvC is a Salmonella effector with phosphothreonine lyase activity on host mitogen-activated protein kinases. Mol Microbiol 67: 1371-1383.
336. Blanc-Potard AB, Solomon F, Kayser J, Groisman EA (1999) The SPI-3 pathogenicity island of Salmonella enterica. J Bacteriol 181: 998-1004.
337. Smith JN, Ahmer BM (2003) Detection of other microbial species by Salmonella: expression of the SdiA regulon. J Bacteriol 185: 1357-1366.
338. Szeto J, Namolovan A, Osborne SE, Coombes BK, Brumell JH (2009) Salmonella-containing vacuoles display centrifugal movement associated with cell-to-cell transfer in epithelial cells. Infect Immun 77: 996-1007.
339. Arbeloa A, Bulgin RR, MacKenzie G, Shaw RK, Pallen MJ et al. (2008) Subversion of actin dynamics by EspM effectors of attaching and effacing bacterial pathogens. Cell Microbiol 10: 1429-1441.
340. Handa Y, Suzuki M, Ohya K, Iwai H, Ishijima N et al. (2007) Shigella IpgB1 promotes bacterial entry through the ELMO-Dock180 machinery. Nat Cell Biol 9: 121-128.

341. Brumell JH, Tang P, Mills SD, Finlay BB (2001) Characterization of Salmonella-induced filaments (Sifs) reveals a delayed interaction between Salmonella-containing vacuoles and late endocytic compartments. Traffic 2: 643-653.
342. Harrison RE, Brumell JH, Khandani A, Bucci C, Scott CC et al. (2004) Salmonella impairs RILP recruitment to Rab7 during maturation of invasion vacuoles. Mol Biol Cell 15: 3146-3154.
343. Kuhle V, Abrahams GL, Hensel M (2006) Intracellular Salmonella enterica redirect exocytic transport processes in a Salmonella pathogenicity island 2-dependent manner. Traffic 7: 716-730.
344. Lee AH, Zareei MP, Daefler S (2002) Identification of a NIPSNAP homologue as host cell target for Salmonella virulence protein SpiC. Cell Microbiol 4: 739-750.
345. Shotland Y, Kramer H, Groisman EA (2003) The Salmonella SpiC protein targets the mammalian Hook3 protein function to alter cellular trafficking. Mol Microbiol 49: 1565-1576.
346. Uchiya K, Barbieri MA, Funato K, Shah AH, Stahl PD et al. (1999) A Salmonella virulence protein that inhibits cellular trafficking. EMBO J 18: 3924-3933.
347. Tobar JA, Carreno LJ, Bueno SM, Gonzalez PA, Mora JE et al. (2006) Virulent Salmonella enterica serovar typhimurium evades adaptive immunity by preventing dendritic cells from activating T cells. Infect Immun 74: 6438-6448.
348. Uchiya K, Nikai T (2008) Salmonella virulence factor SpiC is involved in expression of flagellin protein and mediates activation of the signal transduction pathways in macrophages. Microbiology 154: 3491-3502.
349. Uchiya KI, Sugita A, Nikai T (2009) Involvement of SPI-2-encoded SpiC in flagellum synthesis in Salmonella enterica serovar Typhimurium. BMC Microbiol 9: 179.
350. Birmingham CL, Jiang X, Ohlson MB, Miller SI, Brumell JH (2005) Salmonella-induced filament formation is a dynamic phenotype induced by rapidly replicating Salmonella enterica serovar typhimurium in epithelial cells. Infect Immun 73: 1204-1208.
351. Browne SH, Hasegawa P, Okamoto S, Fierer J, Guiney DG (2008) Identification of Salmonella SPI-2 secretion system components required for SpvB-mediated cytotoxicity in macrophages and virulence in mice. FEMS Immunol Med Microbiol 52: 194-201.
352. Lesnick ML, Reiner NE, Fierer J, Guiney DG (2001) The Salmonella spvB virulence gene encodes an enzyme that ADP-ribosylates actin and destabilizes the cytoskeleton of eukaryotic cells. Mol Microbiol 39: 1464-1470.
353. Kuhle V, Hensel M (2002) SseF and SseG are translocated effectors of the type III secretion system of Salmonella pathogenicity island 2 that modulate aggregation of endosomal compartments. Cell Microbiol 4: 813-824.
354. Kuhle V, Jackel D, Hensel M (2004) Effector proteins encoded by Salmonella pathogenicity island 2 interfere with the microtubule cytoskeleton after translocation into host cells. Traffic 5: 356-370.
355. Ohlson MB, Fluhr K, Birmingham CL, Brumell JH, Miller SI (2005) SseJ deacylase activity by Salmonella enterica serovar Typhimurium promotes virulence in mice. Infect Immun 73: 6249-6259.

356. Lossi NS, Rolhion N, Magee AI, Boyle C, Holden DW (2008) The Salmonella SPI-2 effector SseJ exhibits eukaryotic activator-dependent phospholipase A and glycerophospholipid : cholesterol acyltransferase activity. Microbiology 154: 2680-2688.
357. Rytkonen A, Poh J, Garmendia J, Boyle C, Thompson A et al. (2007) SseL, a Salmonella deubiquitinase required for macrophage killing and virulence. Proc Natl Acad Sci U S A 104: 3502-3507.

Appendices

Table A-1. Description of *Salmonella* secreted effectors. Adapted from [2].

Salmonella effectors that require the SPI-1 TTSS for their translocation.

Effector	Gene Location	Selected Homologues	Activity	Host cell Target(s)	Infection Phenotypes	Stage of Infection	Refs.
SipA (SspA) (STM2882)	SPI-1	*Shigella* IpaA	Actin binding & stabilizing	Actin, T-plastin	Contributes to membrane ruffles and actin rearrangements associated with invasion. Not required for entry, but increases uptake efficiency. Acts as a catalyst for actin polymerization. C-terminus interacts with F-actin and stabilizes filaments. Prevents actin depolymerization by displacing and preventing F-actin interaction with cellular actin depolymerizing proteins ADF and cofilin,. Internal F1 and F2 domains drive SifA focus formation and SipA-SipA interactions, respectively. Potentiates SipC actin polymerization, triggers PMN transmigration, maintains perinuclear SCV positioning by cooperating with SPI-2 effector SifA, disrupts tight junctions, induces CXC chemokine expression.	Invasion & phagocytosis Replication & SCV positioning Pro/anti-inflammatory responses	[14,23,35,39-41,44,45,47, 183,184,301-313]
SipB (SspB) (STM2885)	SPI-1	*Shigella* IpaB	SPI-1 TTSS translocon component	Cholesterol	SPI-1 effector delivery, apoptosis of phagocytes	Invasion & phagocytosis	[74,77,314-317]
SipC (SspC) (STM2884)	SPI-1	*Shigella* IpaC	SPI-1 TTSS translocon component, actin nucleation & bundling	Actin	SPI-1 effector delivery, N-terminus bundles actin filaments. C-terminus nucleates actin assembly leading to filament growth from barbed ends, induces membrane ruffling	Invasion & phagocytosis	[23,39,41,43, 303,317]
SipD (SspD) (STM2883)	SPI-1	*Shigella* IpaD	SPI-1 TTSS needle tip		Regulates SPI-1 translocon assembly and effector secretion	Invasion & phagocytosis	[317]
SopA (STM2066)	Outside SPI-1	Putative EHEC effector (Genbank NP_309587.1)	E3 ubiquitin ligase	HsRMA-1	Target of ubiquitin ligase domain unknown. However, recognized, ubiquitinated, and degraded through HsRMA-1 mediated pathway. Degradation permits Salmonella escape from vacuole into cytoplasm of epithelial cells. Induces PMN transmigration, localizes to mitochondria.	SVC maturation & trafficking	[77,184,278, 307,318,319]
SopB (SigD) (STM1091)	SPI-5	*Shigella* spp. IpgD, cellular 4-phosphatases, synaptojanin	Inositol polyphosphate phosphatase	Cdc42, key substrate likely phosphatidyl inositol-4-5 bisphosphate [$PI(4,5)P_2$]	Invasion: Promotes membrane fission & macropinosome formation, recruits SNARE protein VAMP8 for phagocytosis of bacteria, activates Akt at the plasma membrane which may promote epithelial cell survival. During entry Cdc42 interaction thought to localize effector at plasma membrane. SCV: maintains perinuclear SCV positioning, recruits Rab5 to SCV which in turn recruits Vps34 (a PI3-kinase that phosphorylates PI to PI3P). Monoubiquitination at 9 different lysine residues triggers cellular relocalization from plasma membrane to SCV. E3 ligase that	Invasion & phagocytosis SVC maturation & trafficking Replication & SCV positioning Pro/anti-inflammatory responses	[23,34-38,47,49,77, 184,280,281, 301,303,307, 320-328]

					ubiquitinates SopB unknown. Inflammation: triggers nitric oxide production in macrophages, promotes fluid secretion in calf illeal loops, disrupts tight junctions.		
SopD (STM2945)	Outside SPI-1/SPI-2	*Salmonella* SopD2			Promotes membrane fission & macropinosome formation, works cooperatively with SopB and promotes invasion of T84 cells, required for optimal replication in mouse macrophages, induces fluid secretion in infected ileum	Invasion & phagocytosis Pro/anti-inflammatory responses	[47,69,77,184,307]
SopE[a]	Phage SopEϕ	*Salmonella* SopE2	Guanine exchange factor (GEF) mimic	Rac-1, Cdc42	Induces membrane ruffling & proinflammatory responses, promotes fusion of SCV with early endosomes, disrupts tight junctions. After translocation ubiquitinated and degraded by a proteosome mediated pathway.	Invasion & phagocytosis SCV maturation & trafficking Pro/anti-inflammatory responses	[23,30,30,35, 202,301,303, 310,324,327, 329]
SopE2 (STM1855)	In vicinity of phage remnants	*Salmonella* SopE	GEF mimic	Cdc42	Induces membrane ruffling & proinflammatory responses, increases macrophage iNos expression, disrupts tight junctions	Invasion & phagocytosis Pro/anti-inflammatory responses	[35,77,184,301,303,307,324,330,331]

Salmonella effectors that are secreted by both SPI-1 and SPI-2 TTSS.

Effector	Gene Location	Selected Homologues	Activity	Host cell Target(s)	Infection Phenotypes	Stage of Infection	Refs.
AvrA (STM2865)	SPI-1	*Yersinia* YopJ/P	Cysteine protease, deubiquitinase, acetyl transferase	MKK4/7 IκBα, β-catenin	Inhibits inflammation, represses apoptosis & epithelial innate immunity, stabilizes tight junctions. Deubiquitinates and stabilizes IκBα and B-catenin in epithelial cells. Consequently B-catenin activated while NF-κB activation and apoptosis inhibited.	Pro/anti-inflammatory responses	[79,80,137]
GtgE (STM1055)	Phage Gifsy-2						[213], this study
SteE (STM2585)	Phage Gifsy-3						[332], this study
SlrP (STM0800)	Outside SPI-1/SPI-2	N-terminus: *Salmonella* SifA, SifB, SrfH, SseJ, SspH1/H2 Leucine Rich Repeat: *Salmonella* SspH1/2, GogB C-terminus: *Salmonella* SspH1/2, *Yersinia* YopM, *Shigella* $IpaH_{7.8/9.8}$	E3 ubiquitin ligase	Thioredoxin	Confers host specificity, decreases thioredoxin activity, promotes cell death, interferes with antigen presentation in dendritic cells	Pro/anti-inflammatory responses	[82,89,115,115,141,199]
SpvC (PSLT038)	pSLT (*S.typhimurium*)	*Shigella* OspF, *Pseudomonas syringae* HopAI1	Phosphothreonine lyase		Required for full virulence in mice		[333-335]
SpvD (PSLT037)	pSLT (*S.typhimurium*)						this study
SptP (STM2878)	SPI-1	N-terminus: *Yersinia* YopE, *Pseudomonas aeruginosa* ExoS. C-terminus: cellular tyrosine	GTPase activating protein (GAP) mimic, tyrosine phosphatase	Cdc42, Rac-1, VCP, vimentin	Antagonist of SopE/E2, returns host cytoskeleton to resting state following bacterial entry. N-terminus GAP activity deactivates Rho GTPases Rac and Cdc42. C-terminal tyrosine phosphatase activity targets the AAA+ ATPase VCP	Replication & SCV positioning Pro/anti-inflammatory responses	[23,28,30,30,31,53,284,303,310,324]

		phosphatases, *Yersinia* YopH			(valosin-containing protein). Dephosphorylation of VCP leads to increased bacterial replication. Downregulates proinflammatory responses. Degraded by proteosome mediated pathway. Ubiquitination likely, but not demonstrated.		
SseK1 (STM4157)	Outside SPI-2	*Salmonella* SseK2/3, *Citrobacter rodentium* NleB, EHEC Z4328					[207]
SspH1[b]	Phage Gifsy-3	N-terminus: *Salmonella* SifA, SifB, SrfH, SseJ, SlrP, SspH2 Leucine Rich Repeat: *Salmonella* SspH2, SlrP, GogB C-terminus: *Salmonella* SspH2, SlrP, *Yersinia* YopM, *Shigella* $IpaH_{7.8/9.8}$	E3 ubiquitin ligase	PKN1	LRR domain interacts with PKN1, down-regulates proinflammatory responses	Pro/anti-inflammatory responses	[82,83,115]
SteA (STM1583)	Outside SPI-2				Required for efficient mouse spleen colonization		[29]
SteB (STM1629)	Outside SPI-2		Putative dipicolinate reductase				[29]

Salmonella effectors that require the SPI-2 TTSS for their translocation.

Effector	**Gene Location**	**Selected Homologues**	**Activity**	**Host cell Target(s)**	**Infection Phenotypes**	**Stage of Infection**	**Refs.**
CigR (STM3762)	SPI-3				Hypervirulence phenotype in 129/SVJ mice.		[336], this study
GogB (STM2584)	Phage Gifsy-1	N-terminus: *Yersinia* YopM, *Shigella* $IpaH_{7.8/9.8}$, *Salmonella* SspH1/2, SlrP. C-terminus: *Yersinia* YP2634/Y1471 , rabbit EPEC OrfL, EHEC 0157:H7 Z1829					[3,230]
GtgA (STM1026)	Phage Gifsy-2	GogA (STM2614) PipA (STM1087)					[337], this study
PipB (STM1088)	SPI-5	*Salmonella* PipB2			Targeted with pipB2 to detergent resistant lipid rafts on the SCV and SIF.		[6,66,67]
PipB2 (STM2780)	Outside SPI-2	*Salmonella* PipB		Kinesin-1	Recruits kinesin-1 to SCV, promotes SIF extension by affecting late endosome/lysosone distribution, targeted with PipB to detergent resistant lipid rafts on the SCV and SIF, contributes to cell to cell spread, interferes with antigen presentation in	Replication & SCV positioning Pro/anti-inflammatory responses	[66-68,89,338]

					dendritic cells		
SifA (STM1224)	Outside SPI-2	N-terminus: *Salmonella* SrfH, SifB, SseJ, SspH1/2, SlrP C-terminus: EPEC EspM2/3, *Shigella* IpgB1	GEF mimic, Rab GTPase antagonist	SKIP, Rab9	Required for full virulence in mice, N-terminus interacts with SKIP, C-terminus has WxxxE motif and structure characteristic of a GEF mimic, inhibits Rab9 interaction with SKIP, required for SCV membrane integrity & SIF formation, co-expression with SseJ promotes SIF formation in cells, maintains perinuclear SCV positioning, redirects exocytic vesicles to SCV, interferes with antigen presentation in dendritic cells	Replication & SCV positioning Pro/anti-inflammatory responses	[3,6,55,56,59,60,63,67,68,89,115,139,283,302,339-343]
SifB (STM1602)	Outside SPI-2	N-terminus: *Salmonella* SifA, SrfH, SseJ, SspH1/2, SlrP			Targeted to SCV and SIF		[61,115]
SopD2 (STM0972)	Outside SPI-2	*Salmonella* SopD			Contributes to SIF formation with SifA and SseF/G, required for efficient bacterial replication in macrophages & mice, interferes with antigen presentation in dendritic cells	Replication & SCV positioning Pro/anti-inflammatory responses	[69,89]
SpiC (SsaB) (STM1393)	SPI-2			Hook3, TassC	Interferes with vesicular trafficking via interactions with Hook3 and TassC, role in VAP and SIF formation, controls order of protein export through SPI-2 TTSS, prevents dendritic cells from activating T cells, regulates expression of flagella which affects pro-inflammatory MAPK signaling	SCV maturation & trafficking Pro/anti-inflammatory responses	[6,344-349]
SpvB (PSLT039)	pSLT (*S.typhimurium*)	N-terminus: *Photorhabdus luminescens* TcaC, *Bacillus cereus* VipB2, *Clostridium botulinum* C2 toxin component 1/C3 toxin, *Clostridium perfringens* Iota	ADP ribosyl transferase, inhibits actin polymerisation *in vitro*, depolymerises F-actin upon transfection	Actin	Inhibition of VAP and SIF formation, apoptosis of infected cells via caspase-3, required for full virulence in mice	SCV maturation & trafficking Replication & SCV positioning	[3,115,350-352]
SseB (STM1398)	SPI-2		SPI-2 TTSS Needle Tip				[42,317]
SseC (STM1400)	SPI-2		SPI-2 TTTS translocon component				[42]
SseD (STM1401)	SPI-2		SPI-2 TTTS translocon component				[42]
SseF (STM1404)	SPI-2				Contributes to SIF formation with SifA, SopD2 and SseG, immunoprecipitates with SseG, recuits dynein to SCV, maintains perinuclear SCV positioning, required for formation of microtubule bundles around SCV, redirects exocytic transport vesicles to SCV,	Replication & SCV positioning	[3,64,65,343,353,354]
SseG (STM1405)	SPI-2				Contributes to SIF formation with SifA, SopD2 and SseF, immunoprecipiates with SseF, recuits dynein to SCV,	Replication & SCV positioning	[3,65,210,343,353,354]

					maintains perinuclear SCV positioning, required for formation of microtubule bundles around SCV, redirects exocytic transport vesicles to SCV,		
SrfH (SseI/GtgB) (STM1051)	Phage Gifsy-2	N-terminus: *Salmonella* SifA/B, SlrP, SseJ, SspH1/2 C-terminus: *P. asymbiotica* PAU_02230		Filamin, TRIP6, IQGAP1	Co-localizes with polymerizing actin cytoskeleton, promotes phagocyte motility and rapid septicemia after oral infection		[11,115,175]
SseJ (STM1613)	Outside SPI-2	N-terminus: *Salmonella* SifA/B, SlrP, SrfH, SspH1/2	Deacylase, phospholipase A, glycerophospholipid :cholesterol acyltransferase	Cholesterol	Required for full virulence in mice, over-expression negatively regulates SIF formation in infected cells, destabilizes SCV in ΔsifA mutants, co-expression with SifA promotes SIF formation.	SCV maturation & trafficking Replication & SCV positioning	[3,60-63,115,350, 355,356]
SseK2 (STM2137)	Outside SPI-2	*Salmonella* SseK1/3, *Citrobacter rodentium* NleB, EHEC Z4328					[207]
SseK3[c]	ST64B coliform phage	*Salmonella* SseK1/2, *Citrobacter rodentium* NleB, EHEC Z4328					[207]
SseL (STM2287)	Outside SPI-2		Cysteine protease with deubiquitinase activity	IκBα	Impairs IκBα ubiquitination and degradation but not phosphorylation, inhibits macrophage apoptosis, downregulates inflammatory responses	Pro/anti-inflammatory responses	[84,357]
SspH2 (STM2241)	In vicinity of phage remnants	N-terminus: *Salmonella* SspH1, SlrP, SifA/B, SrfH, SseJ LRR: *Salmonella* GogB C-terminus: *Yersinia* YopM, *Shigella* $IpaH_{7.8}/_{9.8}$	Inhibits actin polymerisation *in vitro*	Filamin Profilin	Remodels SCV associated F actin? Interferes with antigen presentation in dendritic cells, N-terminus localizes protein to apical membrane of epithelial cells, internal LRR domain interacts with C-terminal E3 ubiquitin ligase domain and inhibits ligase activity. Localization to membrane thought to break this association and restrict ubiquitin ligase to particular cellular regions	SCV maturation & trafficking Pro/anti-inflammatory responses	[82,89,115,140]
SteC (STM1698)	Outside SPI-2	Human kinase Raf-1	Serine/ Threonine kinase		Kinase activity required for actin remodeling, associated with VAP phenotype.	SCV maturation & trafficking	[29,71]
SteD (STM2139)	Outside SPI-2				Hypervirulence phenotype in 129/SVJ mice.		this study

Salmonella effectors that are secreted independent of a TTSS.

Effector	**Gene Location**	**Selected Homologues**	**Activity**	**Host cell Target(s)**	**Infection Phenotypes**	**Stage of Infection**	**Refs.**
PagK (STM1867)					Vesicle effector.		(pers. Comm. Hyunjin Yoon and Fred

							Heffron)
PagK-H (STM2585A)					Vesicle effector		(pers. Comm. Hyunjin Yoon and Fred Heffron)
PagC (STM1246)					Vesicle effector		(pers. Comm. Hyunjin Yoon and Fred Heffron)
PagD (STM1244)					Vesicle effector		(pers. Comm. Hyunjin Yoon and Fred Heffron)
SrfN (STM0082)					Vesicle effector		(pers. Comm. Hyunjin Yoon and Fred Heffron)
SssA (STM0359)					Unknown secretion mechanism		this study
SssB (STM1478)		YdgH domain conserved in Enterobacteriaciae			Unknown secretion mechanism, hypervirulence phenotype in 129/SVJ mice.		this study
ZirS (STM1668)					Two-partner secretion with ZirT (STM1669)		[267]

[a] Found in *S*. Typhimurium SL1344 but not 14028 or LT2

[b] Found in *S*. Typhimurium 14028 but not SL1344 or LT2

[c] Found in *S*. Typhimurium 14028 and SL1344 but not LT2

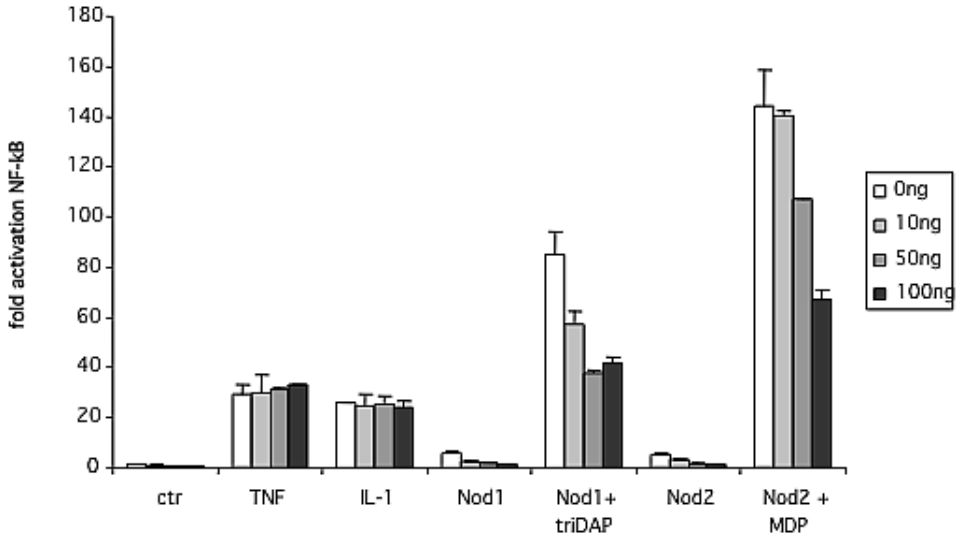

Fig. A-1

SrfH down-regulates NOD signaling in transfected HEK293T cells. HEK293T cells were co-transfected with an NF-κB luciferase reporter, Nod1 and Nod2 expression plasmids, and pIRES2-HsrfH as indicated. The following day cells were treated with TNFα, IL-1, triDAP, or MDP for one hour, and cellular lysates were analyzed for luciferase activity. Data was normalized to β-gal expression from a co-transfected expression plasmid.

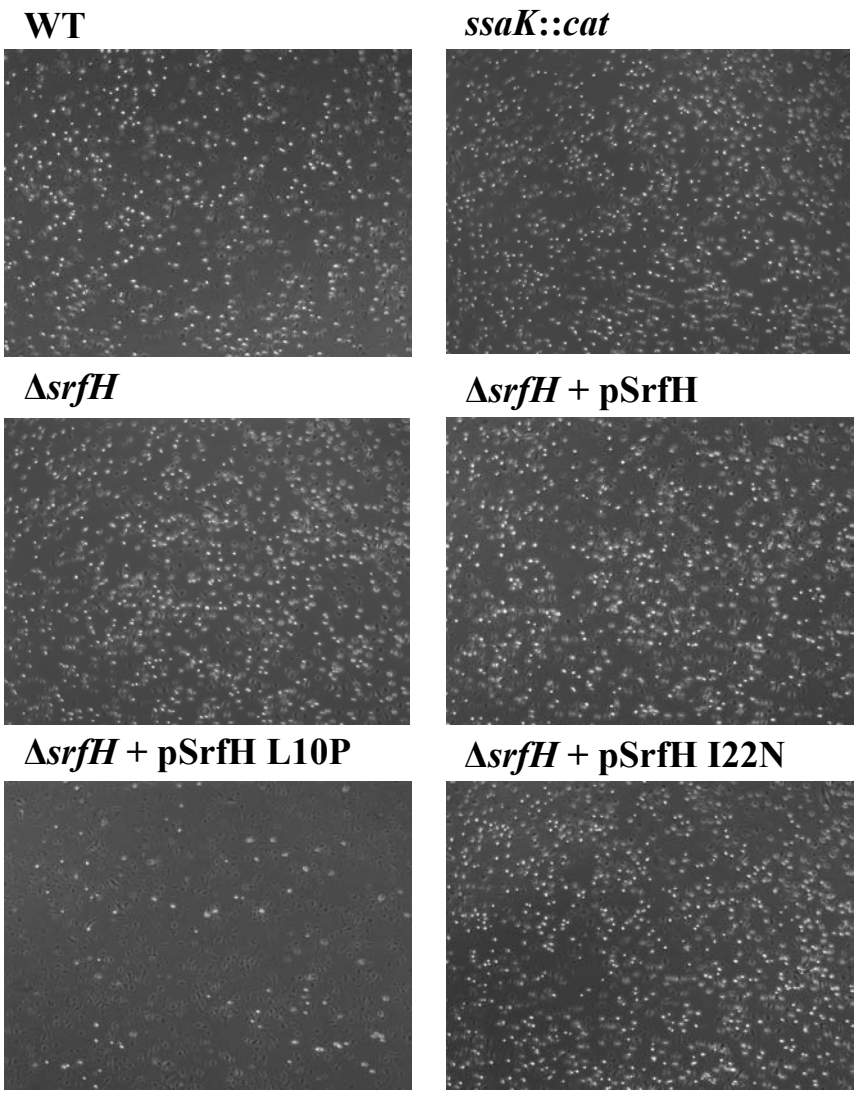

Fig. A-2

SrfH L10P alters the morphology of infected BMDM. BMDM macrophages from Balb/c mice were infected overnight at an MOI =50 with the indicated bacterial strains. The following day 4X phase contrast images of the infected cells were taken. Similar results were obtained with 129/SvJ BMDM.

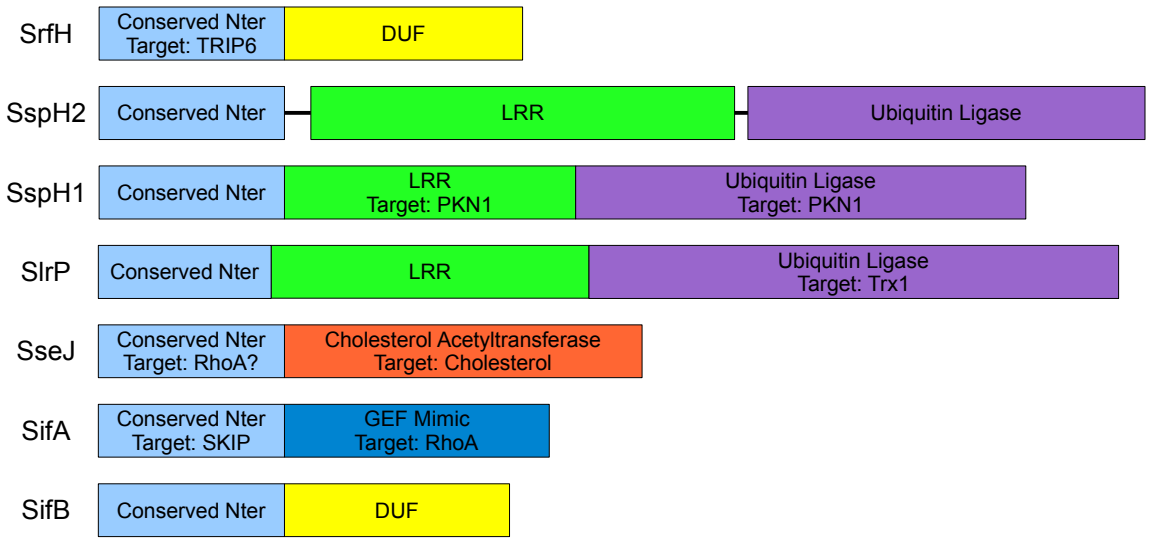

Fig. A-3

Domain map of *Salmonella* effector proteins defined conserved N-terminal homology. Abbreviations: DUF = domain of unknown function, LRR = leucine rich repeat, GEF = guanine nucleotide exchange factor.

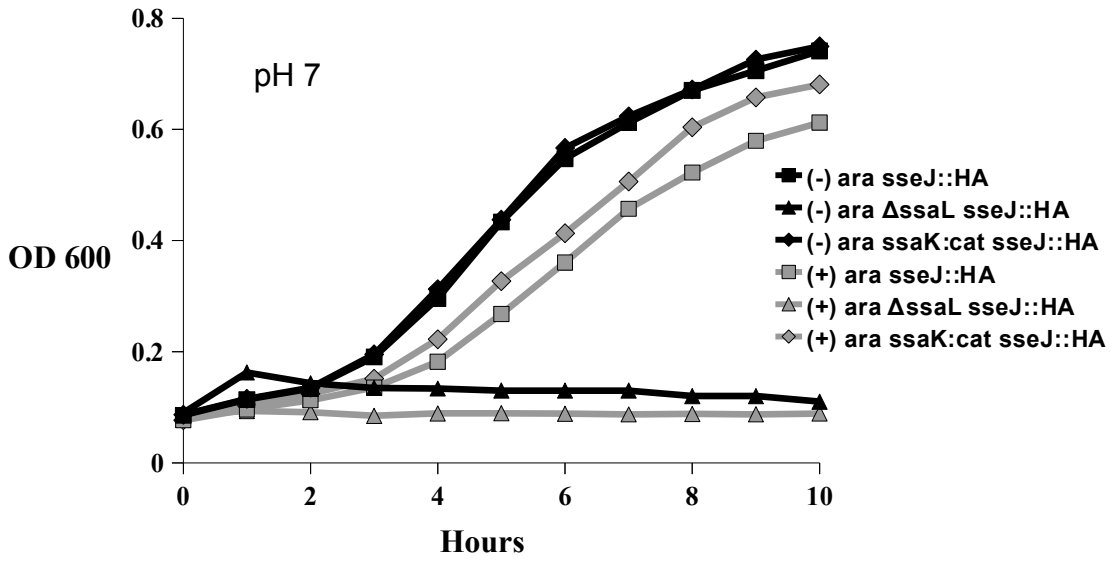

Fig. A-4

An *ssaL* mutant is attenuated for growth at neutral pH. Bacterial strains were normalized to a starting OD_{600}= 0.1 and grown in mLPM, pH 7, ± 0.2% arabinose. Arabinose was added to over-express SsrB from the pBAD*ssrB* plasmid. The difference in growth rates between *ssaL* encoding and non-encoding strains was significant ($P<0.05$).

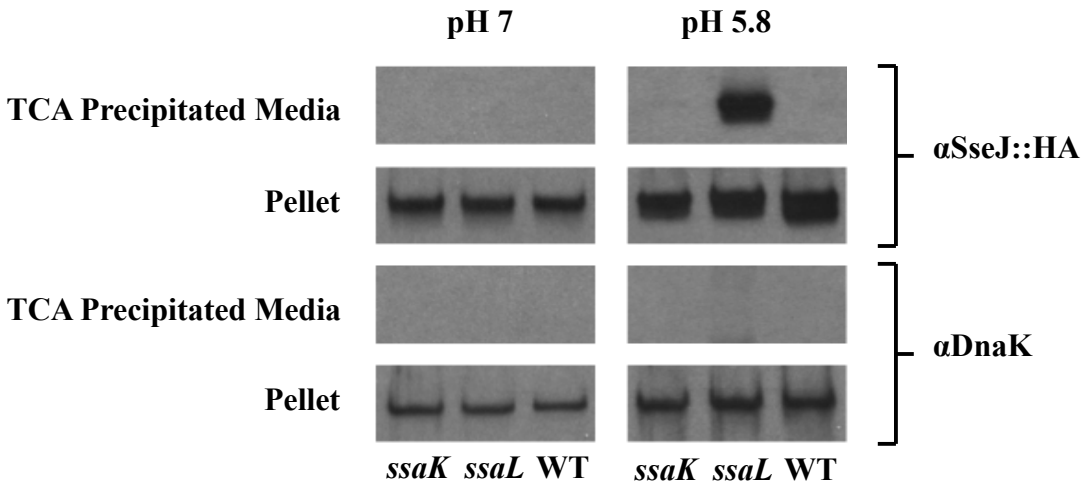

Fig. A-5

pH dependent secretion of SseJ occurs in an *ssaL* mutant. Overnight cultures of the indicated strains were washed and diluted 1:10 into fresh mLPM. After five hours incubation, bacteria were pelleted, and the OD600 was measured. The spent culture supernatants were filtered through a 0.45 μm PVDF membrane and TCA precipitated overnight. Samples were normalized to the OD 600, resolved by SDS PAGE, and analyzed by immunoblotting.

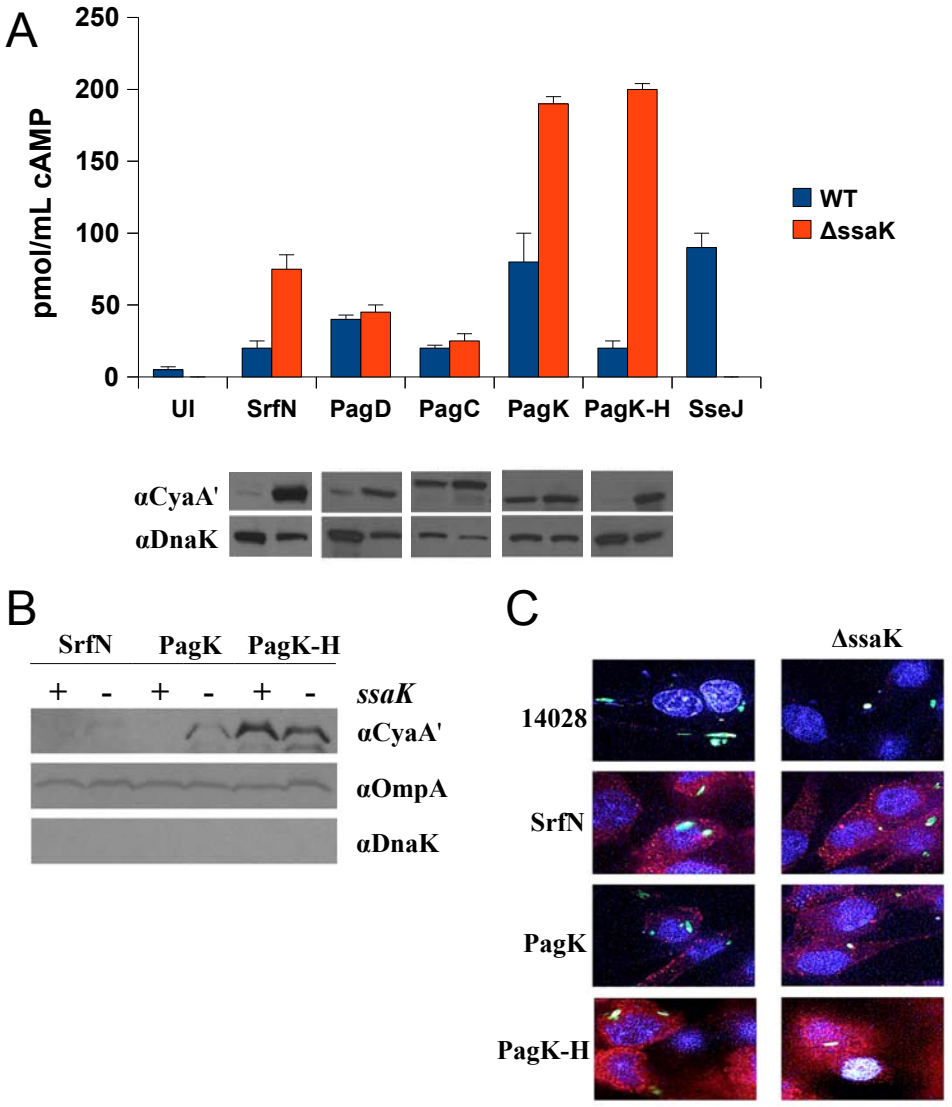

Fig. A-6

Effector proteins that may be secreted in OMV. (A) Secretion of SrfN, PagD, PagC, PagK, and PagK-H is independent of the SPI-2 TTSS. Top: J774 macrophages were infected with *Salmonella* strains harboring chromosomal effector::CyaA' fusions. 18 hours post-infection cAMP levels were measured to evaluate secretion. Bottom: Lysates from infected macrophages were collected 18 hours post infection. Expression of the CyaA fusions was assessed by immunoblotting using CyaA' and DnaK antibodies. (B) Export of SrfN, PagK, and PagK-H via OMV. Vesicles were isolated from *Salmonella* strains expressing CyaA' fusions in LPM and analyzed by immunoblotting. OmpA, a redundant OMV protein, and DnaK, a cytosolic protein, were used as controls. (C) Secretion of SrfN, PagK, PagK-H into host cytosol. Macrophages were infected with wild type and CyaA'-labeled strains for 18 hours and analyzed by immunofluorescence microscopy. Bacteria were transformed with a plasmid expressing ppluGFP (green); nuclei were stained with DRAQ5 (blue); CyaA'-tagged SrfN, PagK, and PagK-H were detected using rabbit anti-CyaA antibody and Alexa 594-labeled goat anti-rabbit IgG (red). Data courtesy Hyunjin Yoon.

A

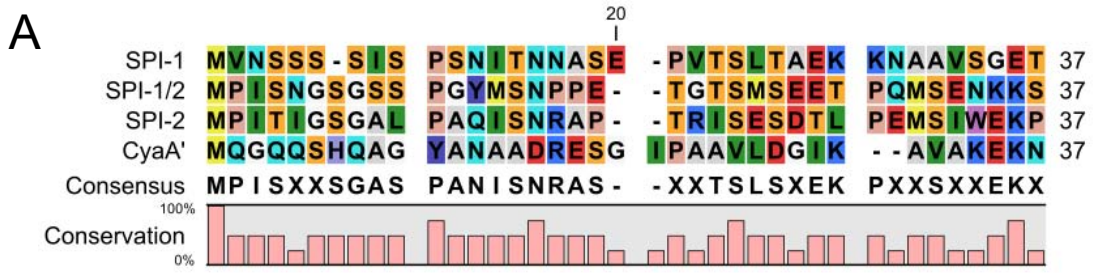

B

	5' Sequence Encoding Shine Dalgarno
R17 Phage	AGGAGGUUUGACCU**AUG**
sipA	AGGAUAACAGAAGAGGAUAUUAAUA**AUG**
steA	AAACACGUUAAUUAAGGAUAACACG**AUG**
srfH	UGUAAAUUUAUAAAGGUUUUUUGUU**AUG**

C

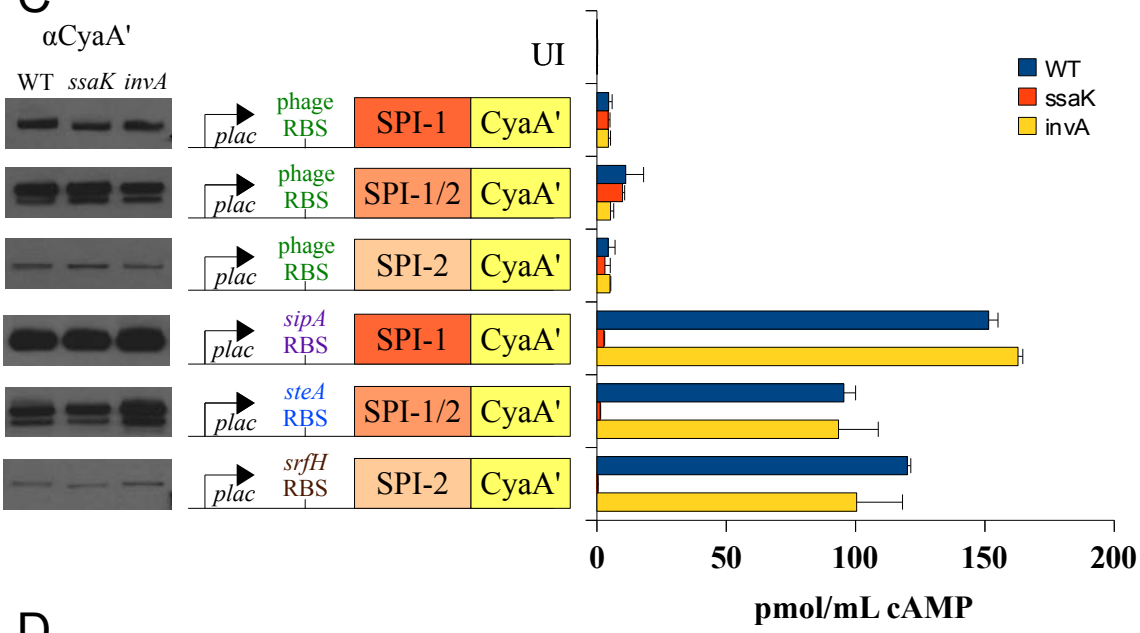

D

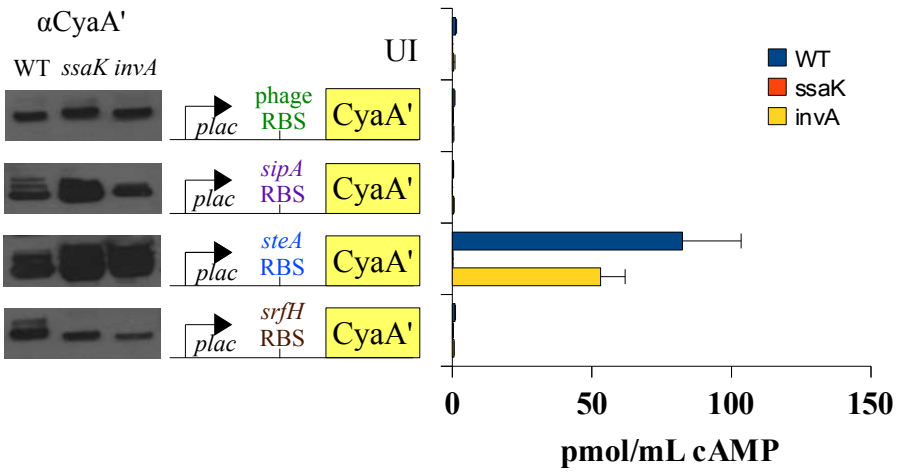

Fig. A-7

The SPI-2 TTS signal is encoded upstream and downstream of the mRNA start codon. (A) Clustal alignment of SIEVE predicted consensus secretion signals for SPI-1, SPI-1/2, and SPI-2 effectors. (B) 5' sequences encoding the RBS of R17 phage, *sipA*, *steA*, and *srfH*. AUG start codon in bold. (C & D) R17 phage, *sipA*, *steA*, or *srfH* RBS were cloned upstream of the SIEVE secretion signals or fused directly to CyaA' as indicated. Expression was driven by *plac* which is constitutive in *Salmonella*. (Left) Immunoblots of the various CyaA' fusions from overnight LB cultures. Samples were normalized to an OD600 = 0.01 (~2 x 10^7 CFU). (Right) J774 macrophages were infected for six hours and secretion was evaluated by cAMP ELISA.